Mag. Katrin Medea-Emma Fantur

Friend or Foe: Iminosugars as Inhibitors and Pharmacological Chaperones of the Human Lysosomal Acid β-Galactosidase

DISSERTATION

zur Erlangung des akademischen Grades einer

Doktorin der Naturwissenschaften

erreicht an der

Technischen Universität Graz

in Zusammenarbeit mit der Universitätsklinik für Kinder- und Jugendheilkunde

Medizinische Universität Graz

Univ.-Prof. Dr.rer.nat. Peter Macheroux

Institut für Biochemie

Technische Universität Graz

2010

Cultivation of mammalian cells, enzymatic measurements (except where indicated), and DNA-based experiments described in this work were conducted at the Laboratory of Metabolic Diseases (PI: Ao.Univ.-Prof. Dr. Eduard Paschke), Department of Pediatrics, Medical University of Graz, Auenbruggerplatz 30, 8036 Graz, Austria.

Experiments with genetically modified organisms, protein purifications, separation and detection of proteins as well as immunofluorescence experiments were conducted at the Laboratory of Protein Biochemistry (PI: Univ.-Prof. Dr. Peter Macheroux), Department of Biochemistry, Graz University of Technology, Petersgasse 12/II, 8010 Graz, Austria or at the Center for Medical Research (ZMF), Medical University of Graz, Stiftingtalstrasse 24, 8010 Graz, Austria.

Loading assays with tritium-labeled G_{M1}-gangliosides, thin layer chromatography of lipid extracts, and liquid scintillation counting were completely performed at the Laboratory of Lysosomal Metabolism Biochemistry (PI: RNDr. Jana Ledvinová, CSc.), Institute of Inherited Metabolic Disorders, First Faculty of Medicine, Charles University in Prague and General University Hospital in Prague, Ke Karlovu 2, 128 08 Prague 2, Czech Republic.

Some parts of this thesis are excerpts from the following publication:

Fantur K, Hofer D, Schitter G, Steiner AJ, Pabst BM, Wrodnigg TM, Stütz AE, Paschke E. DLHex-DGJ, a novel derivative of 1-deoxygalactonojirimycin with pharmacological chaperone activity in human G_{M1}-gangliosidosis fibroblasts. *Mol Genet Metab* 2010; **100**: 262-268.

EIDESSTATTLICHE ERKLÄRUNG

Ich erkläre an Eides statt, dass ich die vorliegende Arbeit selbstständig verfasst, andere als die angegebenen Quellen/Hilfsmittel nicht benutzt, und die den benutzten Quellen wörtlich und inhaltlich entnommene Stellen als solche kenntlich gemacht habe.

Graz, am …………………………   …………………………………………………..

                                                (Unterschrift)

Englische Fassung:

STATUTORY DECLARATION

I declare that I have authored this thesis independently, that I have not used other than the declared sources / resources, and that I have explicitly marked all material which has been quoted either literally or by content from the used sources.

…………………………   …………………………………………………..

            date   (signature)

Für meine Väter im Himmel und meine Mutter auf Erden.

In dankbarer Erinnerung an Werner.

When the going gets tough, the tough get going

(Joseph P. Kennedy, 1888-1969)

Acknowledgements

ABSTRACT

G_{M1}-gangliosidosis (GM1) and Morquio B disease (MBD) are rare, hereditary lysosomal storage disorders caused by mutations in the gene *GLB1*. Its main gene product, human lysosomal acid β-galactosidase (β-Gal) degrades N-linked oligosaccharides present in glycoproteins, G_{M1}-gangliosides in the brain, and keratan sulfate in connective tissues. While GM1 is a phenotypically heterogenous neurodegenerative disorder, MBD is a systemic bone disease without effects on the central nervous system. Some mutations in the *GLB1* gene produce stable β-Gal precursors, normally transported and processed to mature, intralysosomal β-Gal, while others affect precursor stability and intracellular transport resulting in premature protein degradation. Several misfolded enzymes were shown to be sensitive to stabilization by iminosugars, which bind at the active site to provide proper conformation. Thus the stabilized protein may escape from degradation processes, and reach the lysosomes in an active state, as proposed for enzyme enhancement therapy (EET).

In this work the influence of novel derivatives of 1-deoxygalactonojirimycin (DGJ) on the β-Gal activity of cultured GM1 and MBD skin fibroblasts was examined. Furthermore, the effect of selected compounds on natural substrate degradation in GM1 and MBD cells was determined. Several novel iminosugars acting as pharmacological chaperones of β-Gal in specific GM1 fibroblasts were discovered and described in this work. One specific compound, DLHex-DGJ, proved to be a potent competitive inhibitor of β-Gal *in vitro*, and this work describes its effects on activity, protein expression, maturation and intracellular transport *in vivo* in 13 fibroblasts lines with *GLB1* mutations. DLHex-DGJ significantly increased the catalytic activity in six GM1 cell lines, and normalization of transport and lysosomal processing of β-Gal precursors was demonstrated for selected cell lines. Furthermore, DLHex-DGJ and another, similar compound successfully reduced the level of internalized radiolabeled G_{M1}-gangliosides in a specific GM1 cell line, suggesting that reduction of stored material is possible under certain conditions.

Specific antibodies, directed against human β-Gal, were developed with the aid of previously published protocols, and novel approaches to obtain large amounts of the purified human enzyme were tested. Two novel polyclonal anti-β-Gal peptide antibodies were produced and expression of human β-Gal in *E. coli* cells, described in this work, may provide the basis for further development of antibodies directed against the human enzyme.

ZUSAMMENFASSUNG

G_{M1}-Gangliosidose (GM1) und M. Morquio B (MBD) sind seltene, vererbbare lysosomale Speicherkrankheiten, verursacht durch Mutationen im *GLB1* Gen. Das Hauptgenprodukt, die humane lysosomale saure β-Galaktosidase (β-Gal) katalysiert den Abbau von N-glykosidischen Oligosacchariden, G_{M1}-Gangliosid im Gehirn und von Keratansulfat in Bindegeweben. GM1 ist eine neurodegenerative Erkrankung mit phänotypisch heterogenem Erscheinungsbild, während MBD eine systemische Knochenerkrankung ohne Einfluss auf das Zentralnervensystem darstellt. Einige Mutationen des *GLB1* Gens resultieren in stabilen β-Gal Vorläuferproteinen, welche in die Lysosomen transportiert und zum reifen Enzym prozessiert werden, wohingegen andere Mutationen die Stabilität und den Transport des Vorläuferproteins beeinflussen und zum vorzeitigen Proteinabbau führen können. Viele fehlgefaltete Enzyme konnten durch die Bindung von Iminozuckern in ihrem aktiven Zentrum stabilisiert werden, wodurch Abbauprozesse umgangen und die Lysosomen in einem funktionellen Zustand erreicht werden können. Dieses Konzept bildet die Grundlage für die Enzymstabilisierungstherapie.

In dieser Arbeit wurde der Einfluss von neuartigen 1-Deoxygalactonojirimycin-Derivaten auf die β-Gal-Aktivität kultivierter GM1- und MBD-Hautfibroblasten untersucht und ausgewählte Verbindungen wurden bezüglich ihres Effekts auf den Abbau von natürlichen Substraten überprüft. Einige neuartige Iminozucker konnten als pharmakologische Chaperone identifiziert werden und eine bestimmte Verbindung, DLHex-DGJ, erwies sich als stark kompetitiver β-Gal Inhibitor *in vitro*. Die vorliegende Arbeit beschreibt hauptsächlich die Auswirkungen von DLHex-DGJ auf die Enyzmaktivität, Proteinexpression, Reifung und auf den intrazellulären Transport in 13 Fibroblastenzelllinien mit *GLB1* Mutationen. Die Behandlung mit DLHex-DGJ führte zur signifikanten Steigerung der β-Gal-Aktivität in 6 GM1 Zelllinien und die Normalisierung des Transportes, die intralysosomale Prozessierung des β-Gal Vorläuferproteins sowie der Abbau von radioaktiv-markierten G_{M1}-Gangliosiden wurde in bestimmten Zelllinien nachgewiesen.

Spezifische Antikörper gegen die humane β-Galaktosidase konnten unter Zuhilfenahme von publizierten Methoden entwickelt werden und neue Strategien zur Reinigung großer Mengen des humanen Enyzms wurden getestet. In dieser Arbeit wird außerdem die Expression der humanen β-Galaktosidase in *E. coli* Zellen beschrieben, welche möglicherweise eine Grundlage für zukünftige Strategien zur Produktion von Antikörpern bilden könnte.

INDEX

List of abbreviations

#2 w/o dansyl	Methyl N^6-(1,5-dideoxy-D-galactitol-1,5-diyl)-L-lysinate
^{3}H-G_{M1}G	Tritium (^{3}H)-labeled G_{M1}-ganglioside
aa	Amino acids
Aqua dest.	Aqua destillata
β-Gal	Human lysosomal acid β-galactosidase
β-Hex	Human lysosomal β-N-acetylhexosaminidase
BSA	Bovine serum albumin
CBE	Conduritol B Epoxide
d	Day(s)
DGJ	1-Deoxygalactonojirimycin
DLHex-DGJ	Methyl 6-[N^2-dansyl-N^6-(1,5-dideoxy-D-galactitol-1,5-diyl)-L-lysinyl] amino hexanoate
DNJ	1-Deoxynojirimycin
dpm	Disintegrations per rminute
DTT	Dithiothreitol
E. coli	*Escherichia coli*
(r)ER	(Rough) endoplasmic reticulum
EtOH	Ethanol
FCS	Fetal (bovine) calf serum
g	Local gravitational field (1 x g = 9.80665 m/s²)
GM1	G_{M1}-gangliosidosis
hr(s)	hour(s)
IC_{50}	Half maximal inhibitory concentration

ICD-10	International Statistical Classification of Diseases and Related Health Problems (10th edition)
IF	Immunofluorescence
IPTG	Isopropyl β-D-1-thiogalactopyranoside
(k)Da	(Kilo) Dalton
K_i	Apparent inhibition constant
LSD(s)	Lysosomal storage disease(s)
M.	Morbus
MBD	Morquio B Disease
MeOH	Methanol
M_r	Relative molecular mass
nt	Nucleotide(s)
ONC	Overnight culture
PC(s)	Pharmacological chaperone(s)
PCR	Polymerase chain reaction
PhoBI	Phosphate Buffer for Inhibitors
PP	PreScission™ Protease
rpm	Rounds per minute
TLC	Thin layer chromatography
WB	Western blot
w/o	Without
WT	Wildtype

1   INTRODUCTION

1.1   Human β-galactosidases

Human lysosomal acid β-galactosidase (β-Gal; OMIM #611458; EC 3.2.1.23), encoded by the structural gene *GLB1* on chromosome 3p21.33 [Yamamoto *et al*., 1990], is a lysosomally located, hydrolytic enzyme essential for the human body. It belongs to the family of hydrolases (EC 3) and can be further classified as member of the glycosylases (EC 3.2) or, more specifically, of glycoside hydrolases (glycosidases; EC 3.2.1), enzymes catalyzing the hydrolysis of various O- and S-glycosyl compounds.

In fact, two different β-galactosidases are active in lysosomes, the human lysosomal acid β-Gal enzyme described above and galactocerebrosidase (EC 3.2.1.46), a glycoside hydrolase with quite similar substrate specifity. Human lysosomal acid β-Gal (EC 3.2.1.23) from healthy individuals catalyzes hydrolysis of various natural substrates like G_{M1}- and G_{A1} (asialo G_{M1})-gangliosides, keratan sulfate, lactosylceramide, asialofetuin and other galactose-containing oligosaccharides [Callahan, 1999] in the lysosomal compartment. Furthermore, the terminal galactose of the commercially available synthetic substrates 4-methylumbelliferyl-β-D-galactopyranoside or p-nitrophenyl-β-D-galactopyranoside, amongst others, is removed upon enzymatic β-Gal activity. Galactocerebrosidase, on the other hand, catalyzes the removal of galactose residues only from galactosylceramide, lactosylceramide, galactosylsphingosine, and monogalactosyl diglyceride substrates [Pshezhetsky and Ashmarina, 2001]. Both enzymatic activites are required for normal substrate turnover in the lysosomal compartment. Another isoform of lysosomal β-galactosidase, the human senescence-associated β-galactosidase (SA-β-galactosidase), seems to be the result of excessive amounts of the regular lysosomal acid β-Gal protein (EC 3.2.1.23), but its characteristics are very distinct from the enzymes described above. So far, SA-β-galactosidase activity was only detected in cultured cells, specifically in senescent human fibroblast cultures, but not in quiescent or terminally differentiated cells [Kurz *et al*., 2000; Lee *et al*., 2006]. Catalytic activity requires a pH of 6.0 [Dimri *et al*., 1995], whereas the regular β-Gal enzyme has a pH optimum of 4.5-4.75 (Pshezhetsky and Ashmarina, 2001). Furthermore, the activity of SA-β-galactosidase seems to be restricted to smooth muslce cells, ovarian epithel cells, fibroblasts, and keratinocytes [Kurz *et al*., 2000; Pshezhetsky and

Ashmarina, 2001]. Finally, two isoforms of β-galactosidase were purified from human liver [Ho *et al*., 1973; Norden *et al*., 1974], but their features seem to be very different from the lysosomal acid enzyme and they lack detailed characterization to date. However, the present work is exclusively focused on the human lysosomal acid β-galactosidase (β-Gal; EC 3.2.1.23).

1.2   The human lysosomal acid β-galactosidase

Independent from their origin in terms of organism or subcellular localization, all β-galactosidase enzymes catalyze the hydrolysis of terminal, non-reducing (β-1,4 or β-1,3 linked) β-D-galactose residues in β-D-galactosides, although substrate specifities of individual enzymes can be quite different. The human lysosomal acid β-galactosidase catalyzes hydrolysis of G_{M1}- and G_{A1} (asialo G_{M1})-gangliosides, keratan sulfate, lactosylceramide, asialofetuin and other galactose-containing oligosaccharides [Callahan, 1999] as well as hydrolysis of synthetic substrates like 4-methylumbelliferyl-β-D-galactopyranoside or p-nitrophenyl-β-D-galacto-pyranoside.

The catalytic reaction proposed for lysosomal acid β-Gal is based on a Koshland double-displacement mechanism (Figure 1.2.1), involving a covalent glycosyl enzyme intermediate [Zhang *et al*., 1994]. A highly conserved glutamic acid residue at position 268 (Glu268) of the polypeptide chain could be identified as catalytic nucleophile [McCarter *et al*., 1996]. The highly conserved glutamic acid at position 188 (Glu188) was suggested as proton donor, required to complete the reaction and to restore β-Gal to an active state [Callahan, 1999], but this speculation has not been experimentally confirmed. Further highly conserverd amino acid residues, namely an aspartic acid residue at position 332 (Asp332) and the tryptophan at position 273 (Trp273), were also proposed to be involved in the catalytic mechanism [McCarter *et al*., 1997; Callahan, 1999; Vyas, 1991].

Mechanism of a 'retaining'
β-glycosidase

TRP 273   forms "stacks" with
           hexose ring surface
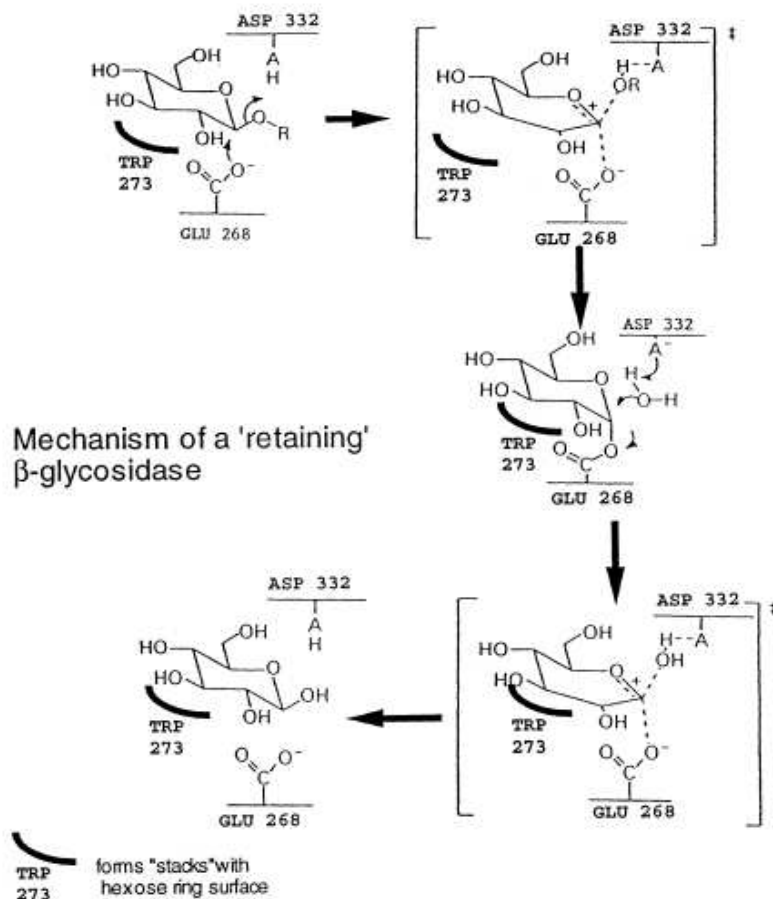
Figure 1.2.1 Catalytic mechanism of a β-configuration retaining family 35 β-galactosidase. β-Gal cleaves its substrates by a Koshland double-displacement mechanism, where Glu268, located at the catalytic site, acts as nucleophile and a galactosyl-enzyme inter-mediate is formed resulting from β-configuration retention. Glu188 was proposed as proton donor, and Trp273 might promote "stacking" between the planar indole ring and the pyranose backbone stabilizing the enzyme-substrate complex. The illustration was adapted from [Callahan, 1999].

The three-dimensional structure of the human enzyme has not been resolved by crystallographic analysis yet, but a computational homology model, based on the crystallographic structure of a beta-galactosidase from *Bacteroides thetaiotaomicron* (RCSB PDB accession number 3D3A), was proposed for this protein and is available in the 3D structure database "MODBASE" [Pieper *et al*., 2009]. Sequence identity between the underlying sequences was calculated as 39%, which is considered a reliable basis for prediction of protein structures [Chothia and Lesk, 1986]. Although homology models have to be handled with care, this specific model was recently used for structural analysis of specific β-galactosidase mutations [Morita *et al*., 2009].

1.2.1   Mutations in the GLB1 gene

The structural gene *GLB1*, encoding the human lysosomal acid β-galactosidase, is located on chromosome 3p21.33 and consists of 16 exons [Yamamoto *et al*., 1990]. Its overall length is

62.5 kb and all intron/exon junctions have been defined [Morreau *et al.*, 1991]. Remarkably, mutations in the *GLB1* gene can result in two different disorders, Morquio B disease (MBD) or G_{M1}-gangliosidosis (GM1) [Groebe *et al.*, 1980; O'Brien, 1989; O'Brien *et al.*, 1976; Okada and O'Brien, 1968]. Both disorders belong to the group of lysosomal storage diseases and are described in detail in section 1.4. Over the past decades, several strategies were pursued to analyze mutations in the *GLB1* sequence. Restrictive analysis methods such as Southern and Northern blotting were soon amended by techniques employing reverse transcription of mRNA, PCR amplification of cDNA, cloning into m13 bacteriophage, and subsequent sequencing [Morreau *et al.*, 1991]. In this way, 140 pathogenic mutations of the *GLB1* gene could be identified [Brunetti-Pierri and Scaglia, 2008; Hofer *et al.*, 2009; Hofer *et al.* 2010]. They include point mutations resulting in amino acid substitutions on the protein level (missense mutations), as well as insertions, duplications, splice site mutations (due to insertions), or nonsense mutations [Suzuki *et al.*, 2001]. *GLB1* mutations described in this work and recently investigated at the Department of Pediatrics in Graz are illustrated in Figure 1.2.1.1.
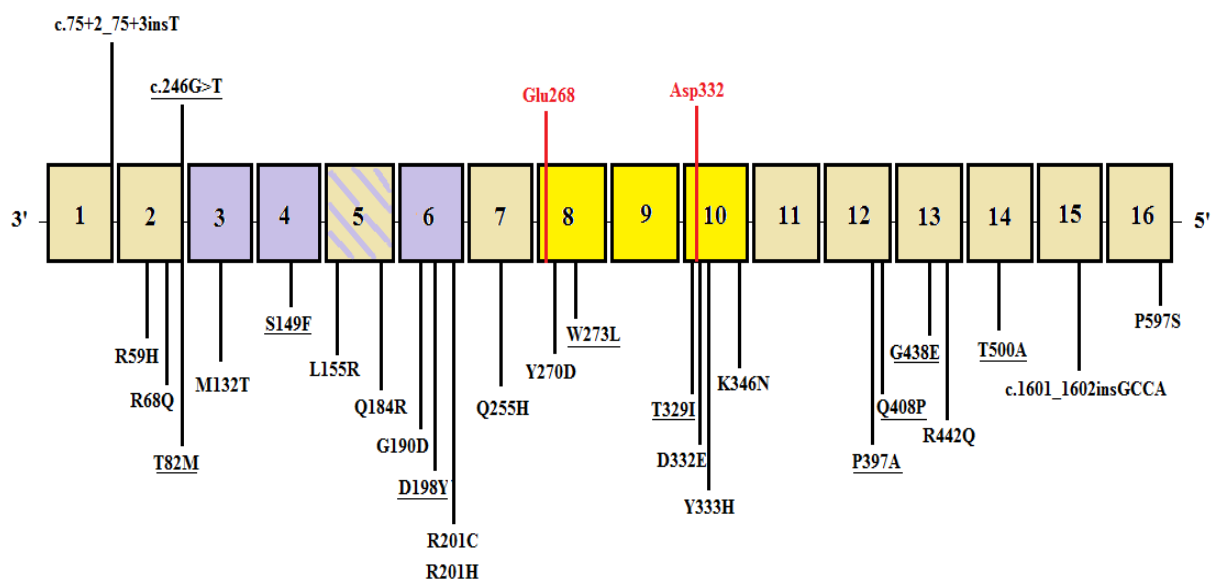
Figure 1.2.1.1 Summary of *GLB1* mutations investigated at the Department of Pediatrics in Graz. Underlined mutations were found in MBD patients in association with the p.W273L allele. The p.S149F and p.T500A alleles have been described to occur independent of the p.W273L mutation in MBD. Exons in blue are skipped in the mRNA of elastin binding protein (EBP, cf. section 1.2.1.1). Additionally, a frame-shift in exon 5 is characteristic for EBP. Yellow exons are the location of presumptive catalytic residues (Glu268; Asp332). For references see [Hofer *et al.*, 2009; Hofer *et al.*, 2010] and text.

Individuals, carrying a single MBD or GM1 allele in association with a healthy allele, are not affected by either disease due to the autosomal recessive mode of inheritance. Homo- or heteroallelic carriers of mutant alleles, however, show mild or even severe phenotypical characteristics, whereas the phenotype-determining allele is not always clearly classifiable [Hofer *et al*., 2009; Hofer *et al*., 2010; Suzuki *et al*., 2001]. A detailed list with mutations described in this work can be found in section 3.7.1. Prenatal diagnosis is available for both G_{M1}-gangliosidosis [Booth *et al*., 1973; Ida *et al*., 1989; Kaback *et al*., 1973; Kleijer *et al*., 1976; Kudoh *et al*., 1978; Lowden *et al*., 1973] and Morquio B [Sheth *et al*., 2002].

1.2.1.1   *Elastin-binding protein, an alternatively spliced GLB1 gene product*

Interestingly, human lysosomal acid β-Gal is not the only protein encoded by the *GLB1* gene [Yamamoto *et al*., 1990]. In fact, it gives also rise to an alternatively spliced, ~67-68 kDa gene product which could be identified as elastin-binding protein (EBP), due to its interaction with tropoelastin fibers and its participation in elastogenesis [Hinek *et al*., 1993]. The *GLB1* gene is composed of 16 exons, and all of them are present in the 2.4 kb mRNA transcript coding for the β-Gal prepropolypeptide. Exon 1 encodes an N-terminal signal peptide and is therefore not part of the β-Gal precursor protein after cleavage. Unlike β-Gal mRNA, the alternatively spliced mRNA transcript (2.0 kb) has a frameshift in exon 5 and is devoid of the exons 3, 4, and 6 [Morreau *et al*., 1989], but contains all other exons of the *GLB1* gene (7-16). The mature protein has a length of 523 aa and its C-terminus differs from the C-terminal end of β-Gal, due to the lysosomal processing of the β-Gal precursor (cf. section 1.3 and Figure 1.3.1). Unlike β-Gal, EBP has no enzymatic activity. EBP and its cellular function is reviewed in section 1.3.2.

1.3 Processing of the human lysosomal acid β-galactosidase

The human lysosomal acid β-galactosidase is synthesized as prepropolypeptide (677 aa), containing an N-terminal signal peptide (23 aa), which directs transportation to the rough endoplasmic reticulum (rER) and entry into this organelle [reviewed in Callahan, 1999]. Therefore, the signal peptide of the nascent polypeptide chain is recognized by a specific signal recognition particle (SRP) in the cytosol, which subsquently binds to the protein thereby decelerating protein translation at ribosomes. Finally, specific SRP-receptors in the membrane

of the rER recognize the complex consisting of SRP, the polypeptide, and ribosomes. Translation is resumed upon docking to this membrane receptor and the polypeptide chain is translated directly into the lumen of the rER [reviewed in Grudnik *et al.*, 2009 and Ni *et al.*, 2006]. After cleavage of the signal peptide and co-translational N-glycosylation processes the resulting precursor protein has a length of 654 aa and a mass of ~84 kDa [reviewed in Callahan, 1999 and Pshezhetsky and Ashmarina, 2001]. A comparative illustration of the β-Gal precursor, its post-translationally processed form, and the elastin-binding protein (EBP) is shown in Figure 1.3.1. Precursor proteins are transported to the Golgi apparatus, where specific mannose residues of oligosaccharide chains are phosphorylated thus producing mannose-6-phosphate residues. This process is catalyzed by the N-acetylglucosamine-1-phosphotransferase [Little *et al.*, 1986; Litte *et al.*, 1987; reviewed in Ni *et al.*, 2006] and the resulting protein has a mass of ~88 kDa [Callahan, 1999]. Phosphorylation of the molecule is essential for sorting processes and trafficking to the lysosomal compartment. Mannose-6-phosphate residues of N-linked oligosaccharides are detected and bound by mannose-6-phosphate receptors in the membrane of the Golgi apparatus [reviewed in Ni *et al.*, 2006]. Subsequently, these complexes are constricted from the Golgi membrane and transported to sorting vesicles in the cytoplasm, where a phosphatase catalyzes cleavage of phosphate groups from the mannose-6-phosphate residues, and the receptor complex disintegrates due to the low pH [Lodish *et al.*, 1999]. Receptor molecules are recycled at this point, while the dephosphorylated β-Gal precursor is transported to the lysosomes. Most lysosomal hydrolases are transported to the lysosomes via the mannose-6-phosphate pathway [Hasilik and Lemansky, 2004].

In lysosomes, the C-terminal end is cleaved by at least two, but yet not fully understood proteolytic processes to form the ~64 kDa mature enzyme [D'Agrosa *et al.*, 1992; Okamura-Oho *et al.*, 1996; Zhang *et al.*, 1994]. The resulting C-terminal fragment has a size of ~20 kDa and was found to remain in tight physical contact with the mature enzyme. Permanent loss of this fragment has been shown to significantly impair the catalytic activity [van der Spoel *et al.*, 2000].
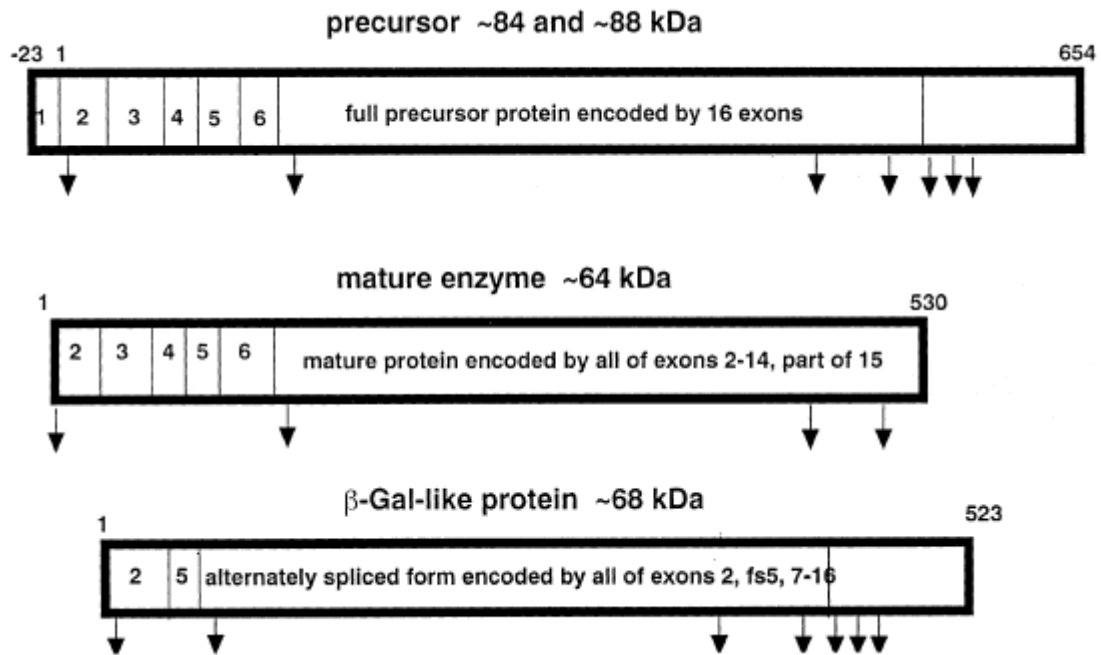
Figure 1.3.1 Processing of the β-galactosidase precursor and elastin binding protein (β-Gal-like protein). The prepropolypeptide (677 aa) still contains the N-terminal signal sequence (-23>1) that directs transportation to the ER. After cleavage of the signal sequence, post-translational modifications, and C-terminal processing in the lysosomal compartment, the mature protein has a length of 530 aa. In contrast, the EBP transcript undergoes alternative splicing (deletion of exons 3, 4, and 6; frameshift in exon 5) to produce an enzymatically inactive protein of 523 aa. Arrows indicate predicted N-glycosylation sites. The illustration was adapted from [Callahan, 1999] in a slightly modified form.

Two serine residues at position 543 and 544 (Ser543 and Ser544) were proposed as initial cleavage site by van der Spoel *et al.*, while additional action of a trypsin-like protease on the resulting large protein domain (arginine residue at position 530; Arg530) was suggested previously [Yamamoto *et al.*, 1990]. Therefore, the mature protein was proposed to have a length of 530 aa. Except for the removal of the N-terminal signal peptide (23 aa), directing transportation of the precursor protein to the rER, the N-terminus of the polypeptide chain is not affected by post-translational modifications [Yamamoto *et al.*, 1990]. Interestingly, both precursor and mature β-Gal display the same kinetic characteristics and are identical in function [Zhang *et al.*, 1994]. Normal, but functionally impaired mature β-Gal is intralysosomally degraded by proteases like cathepsin B, resulting in a ~50 kDa polypeptide and a ~18 kDa fragment (cf. Figure 1.3.2) [Callahan, 1999].

Normal processing

Non-Cathepsin
B-like protease

18 kD ↓ 50 kD
    67kD
18 kD ↓ 50 kD
    64kD

Cathepsin B-like
thiol protease ■

___ 50 kD
18 kD
■ INHIBITED BY LEUPEPTIN
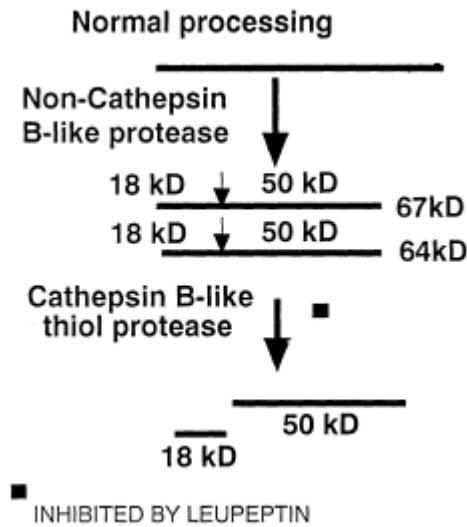
Figure 1.3.2 Post-translational processing of the β-Gal precursor protein in lysosomes. The C-terminal end of the precursor is cleaved and modified by processes involving a non-cathepsin B-like protease to form the mature enzyme (64 kDa). This mechanism is not influenced by the action of the protease inhibitor Leupeptin. Normal degradation of mature β-Gal in the lysosomes results in specific fragments of 18 kDa and 50 kDa. The Cathepsin B-like thiol protease, involved in this process, can be inhibited by Leupeptin. The illustration is adapted from [Callahan, 1999] in a slightly modified form.

1.3.1 Formation of the lysosomal multienzyme complex

Affinity chromatographic purification of β-Gal proteins from various mammalian tissues, including human placenta and liver [Norden *et al*., 1974], provided evidence that β-Gal molecules exist in multiple oligomeric forms and only small amounts might be present in a monomeric form. Such oligomers include 70-80 kDa monomers, 110-170 kDa dimers, 250 kDa tetramers, and 600-700 (~680) kDa multimers [Anderson *et al*., 1978; Frost *et al*., 1978; Hoeksema *et al*., 1979; Hoogeveen *et al*. 1983; Norden *et al*., 1974; Tomino and Meisler, 1975]. Hoogeveen *et al*. could demonstrate that the vast majority (85%) of β-Gal molecules in human skin fibroblasts is present as 600-700 kDa aggregates upon purification under conditions simulating the lysosomal environment in terms of pH and high protein concentration [Hollemans *et al*., 1979]. In contrast to β-Gal monomers (10% in human skin fibroblasts) and other oligomeric forms, the high-molecular-weight aggregates were always found to co-purify with variable amounts of a 32 kDa protein [d'Azzo *et al*., 1982; Hoogeveen *et al*., 1984; Jones *et al*., 1984; Yamamoto *et al*., 1982], later identified as lysosomal carboxypeptidase A (EC 3.4.16.5) and named protective protein/cathepsin A (PPCA) [Barrett *et al*., 1998]. In fact, PPCA consists of two polypeptide chains, a 20 kDa chain and the 32 kDa chain, linked by disulfide bonds [reviewed in Pshezhetsky and Ashmarina, 2001]. PPCA is a multifunctional enzyme with deamidase and esterase activity, expressed at neutral pH, and carboxypeptidase activity at acidic pH [Jackman *et al*., 1990]. The name affix protective protein derives from its ability to protect β-Gal in the complexed form against premature degradation within the

lysosomal compartment. It is further believed to stabilize transportation of the β-Gal precursor to the lysosomes [Pshezhetsky and Ashmarina, 2001; van der Spoel *et al*., 1998; Zhou *et al*., 1996]. Binding of PPCA to β-Gal is essential for subsequent formation of the 600-700 kDa aggregates [Hoogeveen *et al*., 1984]. Later studies revealed two other proteins with masses of 40 kDa and 48 kDa, respectively, binding to the ~680 kDa aggregates and resulting in a 1.27 MDa complex [Pshezhetsky and Ashmarina, 2001] which was therefore designated as lysosomal multienzyme complex (LMC). The 48 kDa protein (α-neuraminidase or sialidase; SIAL; EC 3.2.1.18) catalyzes the hydrolysis of terminal sialic acid residues in oligosaccharides, glycoproteins, glycolipids, colominic acid and synthetic substrates (Dorland *et al*., 1978; Michalski *et al*., 1977; Strecker *et al*., 1977; van Pelt *et al*., 1988). The 40 kDa protein, identified as the N-acetylgalactosamine-6-sulfatase or galactose-6-sulfatase (GALNS; EC 3.1.6.4), specifically catalyzes removal of 6-sulfate groups from N-acetyl-D-galactosamine 6-sulfate in chondroitin sulfate and from D-galactose 6-sulfate units in keratan sulfate [Glössl *et al*., 1979]. The enzyme is actually composed of a 40 kDa polypeptide and a 15 kDa peptide chain.

The ~680 kDa complex can be considered as basic LMC complex, consisting of 100 kDa PPCA dimers and 320 kDa β-Gal tetramers [Hiraiwa *et al*., 1997; Pshezhetsky and Potier, 1993], which is essential for the formation of the 1.27 MDa complex. Several individual studies [reviewed in Pshezhetsky and Ashmarina, 2001] could demonstrate the presence of the following subunits in the 1.27 MDa complex, irrespective of underlying purification methods or sample origins (in terms of tissue):

- 64 kDa β-galactosidase,

- 48 kDa sialidase,

- 40 kDa N-acetylgalactosamine-6-sulfatase, and

- 32 kDa + 20 kDa protective protein/cathepsin A.

However, exact stoichiometric analysis of the lysosomal multienzyme complex is still an ongoing task, due to the high instability of the LMC in low-protein and neutral pH environments and different purification methods.

1.3.2 EBP and the plasma membrane complex

In contrast to β-Gal, EBP is an enzymatically inactive protein with galactolectin properties. The protein is able to bind specifically to elastin fibers, laminin, or type IV collagen [Caciotti *et al*., 2005; Hinek 1996; Hinek *et al*., 1993]. EBP is an essential part of the non-integrin cell surface receptor and one of its main functions in the cell is facilitating tropoelastin transport and its extracellular assembly to elastic fibers [Hinek, 1996]. In fact, EBP can be considered as molecular chaperon of tropoelastin.

The non-integrin cell surface receptor is expressed on all elastin-producing cells like fibroblasts, smooth muscle cells, chondroblasts, leukocytes, and certain cancer cell types [reviewed in Hinek, 1996]. Similar to β-Gal, EBP requires interaction with other proteins to perform all of its tasks. In the case of EBP, two more proteins are necessary for complex formation and its binding to the plasma membrane. The two subunits were identified as protective protein/cathepsin A (PPCA) and sialidase, the same proteins that are also constituents of the lysosomal multienzyme complex (LMC; cf. section 1.3.1). Sialidase is the key protein for anchoring the complex in the plasma membrane, or attaching it to endosomal membranes during recycling of its components [reviewed in Callahan, 1999 and Hinek, 1996].

1.4 Lysosomal storage diseases

So far, approximately 50 different forms of lysosomal storage diseases (LSDs) have been described in the literature [Ballabio and Gieselmann, 2009]. They are primarily characterized by the accumulation of partially degraded or undegraded substances within the lysosomal compartment of various tissues. Quite often, however, storage of material is not limited to lysosomes, but rather extended to other organelles or even to the outside of plasma membranes, hence interfering with various processes on the cellular level [Ballabio and Gieselmann, 2009]. Extracellular heparan sulfate oligosaccharide accumulation in Hurler syndrome (OMIM

#607014), for example, impairs a specific signal transduction cascade by preventing the binding of fibroblast growth factor 2 (FGF-2) to its receptor. As a consequence, the proliferative response of Hurler cells is strongly reduced [Yayon *et al*., 1991] and fibroblast cells show increased rates of apoptosis [Aldenhoven *et al*., 2009; Ballabio and Gieselmann, 2009].

LSDs are classified according to the major storage compound and can therefore be subdivided in lipidoses, gangliosidoses, mucopolysaccharidoses, glycoproteinoses, mucolipidoses and leukodystrophies (cf. ICD-10: E75-E77). A brief overview of the most frequent disorders is given in Table 1.4.1.

Lysosomal storage disorders are caused by mutations in specific genes, which are inherited in the autosomal or x-linked recessive mode of inheritance. The resulting gene products are dysfunctional lysosomal enzymes or proteins which are required for normal substrate turnover, or non-lysosomal proteins (eg. proteins of ER or Golgi apparatus) related to lysosomal degradation mechanism in terms of transport, receptor activity or activation of substrate degradation [reviewed in Ballabio and Gieselmann, 2009]. I-cell disease (Mucolipidosis II; OMIM #252500), for example, is caused by mutations in the GNPTAB gene (gene map locus 12q23.3; OMIM #607840) producing defective N-acetylglucosamine-1-phosphate transferase (EC 2.7.8.15), a Golgi apparatus-located enzyme which phosphorylates mannose-6-phosphate residues of hydrolases destined for transport to the lysosomal compartment in fibroblast cells [Kollmann *et al*., 2010; van Dongen *et al*., 1985]. Due to the missing targeting signal, all mannose-6-phosphate-dependent proteins are transported to the cell surface and secreted into the extracellular space (e.g. serum, culture medium of cultured fibroblasts). Furthermore, large amounts of intracytoplasmic, membrane-bound vacuoles (inclusion bodies) containing undegraded materials like oligosaccharides, lipids, or mucopolysaccharides are characteristic cellular features of individuals afflicted with I-cell disease [Leroy and DeMars, 1967]. Due to the low intracellular activity of most lysosomal hydrolases [Kenyon and Sensenbrenner, 1971] and the cell's disability for normal substrate turnover, the anticipated average life of I-cell patients is <10 years.

Each individual disorder is a very rare condition, although LSDs as a group have an incidence of approximately 1:7,000-8,000 live births [Meikle *et al*., 1999; Poorthuis *et al*., 1999]. The above mentioned disorders I-cell disease and Hurler disease have an incidence of 1:640,000 and 1:100,000, respectively [Aldenhoven *et al*., 2009].

Disorder	Defective enzyme	Storage material
Mucopolysaccharidoses (MPS)		
MPS I (M. Hurler, M. Scheie, M. Hurler/Scheie)	α-Iduronidase	DS, HS, GM2, GM3, SCMAS
MPS II (Hunter)	Iduronate-2-sulfatase	DS, HS, GM2, GM3, SCMAS
MPS IIIA (M. Sanfilippo A)	Heparan N-sulfatase (sulfamidase)	HS, GM2, GM3, GD2, SCMAS, ubiquitin
MPS IIIB (M. Sanfilippo B)	N-Acetyl-α-glucosaminidase	HS, GM2, GM3, GD2, SCMAS, unesterified cholesterol
MPS IIIC (M. Sanfilippo C)	Acetyl-CoA: α-glucosamide N-acetyltransferase	HS, GM2, GM3, GD2
MPS IIID (M. Sanfilippo D)	N-Acetylglucosamide-6-sulfatase	HS, GM2, GM3, GD2
MPS IV A (M. Morquio A)	N-Acetylgalactosamine-6-sulfate-sulfatase	KS, chondroitin-6-sulfate
MPS IV B (M. Morquio B)	β-Galactosidase	KS, oligosaccharides
MPS VI (M. Maroteaux-Lamy)	N-Acetylgalactosamine-4-sulfatase (arylsulfatase B)	DS, GM2, GM3, unesterified cholesterol
MPS VII (M. Sly)	β-Glucuronidase	HS, DS, chondroitin-4- and -6-sulfates
Mucolipidoses (ML)		
ML II (I-cell disease)	N-Acetylglucosamine-1-phosphotransferase	various lipids, mucopolysaccharides, oligosaccharides
ML III (Pseudo-Hurler-Polydystrophy)	N-Acetylglucosamine-1-phosphotransferase	various lipids, mucopolysaccharides, oligosaccharides
Gangliosidoses		
G_{M1}-gangliosidosis	β-Galactosidase	GM1, GA1, GM2, GM3, GD1a, lyso-GM1, glucosylceramide, lactosylceramide, oligosaccharides, keratan sulfate
G_{M2}-gangliosidosis (M. Tay-Sachs)	β-Hexosaminidase A	GM2, GD1aGalNac, GA2, lyso-GM2
G_{M2}-gangliosidosis (M. Sandhoff)	β-Hexosaminidase A and B	GM2, GD1aGalNac, globoside, oligosaccharides, lyso-GM2
Lipidoses		
M. Gaucher I (chronic), II (neuropathic), III (subacute)	β-Glucosidase	GM1, GM2, GM3, GD3, glucosylceramide, glucosylsphingosine
Globoid cell leukodystrophy (M. Krabbe)	Galactocerebroside β-galactosidase	Galactosylceramide, psychosine lactosylceramide, globotriaosylceramide, globotetraosylceramide, fucosylneolactotetraosylceramide
M. Niemann-Pick I and II	Sphingomyelinase	Sphingomyelin, cholesterol, bismonoacylglycerophosphate, GM2, GM3, glucosylceramide, lactosylceramide, globotriaosylceramide, globotetraosylceramide
M. Fabry	α-Galactosidase A	Globotriaosylceramide, galabiosylceramide, globotriaosylsphingosine, blood-group-B glycolipids
Metachromatic leukodystrophy	Arylsulfatase A	Sulfatide, 3-O-sulfolactosylceramide, lysosulfatide, seminolipid, gangliotetraosylceramide-bis-sulfate, GM2

Table 1.4.1 Examples of lysosomal storage disorders. DS = dermatan sulfate; HS = heparan sulfate; GM1, GA1, GA2, GM2, GM3, GD2, GD3, GD1a, lyso-GM1, lyso-GM2, GD1aGalNac = subtypes of gangliosides; SCMAS = subunit c of mitochondrial ATP synthase. The table was adapted from [Ballabio and Gieselmann, 2009].

1.4.1 Morquio B disease

Patients with Mucopolysaccharidosis type IV B or Morquio B disease (MBD; OMIM #253010) suffer from an attenuated variant of Morquio disease [Arbisser *et al*., 1977; Matalon *et al*., 1974] with generalized skeletal dysplasia and corneal clouding, but without affecting the central nervous system (CNS) hence the intelligence is normal. Generally, individuals suffering from MBD are short in stature, and afflicted with platyspondylia, pectus carinatum, odontoid hypoplasia, kyphoscoliosis, and genu valgum [Suzuki *et al*., 2001]. Biochemically the disorder is characterized by accumulation of keratan sulfate and other galactose-containing oligosaccharides in various tissues, but most notably in cartilage and cornea [Arbisser *et al*., 1977; Callahan and Wolfe, 1970; Suzuki *et al*., 1969]. Furthermore, patients show excessive excretion of keratan sulfate in the urine [Giugliani *et al*., 1987, O'Brien *et al*., 1976]. The incidence of MBD is approximately 1:200,000 [Aldenhoven *et al*., 2009] and the patient's anticipated average life span is predicted as >30 years [Suzuki *et al*., 2001].

In MBD fibroblasts, residual β-galactosidase activity against synthetic substrates is below 10% of healthy controls. A specific missense mutation in the *GLB1* gene, corresponding to the mutation p.W273L on the protein level (Trp at position 273 is substituted with Leu), has been shown to be clearly phenotype-specific for MBD [Callahan, 1999; Oshima *et al*., 1991; Paschke *et al*., 2001]. This mutation affects the catalytic domain of β-Gal (cf. Figures 1.2.1 and 1.2.1.1) and has never been detected in GM1 patients. The p.W273L enzyme was suggested to be a "kinetic variant", due to its ability to degrade G_{M1}-gangliosides, but not keratan sulfate [Groebe *et al*., 1980; Okumiya *et al*., 2003; Paschke and Kresse, 1982]. Furthermore, transport to the lysosomes and subsequent processing of the precursor is normal in p.W273L cells [Callahan, 1999]. The tryptophane at position 273 of the polypeptide chain was postulated as substrate binding site by promoting "base stacking" and stabilization of the enzyme-substrate complex [Callahan, 1999; McCarter *et al*., 1997; Vyas, 1991], which may explain the kinetic alterations observed in p.W273L mutants. Other mutations attributed to the MBD phenotype include p.T500A [Hinek *et al*., 2000] and p.S149F [Hofer *et al*., 2009].

1.4.2 G_{M1}-gangliosidosis

In contrast to the systemic bone disease Morquio B, G_{M1}-gangliosidosis (GM1) is a neurosomatic disorder with mild or severe derogation of cognitive functions and delayed psychomotoric development due to atrophy of the brain. Further characteristics of the disorder are hepatosplenomegalia, osteodysplasia and general, mild dysmorphisms [Okada and O'Brien, 1968; Suzuki *et al.*, 2001]. Unlike MBD, the primary storage materials in GM1 cells are G_{M1}-gangliosides. Only minor amounts of stored oligosaccharides or keratan sulfate have been described [Jatzkewitz and Sandhoff, 1963; Suzuki *et al.*, 2001]. G_{M1}-ganglioside accumulation in neurons is the most striking histochemical feature of the disease (3- to 5-fold of normal values), but visceral organs also show abnormal increases of these specific gangliosides, although extraneural levels of G_{M1}-gangliosides are generally very low [Suzuki, 1969; Suzuki *et al.*, 2001]. Depending on the age of onset [O'Brien, 1989], GM1 can be classified in three subtypes:

> ➢ infantile GM1 or type 1 (OMIM #230500),

> ➢ late infantile/juvenile GM1 or type 2 (OMIM #230600), and

> ➢ adult/chronic GM1 or type 3 (OMIM #230650).

The most severe form of G_{M1}-gangliosidosis is type 1 or infantile GM1. Early symptoms can be observed within the first couple of months after birth, followed by rapid neurologic and psychointellectual deterioration [Suzuki *et al.*, 2001]. Furthermore, characteristic macular cherry-red spots can be found in all infantile patients [Hubain *et al.*, 1969], and hepatosplenomegalia plus skeletal dysplasias are also typical symptoms [O'Brien, 1969; O'Brien, 1989]. Consistent with phenotypic observations, storage of G_{M1}-gangliosides and galactose-containing oligoaccharides is at its highest level in infantile GM1 cells. Due to the severity of phenotypic manifestations, the life-span of GM1 type 1 patients is extremely short (<2 years) [Suzuki *et al.*, 2001].

Juvenile and adult GM1 patients, in contrast, display less severe dysmorphic changes, but their neurologic symptoms are severe and progressive. The onset age for type 2 (juvenile) is usually

between 7 month and 3 years, while phenotypical symptoms in the adult form (type 3) typically appear between 3 and 30 years of age. Despite less pronounced disease characteristics (cf. type 1 features) the anticipated average life of the least affected patients is below 30 years [Suzuki *et al.*, 2001]. The incidence for GM1 in general is approximately 1:100,000-200,000 [Sinigerska *et al.*, 2006].

A short summary of MBD and GM1 features is shown in Figure 1.4.2.1. It is important to note that an exact classification of GM1 or MBD patients is not always possible. Phenotypes of both defects can be very heterogenous and might overlap in individual patients, which is a common problem for lysosomal storage diseases in general.

Clinical type	G_{M1} Gangliosidosis			Morquio B disease
	Infantile (Type 1)	Late infantile/ juvenile (Type 2)	Chronic/adult (Type 3)	
Major phenotypic expression	Generalized neurosomatic	Generalized neurovertebral	Localized neurovertebral	Generalized skeletal
Onset	0–6 mo	7 m–3 yr	3–30 yr	5–10 yr
Course	<2 y	1–5 y	10–30 y	>30 y
Central nervous system	Generalized	Generalized	Localized	–
Mental	+++	++	+ or –	–
Major motor	Pyramidal	Pyramidal	Extrapyramidal	–
Peripheral nervous system	–	–	–	–
Muscle	–	–	+ or –	–
Cherry-red spots	+	+ or –	–	–
Hepatosplenomegaly	+	+ or –	–	–
Dysmorphism	+ or –	+ or –	–	–
Skeletal system	Generalized	Localized	Localized	Generalized
Storage				
Ganglioside G_{M1}	+++	++	+	–
Oligosaccharides	+++	++	+	+
Keratan sulfate	+	+	ND	+++
β-Galactosidase	Deficient	Deficient	Deficient	Deficient
Common gene mutation	R482H (Italian) R208C (American)	R201C (Japanese)	I51T (Japanese)	W273L (Caucasian)

ND = not described.

Figure 1.4.2.1 Major clinical types of hereditary β-galactosidase deficiencies. The illustration was adapted from [Suzuki *et al.*, 2001].

In contrast to the findings for the MBD enzyme, β-Gal from GM1 cells is incapable of degrading gangliosides, keratan sulfate, or any other of its substrates [Okumiya et al., 2003; Paschke and Kresse, 1982]. Some GM1-specific mutations result in unstable or misfolded precursor proteins, which are presumably degraded in the cytoplasm by the endoplasmic reticulum-associated protein degradation machinery (ERAD) [reviewed in Fan, 2008]. Other mutations may impair the formation of the multienzyme complex, preventing proper trafficking to the lysosomes. The alleles p.I51T, p.T82M, p.R201H, and p.R201C, described in several juvenile and adult GM1 patients, were shown to express enzyme precursors with impaired stability, diminished aggregation within the multienzyme complex, and rapid subsequent degradation [Chakraborty et al., 1994; Kaye et al., 1997; Oshima et al., 1994; Yoshida et al., 1991]. Residual β-Gal activities of juvenile and adult GM1 fibroblasts often range between 2-8% of healthy controls, while activities in infantile cells are usually below 1%. Surprisingly, a β-galactosidase activity of approximately 10% of the healthy control's activity was proposed as critical level for normal substrate turnover, based on experimental findings for two other lysosomal enzymes, β-N-acetylhexosaminidase (EC 3.2.1.52) and arylsulfatase A (EC 3.1.6.8) [Leinekugel et al., 1992]. A deficiency of these enzymes results in G_{M2}-gangliosidosis or metachromatic leukodystrophy, respectively (cf. Table 1.4.1). Although no experimental data has been presented for β-Gal, this hypothesis may have a significant impact on the development of therapeutic strategies for treatment of lysosomal storage disorders.

1.5 Therapy of lysosomal storage diseases

Treatment of lysosomal storage diseases is sometimes hindered by heterogenous phenotypes even amongst the same group or subtypes and by highly diverse storage characteristics on the molecular level. G_{M1}-gangliosidosis, for example, can be considered as a multisystem disorder (cf. Figure 1.4.2.1), affecting various organs (eg. liver and spleen) and even the CNS, while Morquio B is less affected in terms of organic involvement, but skeletal dysplasia is more pronounced than in GM1 (accumulation of keratan sulfate in cartilage and cornea) [Suzuki et al., 2001]. Due to different primary storage material, MBD and GM1 are not classified in the same group, although both disorders originate from defects in the same gene, *GLB1*, affecting one and the same enzyme, human lysosomal acid β-galactosidase [Yamamoto et al., 1990]. It is

hardly surprising that therapeutic options for MBD might differ from approaches for treating GM1.

Additionally, secondary consequences of storage have to be considered. Quite often inflammation processes are observed in animal models for lysosomal storage disorders [Jeyakumar *et al.*, 2005]. Recently, G_{M1}-ganglioside accumulation was suggested to act as effector of both ER-stress induced and mitochondria-mediated apoptosis of neuronal cells [Sano *et al.*, 2009]. Various other secondary effects have been described in the literature for all kinds of LSDs [reviewed in Platt and Lachmann, 2008], therefore, metabolic cross-reactions have to be evaluated carefully prior considering therapeutic options.

Therapeutic strategies for treating LSDs comprise:

- hematopoietic stem cell therapy (HSCT) or bone marrow transplantation (BMT),

- neural stem cell therapy,

- gene therapy,

- enzyme replacement therapy (ERT),

- substrate reduction therapy (SRT),

- enzyme enhancement therapy (EET) or

- combinations of therapies mentioned above.

A short overwiev of advantages and limitations of each strategy is given in Table 1.5.1.

Therapy /mode of action	Advantages	Limitations
HSCT Transplantation of bone marrow-derived blood stem cells	• Sustained correction after one single procedure • Cross-correction of host's cells by secreted enzymes	• Procedure-related risks and mortality • Not effective in some disaeses • Time required to identify compatible donors • Poor engraftment in tissues like bone, cartilage, and heart
ERT Intravenous infusion of a recombinant enzyme to replace the patient's deficient enzyme	• Long-term experience and documented efficacy in thousands of patients treated (e.g. Gaucher disease) • Registries available to document natural history of disease and efficacy	• Poor distribution of recombinant enzymes in specific tissues • Inability of recombinant enzyme to cross the BBB • Frequent infusions required, with high impact on quality of life • High costs
SRT Oral administration of substances to inhibit the synthesis of sphingolipids and to reduce storage of undegraded material	• Oral administration • Little impact on quality of life	• Limited clinical experience (with the exception of Gaucher disease) • Long-term adverse effects unknown
EET Oral administration of substances to enhance the patient's residual enzyme activity	• Better biodistribution of therapeutic agents • Possibility to target neurodegenerative in LSDs • Oral administration • Little impact on quality of life	• Limited clinical experience • Long-term adverse effects unknown • Only patients with specific responsive mutations amenable to treatment
Gene therapy Vector-mediated insertion of genetic material into an individual's cell and target tissues	• Sustained correction after a single procedure • Cross-correction by enzymes secreted by "factory" organs	• Very limited clinical experience, still under development

Table 1.5.1 Advantages and limitations of therapeutic options for lysosomal storage diseases. The table was adapted from [Parenti, 2009] in a slightly modified form.

Considering the abundance of clinical data, disorders, and applied methods, the author refers to the reviews of [Beck, 2007], [Parenti, 2009], and [Platt and Lachmann, 2008] for a comprehensive experimental description. Enzyme replacement therapy is currently only available for M. Gaucher, M. Fabry, M. Pompe, and mucopolysaccharidosis type I, II, and VI [reviewed in Beck, 2010 and in Wraith, 2009]. Promising therapeutic options for GM1 are described in the following sections.

1.5.1 *Therapy of MBD and GM1*

Currently, there is no treatment available for G_{M1}-gangliosidosis or Morquio B disease. Only symptomatic and supportive therapy can be applied to patients suffering from these disorders. Enzyme replacement therapy (ERT), for example, is not a promising strategy for treatment of MBD patients. Uptake of recombinant enzymes requires interaction with mannose-6-phosphate receptors, which are unavailable in osseous material [reviewed in Wraith, 2009]. Interestingly, an ongoing clinical trial with recombinant N-acetylgalactosamine-6-sulfatase (GALNS; drug name: BMN 110) for ERT of Mucopolysaccharidosis type IVA (MPS IVA, M. Morquio A) showed promising preliminary results in terms of degradation of keratan sulfate and physical fitness [Clinical trial #NCT00884949; drug sponsor: BioMarin Pharmaceutical]. Successful completion of this study may have an impact on further clinical trials with MBD patients. ERT may also be unfeasible in patients suffering from GM1, because the recombinant enzyme is usually retained outside of the brain by the blood-brain barrier [reviewed in Begley *et al*., 2008].

Therapeutic options previously considered for treatment of GM1 include gene therapy, bone marrow transplantation (BMT), substrate reduction therapy (SRT), and enzyme enhancement therapy (EET) [Brunetti-Pierri and Scaglia, 2008; Suzuki *et al.*, 2001]. BMT, for example, was conducted in an infantile GM1 patient, but β-galactosidase activity could not be enhanced and phenotypic characteristics remained unchanged, despite the normalization of white blood cells after receiving an allogenic transplant [Shield *et al.*, 2005]. Amniotic tissue transplantation has been attempted in a patient with MBD [Tylki-Szymańska *et al.*, 1985], but was considered unsuccessful.

Most of these strategies never got off the ground on a large scale in patients. Some applications are still experimental for GM1 and MBD, hence they depend on animal models or cell culture experiments to investigate the potential impact of therapy at the molecular level. Fortunately, animal models are available for G_{M1}-gangliosidosis. On the one hand, GM1 is a naturally occuring disorder among cats, dogs, sheep, and cattle [Suzuki *et al.*, 2001], and on the other hand transgenic mice lacking the β-Gal gene [Hahn *et al.*, 1997; Matsuda *et al*., 1997] or expressing a GM1-specific mutation (p.R201C) [Matsuda *et al*., 2003] have been generated. Adenovirus-mediated gene transfer, for example, was tested in such knock-out mice resulting in elevated levels of β-Gal activity in liver, spleen, and brain, but the effect was temporary

[Suzuki *et al*., 2001]. Furthermore, Suzuki *et al*. demonstrated that early treatment might be critical for successful elimination of clinical or biochemical features of the disease. However, most approaches are still far from reaching clinical application. Furthermore, some strategies are inapplicable for diseases with central nervous system involvement (e.g. G_{M1}-gangliosidosis), as the blood-brain barrier prevents or limits uptake of therapeutic agents like recombinant enzymes in ERT [Begley *et al*., 2008] and therefore, neuronal storage of gangliosides cannot be abolished. Two promising approaches, with the potential to reverse the storage of glycosphingolipids (eg. G_{M1}- or G_{A1}-gangliosides) in G_{M1}-gangliosidosis, are substrate reduction therapy (SRT) [Kasperzyk *et al*., 2005; Radin *et al*., 1982] and enzyme enhancement therapy (EET) [Parenti, 2009]. While SRT aims at blocking the synthesis of the storage product, hence reducing total amounts of stored material within the cells, the EET approach attempts to enhance the defective enzyme's residual activity to levels sufficient for normal substrate degradation. As mentioned before, a critical level of 10% of the healthy control activity has been proposed for normal substrate turnover [Leinekugel *et al*., 1992]. Both SRT and EET utilize iminosugars, usually substrate analogs, which are able to cross the blood-brain barrier due to their small size [Begley *et al*., 2008]. The inhibitory effect of the iminosugars N-butyldeoxygalactonojirimycin (*N*B-DGJ) and N-butyldeoxynojirimycin (*N*B-DNJ) on the ceramide-specific glucosyltransferase that catalyzes the first step in the biosynthesis of all glycosphingolipids was demonstrated by several groups [reviewed in Butters *et al*., 2003b and Beck, 2007]. Furthermore, the brain ganglioside content was markedly reduced after SRT in mouse models for G_{M2}-gangliosidoses [Andersson *et al*., 2004; Platt *et al*., 1997; Platt and Butters, 2004]. *N*B-DNJ is currently approved for SRT of Gaucher disease type 1 patients, and is in clinical trials as therapeutic agent for late-onset Tay-Sachs disease [Butters *et al*., 2005].

1.6 Enzyme enhancement therapy for GM1

Enzyme enhancement therapy (EET) or pharmacological chaperone therapy (PCT) has been proposed as therapeutic agent for GM1 [Beck, 2007; Butters *et al*., 2005; Parenti, 2009]. As described earlier, pharmacological chaperones (PCs) are small iminosugars, representing substate analogs for the respective enzyme, which bind to the enzyme's active site and assist in stabilization or folding of misfolded enzymes in the ER [Fan, 2008]. Thus they prevent premature degradation of lysosomal enzymes by the endoplasmic reticulum-associated protein

degradation (ERAD) in the cytoplasm, and enable proper enzyme transport to the lysosomes via the mannose-6-phosphate pathway (see Figure 1.6.1). Therefore, residual activities of lysosomal enzymes can be increased upon chaperone treatment. However, this chaperone activity could only be demonstrated for certain mutations, producing unstable or misfolded proteins [Iwasaki *et al.*, 2006; Matsuda *et al.*, 2003; Tominaga *et al.*, 2001]. A positive impact of PCs on the "catalytic β-Gal variant", resulting from the Morquio B mutation p.W273L, is therefore unlikely.
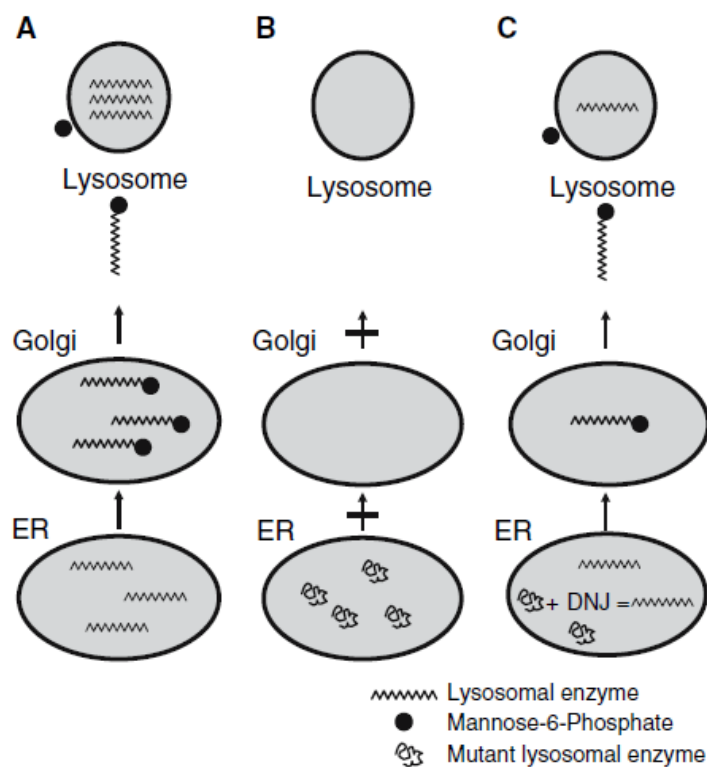
Figure. 1.6.1 Pharmacological chaperones stabilize misfolded proteins in the ER. (A) Lysosomal enzymes are synthesized in the ER, N-glycosylated, and transported to the Golgi apparatus. N-Acetylglucosamine-1-phosphotransferase phosphorylates mannose residues to mannose-6-phosphate, which labels the enzymes for transport to the lysosomal compartment via the mannose-6-phosphate pathway. **(B)** Misfolded enzymes are marked for degradation in the ER, and transported to the cytoplasm for degradation by ERAD (see text). **(C)** Pharmacological chaperones (in this case *N*B-DNJ) assist in stabilization and folding processes of misfolded proteins by binding to the enzyme's active site. The stabilized or correctly folded enzyme is further transported to the Golgi apparatus and labeled with mannose-6-phosphate as described for (A). The figure was adapted from [Beck, 2007].

In contrast to recombinant lysosomal enzymes, pharmacological chaperones have the potential to easily cross the blood–brain barrier and thus they may become beneficial for the treatment of neurodegenerative lysosomal storage diseases like GM1 [Begley *et al.*, 2008; Platt and Lachmann, 2009]. Low costs and the possibility of oral administration are further aspects in favor of EET.

Pharmacological chaperones are usually competitive enzyme inhibitors that display their inhibitory action at high doses *in vitro*, but have been found to enhance the enzyme's activity

when added to the cell culture medium in sub-inhibitory doses [reviewed in Fan, 2008]. However, this effect seems to be mutation-specific [Iwasaki *et al*., 2006; Matsuda *et al*., 2003; Tominaga *et al*., 2001], which might limit its future therapeutic use. Table 1.6.2 gives a short summary of pharmacological chaperones which bind to the active-site of enzymes and have demonstrated chaperone activity in cell culture experiments or clinical trials. The promising pharmacological chaperone *N*-Octyl-4-epi-*β*-valienamine (NOEV) has been in preclinical trials since its presentation by Matsuda *et al*.

Disorder	Active-site-specific chaperones	References
Fabry disease	1-Deoxygalactonojirimycin (DGJ) α-*Galacto*-homonojirimycin α-*Allo*-homonojirimycin β-1-C-Butyl-deoxygalactonojirimycin	Asano *et al*., 2000; Fan *et al*., 1999
Gaucher disease	*N*-Nonyl-deoxynojirimycin (NN-DNJ) *N*-Octyl-2,5-anhydro-2,5-imino-D-glucitol *N*-Octyl-isofagomine *N*-Octyl-*β*-valienamine (NOV) Isofagomine (IFG) Calystegines A_3, B_1, B_2, C_1 1,5-Dideoxy-1,5-iminoxylitol (DIX) α-1-C-Nonyl-DIX α-1-C-Octyl-1-DNJ	Chang *et al*., 2006; Compain *et al*., 2006; Lin *et al*., 2004; Sawkar *et al*., 2002; Sawkar *et al*., 2005; Yu *et al*., 2006
Tay-Sachs and Sandhoff diseases	*N*-Acetyl-glucosamine-thiazoline (NGT) 6-Acetamido-6-deoxycastanospermine (ACAS) Bisnaphthalimide nitro-indan-1-one Pyrrolo[3,4-d]pyridazin-1-one Pyrimethamine (PYR)	Maegawa *et al*., 2007; Tropak *et al*., 2004; Tropak *et al*., 2007
G_{M1}-gangliosidosis	*N*-Octyl-4-epi-*β*-valienamine (NOEV)	Matsuda *et al*., 2003
Pompe disease	*N*-Butyl DNJ DNJ	Okumiya *et al*., 2007; Parenti *et al*., 2007

Table 1.6.2 Identified active-site-specific chaperones for lysosomal storage disorders. The table was adapted from [Fan, 2008].

Several derivatives of 1-deoxynojirimycin (DNJ) or 1-deoxygalactonojirimycin (DGJ; Amigal™) have recently been proposed for EET [Fan, 2008] and tested in clinical trials for treatment of Fabry disease [Benjamin *et al*., 2009; Khanna *et al*., 2010]. The chemical structure of these compounds is shown in Figure 1.6.3. Our collaborators from the Glycogroup,

Department of Organic Chemistry, Graz University of Technology, recently synthesized a series of novel lipophilic and/or ionisable N-modified derivatives of 1-deoxygalactonojirimycin (DGJ). Some of these compounds proved to be competitive inhibitors of lysosomal β-galactosidase [Steiner *et al*., 2008; Schitter *et al*., 2010a; Schitter *et al*., 2010b], and promising results were obtained in preliminary chaperone screenings in G_{M1}-gangliosidosis fibroblasts described in this work.
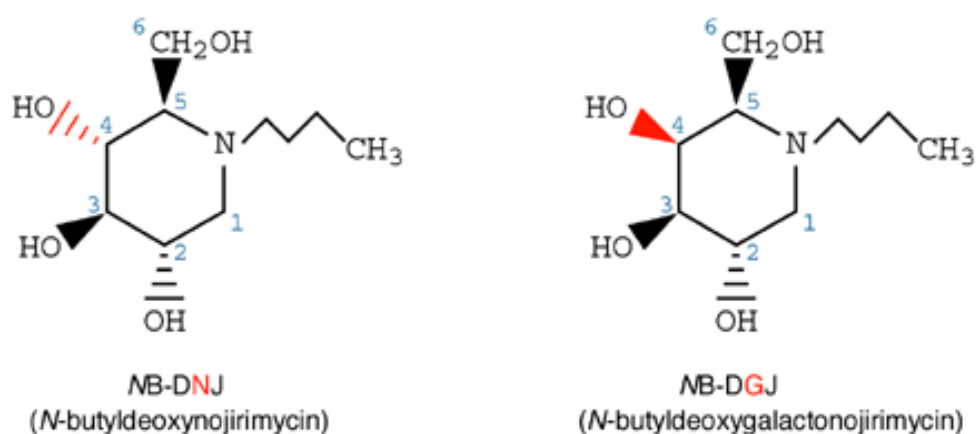
Figure 1.6.3 Molecular structures of the inhibitors *N*B-DNJ and *N*B-DGJ. The graphic was adapted from [Platt and Butters, 2000].

2 AIM

Although the human lysosomal acid β-galactosidase (β-Gal, EC 3.2.1.23) and the consequences of its defects in the human body were first described by Okada and O'Brien in 1968, there are still open questions regarding the enzyme's three-dimensional structure, the catalytic domain and its active-site specific amino acid residues, and how mutations in the β-Gal encoding gene (*GLB1*) can result in two different lysosomal storage disorders (LSDs), Morquio B disease (MBD) and G_{M1}-gangliosidosis (GM1) [Groebe *et al.*, 1980; O'Brien, 1989; O'Brien *et al.*, 1976; Okada and O'Brien, 1968]. A computational homology model on the basis of the crystallographic structure of β-galactosidase from *Bacteroides thetaiotaomicron* was proposed for the human enzyme, and recently used for prediction of structural changes in defective enzymes resulting from MBD- or GM1-specific mutations in the *GLB1* gene (Morita *et al.*, 2009). The proposed catalytic reaction of β-Gal is based on a Koshland double-displacement mechanism, and some amino acid residues participating in the catalytic reaction could be identified [Callahan, 1999]. So far, 140 different *GLB1* mutations have been described [Brunetti-Pierri and Scaglia, 2008; Hofer *et al.*, 2009; Hofer *et al.* 2010], and several mutant alleles could be attributed to a certain phenotype. Some of these mutations were found to alter the kinetic behaviour of the resulting enzyme, while others result in misfolded or unstable proteins which are marked for degradation in the ER and subsequently degraded in the cytoplasm [reviewed in Fan, 2008]. The prognosis of phenotype-genotype relations is an ongoing challenge for several LSDs and also for MBD and GM1. A detailed understanding of phenotypic effects, caused by a certain mutation, would not only improve our knowledge of metabolic interactions, but also be helpful in the development of therapies for treatment of LSDs.

The aim of the present work was the characterization of novel lipophilic and/or ionisable N-modified derivatives of 1-deoxygalactonojirimycin (DGJ), a competitive glycosidase inhibitor with proven pharmacological chaperone activity in Fabry cells [Fan *et al.*, 1999; Ishii *et al.*, 2009; Khanna *et al.*, 2009] and in mouse fibroblasts expressing mutant human β-Gal [Matsuda *et al.*, 2003; Tominaga *et al.*, 2001]. DGJ is currently in phase II clinical trials for enzyme enhancement therapy (EET) of Fabry disease [Butters, 2007]. Several novel iminosugars were synthesized and provided by the Glycogroup, Department of Organic Chemistry, Graz

University of Technology, and subjected to pharmacological chaperone screenings in GM1 and MBD fibroblasts in this work. Furthermore, their inhibitory effect on human lysosomal acid β-Gal was characterized in inhibition assays. Western blotting was performed to assess changes in the expression and maturation of β-Gal in chaperone-treated cells, and immunofluorescence experiments indicated altered enzyme distribution after pharmacological chaperone treatment. To investigate possible chaperone-induced *in vivo* substrate degradation in GM1 and MBD cells, fibroblast cells were loaded with a natural substrate and results were compared to *in vitro* assays using a common synthetic substrate.

Specific anti-β-Gal antibodies were essential for the investigations described in this work. Therefore, another goal of this work was the development of such antibodies. Three different strategies were pursued to obtain polyclonal antibodies or antisera directed against the human enzyme. The purification of overexpressed, secreted β-Gal precursors from the culture medium of CHO cells was previously described in the literature and established at the Department of Pediatrics during this work. Purified β-Gal was used as antigen for the immunization of rabbits. Moreover, antigenic β-Gal peptides were designed and used in immunizations. Finally, the heterologous expression of human β-Gal in *E. coli* cells to obtain large amounts of purified protein was investigated in this work.

3 METHODS AND MATERIALS

PART 1: EXPERIMENTAL PROCEDURES FOR BACTERIAL CELLS

3.1. Bacterial strains

The bacterial strains listed in Table 3.1.1 were used in this work.

E. coli strain	Genotype	Properties	Reference
BL21(DE3)	F⁻ *ompT hsdS*$_B$ (r$_B^-$m$_B^-$) *Gal dcm* (DE3)	widely used expression host strain, *lon* and *ompT* protease deficient, carrier of λDE3 lysogen	[Invitrogen™ 28-0182]
BL21	F⁻ *ompT hsdS*$_B$ (r$_B^-$m$_B^-$) *Gal dcm*	widely used expression host strain, *lon* and *ompT* protease deficient	[Novagen TB009]
BL21(DE3) + [pG-KJE8]	F⁻ *ompT hsdS*$_B$ (r$_B^-$m$_B^-$) *Gal dcm* (DE3) plus pG-KJE8 plasmid	expression host strain transformed with the chaperone plasmid pG-KJE8, *lon* and *ompT* protease deficient	provided by A. Binter, Department of Biochemistry, Graz University of Technology; plasmid was bought from Takara Bio Inc. [Takara A; Takara B]
NovaBlue	*end*A1 *hsd*R17 (rK12⁻ mK12⁺) *sup*E44 thi-1 *rec*A1 *gyr*A96 relA1 *lac* F′[proA⁺B⁺ *lac*IqZΔM15::*Tn*10] (*Tet*R)	general cloning host strain, high transformation efficiency	provided by A. Gruber, Department of Structural Biology, Karl-Franzens-University of Graz

Table 3.1.1 Bacterial strains used in this work.

3.2. Bacterial cell culture methods

3.2.1. *General cultivation methods for E. coli cells*

E. coli strains were maintained in Luria Broth (LB) Medium or on LB Agar Plates. After transformation of competent cells with plasmid DNA, it was necessary to switch to specific LB selection media containing the appropriate substitutes (e.g. antibiotics, induction reagents),

respectively. The optimal growth temperature is 37 °C, but for inducible expression of heterologous proteins it was sometimes necessary, to incubate *E. coli* strains at temperatures between 18 °C and 30 °C.

3.2.1.1. *Storage of E. coli cells*

For long-term storage of bacterial strains, glycerol stocks were prepared by mixing 200 µl bacterial overnight culture (ONC) with 800 µl sterile 80% (v/v) glycerol. Stocks were shock-frozen in liquid nitrogen and stored at -80 °C.

E. coli stocks (host strains, competent cells, and transformants) were always stored at -80 °C. For short-time use, *E. coli* strains were either cultured on selective medium agar plates or in liquid selection medium (e.g. as ONC), and stored at 4 °C.

3.2.2 *Small-scale expression protocol for IPTG-inducible proteins*

The protocol described below was partially adapted from handbooks supplied by the manufacturers of competent *E. coli* cells [Invitrogen™ 28-0182; Novagen TB009].

1. Prepare 5-10 ml ONC of the positive transformant in LB selection medium.

2. Inoculate 50 ml LB selection medium with ONC to an OD_{600} (optical density at 600 nm) of 0.05, and incubate at preassigned temperature until an OD_{600} of 0.4-0.6 has been reached.

3. Induce with isopropyl β-D-1-thiogalactopyranoside (IPTG) at a final concentration of 0.5-1 mM, collect 2 OD units of cell culture for SDS-PAGE (sodium dodecyl sulfate polyacrylamide gel electrophoresis) prior induction, centrifuge sample at 5,000 x g for 20 min or 10,000 x g for 5 min (4 °C), shock-freeze in liquid nitrogen, and store sample at -80 °C.

4. Keep main culture at preassigned temperature for several hours (determine optimal time in preliminary experiments).

5. Collect 2 OD units of cell culture for SDS-PAGE. Store samples at -80 °C until use. Prepare for SDS-PAGE as described in section 3.11.7.

3.2.3 Large-scale expression protocol for IPTG-inducible proteins

The protocol described below was partially adapted from handbooks supplied by the manufacturers of competent *E. coli* cells [Invitrogen™ 28-0182; Novagen TB009].

1. Prepare cultures of positive transformants as described in the small-scale IPTG-induction protocol (step 1 to 5). Use 250-500 ml LB selection medium as main culture. At crucial steps, always collect 2 OD units of the cell culture for SDS-PAGE.

2. After optimal induction time, centrifuge main culture at 3,000 x g for 10 min (4 °C).

3. Wash pellet in 0.9% NaCl.

4. Determine wet weight; for longer storage shock-freeze pellet in liquid nitrogen, and store at -80 °C.

3.3 Plasmids

The following plasmid vectors were used for cloning of the human *GLB1* cDNA:

- pET-21d(+) for C- and N-terminal polyhistidine-tagged fusion proteins

- pGEX-6P-2 for N-terminal GST-tagged full length fusion protein and a fusion peptide

Another plasmid, pG-KJE8, was used in expression studies to facilitate folding of heterologous fusion proteins. This plasmid encodes the bacterial chaperones DnaK, DnaJ, GrpE, GroES, and GroEL, which can be co-expressed with the protein of interest, encoded by a second plasmid.

It also carries the resistance gene for chloramphenicol (Cm^r), allowing co-selection with ampicillin resistant vectors. This plasmid was provided in chemically competent BL21(DE3) cells by A. Binter (Department of Biochemistry, Graz University of Technology). The pG-KJE8 vector was originally purchased from Takara Bio Inc.

The human *GLB1* cDNA was derived from the pcDX-x-*GLB1* vector, kindly provided by A. d'Azzo, St. Jude Children's Research Hospital, Memphis, USA.

Key features of all plasmids used in this work are illustrated in Table 3.3.1 and Figures 3.3.2-5.

Plasmid	Key features	Inducer	Resistant marker	Reference
pET-21d(+)	optional expression of C-terminal polyhistidine-tagged fusion proteins; *T7* promoter	isopropyl β-D-1-thiogalactopyranoside (IPTG)	ampicillin	[Novagen TB036]
pGEX-6P-2	optional expression of N-terminal GST-tagged fusion proteins; *tac* promoter	isopropyl β-D-1-thiogalactopyranoside (IPTG)	ampicillin	originally from GE Healthcare [GE Healthcare 28-9184-51AB]
pG-KJE8	dnaK-dnaJ-grpE groES-groEL chaperones; *araB* and *Pzt1* promoter	L-arabinose tetracycline	chloramphenicol	originally from Takara Bio Inc. [Takara A; Takara B]

Table 3.3.1 Key features of plasmids used in this work.

pET-21a(+) sequence landmarks

T7 promoter	311-327
T7 transcription start	310
T7·Tag coding sequence	207-239
Multiple cloning sites	
(*Bam*H I - *Xho* I)	158-203
His·Tag coding sequence	140-157
T7 terminator	26-72
lacI coding sequence	714-1793
pBR322 origin	3227
bla coding sequence	3988-4845
f1 origin	4977-5432
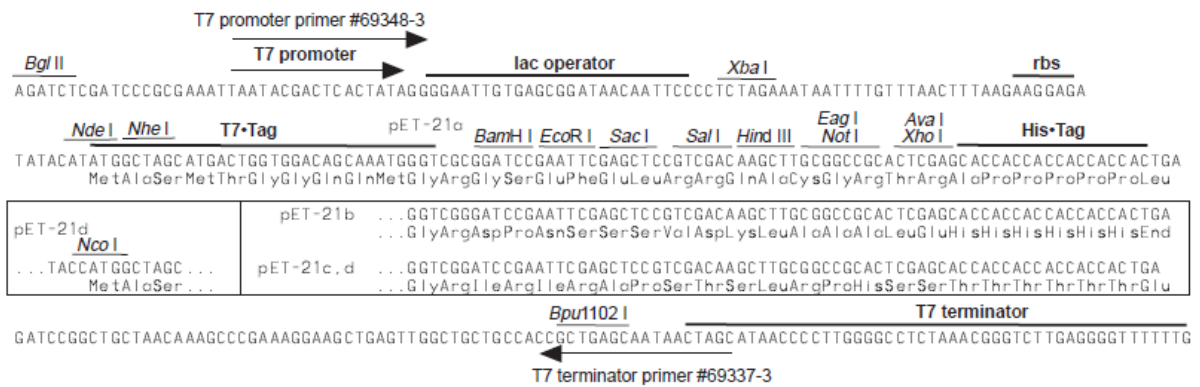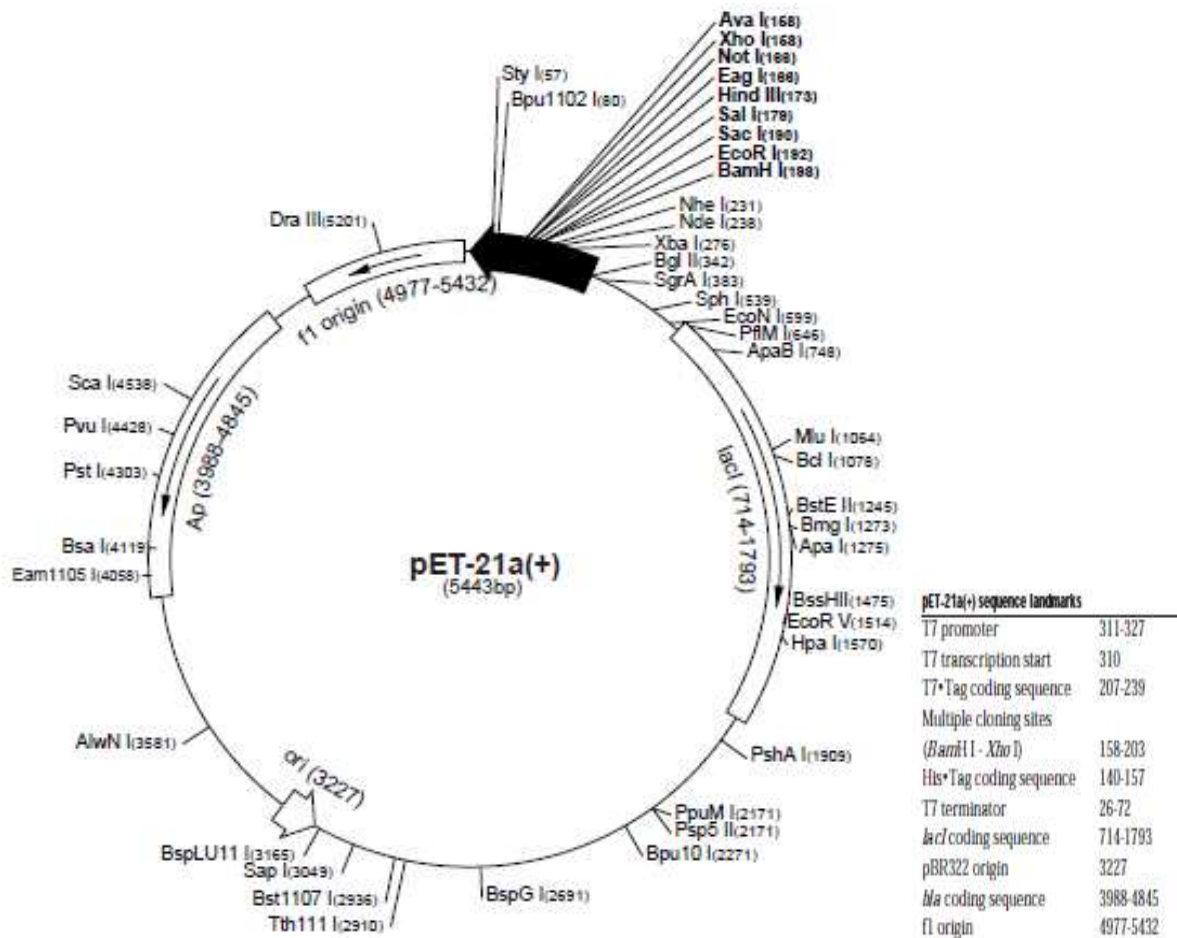
pET-21a-d(+) cloning/expression region

Figure 3.3.2 Vector map of pET-21d(+). The map for pET-21d(+) is the same as pET-21a(+) with the following exceptions: pET-21d(+) is a 5,440 bp plasmid; an *Nco*I site is substituted for the *Nde*I site; as a result, *Nco*I cuts pET-21d(+) at 234, and *Nhe*I cuts at 229. For the rest of the sites, subtract 3 bp from each site beyond position 239 in pET-21a(+). *Nde*I does not cut pET-21d(+).The vector maps of pET-21a(+) and pET-21d(+) were adapted from the Novagen Manual TB036.

Figure 3.3.3 Vector map of pGEX-6P-2. The vector map of pGEX-6P-2 was adapted from the Vector Database (www.lablife.org). The plasmid was originally purchased from GE Healthcare.
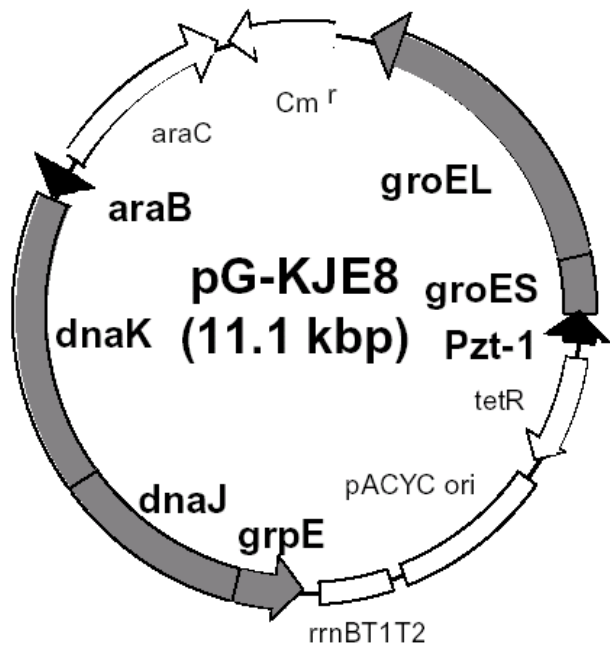
Figure 3.3.4 Vector map of pG-KJ48. The map was adapted from the Takara Bio inc. manual [Takara A].

araB: L-arabinose-inducible promoter
Pzt-1: tetracycline-inducible promoter
Cm^r: chloramphenicol resistance marker
groEL, groES, dnaK, dnaJ, and grpE: chaperone encoding genes.
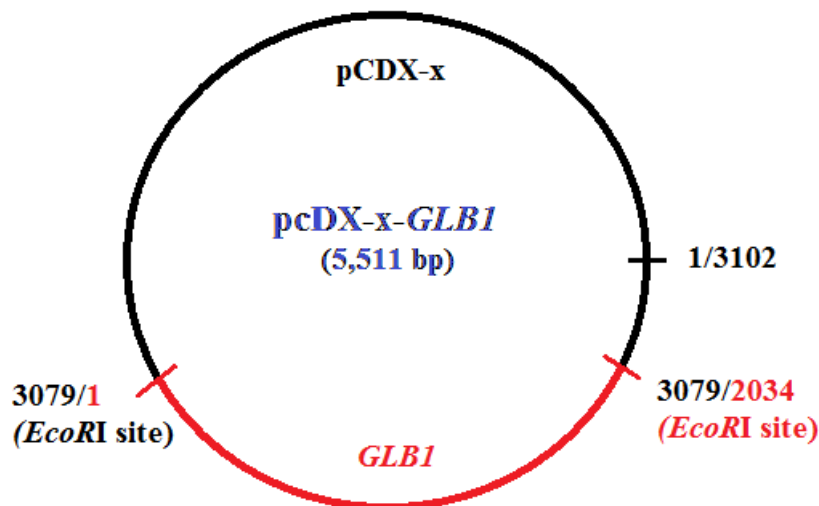
Figure 3.3.5 Vector map of pcDX-x-*GLB1*. The *GLB1* cDNA was cloned into the *EcoR*I restriction site of the pcDX-x vector. This vector was kindly provided by A. d'Azzo, St. Jude Children's Research Hospital, Memphis, USA.

3.3.1 Plasmid DNA purification

Depending on the subsequent application, plasmid DNA was either purified with the QIAprep$^®$ Spin Miniprep Kit ($\leq$ 20 µg DNA), or with the EndoFree$^®$ Plasmid Maxi Kit ($\leq$ 500 µg) according to the manufacturer's protocol [QIAGEN 1034639; QIAGEN 1043788]. In either case, cells from ONCs were harvested at 6,000 x g for 15 min at 4 °C. Miniprep DNA was eluted by addition of 50 µl 10 mM Tris-HCl Buffer (pH 8.0), and Maxiprep DNA was

redissolved in 60 µl of the same buffer. Aliquots were kept for DNA analysis on agarose gels and purified plasmid DNA was stored at -20 °C.

3.4 Cloning of the human *GLB1* cDNA in different bacterial expression vectors

The aim of the different cloning strategies was the establishment of heterologous expression systems for human lysosomal acid beta-galactosidase (β-Gal; EC 3.2.1.23). These expression systems could be extremely useful for production of large amounts of β-Gal fusion proteins, subsequently needed for antibody production against the human protein. Different protein tags would be helpful for the purification of the fusion proteins.

The protein coding sequence (CDS) of the *GLB1* cDNA (NCBI Reference Sequence: NM_000404.2, transcript variant 1) was amplified by polymerase chain reaction (PCR), digested with specific restriction enzymes to produce compatible ends for the ligation with plasmid DNA, and transformed with competent *E. coli* cells. Expression experiments with IPTG were performed to find positive clones with inducible β-Gal fusion protein, and optimized for production of large amounts of soluble β-galactosidase. Tagged fusion proteins were subjected to specific affinity chromatographic methods, to obtain purified, untagged human β-galactosidase protein for immunization of rabbits.

3.4.1 Amplification of the CDS from human GLB1 cDNA by PCR

The purpose of the PCR is the amplification of a specific DNA fragment. This can be achieved by designing both a forward and a reverse primer, complementary to the sequences flanking the desired gene/DNA sequence up- and downstream, respectively. These specific primers are added to the PCR reaction mix (see Table 3.4.1.1 and 3.4.1.2), enabling the DNA polymerase to extend their 3'-hydroxyl-ends in 5'- to 3'-direction with the deoxynucleoside triphosphates (dNTPs) also supplied in the solution.

AmpliTaq Gold® DNA Polymerase (Applied Biosystems™) was the DNA polymerase of choice in most experiments, despite the lack of 3'>5' exonuclease activity (proofreading). PCRs using

the *Pfu* DNA Polymerase (Promega) with proofreading activity were not always successful. Possible amplification mistakes were ruled out by sequence analysis of cloned DNA. Sequencing was performed by the company IBL (Vienna, Austria).

Component	Volume
10x PCR buffer (Applied Biosystems™)	5 µl
dNTP mix (20 mM each; Pharmacia)	0.5 µl
Forward primer (120 µM Stock)	1 µl
Reverse primer (120 µM Stock)	1 µl
DNA (<1 µg DNA/reaction)	1 µl
Aqua dest.	36.25 µl
MgCl$_2$ (25 mM; Applied Biosystems™)	3.5 µl
DMSO	1.5 µl
AmpliTaq Gold® DNA Polymerase (5 u/µl)	0.25 µl
Final volume:	50 µl

Table 3.4.1.1 Reaction mix for PCRs optimized for AmpliTaq Gold® DNA Polymerase (Applied Biosystems™).

Component	Volume
Pfu 10x buffer (+ 20mM MgSO$_4$; Promega)	5 µl
dNTP mix (20 mM each; Pharmacia)	0.5 µl
Forward primer (120 µM Stock)	1 µl
Reverse primer (120 µM Stock)	1 µl
DNA (<0,5 µg/50 µl)	1 µl
Aqua dest.	41 µl
Pfu DNA Polymerase (3 u/µl)	0.5 µl
Final volume:	50 µl

Table 3.4.1.2 Reaction mix for PCRs optimized for *Pfu* DNA Polymerase (Promega).

PCRs in this work were performed using the Eppendorf Mastercycler epgradient S. For successful PCR reactions, it is crucial to optimize not only the reaction mix, but also the times and temperatures for each step of the reaction (Table 3.4.1.3). The first step is the denaturation of the double-stranded DNA to allow for hybridization of single-stranded primers to their complementary DNA sites in the second step (annealing). The annealing temperature depends on the melting temperatures (T_m) of the forward and reverse primer, and should be 3-5 °C below the calculated T_m. Thus it is important to design primers with similar melting

temperatures. The T_m of each primer can be estimated by a simple calculation based on their nucleotide composition:

$$T_m = (4 \times [G + C]) + (2 \times [A + T])\ °C \qquad\qquad [x]\ \text{number of x nucleotides}$$

Annealing is followed by elongation of the primers in 5'>3' direction, producing complementary DNA strands to single-stranded templates. The reaction time depends on the size of the amplified DNA. As a general rule, DNA polymerase needs approximately one minute to amplify a fragment consisting of 1,000 nucleotides. These three steps, denaturation, annealing, and elongation are repeated 25-35 times, yielding billions of copies of the original template. PCR ends with a single elongation step to finish all reactions, and PCR products are kept on 4 °C until use.

Initial denaturation:	2 min [a] 5 min [b]	95 °C	1 cycle
Denaturation:	30 sec	95 °C	
Primer annealing:	30 sec	variable	25- 35 cycles
Elongation:	variable	72 °C	
Final elongation:	7 min	72 °C	1 cycle
Soak:	∞	4 °C	

Table 3.4.1.3 General PCR reaction scheme. [a] *Pfu* DNA Polymerase (Promega); **[b]** AmpliTaq Gold® DNA Polymerase (Applied Biosystems™).

3.4.1.1 Primers

To amplify the CDS encoding the human lysosomal acid β-galactosidase, a modified pcDX-x vector containing the *GLB1* cDNA was used as a template (see Figure 3.3.5). To facilitate purification of the expressed protein, certain protein tags should be attached to the β-Gal protein. This was achieved by cloning of the amplified human β-Gal CDS in specific bacterial vectors, encoding the desired protein tag. For that purpose, the primers for *GLB1* cDNA amplification were designed with short nucleotide stretches, recognized by specific restriction enzymes, and matching the desired restriction sites in the cloning vector, but also with

complementary sequences to the areas flanking the β-Gal CDS. For N-terminal polyhistidine (His®)-tagged β-galactosidase it was necessary to attach the His-Tag® sequence to the primers as well.

Four strategies were pursued to obtain N- or C-terminal tagged β-Gal fusion proteins expressed in *E. coli* cells:

1. C-terminal tagging with polyhistidine ("C-His®-Gal")

2. N-terminal tagging with polyhistidine ("N-His®-Gal")

3. N-terminal tagging with glutathione S-transferase ("N-GST-Gal")

4. N-terminal tagging of a short β-Gal peptide sequence with glutathione S-transferase ("N-GST-Gal-peptide").

The specific primer pairs for each strategy are listed in Table 3.4.1.1.1. Primers containing recognition sites for restriction enzymes were designed with short stabilization stretches as recommended by New England Biolabs® (www.neb.com; Technical Reference > Restriction Endonucleases > Cleavage Close to the End). All primers were produced by TIB® MOLBIOL (Berlin, Germany).

Primer	Sequence (5'>3')	Direction	T_m (°C)	Fragment length
Primer pair for cloning of the C-terminal tagged His®-Gal construct				
GLB1Sfw	CATGCCATGGATGCCGGGGGTTCCTGGTT T	sense	66	
GLB1Srev	CCGCTCGAGTACATGGTCCAGCCATGAATC	antisense	66	2,050 bp
Primer pair for cloning of the N-terminal tagged His®-Gal construct				
NHis2GLBfw	CATGCCATGGCTCACCACCACCACCACCACCCGGGGGTTCCTGGTTCGCAT	sense	78	
NHisGLBrev	CCGCTCGAGTCATACATGGTCCAGCCATGAATCTTTGTTTTTTTGCGGGGGT	antisense	72	2,070 bp
Primer pair for cloning of the N-terminal tagged GST-Gal construct				
GLB1Sal2fw	ACGCGTCGACGTCGGCCATAGCGGCCGCGCCGGGGGTTCCTGGTTCGCATCCT	sense	81	
GLB1Notrev	ATAGTTTAGCGGCCGCATTCTTATCATACATGGTCCAGCCATGAATCTTTG	antisense	69	2,083 bp
Primer pair for cloning of the N-terminal tagged GST-Gal-peptide construct				
GLB1Sal2fw	ACGCGTCGACGTCGGCCATAGCGGCCGCGCCGGGGGTTCCTGGTTCGCATCCT	sense	81	
PepNotrev	ATAGTTTAGCGGCCGCATTCTTATCAACATTTCAGGAATGTTTTATGTGCTCCATCAG	antisense	70	742 bp
Universal primer	**Sequence (5'>3')**	**Direction**	**T_m (°C)**	**Fragment length**
T7 universal primers				
T7Profw	TAATACGACTCACTATAGGG	sense	48	v
T7Terrev	GCTAGTTATTGCTCAGCGG	antisense	51	v
pGEX universal primers (GST)				
pGEX5	GGGCTGGCAAGCCACGTTTGGTG	sense	62	v
pGEX3	CCGGGAGCTGCATGTGTCAGAGG	antisense	62	v

Table 3.4.1.1.1 Primers used in this work. PART 1.

Sequencing primer	Sequence (5'>3')	Direction	T_m (°C)	Fragment length
Primer pairs for sequencing of the C- and N-terminal tagged His®-Gal constructs				
T7Profw	TAATACGACTCACTATAGGG	sense	48	~560 bp
p1rev	CAGGTAATCTGGGTCGGAGGAGCGGAG	antisense	66	
p2fw	CTGTGCAGAGTGGGAAATGGG	sense	56	488 bp
p2rev	CTGCTTCGGTCTTGATTGTGG	antisense	54	
p3fw	AGTGTGAGCCCAAAGGACCC	sense	56	549 bp
p3rev	GGACTCCATTGAGGGGTGAA	antisense	54	
p4fw	ACCGGACAACACTTCCTCAAGA	sense	55	524 bp
p4rev	CCAATAGCGGCCAAGGTTAA	antisense	52	
p5fw	CCCCAGGACACCTTTATCCAGTTTC	sense	59	~450 bp
T7Terrev	GCTAGTTATTGCTCAGCGG	antisense	51	
Primer pairs for sequencing of the N-terminal tagged GST-Gal construct				
pGEX5	GGGCTGGCAAGCCACGTTTGGTG	sense	62	583 bp
p1rev	CAGGTAATCTGGGTCGGAGGAGCGGAG	antisense	66	
p2fw	CTGTGCAGAGTGGGAAATGGG	sense	56	487 bp
p2rev	CTGCTTCGGTCTTGATTGTGG	antisense	54	
p3fw	AGTGTGAGCCCAAAGGACCC	sense	56	549 bp
p3rev	GGACTCCATTGAGGGGTGAA	antisense	54	
p4fw	ACCGGACAACACTTCCTCAAGA	sense	55	525 bp
p4rev	CCAATAGCGGCCAAGGTTAA	antisense	52	
p5fw	CCCCAGGACACCTTTATCCAGTTTC	sense	59	429 bp
pGEX3	CCGGGAGCTGCATGTGTCAGAGG	antisense	62	
Primer pairs for sequencing of the N-terminal tagged GST-Gal-peptide construct				
pGEX5	GGGCTGGCAAGCCACGTTTGGTG	sense	62	583 bp
p1rev	CAGGTAATCTGGGTCGGAGGAGCGGAG	antisense	66	
p2fw	CTGTGCAGAGTGGGAAATGGG	sense	56	403 bp
pGEX3	CCGGGAGCTGCATGTGTCAGAGG	antisense	62	

Table 3.4.1.1.1 Primers used in this work. PART 2. Melting temperatures (T_m) were calculated with the "Oligo Calculator" program (http://www.pitt.edu/~rsup/OligoCalc.html) from the University of Pittsburgh, PA, USA. v = variable.

3.4.2 *Restriction enzyme digestion of DNA*

For cloning of genes in expression vectors it is essential to digest the specific DNA fragment with restriction enzymes. These enzymes are endonucleases which recognize specific, often palindromic, single- or double-stranded DNA sequences, and cut the phosphodiester bonds of both DNA strands to produce free 5'-phosphate and 3'-hydroxyl ends. If the free ends have single-stranded overhangs, they are called cohesive ends, otherwise this procedure results in blunt ends. This allows position-specific cloning of genes into plasmid vectors, which are cut

52

with the same restriction endonuclease(s). As mentioned earlier, restriction sites (recognition sites for restriction enzymes) were integrated in primers for amplification of the β-Gal CDS, and subsequent cloning into vectors. Restriction enzymes were also used to verify positive clones. The general restriction scheme is listed in Table 3.4.2.1.

Component	Volume/Concentration
DNA	0.1-5 µg
10x Restriction Buffer	1x
100x Bovine serum albumin (BSA)	lx
Restriction enzyme 1 (+ Restriction enzyme 2)	10-20 units
Aqua dest. to a final volume of:	20 or 60 µl

Table 3.4.2.1 General DNA digestion scheme.

Details on specific digestion reactions and incubation times can be found on the manufacturer's homepage (New England Biolabs® or Roche). Regardless of other recommendations, BSA (New England Biolabs®) was used in all restriction assays, because higher yields of digested DNA were obtained. The restriction enzymes used for cloning of the β-Gal CDS in bacterial expression vectors are listed in Table 3.4.2.2.

Enzyme	Recognition site	Free ends
*Nco*I (10 U/µl, NEB or Roche)	5'…C$^{\vee}$CATGG…3' 3'…GGTAC$^{\wedge}$C…5'	cohesive
*Xho*I (20 U/µl, NEB)	5'…C$^{\vee}$TCGAG…3' 3'…GAGCT$^{\wedge}$C…5'	cohesive
*Sal*I (20 U/µl, NEB)	5'…G$^{\vee}$TCGAC…3' 3'…CAGCT$^{\wedge}$G…5'	cohesive
*Not*I (10 U/µl, NEB)	5'…GC$^{\vee}$GGCCGC…3' 3'…CGCCGG$^{\wedge}$CG…5'	cohesive
*Sma*I (20 U/µl, NEB)	5'…CCC$^{\vee}$GGG…3' 3'…GGG$^{\wedge}$CCC…5'	blunt
*Nde*I (20 U/µl, NEB)	5'…CA$^{\vee}$TATG…3' 3'…GTAT$^{\wedge}$AC…5'	cohesive
*Msc*I (5 U/µl, NEB)	5'…TGG$^{\vee}$CCA…3' 3'…ACC$^{\wedge}$GGT…5'	blunt
*Sca*I (10 U/µl, Roche)	5'…AGT$^{\vee}$ACT…3' 3'…TCA$^{\wedge}$TGA…5'	blunt

Table 3.4.2.2 Restriction Enzymes used in this work. NEB = New England Biolabs®.

If plasmid DNA was prepared for ligation reactions, the DNA was treated with 1 unit of calf intestinal alkaline phosphatase (CIAP; Invitrogen™) for 5-60 min at 37 °C. CIAP dephosphorylates free 5'-phosphate ends in linearized plasmid vectors, hence preventing re-ligation of free ends.

3.4.3 DNA Ligation

Ligation of amplified β-Gal CDS DNA and plasmid vectors was performed according to the manufacturer's protocol [Invitrogen™ 711-011109] using T4 DNA Ligase (Invitrogen™). Reactions were either performed for 16 hrs at 16 °C, or 3-5 hrs at room temperature (c.f. Table 3.4.3.1).

Reagent	Volume/Concentration
5x Ligase Reaction Buffer (Invitrogen™)	4 µl
Insert : vector molar ratio	3:1
Vector ends	3-30 fmol
Insert ends	9-90 fmol
Total DNA	0.01-0.1 µg (cohesive ends) 0.1-1.0 µg (blunt ends)
T4 DNA Ligase (Invitrogen™)	0.1 unit (cohesive ends) 1.0 unit (blunt ends)
Aqua dest.	fill up to a final volume of 20 µl

Table 3.4.3.1 General ligation conditions used in this work.

3.4.4 Transformation of competent E. coli cells

Transformation of competent *E. coli* cells with plasmid vectors was performed according to the protocol supplied by the particular manufacturer with minor modifications.

3.4.4.1   One Shot® BL21(DE3) cells

Transformation was performed according to the protocol for One Shot® BL21(DE3) chemically competent *E. coli* cells from Invitrogen™ [Invitrogen™ 28-0182]. The heat shock incubation was extended to 50 sec.

3.4.4.2   BL21 cells

Transformation was performed according to the protocol for BL21 competent *E. coli* cells from Novagen [Novagen TB009]. The heat shock incubation was extended to 50 sec.

3.4.4.3   NovaBlue cells

The transformation protocol for competent NovaBlue cells was provided by the Department of Structural Biology, Karl-Franzens-University of Graz.

1. Thaw 100 µl of competent NovaBlue cells on ice.

2. Add 7-8 µl of the ligation reaction to the cells, gently mix by tapping.

3. Incubate on ice for 30 min.

4. Heat 45 sec at 42 °C in a water bath.

5. Incubate on ice for 2 min.

6. Add 300 µl of LB medium to the cells, and incubate for 1 hr at 37 °C under shaking (225 rpm).

7. Briefly centrifuge the cells, and resuspend in 100-200 µl LB medium.

8. Plate 20-200 µl of the transformation reaction onto appropriate selection agar plates and incubate over night at 37 °C.

9. Pick single colonies of transformants, plate onto appropriate plates, or inoculate in LB medium containing the antibiotic(s) for selection.

10. Prepare glycerol stocks and store at -80 °C.

3.4.4.4   BL21(DE3) + [pG-KJE8] cells

The transformation protocol for competent BL21(DE3)+[pG-KJE8] cells was provided by the Department of Biochemistry, Graz University of Technology, and is based on instructions supplied by the manufacturer [Takara A; Takara B].

1. Thaw 100 µl of competent cells on ice, and incubate plasmid vector on ice for 5 min.

2. Add 5 to 10 ng of DNA in a volume of 1 to 5 µl, and gently mix by tapping.

3. Incubate 2 min at 42 °C in a thermoblock.

4. Add 900 µl of LB medium to the cells, and incubate for 30 min at 37 °C under shaking.

5. Plate 100 µl of the transformation reaction directly onto selection agar plates, and briefly centrifuge the residual reaction mix.

6. Resuspend cells in 100 µl LB medium and plate the total volume onto appropriate plates. Incubate over night at 37 °C. Note: The pG-KJE8 plasmid contains a chloramphenicol resistance gene (Cm^r), thus the BL21(DE3)+[pG-KJE8] strain requires a final concentration of 20 µg/ml chloramphenicol for selection.

7. Pick single colonies of transformants, plate onto appropriate plates, or inoculate in LB medium containing the antibiotic(s) for selection.

8. Prepare glycerol stocks and store at -80 °C.

3.4.5 Agarose gel electrophoresis

For separation of DNA fragments, purification of specific DNA bands, and determination of size and concentration, DNA samples were subjected to agarose gel electrophoresis. Samples were mixed with Loading Dye, and applied to agarose gels containing the DNA-intercalating agent ethidium bromide for subsequent UV light visualization. The method utilizes an electric field for separation of different-sized DNA fragments. Due to the phosphoric acid, DNA is negatively charged and moves through the gel pores towards the positively charged end of the

gel chamber. The concentration of agarose in the gel is also important, as high percentage gels have smaller pores, allowing smaller DNA fragments to move faster in the gel.

Agarose gel electrophoresis was performed with 1% agarose gels using the Pharmacia Biotech Electrophoresis System (Power Supply EPS 600). Electric field strength was 8 V/cm. As running buffer, 1x TBE Buffer was used, and DNA was mixed with Loading Dye at the ratio of 10:1. For estimation of DNA size and concentration, the DNA markers pictured in Figure 3.4.5.1 were used.
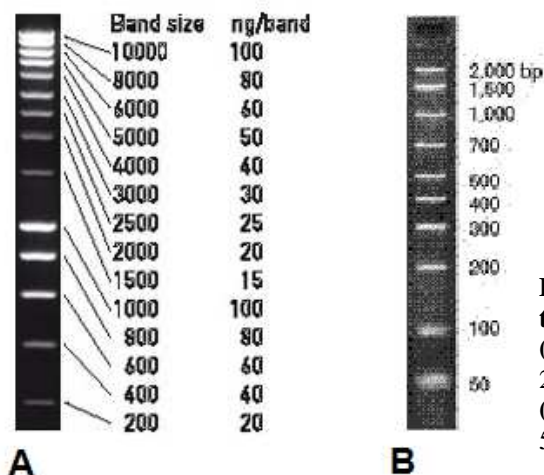
Figure 3.4.5.1 DNA weight markers used in this work.
(A) SmartLadder (Eurogentec, Seraing, Belgium), 200-10,000 bp.
(B) AmpliSize DNA Mol. Ruler (Bio-Rad), 50-2,000 bp.

3.4.5.1 Gel extraction

DNA was extracted from agarose gels with the QIAquick® Gel Extraction Kit according to the manufacturer's protocol [QIAGEN 1051746]. DNA was eluted by addition of 30-50 µl 10 mM Tris-HCl Buffer (pH 8.0). Purified DNA was stored at -20 °C.

3.5 Protein Purification

Heterologously expressed β-galactosidase was tagged with polyhistidine or GST to facilitate protein purification by affinity chromatography.

3.5.1 *Purification of polyhistidine-tagged fusion proteins*

His[®]-tagged proteins were purified by affinity chromatography as recommended by the manufacturer of the Profinity[™] IMAC Resin [Bio-Rad 10001677]. A brief summary is given below.

1. Proceed as described in step 1 to 4 for large-scale expression experiments (section 3.2.3). All subsequent steps are carried out on ice.

2. Resuspend bacterial pellet in 2 ml Lysis Buffer A (pH 8.0)/g wet weight.

3. Sonicate on ice for 5 x 1 min. Pause for 1 min after each run.

4. Centrifuge homogenate at 20,000 x g for 20 min (4 °C); collect samples of cell homogenate, pellet, and supernatant for SDS-PAGE.

5. Optional: Filter supernatant through filter paper to avoid cell debris on the column.

6. Calibrate histidine affinity column (Profinity[™] IMAC Resin; Bio-Rad) with 5-10 bed volumes of Lysis Buffer A (pH 8.0). For column packing and regeneration of the IMAC resin, see manufacturer's protocol [Bio-Rad 10001677]. Purification steps are carried out at 4 °C.

7. Apply the supernatant on nickel affinity column, and allow to flow by gravity.

8. Collect 0.5-2 ml fractions of the flow through.

9. Wash column with 5-10 bed volumes of Wash Buffer A (pH 8.0), and collect 0.5-2 ml fractions.

10. Elute bound proteins with 1-5 bed volumes of Elution Buffer A (pH 8.0), and collect 0.5-2ml fractions.

11. Observe elution procedure by absorbance measurements at 280 nm (A_{280}), and visually control elution efficiency with the Quick Start[™] Bradford Dye Reagent (1x; Bio-Rad) by mixing 10 µl of the sample with 500 µl of the dye. Color changes from red to blue indicate the presence of proteins in the sample [Bio-Rad 4110065].

12. Keep aliquots of each fraction for SDS-PAGE analysis.

13. Pool eluate fractions containing proteins, concentrate, and dialyze or rebuffer against PBS (pH ~7) or a buffer of choice.

3.5.2 *Purification of GST-tagged fusion proteins*

GST-tagged proteins were purified by affinity chromatography as recommended by the manufacturer of the High Affinity GST Resin [GenScript TM0185]. A brief summary is given below.

1. Proceed as described in step 1 to 4 for large-scale expression experiments (section 3.2.3). All subsequent steps are carried out on ice.

2. Resuspend bacterial pellet in ice-cold phosphate buffered saline (PBS, pH ~7), or Lysis Buffer B (pH 7.0). Use 3 ml buffer per 50 ml of culture medium. For 2 x 250 ml culture, resuspend each pellet in 15 ml buffer.

3. Sonicate on ice for 5 x 1 min. Pause for 1 min after each run.

4. Centrifuge homogenate at 20,000 x g for 20 min (4 °C); collect samples of cell homogenate, pellet, and supernatant for SDS-PAGE.

5. Optional: Filter supernatant through filter paper to avoid cell debris on the column.

6. Calibrate GST affinity column (High Affinity GST Resin; GenScript) with 5-10 bed volumes of PBS or Lysis Buffer B (pH 7.0). For column packing and regeneration of the GST affinity resin, see manufacturer's protocol [GenScript TM0185]. Purification steps are carried out at 4 °C.

7. Apply the supernatant on GST affinity column, and allow to flow by gravity.

8. Collect 0.5-2 ml fractions of the flow through.

9. Wash with 5-10 bed volumes of PBS (pH ~7) or Lysis Buffer B (pH 7.0), and collect 0.5-2 ml fractions. Addition of protease inhibitor is optional.

10. Elute bound proteins with 10-15 bed volumes of Elution Buffer B (pH 8.0), and collect 0.5-2 ml fractions.

11. Observe elution procedure by absorbance measurements at 280 nm (A_{280}), and visually control elution efficiency with the Quick Start[™] Bradford Dye Reagent (1x; Bio-Rad) as described earlier [section 3.5.1; Bio-Rad 4110065].

12. Keep aliquots of each fraction for SDS-PAGE analysis.

13. Pool eluate fractions containing proteins, concentrate, and dialyze or rebuffer against PBS (pH ~7) or a buffer of choice.

3.5.3   *Sample concentration and rebuffering*

For volumes up to 5 ml, the Vivaspin 4 columns (MWCO 5,000 or 10,000; Vivascience, Sartorius GmbH) were used to concentrate samples by centrifugation at 4,000 x g for 10 min at 4 °C. For rebuffering, the column was filled at least two times with the buffer of choice after each single concentration step. For details on handling and applicable rotors, see manufacturer's instructions [Sartorius SLU2004-e07 103].

Larger volumes (up to 15 ml) were concentrated in Amicon[®] Ultra-15 Centrifugal Filter Units (MWCO 10,000; Millipore). Centrifugation was performed according to the manufacturer's recommendations [Millipore PR02842] at 4,000 x g for 10 min (4 °C).

3.6   Solubilization of inclusion bodies

The procedures are based on online protocol guidelines from the "Protein Purification Facility" (http://wolfson.huji.ac.il/purification/Protocols/InclBodCont.html), Wolfson Centre for Applied Structural Biology, Hebrew University of Jerusalem, originally described by Middelberg [Middelberg, 2002], with minor modifications.

1. Prepare cell cultures of positive transformants as described for small-scale expression experiments (step 1 to 5; section 3.2.2).

2. Harvest residual main culture (~50 ml) by centrifugation at 3,000 x g for 10 min (4 °C).

3. Wash pellet in 0.9% NaCl.

4. Determine wet weight; for longer storage shock-freeze pellet in liquid nitrogen, and store at -80 °C.

5. Resuspend bacterial pellet in 5 ml PBS (pH 7.4) per 50 ml cell culture. The use of protease inhibitors, lysozyme, or DNase is optional. In this work, a small amount of DNase I (Sigma-Aldrich®) was added to the PBS solution. All subsequent steps are carried out on ice.

6. Sonicate on ice for 5 x 1 min. Pause for 1 min after each run.

7. Centrifuge homogenate at 20,000 x g for 20 min (4 °C); collect samples of cell homogenate, pellet, and supernatant for SDS-PAGE.

8. Completely resuspend pellet after sonication and centrifugation in 2.5 ml Lysis Buffer C (pH 7.6). Mix in a thermoblock or gently vortex for 5 min.

9. Centrifuge at 15,000 x g for 20 min (4 °C), and separate soluble (supernatant) from insoluble (pellet) fraction. Keep 20-40 µl aliquots for SDS-PAGE ("first wash"), and use the pellet for the next step.

10. Repeat step 8 and 9. Keep 20-40 µl aliquots for SDS-PAGE ("second wash"), and use the pellet for the next step.

11. Completely resuspend the pellet in 2.5 ml PBS (pH 7.4) by mixing in a thermoblock, or gently vortexing for 5 min.

12. Fractionate in 10 x 250 µl portions in 1.5 ml Eppendorf tubes, and centrifuge at 15,000 x g for 20 min (4 °C). Separate soluble and insoluble fraction. Keep 20-40 µl aliquots for SDS-PAGE ("third wash"), and use pellets for the next step.

13. Wash each fraction with a different Wash Buffer (see section 3.13, Wash Buffers 1 to 11). Resuspend pellet of each fraction in 250 µl of the respective Wash Buffer, mix in a

thermoblock, or gently vortex for 5 min. Separate soluble from insoluble fraction. Keep 20-40 µl aliquots for SDS-PAGE ("fourth wash"), and use pellets for the next step.

14. Repeat step 13. Keep 20-40 µl aliquots for SDS-PAGE ("fifth wash"), and use pellets for the next step.

15. Repeat step 13 but with PBS (pH 7.4) instead of Wash Buffers. Keep 20-40 µl aliquots for SDS-PAGE ("sixth wash"), and use pellets for the next step.

16. Completely resuspend each pellet with 250 µl Wash Buffer 10 (PBS + 8 M urea, pH 8.1), and mix gently for 60 min in a thermoblock at 4 °C. Centrifuge for 20 min at 15,000 x g (4 °C), and separate soluble from insoluble fraction. Keep 20-40 µl aliquots for SDS-PAGE. The soluble fraction is designated "8 M urea resuspended inclusion bodies", and the pellet consists of "8 M urea insoluble proteins". It might be necessary to add a small volume of Wash Buffer 10 (pH 8.1) to the pellet for SDS gel application.

PART 2: EXPERIMENTAL PROCEDURES FOR MAMMALIAN CELLS

3.7 Mammalian cells

3.7.1 Fibroblast cells

The homoallelic and heteroallelic cell lines listed in Table 3.7.1.1. were used for the experiments described in this work.

Genotype	Exon	Phenotype	Reference
p.I181K/p.I181K	5	infantile GM1	[Hofer *et al*., 2010]
p.R201C/p.R201C	6	juvenile GM1	[Iwasaki *et al*., 2006; Oshima *et al*., 1994; Tominaga *et al*., 2001; Yoshida *et al*., 1991]
p.R201H/p.R457X	6 (+14)	juvenile GM1	[Iwasaki *et al*., 2006; Kaye *et al*., 1997; Nishimoto *et al*., 1991; Tominaga *et al*., 2001]
p.R201H/p.S149F	6 (+4)	adult GM1/Morquio B	[Hofer *et al*., 2009; Iwasaki *et al*., 2006; Kaye *et al*., 1997; Tominaga *et al*., 2001]
p.R201H/p.H281Y	6 (+8)	juvenile GM1	[Iwasaki *et al*., 2006; Kaye *et al*., 1997; Paschke *et al*., 2001, Tominaga *et al*., 2001]
p.R208C/p.W161X	6 (+5)	infantile GM1	[Boustany *et al*., 1993; Hofer *et al*., 2010]
p.C230R/p.C230R	6	infantile GM1	[Hofer *et al*., 2010]
p.Y270D/p.Y270D	8	infantile GM1	[Paschke *et al*., 2001]
p.W273L/p.W273L	8	Morquio B	[Oshima *et al*., 1991]
p.A301V/p.A301V	8	infantile GM1	[Hofer *et al*., 2010]
p.Y333H/p.Y333H	10	infantile GM1	[Hofer *et al*., 2009]
p.G438E/p.G438E	13	adult GM1	[Hinek *et al*., 2000]
p.P549L/p.P549L	15	infantile GM1	[Santamaria *et al*., 2007]

Table 3.7.1.1 Genotypes and phenotypes of human skin fibroblast cells used in this work. Presumptive phenotype determining alleles are in bold letters. GM1 = G_{M1}-gangliosidosis

3.7.2 COS-1 cells

COS-1 cells [Gluzman, 1981], transiently overexpressing the human lysosomal acid β-galactosidase precursor (β-Gal; EC 3.2.1.23), and used for control experiments in this work, were kindly provided by Doris Hofer, Department of Pediatrics, Medical University of Graz. Details on transfection procedures, expression conditions, and cell preparation are described by Hofer *et. al* [Hofer *et al.*, 2009; Hofer *et al.*, 2010].

3.7.3 CHO-K1 cells

Permanent transfection of Chinese hamster ovary (CHO) cells (subclone K1) with human *GLB1* cDNA (NCBI Reference Sequence: NM_000404.2, transcript variant 1), encoding the human lysosomal acid beta-galactosidase (β-Gal; EC 3.2.1.23) was performed by Doris Hofer (Department of Pediatrics, Medical University of Graz) using the nucleofection technique. Nucleofection Kit T and program U-23 were applied according the manufacturer's protocol [Amaxa DCT-1002]. 600 µg/ml geneticin was used for selection.

3.8 Tissue culture methods

3.8.1 General cultivation methods for human skin fibroblasts

Human skin fibroblasts were grown in minimal essential medium (MEM) with Earle's Salts (PAA, Pasching, Austria) containing 10% fetal bovine serum (FCS), 400 µM L-Glutamine (Sigma-Aldrich®), and 50 µg/ml Gentamicin (Gibco®, Invitrogen™) at 37 °C and 5% CO_2. After 7-9 days of incubation, confluent cells were splitted at a ratio of 1:4, and seeded in either 75 cm² or 25 cm² Tissue Culture Flasks, using 15 ml or 7 ml medium, respectively. For that purpose, the medium was removed, and cells were washed twice in sterile PBS (pH 7.1-7.2; LKH Apotheke), followed by trypsinization for 3 min at 37 °C with 4 ml or 2 ml 1x Trypsin-EDTA (PAA, Pasching, Austria). Trypsinization was stopped by addition of 4 ml or 2 ml medium (or PBS), and cells were pelleted by centrifugation for 2 min at 2,500 rpm in a table top centrifuge (Z200A, Hermle). Cell pellets were resuspended in medium and splitted as described above. Unless otherwise stated, cells were also harvested by trypsinization.

All cells used in this study were between the third and nineteenth passages. Materials and reagents were kept sterile, or were sterile filtrated with 0.1 µM filters before use. To reduce the risk of contamination, disposable Corning Costar® Stripettes® were used throughout this work.

3.8.2   Chaperone treatment of cultured human skin fibroblasts (chaperone screenings)

For chaperone screenings, cells from a 25 cm² Tissue Culture Flask were evenly seeded in a 6well Microplate, and grown to semi-confluency as described earlier. Chaperones were added to the culture medium at five different concentrations from 20 to 500 µM, and cells were incubated for 4 more days at 37 °C. One well on each Microplate was used as chaperone-free control, and each well was filled with 4 ml medium ± chaperone. Cells were harvested by scraping using 400 µl of a 0.9% NaCl + 0.01% Triton® X-100 solution. The suspensions were sonicated on ice for 2 x 10 sec, and a break of 30 sec in between. To remove cell debris, homogenates were briefly centrifuged at 13,000 rpm for 2 min in a table top centrifuge (Biofuge pico, Heraeus). Cell homogenates were further prepared for protein determination, β-galactosidase, and β-hexosaminidase assays as described in section 3.11.

Cell lines from eleven GM1 patients, four MBD patients, and four healthy individuals were exposed to DLHex-DGJ (see section 3.9.1) for evaluation of its chaperone effects.

3.8.3   Uptake of natural substrate by cultured human skin fibroblasts (loading assays)

For loading assays with tritium (^{3}H)-labeled G_{M1}-ganglioside (^{3}H-G_{M1}G), cells were cultured in 25 cm² Tissue Culture Flasks (2 flasks per cell line and single experiment), and maintained in minimal essential medium (MEM; 3 ml/flask) with Earle's Salts (PAA, Pasching, Austria) containing 1% fetal bovine serum (FCS), 400 µM L-Glutamine (Sigma-Aldrich®), and 50 µg/ml Gentamicin (Gibco®, Invitrogen™) at 37 °C and 5% CO_2. The low FCS content enhances ^{3}H-G_{M1}G uptake from the culture medium. After 4 days, cells were incubated with the labeled G_{M1}-ganglioside (for preparation see section 3.9.2) at a final radioactivity of 15 million dpm per flask (3 ml medium/flask). Additionally, the β-glucosidase inhibitor Conduritol B Epoxide (CBE) [Datta and Radin, 1988] was added to the culture medium mix at final concentrations of

500 mM. Therefore, 10 µg/µl CBE stocks were prepared in Aqua dest. and diluted in medium. Total incubation time with ^{3}H-G$_{M1}$G + CBE was 5 days.

In some experiments, chaperones were added to the medium as well. If chaperone treatment was required, the compound was applied for a total time of either 4 or 2 days, but in either case after addition of the labeling mixture.

Prior harvesting, the medium was removed carefully and collected in assay tubes. Cells were washed thoroughly with 3 x 2 ml PBS (pH ~7), which was then pooled and collected in fresh assay tubes. Cells were harvested by trypsinization, and the reaction was stopped by addition of 1 ml PBS + 5% BSA per flask. The cell suspensions were collected in fresh assay tubes. Finally, the flasks were washed twice in PBS (pH ~7), and the washing solutions were combined with the cell suspensions. Separate collection of medium and cell material is necessary to track the radioactive material's distribution in the samples. All steps are carried out at room temperature unless otherwise stated. Cell suspensions were centrifuged at 300 x g for 10 min. Supernatants were collected in fresh assay tubes, while cell pellets were resuspended in 0.6 ml PBS (pH ~7), and transferred to fresh 1.5 ml Eppendorf tubes. The original cell suspension tubes were washed once with 0.6 ml PBS, and the washing solutions were combined with the resuspended pellets. Once more, the suspensions were centrifuged and the supernatants were discarded. Pellets should be clearly visible at this point and can be stored at -20 °C until further use. For enzymatic measurements and lipid extractions, cell pellets were resuspended in 150 µl Aqua dest., respectively, pooled (note: 2 flasks were used per cell line and single experiment), and sonicated on ice for 3 x 15 sec. Go through each sample once before starting the second and third run. 200 µl of the resulting cell homogenates were used for lipid extractions, and 100 µl of each sample were stored at 4 °C for *in vitro* enzymatic measurements.

3.8.4 *Overexpression of human lysosomal acid β-galactosidase by transiently transfected CHO-K1 cells*

Permanently transfected CHO-K1 cells were grown to confluency (3-4 days) in Ham's F-12 medium (PAA) containing 10% fetal bovine serum (FCS), 400 µM L-Glutamine (Sigma-Aldrich®), and 50 µg/ml Gentamicin (Gibco®, Invitrogen™) at 37 °C and 5% CO$_2$. Then, CHO-K1 cells were splitted at the ratio of 1:4, and seeded in 75 cm² Tissue Culture Flasks. Splitting

was performed by trypsinization as described for human skin fibroblast. For overexpression and secretion of the human β-galactosidase precursor into the medium, the splitted cells were maintained in CHO-S-SFM II medium + L-Glutamine (Gibco[®], Invitrogen[™]) containing 50 µg/ml Gentamicin (Gibco[®], Invitrogen[™]), but without FCS supplementation for 3 days at 22 °C (5% CO_2), followed by 4 days of incubation at 30 °C (5% CO_2). The lack of FCS in the culture medium and the low incubation temperatures lead to a reduction in growth, therefore it is possible to maintain the CHO-K1 cells over a longer period without splitting. Furthermore, the reduced protein content of the culture medium might facilitate β-Gal purification (see section 3.12.7). To increase the concentration of secreted β-Gal in the medium, culture volumes of 4-8 ml per 75 cm² flask were used instead of 13-15 ml. The medium ("Charge I") was collected and stored at -20 °C until use. Aliquots of the medium were immediately used for β-galactosidase determinations. Fresh CHO-S-SFM II medium + L-Glutamine (Gibco[®], Invitrogen[™]) containing 50 µg/ml Gentamicin (Gibco[®], Invitrogen[™]) was applied to the cells, and incubation was prolonged for 5-7 days at 30 °C (5% CO_2). The collected medium was designated "Charge II" and stored at -20 °C until use, while the CHO-K1 cells were discarded. Typically, 108 x 75 cm² Tissue Culture Flasks were prepared for one experimental round, yielding up to 900 ml of medium, if both charges were combined.

3.9 Substances tested in cell culture

3.9.1 Iminosugars

Several novel lipophilic and/or ionisable N-modified 1-deoxygalactonojirimycin derivatives were synthesized by our cooperation partners from the Glycogroup, Department of Organic Chemistry, Graz University of Technology [Steiner *et al*., 2008; Schitter *et al*., 2010a; Schitter *et al*., 2010b]. Selected compounds were subjected to chaperone screenings and loading assays *in vivo*, as well as *in vitro* assays to determine their inhibitory potential. Some of the substances listed in Table 3.9.1.1 have not been published yet, and are therefore left unspecified.

Internal name	Compound	M_r	Buffer/Solvent
#1	Methyl N^2-dansyl-N^6-(1,5-dideoxy-D-galactitol-1,5-diyl)-L-lysinate	539.65	PhoBI
#2 (DLHex-DGJ)	Methyl 6-[N^2-dansyl-N^6-(1,5-dideoxy-D-galactitol-1,5-diyl)-L-lysinyl]amino hexanoate	652.80	PhoBI
#2 w/o dansyl	Methyl N^6-(1,5-dideoxy-D-galactitol-1,5-diyl)-L-lysinate [unpublished]	306.36	PhoBI
#3	1-Dansylamino-1,2,5-tridesoxy-2,5-imino-D-mannitol	395.52	PhoBI
#4 (DGJ)	1-Deoxygalactonojirimycin	163.17	PhoBI
#4/2 (DGJ HCl)	1-Deoxygalactonojirimycin monohydrochloride	199.63	PhoBI
#6/2	N-(1,1,1,3,3,3-Hexafluoropropyl-2-oxy)hexyl-1,5-dideoxy-1,5-imino-D-galactitol	413.35	PhoBI
#7/3	N-[6-(benzyloxycarbonylamino)hexyl]-1,5-dideoxy-1,5-imino-D-galactitol	396.48	PhoBI
A1	N-(α,α-Di-trifluoromethyl)benzyloxyhexyl-1,5-dideoxy-1,5-imino-D-galactitol	489.45	MeOH
A2	N-(Nonafluoro-t-butyloxy)hexyl-1,5-dideoxy-1,5-imino-D-galactitol	481.35	MeOH
A3	[unpublished]	857.09	MeOH
A4	N-[6-($tert$-butyloxycarbonylamino)hexyl]-1,5-dideoxy-1,5-imino-D-galactitol	362.46	MeOH
A5	N-(6-Dansylamino)hexyl-1,5-dideoxy-1,5-imino-D-galactitol	495.63	MeOH
A6	[unpublished]	608.79	PhoBI

Table 3.9.1.1 Iminosugars used in this work. All compounds were kindly provided by the Glycogroup, Department of Organic Chemistry, Graz University of Technology. PhoBI = Phosphate Buffer for Inhibitors (pH 7.0); MeOH = methanol.

3.9.1.1 *Synthesis of the β-galactosidase inhibitor DLHex-DGJ*

Methyl 6-[N^2-dansyl-N^6-(1,5-dideoxy-D-galactitol-1,5-diyl)-L-lysinyl]amino hexanoate (DLHex-DGJ; MW 652.80; soluble in methanol, dimethylsulfoxide, and water) was synthesized by modification of the glycosidase inhibitor 1-deoxygalactonojirimycin (DGJ) [Asano, 2003; Fantur *et al.*, 2010; Steiner *et al.*, 2008]. For the experiments presented in this work, DLHex-DGJ (Figure 3.9.1.1.1) was dissolved in 10 mM phosphate buffer (pH 7.0) containing 100 mM NaCl, 0.01% NaN_3, and 0.01% Triton (PhoBI). *In vivo*, the total buffer concentration in the media was less than 1% and had no effect on β-Gal activity or cell viability.
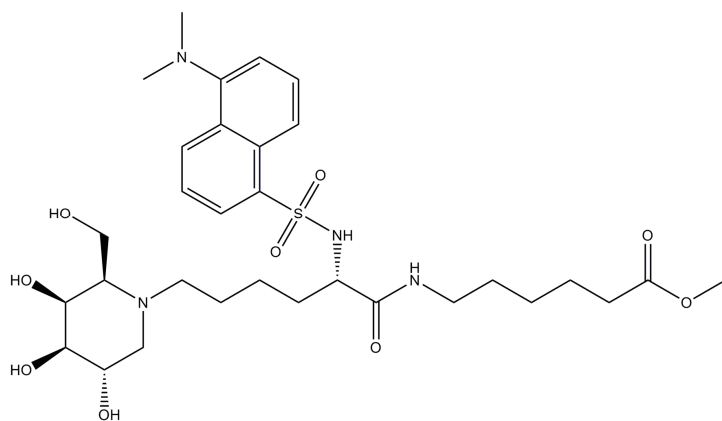
Figure 3.9.1.1.1 Chemical structure of the β-galactosidase inhibitor DLHex-DGJ. Full chemical name: Methyl-6-{[N[2]- (tert- butoxycarbonyl)-N[6]-(1,5 - dideoxy-D- galactitol-1,5-d iyl) -L- lysyl] amino} hexanoate (DLHex-DGJ). The chemical structure is based on the DGJ core, containing an alpha-N-dansyl-substituted L-lysine residue. Dansyl renders the molecule autofluorescent.

3.9.2 Preparation of tritium (^{3}H)-labeled G_{M1}-ganglioside for loading assays

The radiolabeled natural substrate (^{3}H-G_{M1}G) was kindly provided by Jana Ledvinova, Institute of Inherited Metabolic Disorders, First Faculty of Medicine, Charles University in Prague and General University Hospital in Prague, Czech Republic. Loading assays were entirely performed in the laboratory mentioned above, according to protocols provided by Befekadu Asfaw. Similar experiments with other radiolabeled natural substrates, used for examinations of different lysosomal storage disorders have been published by this group [Elleder *et al*., 2005; Keslova-Veselikova *et al*., 2008; Pavlu-Pereira *et al*., 2005]. Briefly, the double bonds of ceramides in G_{M1}-ganglioside molecules were reduced with tritium (^{3}H) gas, and liposome vesicles were prepared as described for A-6-2 radioactive labeling by Asfaw *et al*. [Asfaw *et al*., 1998]. A ^{3}H-G_{M1}G working stock was prepared in 2:1 (v/v) chloroform:methanol at a final concentration of 92 MBq/8ml (2.5 mCu/8ml). For each flask with 3 ml culture medium, 21.7 µl of this stock were used. To prepare the radiolabeled natural substrate for cell culture use, an adequate amount of the stock solution was transferred to a sterile Eppendorf tube, and dried in a gentle stream of nitrogen on a heating block at 40 °C. For larger volumes, the procedure was repeated stepwise. To keep the substrate sterile, the dried substance as well as the lid and outside of the Eppendorf tube were briefly rinsed with a small amount of 2:1 (v/v) chloroform:methanol. Residual liquid was then removed by using a vacuum desiccator for 1 hr at room temperature.The desiccator was finally opened under sterile conditions in a Lamina Flow Clean Bench. The dried substrate was carefully dissolved with 5 µl dimethyl sulfoxide (DMSO) per 21.7 µl of the original ^{3}H-G_{M1}G stock. Prior application to cultivated fibroblast cells, the solution was sonicated on ice for 10 min. A cup horn sonicator (Ultrasonic Homogenizer, 4710 series, Cole-Parmer Co.) cooled with ice water was used to keep the

samples in sterile condition. Sonication is necessary to redissolve the dried sample properly. It is also important to mix the first substrate solution dropwise with small amounts of medium under constant, vigorous shaking and then add the rest of the cultivation medium to evenly distribute the forming micelle vesicles and prevent sticking to the plastic surface.

3.10 Antibodies

In this work, antibodies were used to detect proteins on Western blot (WB) membranes or in immunofluorescence (IF) experiments. Secondary antibodies labeled with either horseradish peroxidase or alkaline phosphatase were used to detect primary antibodies in WB. Colorimetric or chemiluminescent signal detection was performed with the aid of commercial kits (cf. section 3.11.7.4). Secondary antibodies labeled with fluorescent dyes were used in IF experiments to enable detection of immune complexes at specific wavelengths.

3.10.1 Detection of human lysosomal acid *β*-galactosidase

➢ α85 anti-human β-galactosidase antibody produced in rabbits (kindly provided by A. d'Azzo, Department of Genetics and Tumor Cell Biology, St. Jude Children's Research Hospital, Memphis, TN)
WB: dilution 1:1,000 in Milk Blocking Buffer; incubation for 16 hrs at 4 °C
IF: dilution 1:300 in 2% (w/v) BSA in PBS (pH 7.4); incubation for 2 hrs at room temperature

➢ Anti-β-galactosidase peptide antibody 1 produced in rabbits; Eurogentec; order number ZAT08010, rabbit 1269, charge: Purified IgG Vs EP084834 PUR MED
WB: dilution 1:50-1:500 (optimal 1:100) in Milk Blocking Buffer, incubation for 16 hrs at 4 °C

- Anti-β-galactosidase peptide antibody 2 produced in rabbits; Eurogentec; order number ZAT08010, rabbit 1269, charge: Purified IgG Vs EP084835 PUR MED
  WB: dilution 1:50-1:500 (optimal 1:100) in Milk Blocking Buffer, incubation for 16 hrs at 4 °C

3.10.2 Detection of polyhistidine-tagged proteins

- Rabbit Polyclonal anti-6-Histidine antibody (Novus Biologicals®)
  WB: dilution 1:1,000 in Milk Blocking Buffer; incubation for 1 hr at room temperature

3.10.3 Detection of GST-tagged proteins

- Anti-GST antibody produced in goat (Sigma-Aldrich®)
  WB: dilution 1:1,000 in Milk Blocking Buffer; incubation for 1 hr at room temperature

3.10.4 Detection of human peroxisomal catalase

- Anti-Catalase Rabbit pAb (Calbiochem®)
  IF: working concentration 25 µg/ml (dilution in 2% (w/v) BSA in PBS, pH 7.4); incubation for 1.5 hrs at room temperature

3.10.5 Detection of primary antibodies produced in rabbits

- Anti- rabbit -IgG (whole molecule)- alkaline phosphatase antibody produced in goat (Sigma-Aldrich®)
  WB: dilution 1:30,000 in Milk Blocking Buffer; incubation for 1 hr at room temperature

- ImmunoPure® Goat Anti-Rabbit IgG (H+L), Peroxidase Conjugated (ThermoScientific)
  WB: dilution 1 : 750,000 in Milk Blocking Buffer; incubation for 1 hr at room temperature

➢ Fluorescein (FITC) - conjugated AffiniPure Goat Anti - Rabbit IgG (H+L) (Jackson Immuno Research)

IF: dilution 1: 200 in 2% (w/v) BSA in PBS (pH 7.4); incubation for 1 hr at room temperature

3.10.6 *Detection of primary antibodies produced in goats*

➢ Peroxidase AffiniPure Donkey Anti - Goat IgG (H+L) (Jackson Immuno Research)

WB: dilution 1 : 200,000 in Milk Blocking Buffer; incubation for 1 hr at room temperature

3.10.7 *Detection of primary antibodies produced in mice*

➢ Rhodamine (TRITC)- conjugated AffiniPure Sheep Anti- Mouse IgG (H+L) (Jackson Immuno Research)

IF: dilution 1:50 in 2% (w/v) BSA in PBS (pH 7.4); incubation for 1 hr at room temperature

3.11 General laboratory techniques

3.11.1 *Protein determination by Lowry's method*

Protein concentrations were determined in duplicates according to the following protocol, based on the Lowry method [Lowry *et al*., 1951]:

1. Blank: mix 20 µl Aqua dest. with 20 µl 20% (w/v) NaOH solution

   Standard: 40 µl bovine serum albumin (BSA) in 10% (w/v) NaOH (1 mg BSA/ml 10% NaOH)

   Samples: mix 20 µl cell homogenate / sample with 20 µl 20% (w/v) NaOH solution

2. Add 60 µl of 2 N acetic acid.

3. Add 1ml of alkaline $CuSO_4$ solution (1 g/100 ml Aqua dest.) containing

   100 p/v of 3% (w/v) Na_2CO_3 (3 g/100 ml 0.1 N NaOH) in 0.1 N NaOH

   1 p/v of 4% (w/v) potassium sodium tartrate (2 g /100 ml Aqua dest.) in Aqua dest.

   1 p/v of 2% (w/v) $CuSO_4$ in Aqua dest.

   (mix immediately and thoroughly)

4. Incubate for 10 min at room temperature.

5. Add 100 µl of Folin-Ciocalteu's phenol reagent (Merck) diluted 1:3 in Aqua dest., and mix immediately and thoroughly.

6. Incubate for exactly 10 min at room temperature, and determine the absorbance at 623 nm. Optional: Centrifuge sample prior photometric measurement.

Measurements were performed in disposable cuvettes ("Halb-Mikro-Küvetten", Sarstedt) using a Spectrophotometer (UV-1800, Shimadzu), and total protein was quantified according to the following formula:

$$\frac{\text{extinction of sample}}{\text{extinction of standard}} \times 2 = \text{mg protein/ml}$$

3.11.2 Protein determination by Hartree-Lowry's method

Protein concentrations of loading assay samples were determined by a modified Lowry method [Hartree, 1972]. Samples were measured in duplicates according to the following protocol:

1. Samples: mix 15 µl cell homogenate/sample with 185 µl Aqua dest. (the final volume should not exceed 200 µl)

2. Add 200 µl of Hartree Solution A to all tubes, mix, and incubate at 50 °C in a water bath for 10 min.

3. Cool samples to room temperature in cold water for ~5 min.

4. Add 20 µl of Hartree Solution B, mix, and incubate at room temperature for 10 min.

5. Add 600 µl of Hartree Solution C, mix, and incubate at 50 °C in a water bath for 10 min.

6. Cool samples to room temperature in cold water for ~5 min, and determine the absorbance at 650 nm.

Measurements were performed in disposable cuvettes ("Halb-Mikro-Küvetten", Sarstedt) using the ATI Unicam, UV/VIS Spectrometer UV4 against water. Calculations were based on the following BSA calibration curve:

BSA [µg per tube]	0	5	10	15	20
BSA (0.1 mg/ml) [µl]	0	50	100	150	200
H_2O [µl]	200	150	100	50	0

All concentrations were measured in duplicates. Data was obtained as µg protein/15 µl sample, and manually converted to mg protein/ml.

3.11.3 Determination of β-galactosidase activity (standard β-Gal assay)

Fibroblast cells were harvested by trypsinization or scraping as described earlier, and prepared in a 0.9% NaCl solution containing 0.01% (w/v) Triton® X-100. Cells from 75 cm² flasks were resuspended in 0.5-1 ml, cells from 25 cm² flasks in 0.2-0.5 ml, and cells from 6well Microplates in 0.4 ml NaCl/Triton. After sonication (2 x 10 sec; Branson Sonifier II, W-250), the samples were centrifuged for 2 min at 13,000 rpm in a table top centrifuge (Biofuge pico, Heraeus) to remove the cell debris. For β-Gal assays, cell homogenates were diluted with 0.9% NaCl to a total protein concentration of 40 µg in a volume of 20 µl, transferred to assay tubes, and mixed with prewarmed (37 °C) β-Gal Substrate Solution A. Enzyme blanks were mixed with equal amounts of β-Gal Buffer A (pH 4.0), while substrate blanks were prepared with 20 µl 0.9% NaCl instead of cell homogenates. The reaction was started by incubation for 30 min at 37 °C in a water bath, and stopped by addition of 2.5 ml Stop Buffer A (pH 10.4). The amount

of hydrolyzed 4-methylumbelliferone was determined with a Luminescence Spectrometer (LS50B, PerkinElmer) using a Quartz SUPRASIL® Cuvette (10 mm; Hellma), and the following parameters:

Excitation wavelength:	360 nm
Emission wavelength:	450 nm
Excitation slit:	10.0 or 13.0 nm
Emission slit:	6.2 nm
Integration time:	1 sec
Emission filter:	390 nm Cut-off
Detector voltage:	800

A 0.09 µM solution of 4-methylumbelliferone was used as standard (4-MU Standard A), while Stop Buffer A (pH 10.4) served as standard blank. Assays were performed in triplicates, unless otherwise stated. Enzyme activities were calculated according to the following formula:

$$\frac{\text{4-MU Standard\_a [0.09 µM] * assay volume [2,620 µl]}}{\text{Standard\_b [intensity] * t [30 min] * sample volume [20 µl]}} = \beta\text{-Gal factor}$$

The intensity values from spectrofluorometric measurements were multiplied by the β-Gal factor, and if samples were diluted (prior incubation!), also by the dilution factor to obtain enzyme activities in mU/ml. For assessment of mU/mg protein, this value was divided by the total protein concentration (mg protein/ml). Finally, the mU/mg were multiplied by the factor 60 to obtain nmol/hr/mg protein.

3.11.4 Alternative determination of β-galactosidase activity (alternative β-Gal assay)

Fibroblast cells were harvested and homogenized as described for loading assays (cf. section 3.8.3 and 3.12.4) without removing the cell debris by centrifugation. For alternative β-Gal assays [Wenger and Williams, 1991], cell homogenates were diluted with Aqua dest. to a total protein concentration of 2.5 µg in a volume of 20 µl, mixed with 20 µl of prewarmed (37 °C) β-Gal Substrate Solution B, and incubated for 60 min in a thermoblock at 37 °C. Enzyme blanks were prepared with Aqua dest. instead of homogenates. The reaction was terminated by addition of 0.6 ml Stop Buffer B (pH 10.6), and the amount of hydrolyzed 4-

methylumbelliferone was determined with the PerkinElmer LS50 B Luminescence Spectrometer (excitation: 365 nm, emission: 448 nm), using a Quartz SUPRACIL® Micro Cuvette (PerkinElmer). The standard curve was prepared as follows:

c [nmol 4-MU/ml]	0.2	0.4	0.6
1 µM 4-MU Standard B [µl]	240	240	360
Stop Buffer B (pH 10.6)	960	360	240

Assays were performed in duplicates, or singles if sample material was limited. Enzyme activities were calculated according to the following formula:

$$\frac{c \ [nmol/ml] * assay\ volume\ [ml]}{mg\ of\ protein * t\ [hrs]} = \frac{c * 0.64}{0.0025 * 1} = [nmol/hr/mg\ protein]$$

Note: If samples were diluted in Stop Buffer for spectrofluorometric measurement, the dilution factor was integrated in the formula. This was done by multiplying either "c" (if samples were diluted after the reaction), or "nmol/hr/mg protein" (sample dilution prior incubation) by the dilution factor.

3.11.5 Determination of β-hexosaminidase activity (standard β-Hex assay)

For β-hexosaminidase (β-Hex, β-N-acetylhexosaminidase; EC 3.2.1.52) assays, cells were prepared in the same manner as for β-Gal determinations. 10 µl of cell homogenates (dilutions corresponding to 1-4 µg total protein) were mixed with 90 µl of 0.9% NaCl and prewarmed (37 °C) 100 µl β-Hex Substrate Solution A, and incubated at 37 °C in a water bath for 20 min. Enzyme blanks were mixed with equal amounts of β-Hex Buffer A (pH 4.6), while substrate blanks were prepared with 10 µl 0.9% NaCl instead of cell homogenates. Reaction was stopped by adding 2.5 ml Stop Buffer A (pH 10.4). The mode of fluorescence detection and standards were the same as described for β-Gal assays. β-Hex assays were performed in triplicates, unless otherwise stated.

Enzyme activities were calculated according to the following formula:

$$\frac{\text{4-MU Standard\_a [0.09 µM] * assay volume [2,700 µl]}}{\text{Standard\_b [intensity] * t [20 min] * sample volume [10 µl]}} = \text{β-Hex factor}$$

The intensity values from spectrofluorometric measurements were multiplied by the β-Hex factor, and if samples were diluted (prior incubation!), also by the dilution factor to obtain enzyme activities in mU/ml. For assessment of mU/mg protein, this value was divided by the total protein concentration (mg protein/ml). Finally, the mU/mg were multiplied by the factor 60 to obtain nmol/hr/mg protein.

3.11.6 *Alternative determination of β-hexosaminidase activity (alternative β-Hex assay)*

Fibroblast cells were harvested and homogenized as described for loading assays (cf. section 3.8.3 and 3.12.4) without removing the cell debris by centrifugation. For alternative β-Hex assays [Wenger and Williams, 1991], cell homogenates were diluted with Aqua dest. to a total protein concentration of 0.25 µg in a volume of 20 µl, mixed with 20 µl of prewarmed (37 °C) β-Hex Substrate Solution B, and incubated for 15 min in a thermoblock at 37 °C. Enzyme blanks were prepared with Aqua dest. instead of homogenates. The reaction was terminated by addition of 0.6 ml Stop Buffer B (pH 10.6). The amount of hydrolyzed 4-methylumbelliferone was determined with the PerkinElmer LS50 B Luminescence Spectrometer (excitation: 365 nm, emission: 448 nm) using a Quartz SUPRACIL® Micro Cuvette (PerkinElmer). The standard curve was prepared as described for alternative β-Gal assays.

Assays were performed in duplicates, or singles if sample material was limited. Enzyme activities were calculated according to the following formula:

$$\frac{\text{c [nmol/ml] * assay volume [ml]}}{\text{mg of protein * t [hrs]}} = \frac{c * 0.64}{0.00025 * 0.25} = \text{[nmol/hr/mg protein]}$$

Note: If samples were diluted in Stop Buffer for spectrofluorometric measurement, the dilution factor was integrated in the formula. This was done by multiplying either "c" (if samples were diluted after the reaction), or "nmol/hr/mg protein" (sample dilution prior incubation) by the dilution factor.

3.11.7   Separation and detection of proteins

3.11.7.1   Mammalian sample preparation

Thirty micrograms total protein of cell homogenates from human skin fibroblasts, CHO-K1 cells, or COS-1 cells were analyzed, unless otherwise stated. For experiments with mammalian cells, the premixed NuPAGE® LDS 4x LDS Sample Buffer (Invitrogen™) and NuPAGE® Sample Reducing Agent 10x (Invitrogen™) were added to the samples according to the following scheme:

Sample volume	4x LDS Sample Buffer	10x Reducing Agent
10 µl	3 µl	1 µl
15 µl	5 µl	2 µl
20 µl	7 µl	3 µl
25 µl	9 µl	4 µl

Samples were centrifuged briefly, denatured by heating for 10 min at 70 °C in a thermoblock, and centrifuged one more time prior application of the total volume to the SDS gel.

3.11.7.2   E. coli sample preparation

Samples were mixed 1:1 with 2x Laemmli Sample Buffer [Laemmli, 1970] and briefly centrifuged prior heat denaturation at 95 °C for 10 min. After another short centrifugation, the samples were applied to the SDS gel. Typically, a total volume of 30 µl was applied to the SDS gel. For some preliminary induction experiments it was necessary to pellet the cells, add 80 µl

of 1x Laemmli Sample Buffer, and load 10 µl of the mixture onto the SDS gel after heat denaturation.

3.11.7.3 SDS-PAGE

Sodium dodecyl sulfate polyacrylamide gel electrophoresis (SDS-PAGE) was conducted in Mini-PROTEAN® 3 Cells (Bio-Rad), using either self-made 10% polyacrylamide gels or 10% Tris-HCl ready gels (50 µl slot volume, 10 wells; Bio-Rad), according to the Laemmli method [Laemmli, 1970]. Preparation of 10% polyacrylamide gels was performed as described in the Bio-Rad user manual [Bio-Rad 4006157], using 1.5 mm spacer plates and appropriate combs (10 wells).

At least one slot of each gel was loaded with a specific protein molecular weight marker. Depending on the size of the proteins in question, one of three different weight markers (Figure 3.11.7.3.1) was used in this work, the 1x SeeBlue® Plus2 Pre-Stained Standard (Invitrogen™), 1x BenchMark™ Prestained Protein Ladder (Invitrogen™), and the LMW-SDS Marker (GE Healthcare). Gels were run for 30 min at 50 volt using the PowerPac HC™ 250 V (Bio-Rad), then switched to 150 volt for 45-60 min, until the lowest band of the weight marker reached the bottom of the gel. Voltage was kept constant throughout electrophoresis. A Tris-glycine system was used as running buffer.

Band No.	Apparent Molecular Weight
1	181.8 kDa
2	115.5 kDa
3	82.2 kDa
4	64.2 kDa*
5	48.8 kDa
6	37.1 kDa
7	25.9 kDa
8	19.4 kDa
9	14.8 kDa
10	6.0 kDa

*Orientation band (pink in color)

	Tris-Glycine
Myosin	250
Phosphorylase	148
BSA	98
Glutamic Dehydrogenase	64
Alcohol Dehydrogenase	50
Carbonic Anhydrase	36
Myoglobin Red	22
Lysozyme	16
Aprotinin	6
Insulin, B Chain	4

NuPAGE® Novex Bis-Tris 4-12% Gel

Figure 3.11.7.3.1 Characteristics of the (A) BenchMark™ Prestained Protein Ladder (Invitrogen™) and the (B) SeeBlue® Plus2 Pre-Stained Standard (Invitrogen™). Illustrations were adapted from the respective user manual.

For detection of proteins, SDS gels were either stained with the SimplyBlue™ SafeStain (Invitrogen™) according to Invitrogen's™ instruction manual [Invitrogen™ MAN0000735], or subjected to Western blotting.

3.11.7.4 Western blotting

Blotting was performed in Mini Trans-Blot® Electrophoretic Transfer Cells (Bio-Rad). The equipment was assembled according to manufacturer's protocol [Bio-Rad M1703930]. Proteins were transferred to nitrocellulose membranes (0.45 µM pores size; Invitrogen™) by an electric current of 300 mA (constant) for 2 hrs at room temperature, using a running buffer based on the Tris-glycine system. For hybridization, membranes were briefly washed in 1x TBS Buffer (pH 7.6), transferred to suitable plastic boxes with lids, and pre-blocked for 1 hr at room temperature with 10-15 ml Blocking Buffer (5% non-fat milk or 3% BSA). All steps during hybridization were performed under moderate shaking. Membranes were washed briefly in 3 x 15 ml 1x TBS, and subsequently incubated with 10-12 ml primary antibody dilution in Blocking Buffer. After another washing step with 3 x 15 ml 1x TBS (8 min each), membranes

were incubated with 10-12 ml secondary antibody dilution in Blocking Buffer, followed by a final washing step as indicated above.

Depending on the secondary antibody's labeling, membranes were developed either with the Bio-Rad Alkaline Phosphatase Conjugate Substrate Kit (Bio-Rad), or the SuperSignal® West Pico Chemiluminescent Substrate Kit (Thermo Scientific).

Alkaline Phosphatase Reaction:
- Dilute 320 µl of 25x Color Development Buffer in 8 ml Aqua dest. before use.
- Add 80 µl of AP Color Reagent A and B, respectively.
- Immerse membrane in solution under shaking until the color reaction is completed (30 sec to 1 hr).
- Wash membranes with 2 x 15 ml Aqua dest. (7 min each).
- Air-dry membrane on glass plate.

Horseradish Peroxidase Reaction:
- Gently mix 4 ml of SuperSignal® West Pico Luminol / Enhancer and 4 ml SuperSignal® West Pico Stable Peroxide.
- Immerse membrane in solution without shaking for 5 min.
- Remove the blot and place it in a plastic cover. (remove air bubbles carefully)
- Place plastic covered blot in film cassette and adjust X-ray film (Amersham Hyperfilm™ MP, GE Healthcare); cut off one corner for orientation, and expose for 30 sec to 1 hr at room temperature.
- Films were developed with the CURIX 60™ table-top processor (AGFA).

3.12 Specific laboratory techniques

3.12.1 Immunostaining

Fibroblast cells were sparsely seeded on glass coverslips placed in 35 x 10 mm Tissue Culture Dishes (Becton Dickinson), and maintained in minimal essential medium at 37 °C (5% CO_2) for 24 hrs. If required, cells were incubated with chaperones for up to 3 more days at 37 °C. After washing the cells twice with cold PBS buffer (pH 7.4), they were fixed with ice-cold methanol for 8 min at -20 °C, briefly dried and subsequently washed once with PBS (pH 7.4). Typically, cells were incubated for 2 hrs at room temperature with the primary antibody (diluted in 2% (w/v) BSA in PBS, pH 7.4). Secondary antibodies (diluted as described above) were applied for 1 hr at room temperature under light protection. Washings after antibody incubations were performed with Rinsing Solution. Additional washing steps with PBS (pH 7.4), Aqua dest., and 2x SSC Buffer (pH 7.0) were conducted, if cell nucleus counterstaining with propidium iodide (Invitrogen™) was necessary. After washing twice with 2x SSC Buffer (pH 7.0), cells were incubated with the propidium iodide solution (1.5 ml 2x SSC + 18 µl propidium iodide; final concentration 12 µg/ml) for 30 min at room temperature and under light protection, followed by three thorough washing steps with 2x SSC Buffer (pH 7.0). If no propidium iodide was used, glass coverslips were briefly washed in ethanol, and air-dried prior mounting on glass slides. No ethanol was used in the propidium iodide experiments, due to unwanted scouring effects.

Coverslips were mounted on glass slides with Mowiol (Hoechst) and observed with an Olympus IX51 inverted research microscope equipped with standard filters and a 100-fold oil immersion objective. Images were acquired with the Color View III camera system and the Analysis B Software.

3.12.2 Determination of IC_{50}

Modified β-Gal assays were used to estimate the half maximal inhibitory concentration (IC_{50}) of putative β-Gal inhibitors. For triplicate assays, confluent fibroblast cells (3 x 75 cm² flasks) from healthy individuals were harvested by trypsinization, resuspended in 1.5 ml 0.9% NaCl

containing 0.01% Triton$^®$ X-100, sonicated and centrifuged as described earlier. For inhibiton assays, 20 µl of cell homogenate (40 µl total protein) were mixed with 90 µl of prewarmed (37 °C) β-Gal Substrate Solution A, and 10 µl of inhibitor solution (in MeOH or PhoBI) in final concentrations of 0.001-100 µM. Substrate blanks contained 20 µl 0.9% NaCl instead of cell homogenates, while enzyme blanks were made with β-Gal Buffer A (pH 4.0) without β-Gal substrate. Samples were incubated for 30 min at 37 °C in a water bath, and the reaction was stopped by addition of 2.5 ml stop buffer. The amount of hydrolyzed 4-methylumbelliferone was determined as described earlier. Data analysis was performed with the Microcal$^{™}$ Origin$^®$ v6.0 software, using the IC_{50} module based on sigmoid curve fitting.

3.12.3 Determination of Ki

For enzyme kinetic experiments, cells from healthy individuals were prepared as described for IC_{50} measurements. To determine the apparent inhibition constant (K_i), fixed concentrations of each potential inhibitor were used while varying the β-Gal substrate concentrations from 100 to 450 µM. For that purpose, a 0.6 mM β-Gal Substrate Solution was used as main substrate stock, and different volumes of this stock solution were added to the assay mixture, which had a final volume of 120 µl. 20 µl of cell homogenates were used, and the difference in volume (10 µl to 80 µl) was made up of inhibitor solution. Adequate inhibitor stocks (in MeOH or PhoBI) were prepared to achieve the final inhibitor concentrations in the assays. For a single experiment, one set of controls without inhibitor addition, and at least two sets with different inhibitor concentrations were tested for each substance. The highest reliability of data was obtained with three individual experimental setups per substance, but most compounds were only tested once in preliminary experiments. Final inhibitor concentrations in the assay were chosen individually and in accordance with inhibition curve results (see IC_{50} calculation). Samples were incubated for 30 min at 37 °C, and measured spectrofluorometrically as described for standard β-Gal assays. Data analysis was performed with Microcal$^{™}$ Origin$^®$ v6.0, using a non-linear curve fitting module based on the Michaelis-Menten equation for competitive inhibitors.

3.12.4 Lipid extraction from ^{3}H-G$_{M1}$G-loaded human skin fibroblasts

Cell homogenates from loading assay experiments were prepared as described in section 3.8.3. Subsequent steps were carried out at room temperature, unless otherwise stated. 200 µl of each cell homogenate were transferred to pyrex tubes, and mixed with 800 µl of 2:1 (v/v) chloroform:methanol. The solvent:sample ratio should always be 4:1. After vigorous shaking, samples were centrifuged at 300 x g for 10 min for phase separation. The upper, aqueous phase was carefully removed and saved to a fresh pyrex tube without disturbing the interphase consisting of proteins. The interphase is not always clearly visible, but due to possible interference (deformation of zones) during thin layer chromatography of lipid extracts, it should always be removed. It is not necessary to remove the protein phase with a pipette, as it will stick to the glass tubes after separately removing the upper and lower phase. The lower, lipid phase was carefully removed by pipetting, and transferred to a fresh pyrex tube, while the original pyrex tubes were washed with 800 µl chloroform:methanol. Wash fractions were combined with the lipid phases (final volume of 1.6 ml each) and these lipid extracts were dried in a gentle stream of nitrogen on a heating block at 40 °C. At this point, it is very important to continue the experimental procedures, as autoradiolysis might occur in the concentrated samples.

3.12.5 Thin layer chromatography of lipid extracts from ^{3}H-G$_{M1}$G-loaded fibroblast cells

For semi-quantitative analysis of ^{3}H-labeled material in lipid extracts from fibroblast cells, aliquots of cell homogenates were subjected to thin layer chromatography (TLC). Therefore, dried, concentrated samples from lipid extractions were dissolved in 50 µl of 2:1 (v/v) chloroform:methanol, thoroughly vortexed, and applied to silica gel 60 TLC plates (Merck). The plates were dehumidified for 30 min at 120 °C prior use. A mixture of chloroform:methanol:CaCl$_2$ (0.2%) at the ratio of 60:35:04 (v/v/v) was used as mobile phase. CaCl$_2$ (0.2%) was added to the mobile phase to improve ganglioside resolution. The exact position of each sample was marked on the silica plates, and application was performed dropwise. To identify characteristic degradation products, the following radiolabeled ("hot") and unlabeled ("cold") standards were applied to silica gels:

- (^{3}H) G_{M1}-ganglioside, stock: 92 MBq, 5 µl per application,

- (^{3}H) G_{M2}-ganglioside, stocks: 1.02 GBq or 15 nM/1.5µl, 2-20 µl per application,

- G_{M3}-ganglioside, stock: 10 nM/2.5µl, 5-10 µl per application,

- (^{3}H) lactosylceramide, stocks: 37 MBq or 1 nM/2 µl, 7.5-10 µl per application,

- (^{3}H) glucosylceramide, stocks: 180 MBq or 1 mM, 5-15 µl per application,

- (^{3}H) sphingomyelin, stock: 0.7 MBq/3.5 ml, 10 µl per application.

TLC was performed in a glass tank saturated with the mobile phase, until the solvent front had almost reached the top of the silica gel (~90 min; 0.5 cm free of solvent). After air-drying, the silica plates were analyzed with the Raytest TLC Analyzer v2.05, and peak area calculations were performed with the Rita TLC Analysis software (v1.93.002). Silica gels with cold standards were developed with 0.5% Orcinol in 2M H_2SO_4 (dissolved in EtOH) by spraying the Orcinol solution evenly onto the plates. Finally, spots were visualized by drying the silica gels at 105 °C, and retention factors were calculated manually. Therefore, the distance from the start line to the center of the respective lipid spot was sized and divided by the distance covered by the solvent front. Retention factors (RF) of lipids on the "cold" plates are comparable to RF values on "hot" plates.

3.12.6 *Liquid scintillation counting in ^{3}H-G_{M1}G-loaded medium and fibroblast cells*

For another quantitative analysis of ^{3}H-labeled material in the culture medium and cell homogenates, 10 µl aliquots of collected samples (cf. section 3.8.3) were transferred to scintillation vials, mixed with 5 ml of Liquid Scintillation Cocktail BCS (GE Healthcare), and measured with the Beckman LS 6000IC Scintillation Counter. Pure Scintillation Cocktail BCS was used as a blank. Due to limited sample material, measurements could not be performed in duplicates. Radioactivity was measured in disintegrations per minute (dpm) in 10 µl sample volume.

The following calculations were performed to obtain dpm in cells per mg protein:

Calculation of total dpm in cells or medium:

$$\frac{\text{(dpm in 10 µl)} * \text{(total sample volume)}}{10 \text{ µl}} = \frac{\text{(dpm in 10 µl)} * \text{(300 µl cell homogenate or 6,000 µl medium)}}{10 \text{µl}}$$

Calculation of % dpm in cells or medium:

$$\frac{\text{(total dpm cells or medium)} * 100}{\text{(total dpm cells)} + \text{(total dpm medium)}}$$

Calculation of µg protein in 300 µl cell homogenate:

(µg protein/µl) x (total sample volume; 300 µl)

Calculation of dpm cells/mg protein:

$$\frac{\text{(total dpm cells)} * 1000}{\text{(µg protein in 300 µl cell homogenate)}}$$

3.12.7 Purification of overexpressed human lysosomal acid β-galactosidase from CHO-K1 cell culture medium

The protocol is based on previously published affinity chromatographic methods [Hubbes *et al*., 1992; Zhang *et al*., 1994], and was slightly modified. All steps were carried out at 4 °C, unless otherwise stated.

1. Precipitate proteins from CHO-K1 cell medium by addition of 50% (w/v) ammonium sulfate. Mix by stirring for 60 min on a magnetic stirrer at 4 °C, and then allow to stand at 4 °C for 24 hrs. Keep aliquot for SDS-PAGE prior precipitation. Note: Reduced protein content in the culture medium (e.g. no or low FCS) might facilitate protein purification.

2. Centrifuge the solution at ≥10,000 x g for 30 min (4 °C). Keep samples of supernatant and pellet for SDS-PAGE. Optional: Repeat step 1 and 2, and pool pellets.

3. Completely resuspend pellet in a small volume of Phosphate Buffer I (pH 7.0), and dialyze as follows:

   1 x 5 L Phosphate Buffer I (pH 7.0) for 3-5 hrs,
   1 x 5 L Sodium Acetate Buffer I (pH 4.3) for 3-5 hrs, and
   1 x 5 L Sodium Acetate Buffer I (pH 4.3) over night.

   The protein solution should have a pH of 4.3 after dialysis (check pH!).

4. Centrifuge at 3,000 x g for 20 min (4 °C). This step is necessary to remove protein precipitates formed during acidification.

5. Filter supernatant through filter paper and keep sample for SDS-PAGE.

6. Equilibrate the p-Aminophenyl β-D-thiogalactopyranoside-Agarose (PATG) affinity resin (Sigma-Aldrich®) with 5-10 bed volumes of Sodium Acetate Buffer I (pH 4.3).

7. Mix supernatant and PATG-resin, and gently rotate batch over night at 4 °C in an overhead shaker.

8. Prepare a FPLC column for PATG affinity chromatography. Attention should be paid to packing as the sample is already batched with the resin. For general packing instructions, see manufacturer's protocols [Pharmacia A]. In this work, the ÄKTAexplorer™ FPLC system (Amersham Pharmacia Biotech) and a XK 16/20 Column (GE Healthcare) were used, and data was analyzed with the UNICORN™ software.

9. Apply residual sample solution to the column at a flow rate of ≤ 1 ml/min. Fractionate flow through, and keep aliquots for SDS-PAGE.

10. Wash column with 5-10 bed volumes of Sodium Acetate Buffer I (pH 4.3). Fractionate, and keep aliquots for SDS-PAGE.

11. Elute bound proteins with 1-10 bed volumes of freshly prepared Elution Buffer GL (pH 7.0) at a flow rate of ≤ 0.2 ml/min. Fractionate, and keep aliquots for SDS-PAGE. Observe elution procedure by absorbance measurements at 280 nm (A_{280}).

12. Immediately pool eluate fractions, and concentrate eluate using the centrifugal filter devices described in section 3.5.3.

13. When using these devices for rebuffering, concentrate sample to ≤ 0.5 ml, fill up with Phosphate Buffer I (pH 7.0) + 0.1 mM dithiothreitol (DTT), and concentrate again to a final volume of ≤ 0.5 ml. Repeat this step at least twice. Alternatively, the concentrated eluate can be dialyzed against 1 x 5 L Phosphate Buffer I + 0.1 mM DTT (pH 7.0) for 3-5 hrs. Keep aliquot for SDS-PAGE.

3.13 Media, buffers, and solutions

E. coli selection media and antibiotics

LB Medium:

Dissolve 12.5 g Luria Broth in 500 ml Aqua dest. by heating to ~100 °C. Add appropriate antibiotic after cooling to 50 °C, and sterile filtrate using a 0.1 µM filter.
All selection media are based on this formulation.

LBA Medium:
(100 µg ampicillin/ml)

Add 500 µl ampicillin of a 100 mg/ml stock to 500 ml LB Medium prior filtration.

LBAC Medium:
(50 µg ampicillin/ml)
(20 µg chloramphenicol/ml)

Add 250 µl ampicillin of a 100 mg/ml stock, and 100 µl chloramphenicol of a 100 mg/ml stock to 500 ml LB Medium prior filtration.

LBAC-AT Medium:
(0.5 mg L-arabinose/ml)
(5 ng tetracycline/ml)

Add 1 ml L-arabinose of a 250 mg/ml stock, and 15.6 µl tetracycline of a 160 µg/ml stock to 500 ml LBAC Medium prior filtration.

LBA Agar Plates:
(100 µg ampicillin/ml):

Dissolve 10 g Luria Agar in 250 ml Aqua dest. by heating to ~100 °C. Add 250 µl sterile filtrated ampicillin (stock: 100 mg/ml) after cooling to 50 °C, and quickly pour into petri dishes. **Note:** It was not possible to use an autoclave, which is the proper way to sterilize medium and agar!

LBAC Agar Plates:
(100 µg ampicillin/ml)
(20 µg chloramphenicol/ml)

Dissolve 10 g Luria Agar in 250 ml Aqua dest. by heating to ~100 °C. Add 250 µl sterile filtrated ampicillin (stock: 100 mg/ml) and 50 µl chloramphenicol (stock: 100 mg/ml) after cooling to 50 °C, and quickly pour into petri dishes. **Note:** It was not possible to use an autoclave, which is the proper way to sterilize medium and agar!

S.O.C. Medium:

2% tryptone
0.5% yeast extract
10 mM sodium chloride
2.5 mM KCl
10 mM $MgCl_2$
10 mM $MgSO_4$
20 mM glucose
S.O.C. medium was purchased from Invitrogen™.

Ampicillin stocks:
(100 mg/ml)

Dissolve 300 mg ampicillin in 1.5 ml ethanol, followed by 1.5 ml Aqua dest., and sterile filtrate. Store in aliquots at -20 °C.

Chloramphenicol stocks:
(100 mg/ml)

Dissolve 300 mg Chloramphenicol in 3 ml ethanol. Sterile filtrate and store in aliquots at -20 °C.

Tetracycline stocks:
(160 µg/ml)

To prepare a 16 mg/ml main stock, dissolve 80 mg tetracycline in 5 ml 70% (v/v) ethanol and sterile filtrate. Dilute 1:100 in 70% (v/v) ethanol to prepare 160 µg/ml working stocks, and store in aliquots at -20 °C.

Induction reagents

L-Arabinose stocks: **(250 mg/ml)**	Dissolve 500 mg L-arabinose in 2 ml Aqua dest., sterile filtrate, and store aliquots at -20 °C.

1 M IPTG stocks: Dissolve 238.3 mg isopropyl β-D-1-thiogalactopyranoside (IPTG) in 1 ml Aqua dest. and sterile filtrate. Store in aliquots at -20 °C.

Agarose gel electrophoresis

10x TE Buffer:
5 ml 2 M Tris-HCl
2 ml 0.5 M ethylenediaminetetraacetic acid (EDTA)
93 ml Aqua dest.

Loading Dye:
Prepare 0.5%(w/v) bromophenol blue (BPB) solution by dissolving 0.05 g BPB in 10 ml 1x TE buffer.
1 ml 0.5% BPB solution
+ 4 ml 1x TE buffer
+ 5 ml glycerol
The sample:loading dye ratio for gel electrophoresis is 10:1.

20x TBE Buffer, pH 8.0:
108 g Tris base
+ 55 g boric acid
+ 40 ml 0.5 M ethylenediaminetetraacetic acid (EDTA), pH 8.0
Fill up to 500 ml with Aqua dest. and dilute in Aqua dest. to prepare 1x TBE buffer for agarose gel electrophoresis.

1% (w/v) Agarose Gels:
Completely dissolve 2.5 g agarose (Biozym® LE GP Agarose) in 250 ml 1x TBE buffer (pH 8.0) at maximal heat on a magnetic stirrer. Briefly cool the solution by rinsing the flask with water. Add 0.5-2.5 µl ethidium bromide (Invitrogen™) and carefully mix before pouring the gels.

Purification of polyhistidine-tagged fusion proteins

Lysis Buffer A, pH 8.0:	50 mM NaH$_2$PO4 x H$_2$O
	300 mM NaCl
	10 mM imidazole

Wash Buffer A, pH 8.0:	50 mM NaH$_2$PO4 x H$_2$O
	300 mM NaCl
	20 mM imidazole

Elution Buffer A, pH 8.0:	50 mM NaH$_2$PO4 x H$_2$O
	300 mM NaCl
	150 mM imidazole

Purification of GST-tagged fusion proteins

Lysis Buffer B, pH 7.0:	50 mM Tris-HCl
	150 mM NaCl
	1 mM EDTA
	1 mM DTT

Elution Buffer B, pH 8.0: For a 10 mM buffer, dissolve 0,154 g reduced glutathione in 50 ml of a 50 mM Tris-HCl buffer, pH 8.0. Prepare freshly before use!

Solubilization of inclusion bodies

Lysis Buffer C, pH 7.6: Supplement 50 ml PBS (pH 7.4) with 1% (v/v) Triton® X-100.

Wash Buffers 1 to 11:   Supplement 50 ml PBS (pH 7.4) with one of the following detergents/denaturants:

Wash Buffer 1, pH 7.6	3 g	urea [1 M]
Wash Buffer 2, pH 7.7	6 g	urea [2 M]
Wash Buffer 3, pH 7.8	12 g	urea [4 M]
Wash Buffer 4, pH 7.5	0.1 g	N-lauroyl-sarcosine [0.2% w/v]
Wash Buffer 5, pH 7.5	0.25 g	N-lauroyl-sarcosine [0.5% w/v]
Wash Buffer 6, pH 7.6	0.5 g	N-lauroyl-sarcosine [1% w/v]
Wash Buffer 7, pH 7.4	0.5 ml	Tween®-20 [1% v/v]
Wash Buffer 8, pH 7.6	0.5 g	CHAPS (3-[(3-Cholamidopropyl)dimethyl ammonio]-1-propanesulfonate) [1% w/v]
Wash Buffer 9, pH 7.5	0.5 g	guanidine hydrochloride [1% w/v]
Wash Buffer 10, pH 8.1	24.03 g	urea [8 M]

Hartree-Lowry protein determination

Hartree BSA stocks: Dissolve 1 mg bovine serum albumin (BSA) in 1 ml Aqua dest.
(0.1 mg BSA/ml)   and check the absorbance at 280 nm ($A_{280} = 0.67$). Calculate the exact concentration and make appropriate dilutions to a final concentration of 0.1 mg/ml. The 0.1 mg/ml stocks are used for calibration curves. Freeze aliquots at -20 °C.

Hartree Solution A: 2 g potassium sodium tartrate
90 g Na_2CO_3 anhydrous
450 ml 1 M NaOH
Fill up to 1 L with Aqua dest. and store at 4 °C.

Hartree Solution B: 2 g potassium sodium tartrate
1 g $CuSO_4$ x $5H_2O$
10 ml 1 M NaOH
Fill up to 100 ml with Aqua dest. and store at 4 °C.

Hartree Solution C: 1 ml Folin-Ciocalteu's phenol reagent (Merck)
14 ml Aqua dest.
Prepare freshly before use.

β-Gal Buffer A, pH 4.0:	100 mM trisodium citrate dihydrate (2.941 g/100 ml)
	100 mM citric acid monohydrate (2.1 g/100 ml)
	100 mM NaCl (0.5844 g/ 100 ml)
	0.02% NaN_3 (20 mg/100 ml)
	Mix trisodium citrate dehydrate solution and citric acid monohydrate solution to pH 4.0. Add NaCl and NaN_3, and adjust to pH 4.0.

β-Gal Buffer B, pH 4.0:	100 mM citric acid monohydrate (2.1 g/100 ml)
	200 mM Na_2HPO_4 x $2H_2O$ (3.56 g/100 ml)
	100 mM NaCl (0.5844 g/100 ml)
	Mix 122.9 ml of citric acid monohydrate solution and 77.1 ml Na_2HPO_4 x $2H_2O$ solution to pH 4.0. Add NaCl and adjust to pH 4.0.

β-Gal Substrate Solution A:	0.5 mM 4-methylumbelliferyl-β-D-galactopyranoside in β-Gal Buffer A (pH 4.0)

β-Gal Substrate Solution B:	2 mM 4-methylumbelliferyl-β-D-galactopyranoside in β-Gal Buffer B (pH 4.0)

0.6 mM β-Gal Substrate Solution:	0.6 mM 4-methylumbelliferyl-β-D-galactopyranoside in β-Gal Buffer A (pH 4.0)

Stop Buffer A, pH 10.4:	400 mM glycine/NaOH

Stop Buffer B, pH 10.6:	200 mM glycine/NaOH

4-MU Standard A: Prepare 562.5 µM stocks by dissolving 1.115 mg 4 - methylumbelliferone in 10 ml Stop Buffer A (pH 10.4). Fractionate and freeze at -20 °C. Dilute 16 µl of stock in10 ml Stop Buffer A, and add 300 µl of this dilution to 2.7 ml Stop Buffer A (= Standard_b; final concentration of 0.09 µM); Stop Buffer A serves as Standard_a in enzymatic measurements.

4-MU Standard B: Prepare 500 µM stocks by dissolving 8.81 mg 4-methylumbelliferone in 100 ml Aqua dest., and dilute to 50 µM 4-MU stocks. Check the absorbance at 323 nm (A_{323} = 0.744) and store aliquots at -20 °C. Prepare calibration solution just prior use by diluting the 50 µM stocks to 1 µM with Stop Buffer B (pH 10.6).

β-Hex determination

β-Hex Buffer A, pH 4.6:   100 mM trisodium citrate dihydrate (2.941 g/100 ml)

100 mM citric acid monohydrate

0.04% NaN_3 (20 mg/100 ml)

0.2% bovine serum albumin (0.2 g/100 ml)

Mix trisodium citrate dehydrate solution and citric acid monohydrate solution to pH 4.6. Add BSA and NaN_3, and adjust to pH 4.6.

β-Hex Buffer B, pH 4.4:   100 mM citric acid monohydrate (2.1 g/100 ml)

200 mM Na_2HPO_4 x $2H_2O$ (3.56 g/100 ml)

0.05% (w/v) bovine serum albumin (BSA)

Mix citric acid monohydrate solution and Na_2HPO_4 x $2H_2O$ solution to pH 4.4. Add BSA and adjust to pH 4.0.

β-Hex Substrate Solution A: 1 mM 4-methylumbelliferyl-N-acetyl-β-D-glucosaminide in β-Hex Buffer A (pH 4.6)

β-Hex Substrate Solution B: 5 mM 4-methylumbelliferyl-N-acetyl-β-D-glucosaminide in β-Hex Buffer B (pH 4.4)

SDS-PAGE

2x Laemmli Sample Buffer:

1 ml 0.5 M Tris-HCl (pH 6.8)

400 mg sodium dodecyl sulfate (SDS)

300 mg dithiothreitol (DTT)

20 mg Brilliant Blue R

2 g glycerol

10 ml Aqua dest.

Add exactly 10 ml Aqua dest., do not fill up! Make aliquots and freeze at -20 °C.

Resolving gel 10%:
(2 x 1.5 mm gels)

4.8 ml Aqua dest.

2.5 ml Rotiphorese® Gel 40 (19:1) (Roth®)

2.5 ml Tris-HCl (1,5 M, pH 8.8)

100 µl 10% (w/v) SDS solution, mix carefully

100 µl 10% (w/v) ammonium persulfate (APS), mix carefully

10 µl TEMED, mix carefully

Pour within 30 sec and overlay with 2-propanol carefully.

Wait 20 min for polymerization.

Pour off 2-propanol when gel has polymerized.

Stacking gel 10%:
(2 x 1.5 mm gels)

950 µl Aqua dest.

500 µl Rotiphorese® Gel 40 (19:1) (Roth®)

260 µl Tris-HCl (1 M, pH 6.8)

20 µl 10% (w/v) SDS solution, mix carefully

20 µl 10% (w/v) APS, mix carefully

2 µl TEMED, mix carefully

Pour within 30 sec and insert comb.

Wait 20 min for polymerization.

Resolving gel 12.5%:	2.99 ml Aqua dest.
(2 x 0.75 mm gels)	3.12 ml Rotiphorese® Gel 40 (19:1) (Roth®)
	3.75 ml Tris-HCl (1,5 M, pH 8.8)
	50 µl 10% (w/v) SDS solution, mix carefully
	48 µl 10% (w/v) APS, mix carefully
	10 µl TEMED, mix carefully
	Pour within 30 sec and overlay with 2-propanol carefully.
	Wait 20 min for polymerization.
	Pour off 2-propanol when gel has polymerized.

Stacking gel 5%:	3.69 ml Aqua dest.
(2 x 1.5 mm gels)	562.5 µl Rotiphorese® Gel 40 (19:1) (Roth®)
	625 µl Tris-HCl (0.5 M, pH 6.8)
	25 µl 10% (w/v) SDS solution, mix carefully
	25 µl 10% (w/v) APS, mix carefully
	5 µl TEMED, mix carefully
	Pour within 30 sec and insert comb.
	Wait 20 min for polymerization.

1.5 M Tris-HCl, pH 8.8:	Dissolve 27.43 g Tris base in 80 ml Aqua dest. and adjust pH 8.8 with HCl. Fill up to 150 ml with Aqua dest. and store at 4 °C.

1 M Tris-HCl, pH 6.8:	Dissolve 12 g Tris base in 60 ml Aqua dest. and adjust pH 6.8 with HCl. Fill up to 100 ml with Aqua dest. and store at 4 °C.

0.5 M Tris-HCl, pH 6.8:	Dissolve 12.114 g Tris base in 200 ml Aqua dest. and adjust pH 6.8 with HCl. Fill up to 200 ml with Aqua dest. and store at 4 °C.

10% (w/v) APS:	Dissolve 100 mg ammonium persulfate (APS) in 1 ml Aqua dest. and store at 4 °C. Prepare freshly every 2 weeks.

10% (w/v) SDS: Dissolve 10 g sodium dodecyl sulfate (SDS) in 90 ml Aqua dest. and fill up to 100 ml with Aqua dest.. Store at room temperature.

10x Running Buffer:

30.3 g Tris base [250 mM]
144.1 g glycine [192 mM]
10.0 g SDS [0.1% (w/v)]
Fill up to 1 L with Aqua dest..
Dilute 100 ml 10x stock with 900 ml Aqua dest. for final use.

Coomassie Dye:

7.5% (v/v) 100% acetic acid (glacial) [37.5 ml/500 ml]
50% (v/v) 100% ethanol [250 ml/500 ml]
0.25% (w/v) Brilliant Blue R [1.25 g/500 ml]
42.5% (v/v) Aqua dest. [212.5 ml/500 ml]

Coomassie Destaining Solution:

7.5% (v/v) 100% acetic acid (glacial) [75 ml/L]
20% (v/v) 100% ethanol [200 ml/L]
72.5% (v/v) Aqua dest. [725 ml/L]

Low Molecular Weight-SDS Marker:
(LMW-SDS Marker)

Dissolve LMW-SDS Marker powder (GE Healthcare) in 100 µl 1x Running Buffer, and fractionate in 10 µl aliquots. Mix 1:1 with 2x Laemmli Sample Buffer and centrifuge briefly. Incubate 5 min at 95 °C, centrifuge and freeze at -20 °C.

10x TBS:

24.2 g Tris base [200 mM]
80 g NaCl [1.37 M]
Dissolve in 800 ml Aqua dest. and adjust pH 7.6 with concentrated HCl.
+ 10 ml Tween® 20
Fill up to 1 L with Aqua dest..
Dilute 100 ml 10x stock with 900 ml Aqua dest. for final use.

Western blotting

Transfer Buffer: 100 ml 10x Running Buffer (see SDS-PAGE)

200 ml methanol

700 ml Aqua dest.

5% (w/v) Milk Blocking Buffer: Dissolve 50 g non-fat dry milk (Bio-Rad) in 1x TBS and adjust pH to 7.4. Fill up to 1 L with Aqua dest. and prepare 50 ml aliquots. Store at -20 °C.

3% (w/v) BSA Blocking Buffer: Dissolve 30 g bovine serum albumin (BSA) in 1x TBS and adjust pH to 7.4. Fill up to 1 L with Aqua dest., filtrate and prepare 50 ml aliquots. Store at -20 °C.

Immunostaining

2% (w/v) BSA Solution: Dissolve 2 g bovine serum albumin (BSA) in 100 ml PBS (pH 7.4) and add 0.04% NaN_3. Store at 4 °C.

Rinsing Solution: Mix 50 µl Tween® 20 with 100 ml PBS (pH 7.4). Store at 4 °C.

2x SSC Buffer, pH 7.0:   30 mM tri-sodium citrate dihydrate

30 mM citric acid monohydrate

300 mM NaCl

Dissolve 8.82 g tri-sodium citrate dehydrate in 1 L Aqua dest., and prepare a citric acid solution by dissolving 6.3 g in 1 L Aqua dest.. Mix solution to a final pH of 7.0, add 0.3 M NaCl and adjust pH.

Mowiol Solution: Dilute 5 g Mowiol (Hoechst) in 18.5 ml PBS (pH 7.4), add 5 ml 87% (w/v) glycerol, and incubate for 16hrs at room temperature. Centrifuge mixture at 12,000 rpm and dilute in Aqua dest. if necessary. Store at 4 °C.

Buffer for iminosugars

Phosphate Buffer for Inhibitors, pH 7.0:
(PhoBI)

10 mM Na_2HPO_4 x $2H_2O$
10 mM NaH_2PO_4 x H_2O
100 mM NaCl
0.01% NaN_3
0.01% Triton® X-100
Mix Na_2HPO_4 x $2H_2O$ solution and NaH_2PO_4 x H_2O solution to pH 7.0. Add NaCl, Triton, and NaN_3, and adjust to pH 7.0.

Purification of β-galactosidase from CHO-K1 medium

Phosphate Buffer I, pH 7.0:

10 mM Na_2HPO_4 x $2H_2O$
10 mM NaH_2PO_4 x H_2O
100 mM NaCl
0.02% NaN_3
Mix Na_2HPO_4 x $2H_2O$ solution and NaH_2PO_4 x H_2O solution to pH 7.0. Add NaCl and NaN_3. Adjust to pH 7.0.

Sodium Acetate Buffer I, pH 4.3:

20 mM sodium acetate
300 mM NaCl
0.1 mM DTT
Adjust pH 4.3 with acetic acid (glacial) 100%.

Elution Buffer GL, pH 7.0:

10 mM Na_2HPO_4 x $2H_2O$
10 mM NaH_2PO_4 x H_2O
1 M NaCl
0.1 mM DTT
100 mM D(-)-Galactonic acid-γ-lactone
Mix Na_2HPO_4 x $2H_2O$ solution and NaH_2PO_4 x H_2O solution to pH 7.0. Add NaCl, DTT, and galactonolactone, and adjust to pH 7.0. Always prepare freshly!

4 RESULTS

4.1 Cloning of a C-terminal tagged *GLB1-HIS* construct

To obtain C-terminal polyhistidine-tagged β-Gal protein, the protein coding sequence (CDS) of the *GLB1* gene (NCBI #NM_000404.2; transcript variant 1), encoding the human lysosomal acid β-galactosidase (EC 3.2.1.23), was cloned into the pET-21d(+) plasmid (Novagen). This plasmid satisfied all desired criteria such as providing an integrated C-terminal His-Tag® sequence, a strong promoter (T7) for rapid and high-yield protein expression, an adequate multiple cloning site, and a convenient resistance marker (ampicillin) for plasmid selection. However, pET-21d(+) is a rather large plasmid (5,440 bp), and long insert sequences like the *GLB1* CDS (2,034 bp) might cause problems during cloning. Therefore, the possibility of cloning both the full length sequence and a specific, short segment of the *GLB1* CDS was considered. If well-chosen, the latter strategy would produce a smaller β-Gal peptide, likewise capable of inducing an immune response against the antigen.

The optimal sites for cloning of the full length *GLB1* CDS into pET-21d(+) were the restriction sites for *XhoI* (158) and *NcoI* (234), located in the multiple cloning site (MCS) of the plasmid (Figure 4.1.1.). Both enzymes are unique cutters in the target vector, but do not cut the *GLB1* CDS. The *XhoI* restriction site is adjacent to the His-Tag® coding region (140-157). For cloning purposes it was necessary to generate an insert containing the *NcoI* restriction site right before the start codon, and the *XhoI* sequence directly after the last β-Gal encoding nucleotide (5'>3').
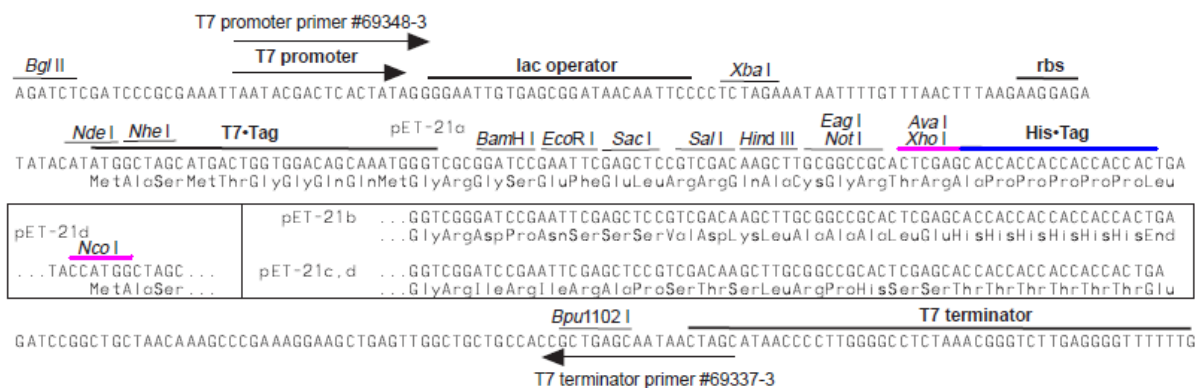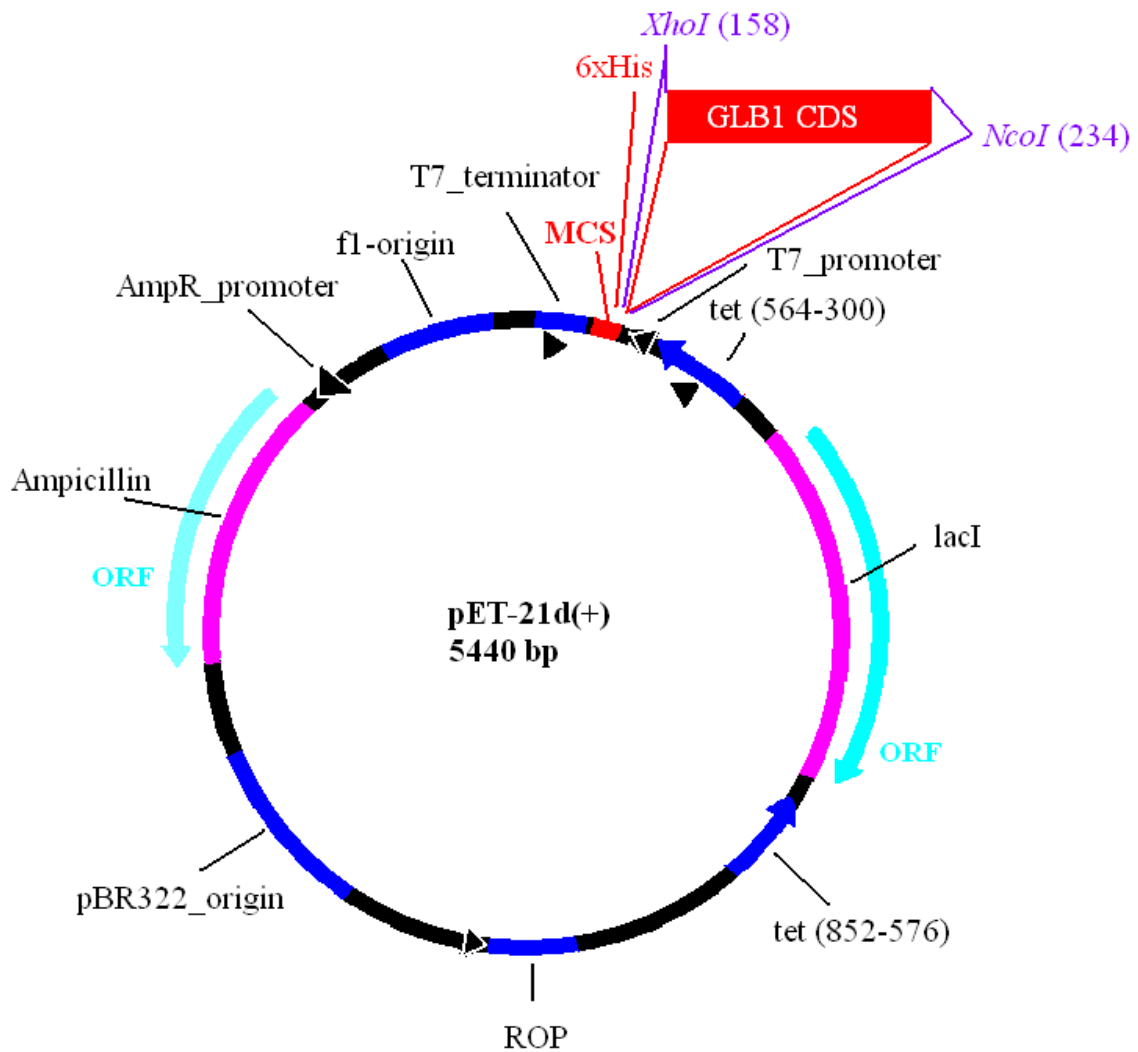
Figure 4.1.1 Vector map of pET-21d(+) and location of cloned *GLB1 CDS* insert. Numbers indicate the positions within the vector. The insert was integrated between the *Xho*I and *Nco*I restriction sites. A His-Tag® sequence is located adjacent to the *Xho*I restriction site of the vector. Vector maps and features were adapted from the Novagen Manual TB036 and from the Vector Database (www.lablife.org).

4.1.1 Amplification and preparation of the GLB1 CDS insert

The protein coding sequence (CDS) of the *GLB1* gene (NCBI #NM_000404.2, transcript variant 1) was amplified by polymerase chain reaction (PCR) using the pcDX-x-[*GLB1*] vector DNA (5,511 bp) as a template. This vector was constructed and provided by A. d'Azzo, St. Jude Children's Research Hospital, Memphis, USA. Briefly, the *GLB1* cDNA was integrated into the pcDX-x plasmid (3,102 bp) at the *EcoR*I cloning site. The total size of the *GLB1* insert is 2,409 bp, consisting of the *GLB1* CDS (2,034 bp), non-coding regions flanking the β-Gal coding sequence, and short stabilization stretches adjacent to the *EcoR*I restriction sites. The non-coding regions result from cDNA synthesis of 5' and 3' untranslated regions (UTRs), and the poly(A) tail in the mRNA template (Figure 4.1.1.1).
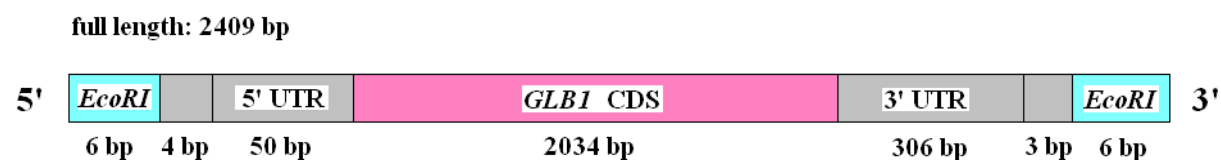
Figure 4.1.1.1 Features of the *GLB1* cDNA cloned into the pcDX-x vector. Sequence length is indicated below each fragment. UTR = untranslated region.

For a detailed list of PCR primers and conditions see section 3.4.1. The forward primer (Glb1Sfw) was designed to hybridize to 18 nucleotides of the *GLB1* CDS, beginning with the first nucleotide of the start codon. Additionally, the primer featured a 5'-overhang containing the sequence for *NcoI* restriction (C$^\vee$CATGG), and a short nucleotide stretch for improving cleavage efficiency as recommended by the manufacturer (http://www.neb.com/nebecomm/tech_reference/restriction_enzymes/cleavage_olignucleotides.asp).

The antisense primer (Glb1Srev) was similarly designed with 5'-overhangs for digestion with *XhoI* (C$^\vee$TCGAG*)*, a stabilization sequence, and hybridization to the last 21 nucleotides upstream of the stop codon in the *GLB1* CDS. It is crucial to eliminate the stop codon in this manner, since the PCR product was inserted upstream right before the His-Tag® sequence in pET-21d(+), thus enabling a read-through from the β-Gal start codon and across the His-Tag® stretch. A stop codon is integrated in the plasmid sequence itself downstream right after the

His-Tag® coding region. Expression of this construct would result in β-Gal protein, which is tagged with polyhistidine on its C-terminal end.

PCR was performed in 30 cycles with an elongation time of 4 min each, and annealing at 58 °C. *Pfu* DNA Polymerase (Promega) with 3'>5' exonuclease activity (proofreading) was used for DNA amplification. The resulting PCR product was verified by agarose gel electrophoresis, and subsequently purified from the agarose gel using the QIAquick Gel Extraction Kit (QIAGEN; cf. section 3.4.5.1). This step is necessary to remove primers, dNTPs, and salts from the PCR product, as they would interfere with further DNA manipulation techniques. Prior cloning of the *GLB1* CDS insert into the target vector, free ends were produced by double digest of the insert and vector DNA with the restriction enzymes *NcoI* and *XhoI*. The conditions are given in Table 4.1.1.2. In addition, the pET-21d(+) plasmid was treated with calf intestinal alkaline phosphatase (CIAP; Invitrogen™) for one hour at 37 °C to prevent re-ligation of free ends.

Component	Volume
Insert or plasmid DNA (1-5 µg)	variable
10x restriction buffer NEB 2	6 µl
100x purified bovine serum albumin (BSA) (10 mg/ml, NEB)	0.6 µl
NcoI (10 U/µl; NEB)	3 µl
XhoI (20 U/µl; NEB)	3 µl
Aqua dest. to final volume of:	60 µl

Table 4.1.1.2 Digestion assay with the restriction enzymes *NcoI* and *XhoI*. NEB = New England Biolabs®

Again the DNA was applied to agarose gels and extracted from the gel as mentioned above. Finally, the *GLB1* CDS insert and pET-21d(+) DNA were ligated using 140 ng insert DNA (~2.1 kb) and 120 ng vector DNA (~5.4 kb) according to the protocol provided by the manufacturer (see section 3.4.3). Briefly, the reaction was catalyzed by addition of 1 µl T4 DNA Ligase (1 U/µl; Invitrogen™) and incubation for 2 hrs at room temperature. The necessary amounts of DNA were calculated according to the following scheme:

(kb insert DNA / kb vector DNA) x ng vector DNA x 3 = ng insert DNA [ratio i:v = 3:1]

4.1.2 Transformation of BL21(DE3) cells and selection of positive transformants

Transformation of chemically competent *E. coli* One Shot® BL21(DE3) cells with 3 µl of the ligation reaction (13 ng/µl) was performed according to the Invitrogen™ user manual [Invitrogen™ 28-0182]. Positive clones were selected on Luria Agar plates containing 100 µg/ml ampicillin (LBA plates; see section 3.13) by incubation over night at 37 °C. Due to direct cloning into the expression host strain, the number of positive transformants was low. Only 12 and 16 transformants were visible on the selection media after overnight incubation respectively, and all of them were picked and grown separately as overnight cultures in Luria Broth medium supplemented with 100 µg/ml ampicillin (LBA medium; see section 3.13) for preparation of glycerol stocks and further experiments.

To verify successful insert integration, vector DNA of 12 selected transformants (from agar plate 2; subsequent designation of transformants: T-2/x) was purified using the QIAprep® Spin Miniprep Kit (QIAGEN), and digested with specific restriction enzymes. The restriction enzymes used to identify pET-21d(+)-[*GLB1-HIS*] constructs and anticipated products sizes are shown in Table 4.1.2.1. Digestion assay procedures are given in Table 4.1.2.2.

Restr. enzyme	Position of restriction site:			Fragment size after restriction:
	Pos. of cut in pET-21d(+) (circular)	Pos. of cut in *GLB1* CDS (linear)	Pos. of cut in pET-21d(+)-[*GLB1-HIS*] C-terminal His-Tag® (circular)	pET-21d(+)-[*GLB1-HIS*] C-terminal His-Tag®(circular)
SmaI	no cut	366, 1783	411, 1828	1,417 bp 5,984 bp
NdeI	no cut	1119, 1329	863, 1073	210 bp 7,191 bp
NcoI	234	no cut	2195	7,401 bp (linear)
XhoI	158	no cut	158	7,401 bp (linear)
NcoI + XhoI	158, 234	no cut	158, 2195	2,037 bp 5,364 bp

Table 4.1.2.1 Restriction site positions of selected enzymes and fragment sizes after DNA digestion.

Restriction sites in Table 4.1.2.1 were calculated with the Webcutter 2.0 software (http://rna.lundberg.gu.se/cutter2/).

Component	Volume
Insert or plasmid DNA (1-5 µg)	variable
10x restriction buffer NEB 2 or NEB 4	2 µl
100x purified bovine serum albumin (BSA) (10 mg/ml, NEB)	0.2 µl
SmaI (20 U/µl) *or NdeI* (20 U/µl) *or* *NcoI* (10 U/µl) + *XhoI* (20 U/µl)	1 µl
Aqua dest. to final volume of:	20 µl

Table 4.1.2.2 Preparation of DNA restriction digests for examination of positive clones.
NEB = New England Biolabs®

After *SmaI* digests (3 hrs at 25 °C), 8 of 12 tested transformants clearly showed two bands on the agarose gel (Figure 4.1.2.3), corresponding to the anticipated sizes listed in Table 4.1.2.1. The *SmaI* cut in linear insert DNA produces three fragments in the size of 251 bp, 366 bp, and 1,417 bp (lane 13). Both small fragments were clearly visible on the gel photo, but hard to see in the picture below. In contrast to negative transformants, the DNA band of 1,417 bp is also present in positive transformants (T2/1, T2/4, T2/5, T2/6, T2/7, T2/9, T2/11, T2/12). Fragment sizes are based on cutting positions calculated with the program Webcutter 2.0 (http://rna.lundberg.gu.se/cutter2/) on the basis of the *GLB1* protein coding sequence (NM_000404.2; transcript variant 1 2034 bp).
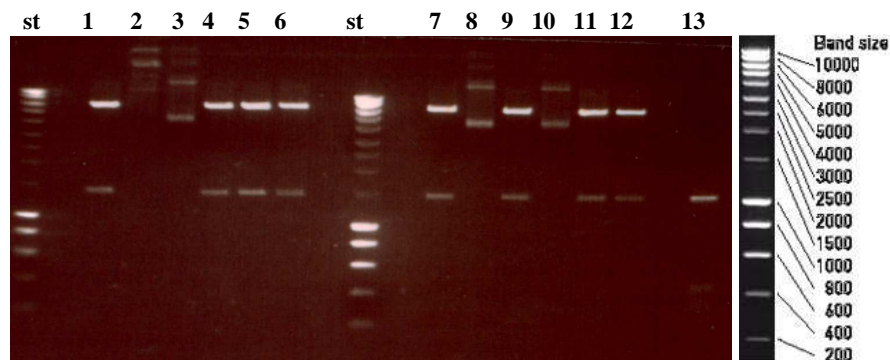
Figure 4.1.2.3 DNA restriction digests from transformants T2/1-T2/12 with *SmaI* (3 hrs). DNA from plasmid preparations was used for restriction digests, and the *GLB1* CDS (insert DNA) was used as a control. **(st)** 10 µl SmartLadder (Eurogentec); **(1)-(6)** 20 µl *SmaI* digested DNA of T2/1-T2/6; **(7)-(12)** 20 µl *SmaI* digested DNA of T2/7-T2/12; **(13)** 20 µl *SmaI* digested insert DNA (clean PCR product).

Additional digests were performed on the *SmaI*-positive clone T2/4 using *NdeI* (37 °C over night) and a combination of *NcoI/XhoI* (37 °C over night or 3.5 hrs), respectively (Figure 4.1.2.4). When digested with *NdeI*, the positive transformant T2/4 showed bands of 210 bp and

105

7,191 bp, while negative transformants were not cut at all by this enzyme (Figure 4.1.2.4, B). As expected, the digested insert control displayed bands of 210 bp, 705 bp, and 1,119 bp (lane 6). After *NcoI*/*XhoI* double digests of T2/4 DNA, the two anticipated bands of 2,037 bp and 5,364 bp were visible on the agarose gel (Figure 4.1.2.4, lanes 7+10), but also small amounts of uncut DNA. Neither *Nco*I nor *Xho*I cut in the *GLB1* CDS, thus the size of the PCR product was not changed (Figure 4.1.2.4, lanes 9+12.). Results of the restriction digests clearly showed that transformant T2/4 has successfully taken up the pET-21d(+)-[*GLB1-HIS*] vector.
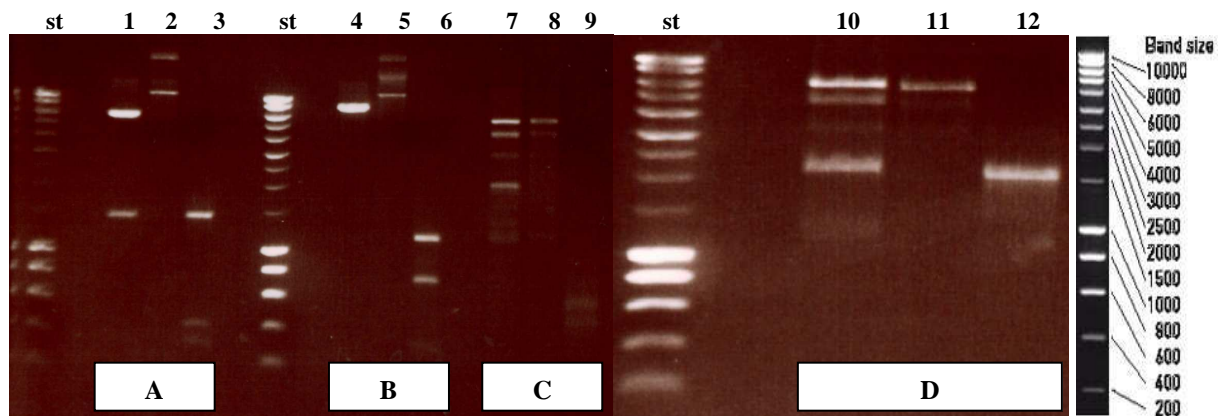
Figure 4.1.2.4 DNA restriction digests of the positive transformant T2/4 and controls with *SmaI*, *NdeI*, and *NcoI/XhoI*, respectively. DNA from plasmid preparations was used for restriction digests, and the *GLB1* CDS (insert DNA) was used as additional control. **(A)** *SmaI* (ON); **(B)** *NdeI* (ON); **(C)** *NcoI/XhoI* (ON); **(D)** *NcoI/XhoI* (3.5 hrs). **(st)** 10 µl SmartLadder (Eurogentec); **(1)**+**(4)**+**(7)**+**(10)** 20 µl T2/4 DNA; **(2)**+**(5)**+**(8)**+**(11)** 20 µl negative control DNA (pET-21d(+)); **(3)**+**(6)**+**(9)**+**(12)** 20 µl insert DNA (clean PCR product). ON = over night.

To eliminate any possibility of replication errors, DNA sequence analysis (forward and reverse) was performed by the Austrian company IBL (Vienna). The PCR products were provided by our lab. Five different primer pairs (see section 3.4.1.1) were necessary to generate short, overlapping DNA stretches, adding up to the full length *HIS-GLB1* insert (Figure 4.1.2.5). In accordance with the lab custom, AmpliTaq Gold® DNA Polymerase (Roche) was used for the reactions. PCRs were conducted according to the Taq Polymerase scheme (cf. section 3.4.1) in 35 cycles, with 55 °C annealing temperature and an extension time of 2 min, respectively. Direct comparison of DNA sequence analysis results with the target sequence showed no alterations in the cloned sequence. Therefore, the positive clone T2/4 should be able to express C-terminally polyhistidine-tagged human lysosomal acid β-galactosidase (C-His®-Gal).
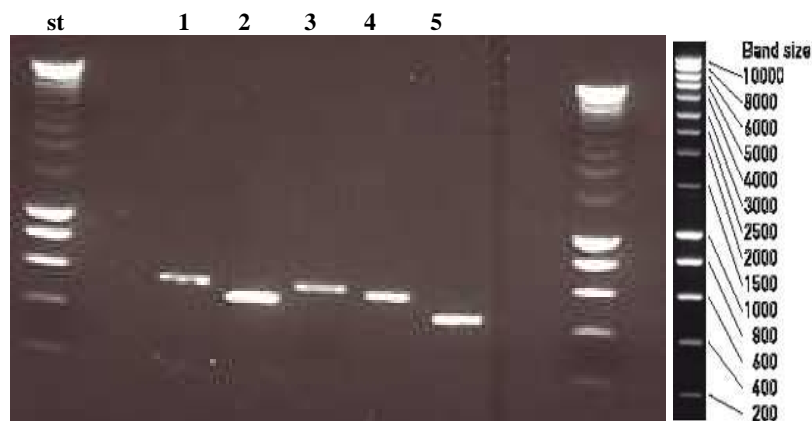
Figure 4.1.2.5 PCR amplification of the fusion protein encoding region from the positive transformant T2/4 for DNA sequencing. (st) 10 µl SmartLadder (Eurogentec); lanes 1-5: 5 µl PCR products obtained with the primer pairs listed in Table 3.4.1.1.1. The following product sizes were obtained: **(1)** ~560 bp; **(2)** 488 bp; **(3)** 549 bp; **(4)** 524 bp; **(5)** ~450 bp.

4.2   Cloning of an N-terminal tagged *HIS-GLB1* construct

A second, quite similar cloning strategy was pursued to obtain N-terminal polyhistidine-tagged β-Gal protein. Some heterologously expressed proteins showed increased intracellular stability when N-terminally tagged with polyhistidine, while C-terminal tagged fusion proteins were rapidly degraded by host proteases. The C-terminal end of the human β-Gal precursor undergoes post-translational, intralysosomal proteolytic processes to form the mature enzyme (cf. section 1.3). Two serine residues at position 543 and 544 (Ser543 and Ser544) and an arginine at position 530 (Arg530) are involved in these poorly understood cleavage processes [van der Spoel *et al*., 2000; Yamamoto *et al*., 1990]. It was expected that the resulting His®-β-Gal fusion protein might be more stable in the *E. coli* expression host cells than the C-terminal tagged β-Gal-His® fusion protein.

For cloning of an N-terminal polyhistidine-tagged construct into the pET-21d(+) plasmid, it was necessary to amplify the CDS of *GLB1* (NCBI #NM_000404.2, transcript variant 1) with an additional sequence encoding the His-Tag®. The pET-21d(+) plasmid features the His-Tag® sequence for C-terminal tagging only, thus the desired new His-Tag® must be created as part of the insert. In contrast to the C-terminal construct, where the polyhistidine sequence was adjacent to the *XhoI* restriction site of the plasmid, the N-terminal polyhistidine stretch must be located downstream right after the *NcoI* site. Another major difference is the position of the start and stop codon in the PCR-generated insert. In order to express the fusion protein, starting with the N-terminal His-Tag®, it was necessary to create a construct containing a start codon (ATG) between the *NcoI* site and the polyhistidine encoding region, followed by the *GLB1*

CDS, and a stop codon upstream right before the *XhoI* sequence. The stop codon prevents a read-through to the His-Tag® sequence originally featured in the plasmid.

4.2.1 Amplification and preparation of the GLB1 CDS insert

To realize this concept, a new primer pair was designed and used for the PCR amplification of the *GLB1* CDS, with pcDX-x-[*GLB1*] as template. The forward primer (NHis2GLBfw) featured a 5'-overhang containing sequences for *NcoI* restriction (C$^\vee$CATGG) including a stabilization stretch, two more nucleotides of the plasmid sequence to maintain the open reading frame (ORF), the His-Tag® coding region, and finally the sequence to hybridize to 20 nucleotides of the *GLB1* CDS (pos. 4-23). The antisense primer (NHisGLBrev) was designed with a short 5'-overhang including the *XhoI* restriction site with a stabilization stretch, and the *GLB1* CDS hybridizing sequence (pos. 1992-2034; 43 nucleotides) including the stop codon (Figure 4.2.1.1).
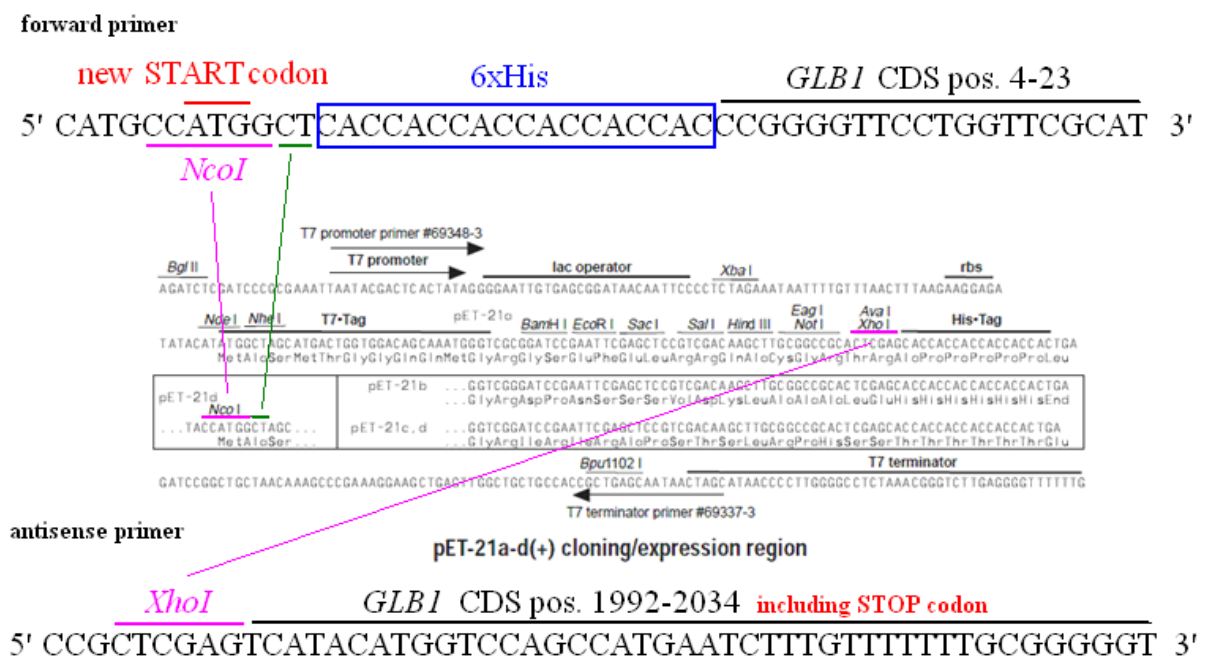
Figure 4.2.1.1 Location of cloned *GLB1* CDS insert in the pET-21d(+) vector sequence. Numbers indicate the positions within the vector. The insert was integrated between the *Xho*I and *Nco*I restriction sites. A His-Tag® sequence was inserted adjacent to the *Nco*I restriction site of the vector. Sequence illustration was adapted from the Novagen Manual TB036.

PCR was performed in 35 cycles with an elongation time of 4 min each, and annealing at 68.5 °C. The AmpliTaq Gold® DNA Polymerase (Roche) was used instead of the *Pfu* DNA Polymerase (Promega), although the Taq Polymerase had no proofreading activity. This deficiency was tolerated, because PCRs using *Pfu* Polymerase were always problematic. Furthermore, DNA sequence analysis of the resulting construct was performed to identify potential replication errors like point mutations, insertions, or deletions. The following procedures are basically the same as described in section 4.1 (cf. also section 3.4). Insert and plasmid DNA was digested with *NcoI* (10 U) and *XhoI* (20 U) for 6 hrs at 37 °C, followed by dephosphorylation of plasmid DNA for 30 min at 37 °C by addition of 1 µl CIAP. Digested DNA was checked on agarose gels, cleaned from the gels, and ligated for 16 hrs at 16 °C. For the ligation reaction, 100 ng plasmid DNA (5.44 kb) and 120 ng insert (~2.1 kb) DNA were used [ratio i:v = 3:1]. DNA amounts are based on calculations with the Ligation calculator (http://www.insilico.uni-duesseldorf.de/Lig_Input.html).

4.2.2 Transformation of BL21(DE3) cells and selection of positive transformants

A general cloning host strain was transformed with the ligation reaction instead of direct transformation of BL21(DE3) expression cells. This procedure increases the yield of positive transformants, and can also prevent loss of the vector during long-term storage. The cloning host of choice was the *E. coli* NovaBlue strain. As NovaBlue cells were not commercially available, they were kindly provided by Astrid Gruber (Department of Structural Biology, Karl-Franzens-University, Graz). Transformants were selected on LBA plates and incubated over night at 37 °C. From hundreds of colonies, four were picked and grown separately as overnight culture (ONC) in LBA medium to prepare glycerol stocks for further experiments. Plasmid DNA was purified with the QIAprep Spin Miniprep Kit (QIAGEN) and used as template in PCRs to verify insert integration. PCR was performed with T7 universal primers according to the Taq DNA Polymerase scheme (cf. section 3.4). The primer sequences were derived from commercially available T7 primers, but synthesized by TIB® MOLBIOL (Berlin, Germany). Reaction was performed in 35 cycles, with an annealing temperature of 55 °C, and 4 min elongation time. Results are shown in Figure 4.2.2.1.
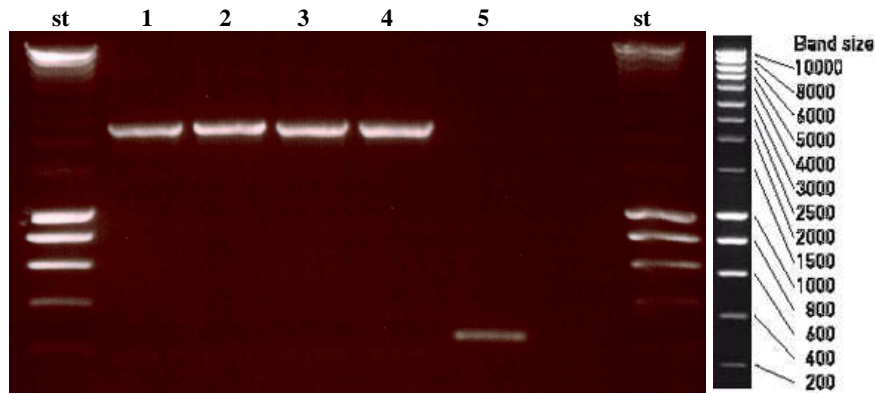
Figure 4.2.2.1 PCR amplification of insert DNA from transformants T1-T4 and negative control. DNA from plasmid preparations was used as PCR template, and the region between the T7 universal primer binding sites was amplified. **(st)** 10 µl SmartLadder (Eurogentec); **(1)-(4)** 6 µl PCR product from transformants T1-T4, respectively; **(5)** 6 µl PCR product from negative control plasmid, pET-21d(+).

On the agarose gel, all four tested transformants showed a ~2.1 kb band corresponding to the insert size (calculated 2,070 bp), while the negative control displayed only a small ~300 bp band, resulting from amplification of the MCS sequence between the primer binding sites in the empty vector (calculated 256 bp). After insert verification, *E. coli* One Shot® BL21(DE3) cells (Invitrogen™) were transformed with the pET-21d(+)-[*HIS-GLB1*] vector according to the Invitrogen™ protocol, and transformants were selected on LBA plates by overnight incubation at 37 °C. Vector DNA for this transformation was prepared from transformant T1 (cf. lane 1). As expected, transformation efficiency was much higher compared to the direct cloning strategy described in section 4.1. From thousands of transformants, one was picked and grown as ONC for subsequent glycerol stock and DNA preparation. This transformant was also denominated T1, and subsequent citations refer to this specific clone (BL21(DE3)-pET-21d(+)-[*HIS-GLB1*]).

DNA sequence analysis (forward and reverse) of the fusion protein encoding region was performed by IBL (Vienna). The PCR products were provided by our lab, and reactions were performed with the primers and conditions described in section 3.4.1.1. Direct comparison of DNA sequence analysis results with the target sequence showed no alterations in the cloned sequence. Therefore, the positive clone T1 should be able to express N-terminally polyhistidine-tagged human lysosomal acid β-galactosidase (N-His®-Gal).
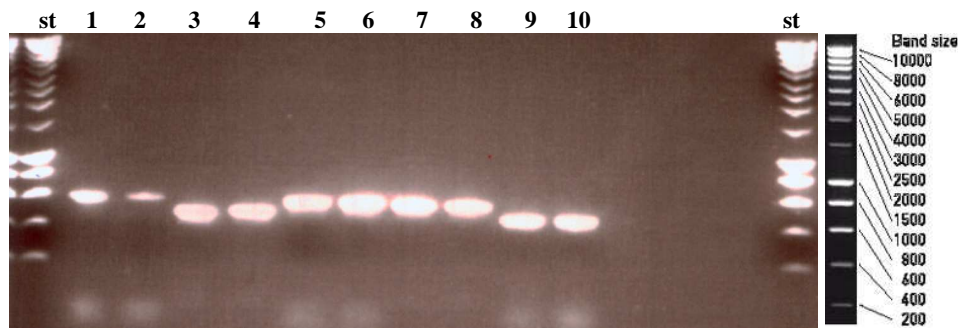
Figure 4.2.2.2 PCR amplification of the fusion protein encoding region from the positive transformant T1 for DNA sequencing. (st) 10 µl SmartLadder (Eurogentec); **lanes 1-10:** 10 µl PCR products obtained with the primer pairs listed in Table 3.4.1.1.1. The following product sizes were obtained: **(1)+(2)** ~560 bp; **(3)+(4)** 488 bp; **(5)+(6)** 549 bp; **(7)+(8)** 524 bp; **(9)+(10)** ~450 bp.

4.3   Cloning of N-terminal tagged *GST-GLB1* constructs

A third strategy was pursued for cloning the *GLB1* CDS into a bacterial vector and its subsequent expression in *E. coli* cells. Therefore, β-Gal protein was tagged with glutathione S-transferase (GST; M_r 26,000), a soluble protein readily expressed in appropriate host cells, and often helpful for stabilization of the fusion protein. To increase the chances of success, the full *GLB1* CDS as well as a reduced sequence was fused with the *GST* gene, respectively. The nucleotide sequence corresponding to position 4-690 of the *GLB1* CDS and producing a β-Gal peptide chain of 229 aa was chosen for this purpose. The fusion protein consisting of the β-Gal sequence plus the 244 aa GST-tag (in total 473 aa) was denominated N-GST-Gal-peptide. It features the highly conserved residue Glu188 (cf. section 1.2), which was proposed as potential proton donor in the enzyme's catalytic reaction [Callahan, 1999]. The active site nucleophile Glu268 [Zhang *et al*., 1994] is not part of the truncated protein. BLAST searches (blastp; http://blast.ncbi.nlm.nih.gov) indicated a high antigenic specificity for this sequence, which is essential for obtaining anti-human-β-galactosidase antibodies after immunization of rabbits with the purified peptide. Solubility predictions were performed with programs available on the ExPASy Proteomics Server (Swiss Institute of Bioinformatics; http://www.expasy.ch).

The pGEX-6P-2 plasmid (provided by the Department of Structural Biology, Karl-Franzens-University, Graz; originally from GE Healthcare) was used as cloning vector. Its characteristic features include the *GST* gene for production of N-terminally tagged GST fusion proteins, the strong hybrid promoter *tac*, and the ampicillin resistance marker, amongst others. The main

111

advantage of N-terminal GST-tags is the high-level and stable expression of GST, which brings forward the expression of the fused protein and might increase the stability and solubility of the target protein.

The restriction sites for *SalI* (965) and *NotI* (976) in the MCS were chosen as insert cloning sites. Both enzymes do not cut the *GLB1* CDS, but are unique cutters in the target vector. The sites are located near the 3'-terminal end of the *GST* gene (258-993), allowing site specific insertion of *GLB1* DNA for the generation of N-terminal tagged GST-β-Gal fusion protein (Figure 4.3.1).
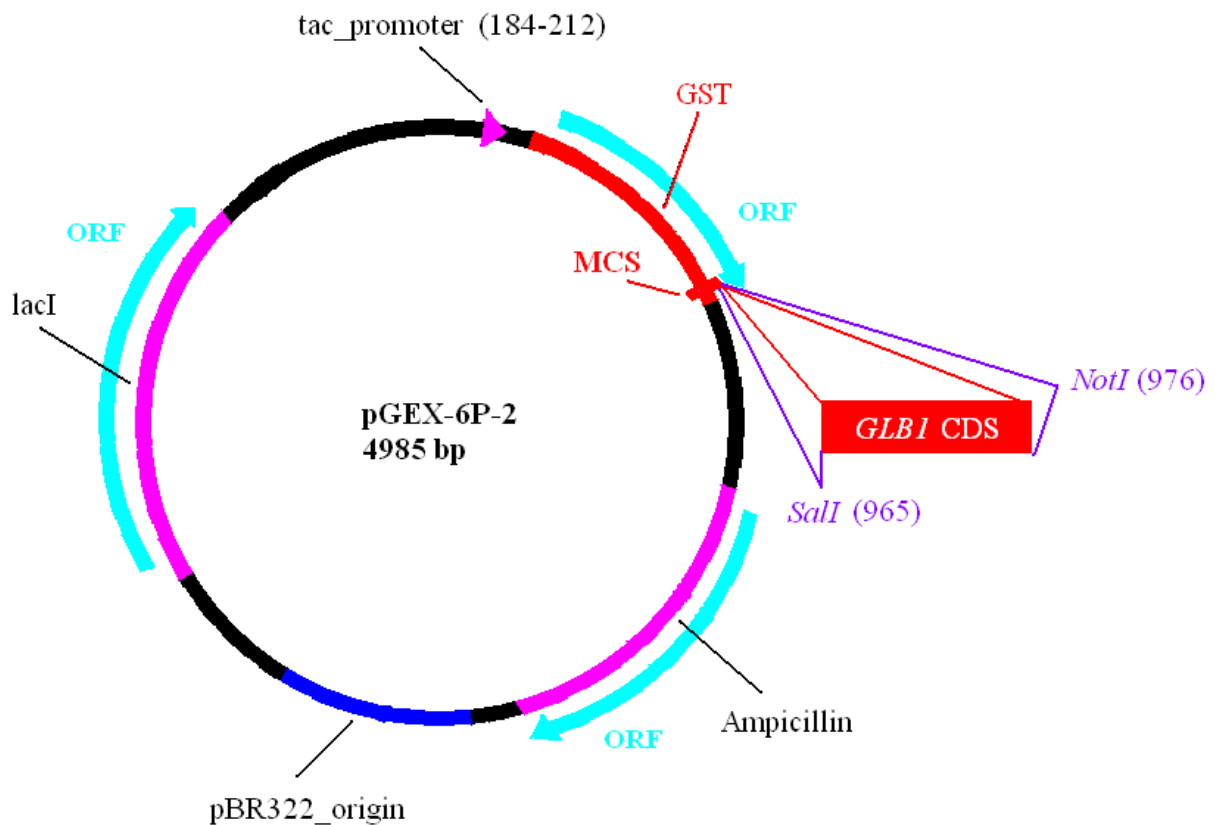
Figure 4.3.1 Vector map of pGEX-6P-2 and location of cloned *GLB1 CDS* insert. Numbers indicate the positions within the vector. The insert was cloned between the *Not*I and *Sal*I restriction sites, which are both integrated in the GST sequence, encoding an N-terminal GST-tag. Vector features were adapted from the Vector Database (www.lablife.org).

4.3.1 Amplification and preparation of the GLB1 CDS inserts

Again, the pcDX-x-[*GLB1*] vector DNA was used as PCR template for amplification of the full length, and the shortened CDS of *GLB1*, respectively. The forward primer (Glb1Sal2fw) was designed to hybridize to the first 23 nucleotides downstream the start codon of the *GLB1* CDS (pos. 4-26), and with a 5'-overhang containing the restriction site for *SalI* (G$^\vee$TCGAC) plus a stabilization stretch of 23 nt, surrounding the *SalI* sequence. This necessary stabilization sequence will inevitably be a part of the translated fusion protein. The antisense primer (Glb1Notrev) binds to the last 28 nt of *GLB1* CDS (pos. 2007-2034), and features the restriction site for *NotI* (GCGGCCGC) as well as stabilization sequences as 5'-overhang. For amplification of the peptide sequence, a second antisense primer (PepNotrev) was created. In contrast to Glb1Notrev, it hybridizes to pos. 659-690 of the *GLB1* CDS (32 nt). A stop codon sequence was attached to the 3'-terminal end of the *GLB1* sequence. Several attempts to amplify the full length target sequence with the *Pfu* DNA Polymerase failed, thus the AmpliTaq Gold® DNA Polymerase was used again. PCR amplification was performed according to the Taq Polymerase protocol (see section 3.4) in 35 cycles, with an annealing temperature of 63 °C and an elongation time of 4 min, respectively. For amplification of the peptide sequence, the *Pfu* DNA Polymerase was used. PCR was conducted according to the Promega scheme (35 cycles, 68 °C annealing, and 4 min elongation). After PCR product purification, insert and plasmid DNAs were double digested with *SalI* (20 U) and *NotI* (10 U) for 17 hrs at 37 °C. Additionally, plasmid DNA was dephosphorylated by addition of 1 µl CIAP for 30 min at 37 °C. Digested DNA was purified agarose gels and used for the ligation reaction. Briefly, 100 ng plasmid DNA (~5 kb) were ligated with 130 ng full length insert (~2.1 kb), or 64 ng peptide insert (~700 bp) for 16 hrs at 16 °C, respectively. Calculations were based on the insert:vector ratio of 3:1 and performed with the Ligation Calculator (http://www.insilico.uni-duesseldorf.de/Lig_Input.html).

4.3.2 Transformation of BL21 cells and selection of positive transformants

NovaBlue cells were transformed with either ~110 ng (full length construct), or ~80 ng vector DNA (peptide construct). Transformants were selected on LBA plates and incubated over night at 37 °C. The agar plate with the full length construct showed only one colony, while the peptide construct plate contained ~50 colonies. Positive transformants were picked and grown

as ONC for preparation of glycerol stocks and further experiments. Vector DNA (minipreps) was prepared from 12 peptide construct transformants (T1p-T12p), and the one full length construct clone (T1f), respectively. To verify successful insert integration, vector DNAs were double digested with *NotI* (10 U) and *SalI* (20 U) for 5 hrs at 37 °C. Results are illustrated in Figure 4.3.2.1. Upon double digestion, vector DNAs of each clone clearly showed two bands corresponding to the size of the empty vector (~5 kb) and the insert (2.1 kb or 700 bp), respectively.
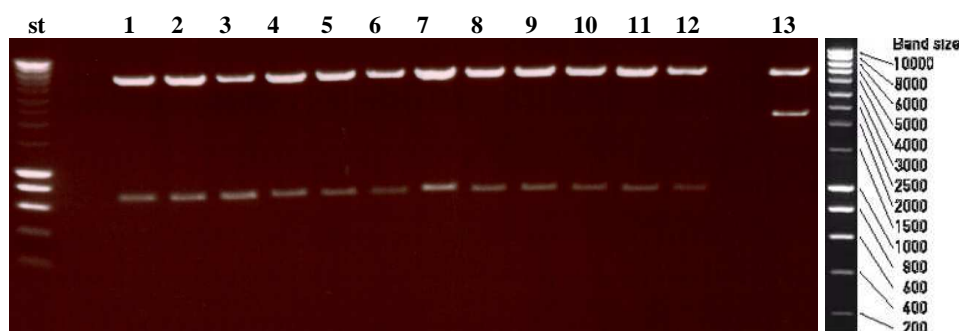
Figure 4.3.2.1 DNA restriction digests of positive transformants T1p-T12p and T1f with *NotI/SalI* (5 hrs). DNA from plasmid preparations was used for restriction digests **(st)** 10 µl SmartLadder (Eurogentec); **lanes 1-12:** 20 µl DNA from T1p-T12p, respectively; **(13)** 20 µl DNA from T1f.

An appropriate expression host strain, in this case *E. coli* BL21, was transformed with vector DNA containing the full length or the peptide construct sequence, respectively. Cells were selected on LBA plates and incubated over night at 37 °C. Each plate contained hundreds of colonies, but only one was picked from each plate (T1p and T1f), and cultivated as ONC for glycerol stocks and vector DNA preparation (minipreps). In addition to restriction enzyme digests with *SmaI* (15 hrs at 25 °C) and *NotI/SalI* (15 hrs at 37°C), respectively, positive transformants were checked by PCR with the universal primers pGEX3 and pGEX5, or p2fw and pGEX3 (cf. Table 3.4.1.1.1). Amplification was performed in 35 cycles (annealing 62 °C, elongation 4 min or annealing 55 °C, elongation 2 min) using AmpliTaq Gold® DNA Polymerase (Roche). PCR and restriction digest products are shown in Figure 4.3.2.2. All DNA bands illustrated in this figure were consistent with predicted DNA sizes (lanes 1+2: ~2.3 kb; lanes 3+4: ~200 bp; lane 5: ~900 bp; lane 6: ~200 bp; lane 7: ~350 bp; lane 8: no product; lane 9: linearization; lane 10: ~5.3 kb and ~370 bp; lane 11: linearization; lane 12: ~5 kb and ~800 bp).

Figure 4.3.2.2 Verification of correct insert integration in vector DNA of the positive transformants T1f and T1p. DNA from plasmid preparations was used for restriction digests and as template for PCRs. The region between the universal pGEX primer binding sites, and an internal *GLB1* CDS region was amplified. **(A)** pGEX3+pGEX5; **(B)** p2fw+pGEX3; **(C)** *Sma*I (15 hrs); **(D)** *Not*I/*Sal*I (15 hrs) **(st)** 10 µl SmartLadder (Eurogentec); **(1)+(2)** 25 µl T1f DNA; **(3)+(4)** 25 µl negative control DNA (pGEX-6P-2); **(5)+(7)+(10)+(12)** 10 µl T1p DNA; **(6)+(8)+(9)+(11)** 10 µl negative control DNA (pGEX-6P-2).

Both vectors, pGEX-6P-2-[*GST-GLB1*-f] (full length construct) and pGEX-6P-2-[*GST-GLB1*-p] (peptide construct), were partially sequenced in forward and reverse mode to verify correct insert integration and accurate nucleotide sequence. Again, DNA sequencing was performed by IBL using PCR products provided by our lab. Five different primer pairs were used for generation of overlapping sequences containing the full length construct, and two primer pairs for the short peptide coding sequence (cf. Table 3.4.1.1.1). Direct comparison of DNA sequence analysis results with the target sequence showed no alterations in the cloned sequence. Therefore, the positive clones T1f and T1p should be able to express N-terminally GST-tagged human lysosomal acid β-galactosidase (N-GST-Gal or N-GST-Gal-peptide).

Figure 4.3.2.3 PCR amplification of the fusion protein encoding region from the positive transformants T1f and T1p for DNA sequencing. (st) 10 µl SmartLadder (Eurogentec); **lanes 1-14:** 5 µl PCR products obtained with the primer pairs listed in Table 3.4.1.1.1. The following product sizes were obtained: **(1)+(2)** 583 bp; **(3)+(4)** 487 bp; **(5)+(6)** 549 bp; **(7)+(8)** 525 bp; **(9)+(10)** 429 bp; **(11)+(12)** 583 bp; **(13)+(14)** 403 bp.

4.3.3 Transformation of BL21(DE3)-[pG-KJE8] cells

For co-expression of GST-tagged β-Gal proteins and selected *E. coli* chaperones, chemical competent BL21(DE3) cells containing the pG-KJE8 (Takara Bio. Inc.) plasmid were transformed with pGEX-6P-2-[*GST-GLB1*-f] vector DNA (cf. Figure 4.3.1) according to the procedures described in section 3.4.4.4. The pG-KJE8 plasmid contains the genes for expression of certain *E. coli* chaperones, and is compatible for co-expression with pET-21d(+) in *E. coli* BL21 or BL21(DE3) cells. Co-expression of chaperones with the protein of interest might facilitate proper folding of the heterologously expressed protein, thus increasing stability and solubility in the host cells. BL21(DE3) cells already transformed with the pG-KJE8 vector were kindly provided by the Department of Biochemistry, Graz University of Technology.

Transformants were selected on LBAC Agar Plates and incubated over night at 37 °C. From a few tens of positive transformants, 10 were picked and grown as ONCs for further experiments and glycerol stock preparation. Even though growth on selection medium was indicating positive transformation with GST-β-Gal, PCR was conducted to verify vector uptake into BL21(DE3)-[pG-KJE8] cells. Reaction was performed according to the protocol for AmpliTaq Gold® DNA polymerase (see section 3.4), using the primers pGEX5 (sense) and p1rev (antisense) for specific amplification of a short DNA stretch from the 5'-terminal end of the *GST-GLB1* construct. The p1rev primer was designed to bind only in *GLB1* sequences. Annealing was performed at 62 °C and DNA strands were extended for 2 min per cycle. The resulting PCR product (583 bp) was present in the tested positive transformants, as well as in the positive controls (data not shown). One of verified positive transformants was chosen for expression and is subsequently designated as T1f-chap.

4.4 Heterologous protein expression for antibody development

The purpose of constructing C- or N-terminal tagged β-Gal proteins and expression in *E. coli* was solely the large-scale purification of human lysosomal acid β-galactosidase and subsequent immunization of rabbits for production of polyclonal anti-β-Gal-antibodies. In this work *E. coli* was chosen as expression host because it is the best-known model organism, maintanance is cheap and uncomplicated, and heterologous protein expression is often fast and rather easy compared to eukaryotic cells like yeast or insect cells.

A big disadvantage of the *E. coli* expression system, however, is the disability to correctly fold heterologous proteins, in particular eukaryotic proteins, because *E. coli* lacks the typical cell machinery of eukaryotic cells. The main difference between Bacteria/Archea and Eukaryotes is that the latter have membrane-bound organelles and a nucleus, enabling them to establish sophisticated protein modification and transportation systems within different organelles. Thus, incorrectly folded, hence insoluble (inclusion bodies) or toxic proteins are a common problem when using *E. coli* as expression host for eukaryotic proteins. However, several methods have been developed to overcome these obstacles and *E. coli* is still a popular choice for heterologous protein expression.

4.4.1 *Expression of the C-terminal tagged GLB1-HIS construct*

The theoretical size of the fusion protein was calculated as ~77 kDa, using the program "Compute pI/Mw" from the ExPASy Proteomics Server (Swiss Institute of Bioinformatics; http://www.expasy.ch), and based on the 685 aa fusion protein sequence provided in the appendix. In fact, the human lysosomal acid β-galactosidase precursor has a mass of 84 kDa, while the lysosomally processed, mature enzyme is truncated to 64 kDa. As the computational calculation did not consider protein glycosylations or other post-translational modifications, the actual mass of proteins on SDS gels can differ from the calculated mass. In case of expression in *E. coli*, there are no post-translational modifications to take into account hence the anticipated mass of the polyhistidine-tagged fusion protein was approximately 77 kDa.

Prior large-scale expression of the desired protein, preliminary experiments were conducted to find optimal growth conditions and isopropyl β-D-1-thiogalactopyranoside (IPTG) concentrations for induction of the fusion protein. For these small-scale experiments, an overnight culture (ONC) of the positive transformant *E. coli* BL21(DE3)-[pET-21d(+)-*GLB1-HIS*] (T2/4) was set up in LBA medium as starter culture. Furthermore, a positive and negative control (*E. coli* BL21(DE3)-[pET21d(+)]; empty plasmid) was cultivated in LBA medium and treated like T2/4 in subsequent procedures. BL21(DE3)pLysS cells, transformed with the pET-14b plasmid containing the gene for *E. coli* β-galactosidase (*lacZ*), served as induction control (Induction Control A, Invitrogen™). 50 ml LBA medium were inoculated with the respective

strain to an optical density (OD at 600 nm) of 0.05 and incubated until an OD_{600} of ~0.4 was attained. At this point, samples for SDS-PAGE were retrieved by collecting cells corresponding to 2 OD units. Cells were pelleted by centrifugation at 5,000 x g for 20 min (4 °C) or 10,000 x g for 5 min (4 °C), shock-frozen in liquid nitrogen, and stored at -80 °C. Main cultures were supplemented with IPTG to induce protein expression and incubated for several hours at preassigned temperatures. Samples for SDS-PAGE were collected on the hour and processed as described above.

The tested small-scale expression conditions for C-terminally His®-tagged β-galactosidase are given in Table 4.4.1.1. Induction Control A was positive in each experiment while the negative control showed no induced protein.

Temp.	Final IPTG concentration			Incub. time after induction
	0.5 mM	0.6 mM	1 mM	
18 °C	n.d.	low expression of ~30 kDa protein	n.d.	1-4 hrs
25 °C	n.d.	low expression of ~30 kDa protein	n.d.	1-4 hrs
37 °C	low expression of ~30 kDa protein	n.d.	low expression of ~30 kDa protein	1-5 hrs

Table 4.4.1.1 Small-scale expression conditions for induction of C-His®-Gal in *E. coli* BL21(DE3)-[pET-21d(+)-*GLB1-HIS*] (T2/4). Results were obtained by SDS-PAGE. n.d. = not determined.

Unfortunately, none of the tested conditions resulted in the expression of the full length human β-galactosidase precursor. SDS gels never showed an induced protein band in the size of the cloned construct (~77 kDa), but rather a small fragment of approximately 30 kDa. However, this band was not always clearly distinguishable from the negative control's or uninduced cell's bands. To further examine heterologous expression in this transformant, T2/4 was cultured in 100 ml LBA medium at 37 °C until an OD_{600} of ~0,5 was attained, induced with a final IPTG concentration of 0.5 mM, and harvested after 5 more hours at 37 °C. Cells of the total culture were pelleted by centrifugation at 3,000 x g for 10 min at 4 °C. Additionally, samples of uninduced and induced cells were prepared for SDS-PAGE as described earlier. The cell pellet of the total culture was resuspended in 6 ml (3 ml/50 ml culture volume) ice-cold phosphate buffered saline (PBS, pH 7,4), homogenized by sonication (5 x 1 min on ice with a break of 1 min after each run), and centrifuged at 18,000 rpm (Sorvall RC5B-Plus, F21S rotor) for 30 min

at 4 °C. The supernatant was collected and samples from the cell homogenate, the supernatant, and the pellet after centrifugation were collected for SDS-PAGE, respectively. SDS-PAGE samples were prepared as described in section 3.11.7 and applied to 10% Tris-HCl gels (Bio-Rad). Results are shown in Figure 4.4.1.2.
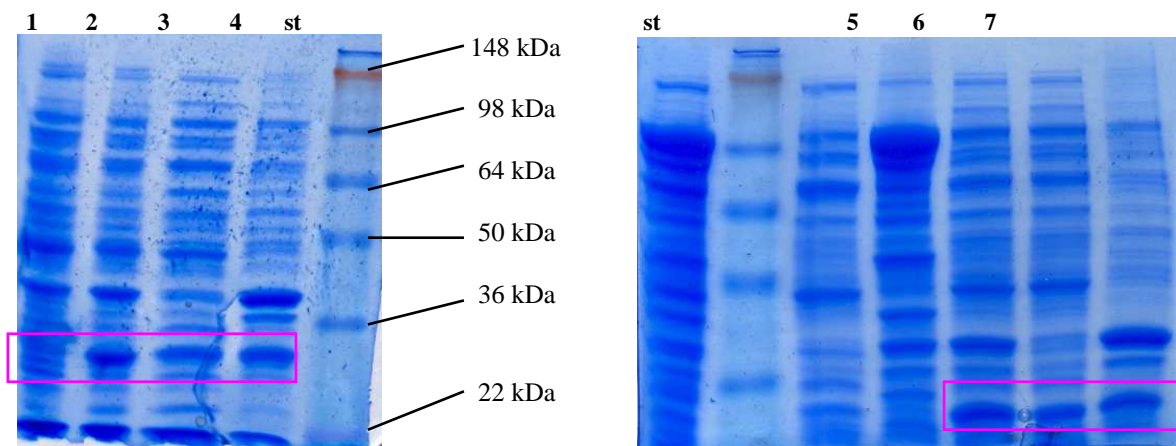
Figure 4.4.1.2 SDS-PAGE of C-His®-Gal induction in T2/4 with 0.5 mM IPTG. Cells were disrupted by sonication and centrifuged to separate soluble from insoluble proteins (except lane 1+2). **(st)** 20 µl SeeBlue® Plus2 (Invitrogen™); **(1)** 10 µl uninduced T2/4; **(2)** 10 µl T2/4 after 5 hr induction with 0.5 mM IPTG; **(3)+(6)** 30 µl supernatant; **(4)+(7)** 30 µl pellet after sonication and centrifugation; **(5)** 30 µl cell homogenate. 10% Tris-HCl ready gels (Bio-Rad), running buffer: Tris/glycine.

In accordance with all previous expression tests, there was an additional band of ~30 kDa when T2/4 was induced with 0.5 mM IPTG. This band was also slightly visible in uninduced cells, probably due to basal expression of proteins. Interestingly, the protein was present in the soluble and insoluble fraction as demonstrated by centrifugation of the cell homogenate (Figure 4.4.1.2, lanes 3, 6, 4, and 7). The presence of this band in the pellet fraction might indicate semi-optimal cell disruption or separation and should be optimized. However, all sonication steps of *E. coli* cells in this work were performed with optimal equipment in the lab of the Biochemistry Department, Technical University of Graz. Unfortunately, there never was an induced band in the size of the full length β-Gal-His® construct (estimated ~77 kDa) or close-by.

4.4.1.1 Purification of the C-terminal polyhistidine-tagged proteins by nickel-affinity chromatography

To purify the potential His®-tagged protein (~30 kDa), another experiment was set up in a similar way, using 2 x 250 ml LBA medium for cultivation of T2/4 at 37 °C, and protein induction with a final IPTG concentration of 0.5 mM. Samples for SDS-PAGE were collected before and after induction, and total cell cultures were pelleted after 4 hrs at 37 °C by centrifugation at 5,000 x g for 10 min (4 °C). The resulting pellet (1.3 g wet weight) was resuspended in 3 ml lysis buffer A and prepared for nickel-column purification as described in section 3.5.1. Briefly, the resuspended cells were sonicated, centrifuged, and filtered through a filter paper prior application to the column. During collection of the samples, visual protein determinations were performed using the Quick Start™ Bradford Dye Reagent (1x; Bio-Rad). Therefore, 10 µl of the sample were mixed with 500 µl of the dye and a color change from red to blue indicated the sample's protein content. Blue eluate fractions were pooled, concentrated in Vivaspin 4 ultrafiltration columns (5,000 MWCO PES; Vivascience, Sartorius GmbH), and rebuffered in 10 mM phosphate buffer (pH 7.0), containing 100 mM NaCl to a final volume of 1 ml. Samples of each purification fraction were subjected to SDS-PAGE (Figure 4.4.1.1.1) and Western blotting (Figure 4.4.1.1.2).
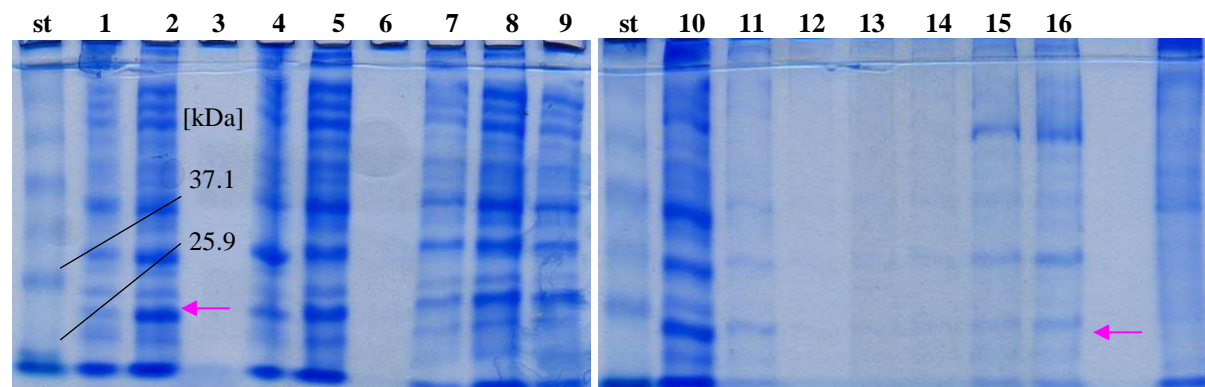
Figure 4.4.1.1.1 SDS-PAGE of fractions from purification of a putative polyhistidine-tagged fusion protein. (st) 25 µl BenchMark™ (Invitrogen™); (1) 10 µl uninduced T2/4; (2) 10 µl T2/4 after 4 hr induction with 0.5 mM IPTG; (3) 20 µl medium; (4) 20 µl pellet after sonication and centrifugation, 1:10 dilution; (5) 20 µl supernatant, 1:10 dilution; (6)-(9) 20 µl flow through fractions, 1:10 dilutions; (10)-(14) 20 µl wash fractions, 1:10 dilutions; (15) 20 µl eluate pool; (16) 20 µl concentrated and rebuffered eluate. 10% polyacrylamid gels, running buffer: Tris/glycine.

The purification of the 30 kDa protein was not successful as demonstrated in Figure 4.4.1.1.1. The same proteins that were found in the flow through fractions (lanes 6-9) were also found in the eluate fractions (eluate pool in lane 15), indicating no specific binding to the nickel-column. Interestingly, an antibody directed against human β-galactosidase (α85 anti-human β-galactosidase antibody; see section 3.10.1) reacted with several proteins in the eluate fractions (Figure 4.4.1.1.2, lanes 6-8).

The β-Gal antibody seemed to recognize the same proteins on the second blot. Unfortunately, this blot was not ideal for comparison and development times are different for both blots. Western blots could not be repeated due to antibody shortage. Some of the most prominent bands in the eluate fractions were also present in the uninduced control (lane 17) and in the negative control (lanes 4 and 5). Western blot results also implied unsuccessful protein purification as seen in Figure 4.4.1.1.1. However, it was difficult to localize the 30 kDa protein in these blots. For orientation purpose, samples from human fibroblast and COS-1 homogenates were applied together with the *E. coli* samples. The human lysosomal acid β-Gal precursor (84 kDa) was clearly detectable in all lanes (1-3, red arrows), where COS-1 cells showed the strongest signal due to overexpression of the precursor. The juvenile GM1 sample shows also some β-Gal specific degradation bands (<37 kDa) [Okamura-Oho *et al.*, 1996]. Mature β-Gal enzyme (64 kDa) is only present in healthy control cells (lane 2, blue arrow). A correctly expressed heterologous fusion protein should therefore be detected in a height between those two bands in the *E. coli* lanes. The topmost bands in all fractions would correspond to the calculated size, but SDS-PAGE never showed a significantly induced band in that position (cf. Figure 4.4.1.2), and this band is also present in the negative controls (WB, lanes 4 and 5).
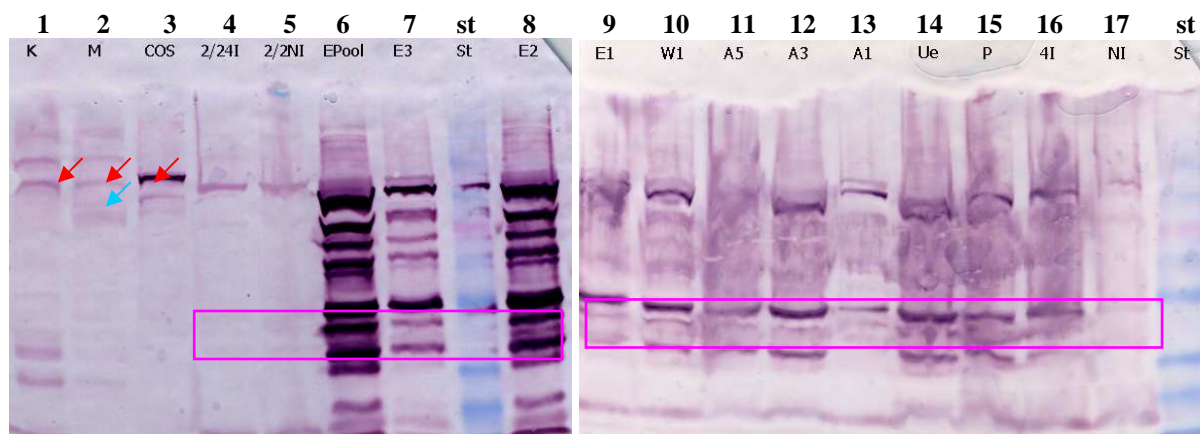
Figure 4.4.1.1.2 Western blot detection of β-Gal immunoresponsive material in T2/4 fractions. Blots were hybridized with α85 anti-human β-galactosidase antibody. Membrane 1 was developed with the AP Substrate Kit (Bio-Rad) for 30 min, and membrane 2 for 15 min. **(st)** 20 µl BenchMark™ (Invitrogen™); **(1)-(3)** cell homogenates of juvenile GM1 **(1)**, healthy control **(2)**, and COS-1 cells **(3)**; **(4)** 20 µl negative control after 4 hr induction with 0.5 mM IPTG; **(5)** 20 µl uninduced negative control; **(6)** 20 µl eluate pool; **(7)-(9)** 20 µl eluate fractions; **(10)** 20 µl wash fraction; **(11)-(13)** 20 µl flow through fractions; **(14)** 20 µl supernatant; **(15)** 20 µl pellet after sonication and centrifugation; **(16)** 20 µl T2/4 after 4 hr induction with 0.5 mM IPTG; **(17)** 20 µl uninduced T2/4. 10% polyacrylamid gels, running buffer: Tris/glycine; nitrocellulose membranes.

To elucidate this problem, the eluate fraction was subjected to another Western blot experiment, and nitrocellulose membranes were hybridized with an anti-polyhistidine antibody. Surprisingly, the anti-6-histidine antibody (Novus Biologicals®) and the anti-β-Gal antibody reacted with the same proteins in the eluate fraction (Figure 4.4.1.1.3). To rule out any negative influence of the secondary antibody, another membrane containing the eluate sample was hybridized only with the secondary antibody. No signal was detected, even after color reactions of more than one hour (data not shown).

Altogether, the results of induction experiments and Western blots indicate low expression of soluble but unstable, rapidly degraded C-terminally polyhistidine-tagged human β-galactosidase protein in *E. coli*. The fusion protein seemed to be cleaved at specific positions resulting in at least seven major fragments (including the ~30 kDa protein) clearly detectable in Western blots by both anti-β-Gal and anti-6-histidine antibodies. The main advantage of Western blots compared to SDS-PAGE is the higher sensitivity of protein detection, which may explain the difficulties to see (over)expressed proteins on SDS gels.

Figure 4.4.1.1.3 Western blot detection of β-Gal and histidine immunoresponsive material in T2/4 fractions. Blots were hybridized with either α85 anti-human β-galactosidase antibody **(lanes 1-3)**, or anti-6-histidine antibody **(lane 4)**. Membrane 1 was developed with the AP Substrate Kit (Biorad) for 30 min, and membrane 2 for 5 min. **(st)** 20 µl BenchMark™ (Invitrogen); **(1)+(4)** 20 µl eluate pool; **(2)+(3)** 20 µl eluate fractions. 10% polyacrylamid gels, running buffer: Tris/glycine; nitrocellulose membranes.

4.4.2 Expression of the N-terminal tagged HIS-GLB1 construct

To possibly overcome the problems arising from a C-terminal tagged fusion protein in terms of decreased stability (e.g. action of C-terminal processing peptidases), an N-terminal tagged *HIS-GLB1* construct was cloned and expressed in *E. coli* BL21(DE3) cells under the conditions listed in Table 4.4.2.1 for small-scale induction experiments. Cells were prepared for small-scale induction experiments as described in section 4.4.1 and 3.2.2.

Temperature	Final IPTG concentration	Incubation time
	1 mM	**after induction**
30 °C	low expression of ~30 kDa protein	1-4 hrs, 21 hrs
37 °C	low expression of ~30 kDa protein	1-4 hrs

Table 4.4.2.1 Small-scale expression conditions for induction of N-His®-Gal in *E. coli* BL21(DE3)-[pET-21d(+)-*HIS-GLB1*] (T1). Results were obtained by SDS-PAGE.

As specified for C-His®-Gal, the theoretical size of the N-His®-Gal fusion protein was calculated as ~77 kDa with the program "Compute pI/Mw" (ExPASy, Swiss Institute of Bioinformatics), based on the 684 aa fusion protein sequence provided in the appendix. Significant overexpression of a full length β-Gal protein, tagged with polyhistidine, was unsuccessful, but a ~30 kDa protein was slightly induced with IPTG (Figure 4.4.2.2, blue arrow). A red arrow indicates the possible location of a low expressed, full length fusion protein, in the size of the target protein. To confirm the identity of the induced band(s), Western blots were performed using the same fractions as in Figure 4.4.2.2.
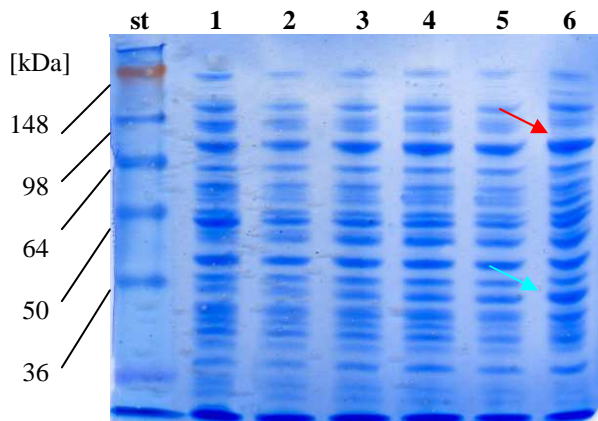
Figure 4.4.2.2 SDS-PAGE of N-His®-Gal induction in T1 with 1 mM IPTG. Cells were cultured in LBA medium to an OD_{600} of 0.6, and induced with IPTG. **(st)** 25 µl SeeBlue® Plus2 (Invitrogen); **(1)** 10 µl uninduced T1; **(2)-(6)**: 10 µl T1 after induction at 30 °C for 1 hr **(2)**, 2 hrs **(3)**, 3 hrs **(4)**, 4 hrs **(5)**, 21 hrs **(6)**. 10% Tris-HCl ready gels (Biorad), running buffer: Tris/glycine.

In contrast to the previous blots (cf. Figure 4.4.1.1.2), nitrocellulose membranes were hybridized with the anti-β-galactosidase peptide antibody 1 (Eurogentec) for detection of β-Gal immunoreactive material. This specific antibody was designed in cooperation with the company Eurogentec, and was only available in a later phase of this work (see section 4.5.2). Results are shown in Figure 4.4.2.3. The blots are all products from one and the same nitrocellulose membrane. First, the membrane was hybridized with the anti-β-Gal antibody followed by the appropriate secondary antibody, and developed for 30 sec using the SuperSignal® West Pico Chemiluminescent Substrate Kit (Thermo Scientific). To detach the hybridized primary and secondary antibodies, the membrane was stripped with 10 ml Restore™ Western Blot Stripping Buffer (Thermo Scientific) for 10 min at room temperature. Then it was hybridized with the anti-6-histidine antibody and its appropriate secondary antibody. A development time of 30 sec, as tested for β-Gal blots, produced only weak polyhistidine-tag signals hence development was repeated, but for the maximum time (~1 hr). The detected proteins bands, both with the anti-β-Gal and anti-6-Histidine antibody, had a striking resemblance to proteins detected in the C-terminal His®-tagged β-Gal transformant (cf. Figure 4.4.1.1.3). It should be noted that different anti-β-Gal antibodies as well as different secondary antibodies were used, which makes this result even more remarkable.
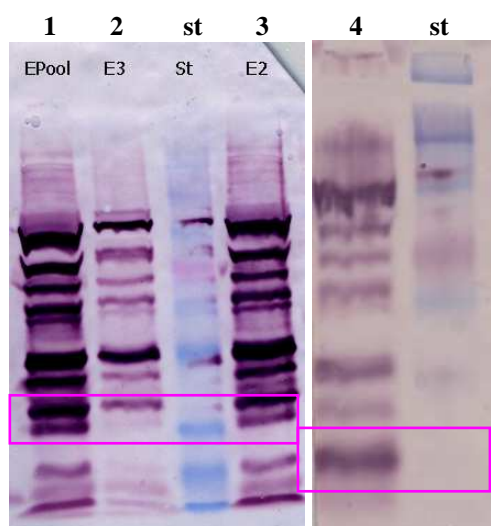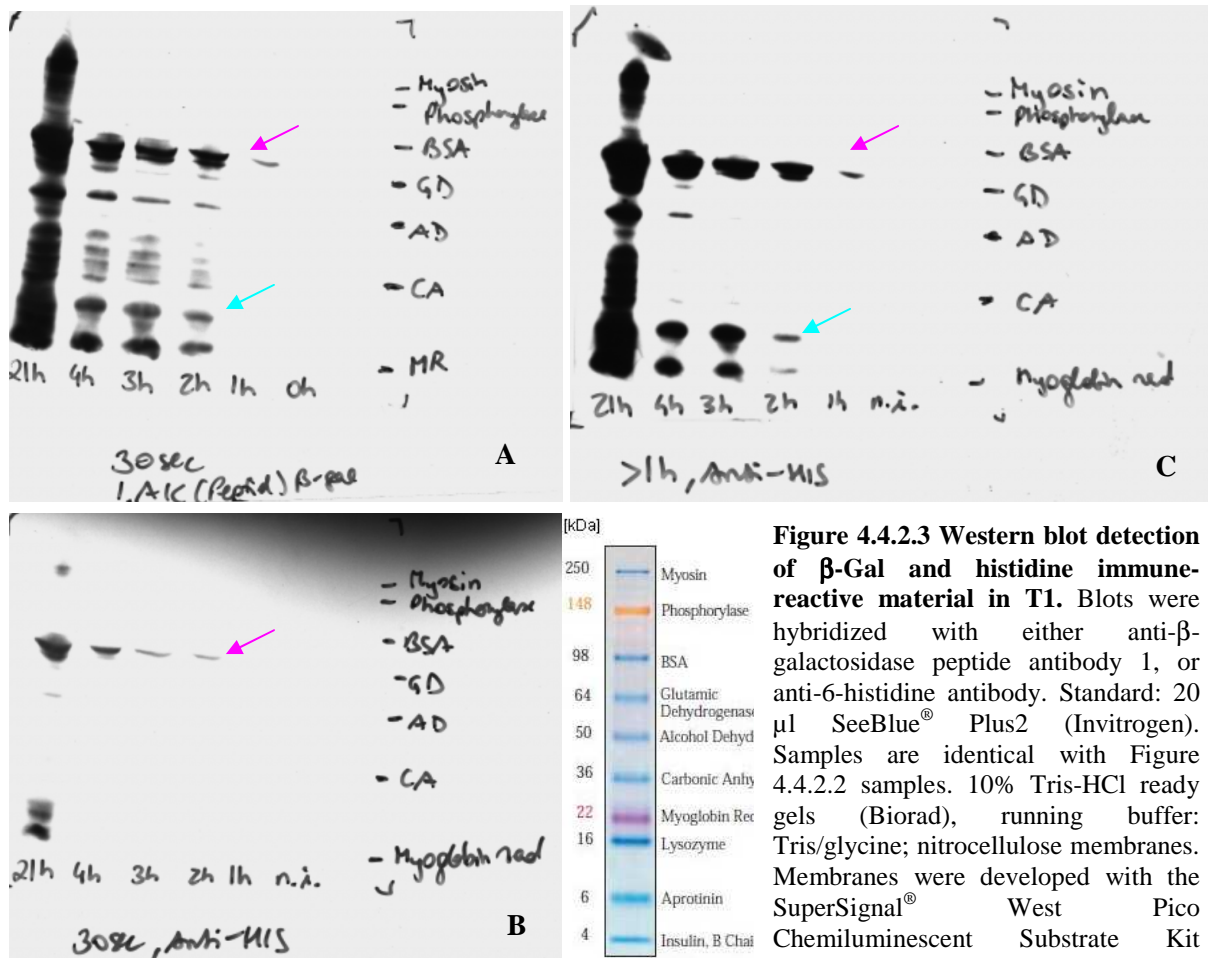
Figure 4.4.2.3 Western blot detection of β-Gal and histidine immune-reactive material in T1. Blots were hybridized with either anti-β-galactosidase peptide antibody 1, or anti-6-histidine antibody. Standard: 20 µl SeeBlue® Plus2 (Invitrogen). Samples are identical with Figure 4.4.2.2 samples. 10% Tris-HCl ready gels (Biorad), running buffer: Tris/glycine; nitrocellulose membranes. Membranes were developed with the SuperSignal® West Pico Chemiluminescent Substrate Kit (Thermo Scientific) Kit for the times indicated below the blots.

Although the uninduced transformant showed a rather clear protein band in the size of full-length β-Gal fusion protein (due to basal protein expression) on SDS gels, no β-Gal was detected in this fraction on Western blots. Actually, the Western blot system is more sensitive for protein detection than staining of SDS gels with Coomassie Blue. Even the extended development of the blot previously hybridized with the anti-6-histidine antibody showed no signal in the lane of the uninduced T1. This result puts interpretations of the upper bands on the SDS gel (Figure 4.4.2.2) into question. It is therefore likely that the upper bands observed on the SDS gel are composed of various proteins of the same size, one of them being the target protein. The longer the incubation time after IPTG induction, the more β-Gal and polyhistidine immunoreactive material was found in the fractions. The detected bands are exactly the same for both antibodies. These results clearly indicate low level expression of an N-terminally polyhistidine-tagged full-length β-Gal protein in *E. coli*, which is again rapidly degraded in the

cytoplasm of the host strain, as seen before in transformants carrying the C-terminal *GAL-HIS* construct.

4.4.3 Expression of N-terminal tagged GST-GLB1 constructs

Previous experiments suggested rapid degradation of the heterologously expressed fusion protein in the bacterial cells hence a different strategy was pursued aiming at the expression of β-Gal with improved stability. One way of achieving that aim could be the co-expression of a stable protein-tag like the glutathione S-transferase (GST) or maltose binding protein (MBP). These protein-tags are available in commercial vectors, optimized for high expression of stable and soluble GST or MBP protein. Tagging the protein of interest to one of these proteins may improve the solubility and stability of the fusion partner, especially if tagging is performed on the N-terminal end of resulting fusion protein. However, these tags do not guarantee successful expression of soluble fusion proteins, but tracking the fate of the protein of interest is much easier with large protein tags. In contrast to the small polyhistidine-tag, GST (~26 kDa) or MBP (~42 kDa) can easily be located on SDS gels, facilitating analysis of small-scale induction experiments.

4.4.3.1 Expression of full length human lysosomal acid β-galactosidase

The theoretical size of the N-terminally GST-tagged full-length β-galactosidase was calculated as ~104 kDa with the program "Compute pI/Mw" (ExPASy; Swiss Institute of Bioinformatics), based on the 920 aa fusion protein sequence provided in the appendix, and neglecting post-translational modifications. The conditions for expression of N-GST-Gal in transformant T1f are listed in Table 4.4.3.1.1.

Temperature	Final IPTG concentration		Incub. time
	0.5 mM	**1 mM**	**after induction**
25 °C	high expression of insoluble protein in large-scale experiments	high expression of insoluble protein in large-scale experiments	1-5 hrs, 20 hrs
37 °C	high expression of insoluble protein in large-scale experiments	high expression of insoluble protein in large-scale experiments	1-20 hrs with 0,5 mM 1-5 hrs + 21 hrs with 1 mM

Table 4.4.3.1.1 Expression conditions for induction of N-GST-Gal in *E. coli* BL21-[pGEX-6P-2-*GST-GLB1*-f] (T1f). Results were obtained by SDS-PAGE.

In all tested large-scale conditions, the full-length fusion protein was expressed in high amounts, but in an insoluble form (inclusion bodies). Figure 4.4.3.1.2 clearly shows the overexpressed fusion protein band in the height of the predicted size (~104 kDa, red arrow). However, the protein is only present in the homogenate fraction after sonication of the cells, and in the pellet fraction after centrifugation of the cell homogenate. The supernatant was applied to a GST affinity column and purified as described in section 3.5.2. Protease inhibitors were not used during the purification process. The eluate fractions were pooled, concentrated and rebuffered in PBS (pH 7.4). Due to inclusion body formation of the fusion protein (lane 3), no protein could be purified via affinity chromatography, hence the protein of interest is absent in the eluate (lane 4).
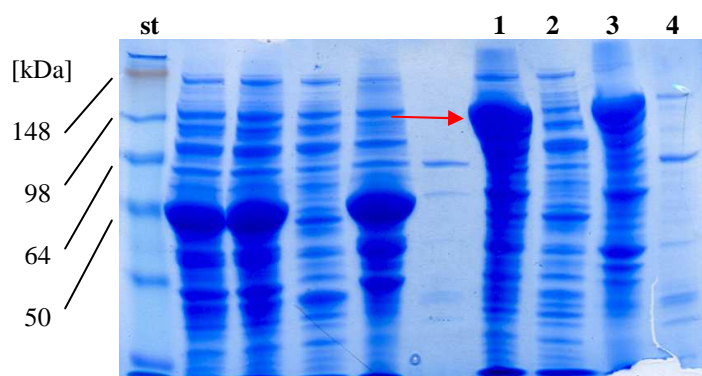
Figure 4.4.3.1.2 SDS-PAGE of fractions from purification of the GST-tagged full length β-galactosidase. β-Gal was induced with 1 mM IPTG for 4 hrs at 37 °C. **(st)** 20 µl SeeBlue® Plus2 (Invitrogen); **(1)** 30 µl cell homogenate; **(2)** 30 µl supernatant; **(3)** 30 µl pellet after sonication and centrifugation; **(4)** 30 µl concentrated and rebufferd eluate. 10% Tris-HCl ready gels (Biorad), running buffer: Tris/glycine.

To increase the probability of correctly folded, soluble expressed protein, N-GST-Gal expression was induced at suboptimal growth temperatures with different IPTG concentrations. Unfortunately, these conditions were not able to improve the solubility of the GST-tagged β-Gal protein (Figure 4.4.3.1.3). The vast majority of the protein was still found in the pellet

fraction (lanes 3 and 6, red arrow). However, the pGEX-6P-2 plasmid containing the GST-tag sequence proved to be a good choice, because it resulted in high expression levels of the fusion protein, clearly visible on SDS gels. This result provided the basis for another attempt, the co-expression of the fusion protein and specific *E. coli* chaperones, assisting in proper protein folding.
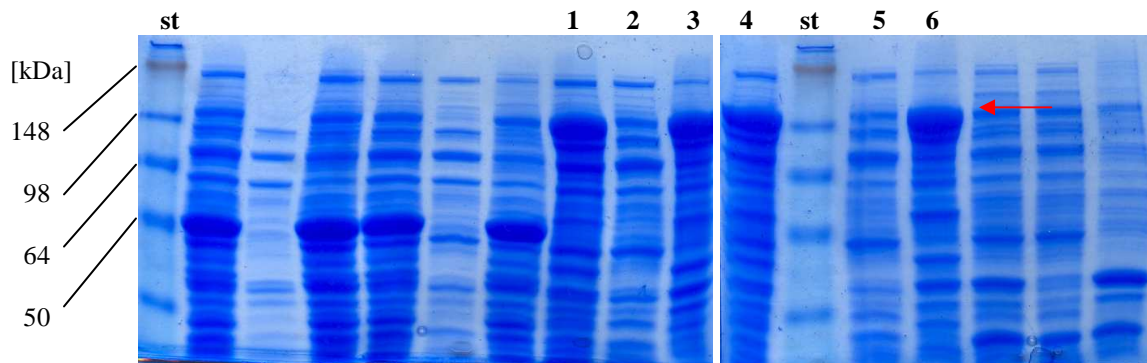
Figure 4.4.3.1.3 SDS-PAGE of induction conditions for expression of the GST-tagged full length β-galactosidase in T1f. β-Gal was induced for 4 hrs at 25 °C with either 0.5 mM **(lanes 1-3)** or 1 mM IPTG **(lanes 4-5)**. **(st)** 20 µl SeeBlue® Plus2 (Invitrogen™); **(1)+(4)** 30 µl cell homogenate; **(2)+(5)** 30 µl supernatant; **(3)+(6)** 30 µl pellet after sonication and centrifugation. 10% Tris-HCl ready gels (Bio-Rad), running buffer: Tris/glycine.

4.4.3.2 Expression of full length human lysosomal acid β-galactosidase with the aid of molecular chaperones

Molecular chaperones are interactive, often highly conserved proteins, naturally occuring in both bacterial and eukaryotic cells, which assist in proper protein folding of nascent proteins, but also participate in protein degradation processes [reviewed in Arndt *et al.*, 2007 and Brodsky, 2007]. Heat shock proteins are probably the best-known and characterized chaperones in *E. coli* and in general [reviewed in De Maio, 1999 and Li and Srivastava, 2004]. They are typically expressed in the bacterial cytoplasm under stress conditions, thus they were designated with the prefix Hsp (e.g. Hsp60, Hsp70). In human cells, the situation is more complex and still far from elucidation. A large quantity of human chaperone families is located in the endoplasmic reticulum (ER), where proteins are synthesized and folding processes take place to form native state proteins [reviewed in Buck *et al.*, 2007]. It should be noted that not all proteins require the action of a chaperones for proper folding and transportation to their target location. The influence of bacterial chaperones on the expression of recombinant proteins

has to be evaluated carefully. Overexpression of molecular chaperones may facilitate stabilization or folding of specific heterologously expressed proteins, but overproduction could also result in inhibiton of cell growth and premature cell death [Hoffmann and Rinas, 2004].

Successful co-expression of chaperones and heterologous proteins to improve solubility and stability was demonstrated by several groups [reviewed in Hoffmann and Rinas, 2004]. A wide range of chaperone expression vectors is commercially available, encoding either one specific chaperone or a set of chaperones that are actually interaction partners, and able to initiate an entire protein folding cascade in the bacterial cells. Of course, these processes occur naturally in *E. coli* without chaperone vectors, but the crucial point might be the overexpression of certain chaperones, as the cellular machinery is well adapted in terms of handling its own resources, but expression of heterologous proteins is certainly more energy demanding.

The plasmid pG-KJE8 (Takara Bio Inc.) was chosen for co-expression experiments [Takara A]. It contains the *E. coli* chaperones listed in Table 4.4.3.2.1. and the resistant marker for chloramphenicol, enabling co-selection with the pGEX-6P-2 plasmid (ampicillin). The chaperone encoding genes under the control of the *araB* promoter are inducible by addition of L-arabinose to the growth medium, and the genes under control of the *Pzt1* promoter can be induced with tetracycline. For further details and the vector map see section 3.3.

Heat shock protein/Chaperone	Alternative name	Size
Hsp70	DnaK	~70 kDa
Hsp40	DnaJ	~40 kDa
Hsp-70 cofactor	GrpE	~22 kDa
Hsp60	GroEL	~60 kDa
HspE1	GroES	~10 kDa

Table 4.4.3.2.1 Molecular chaperones featured in the pG-KJE8 plasmid (Takara Bio Inc.)

The tested expression conditions for N-terminally GST-tagged β-galactosidase and co-expression of chaperones are listed in Table 4.4.3.2.2. Induction was performed according to the manufacturer's recommendation [Takara A; Takara B].

Temp.	Final IPTG concentration	Incub. time
	1 mM	after induction
25 °C	<u>high expression</u> of insoluble protein in large-scale experiments	2, 4, 20 hrs
30 °C	<u>high expression</u> of insoluble protein in large-scale experiments	4, 8, 15, 20 hrs

Table 4.4.3.2.2 Expression conditions for induction of N-GST-Gal in *E. coli* BL21(DE3)-[pG-KJE8]-[pGEX-6P-2-*GST-GLB1*-f] (T1f-chap). Results were obtained by SDS-PAGE.

In one preliminary experiment, 250 ml LBAC-AT medium (see section 3.13) were inoculated with the positive transformant T1f-chap to an OD_{600} of 0.05. Cells were grown at 25 °C until an OD_{600} of ~0,4 was attained, induced with IPTG at a final concentration of 1 mM, and cultivated for 20 hrs at the same temperature. Samples (2 OD units) were taken from uninduced and induced cells (2, 4 and 20 hrs) and prepared for SDS-PAGE as described previously (cf. section 3.11.7). 100 ml of the main culture were harvested after induction for 4 hrs, and another 100 ml after 20 hrs. Cells from each pellet were prepared by centrifugation at 3,000 x g for 10 min (4 °C), washed in 0.9% NaCl, resuspended in 1 ml Lysis Buffer B, and homogenized by sonication (5 x 1 min). After centrifugation of the cell homogenates (20,000 x g, 20 min, 4 °C), 20 µl aliquots of the homogenates, the supernatants, and the pellets after sonication and centrifugation were treated with 2 units of PreScission™ Protease (GE Healthcare) for 16 hrs at 4 °C. Treatment of all fractions was performed to investigate the cleavage qualities, e.g. if GST can be cleaved off in the insoluble protein fraction by the PreScission™ Protease (PP). However, it was hoped that co-expression of molecular chaperones solubilizes the N-GST-Gal protein, increasing the possibility of cleavage by PP.

Results of this experiment are shown in Figure 4.4.3.2.3. There was no difference in the protein pattern of PP-treated and untreated cells. PreScission™ Protease could not cleave the GST-tag from the insoluble fusion protein, indicating not only misfolding of the β-Gal protein, but maybe also GST itself, or GST it is inaccessible due to steric hindrance by misfolded β-Gal motifs. The extra band (~46 kDa) in lanes 9-14 (best seen in lane 11; red arrow) is the PP enzyme itself, which could be co-purified with positively cleaved, free GST fragments on the GST affinity column. Unfortunately, the solubility of the N-GST-Gal was not affected by chaperone co-expression, hence the protein remained insoluble and was mainly present in the pellet fraction after sonication and centrifugation. Furthermore, it seems that also a certain amount of the chaperones was present in the insoluble fraction, especially the low-sized chaperones DnaJ and GrpE. Higher amounts of soluble expressed proteins, including

chaperones, were found after 20 hrs (lanes 8 and 14). However, the amount of soluble N-GST-Gal was rather low compared to the insoluble fraction or chaperones expressed in the soluble fraction itself. Chaperone overexpression alone is shown in lane 15 (IPTG-uninduced T1f-chap). The protein sizes are almost consistent with the predicted sizes listed in Table 4.4.3.2.1. Differences might occur due to different SDS gel/running buffer systems.
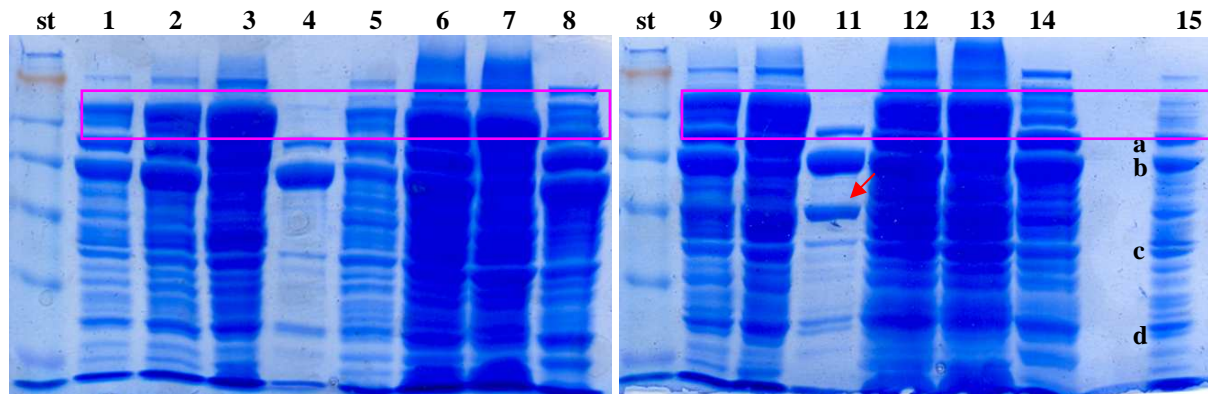
Figure 4.4.3.2.3 SDS-PAGE of induction conditions for expression of the GST-tagged full length β-galactosidase with the aid of chaperones in T1f-chap. β-Gal was induced with 1 mM IPTG at 25 °C for 4 hrs **(lanes 1-4 and 9-11)**, and 20 hrs **(lanes 5-8 and 12-14)**. Additionally, some samples were treated with PreScission™ Protease **(lanes 9-14)**. **(st)** 20 µl SeeBlue® Plus2 (Invitrogen™); **(1)+(5)** 30 µl cells prior sonication; **(2)+(6)+(9)+(12)** 30 µl cell homogenate; **(3)+(7)+(10)+(13)** 30 µl pellet after sonication and centrifugation; **(4)+(8)+(11)+(14)** 30 µl supernatant; **(15)** 10 µl uninduced T1f-chap with expressed chaperones. **(a)** DnaK (~70 kDa); **(b)** GroEL (~60 kDa); **(c)** DnaJ (~40 kDa); **(d)** GrpE (~22 kDa). 10% Tris-HCl ready gels (Bio-Rad), running buffer: Tris/glycine.

A similar experiment was performed with an induction temperature of 30 °C, and 50 ml of the main culture were harvested after 4 hrs, 8 hrs, 15 hrs, and 20 hrs, respectively. Cell pellets were prepared as previously described and homogenates, supernatants, and pellets after sonication and centrifugation were subjected to SDS-PAGE (Figure 4.4.3.2.4). For better visual analysis, the homogenate and pellet fractions were diluted 1:10 in Lysis Buffer B prior application to the SDS gels, while the supernatant fraction was applied undiluted. The results are consistent with previously obtained data from preliminary experiments, where both chaperone and N-GST-Gal expression was as its highest level well after 8 hrs induction time (lanes 9 and 12), but in either case overexpression of soluble fusion protein was not sufficient for large-scale purifications to provide antigens for antibody development.
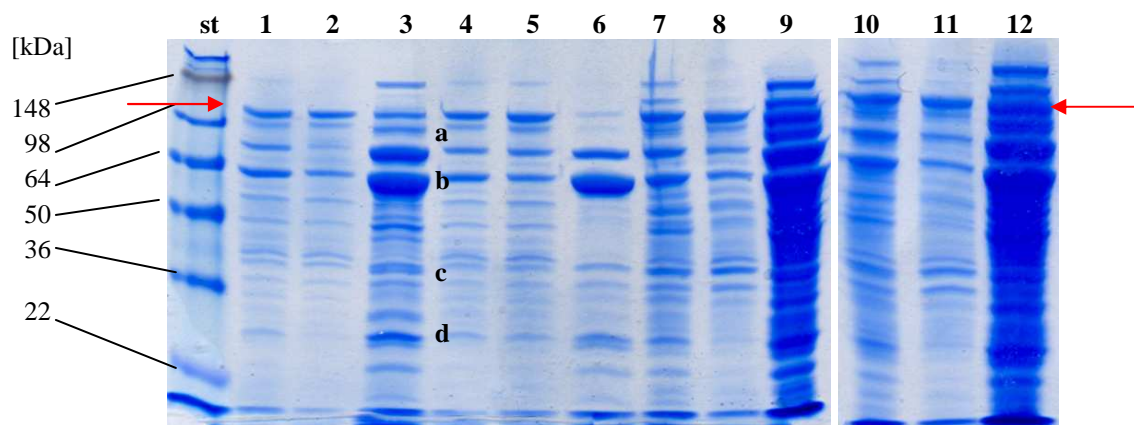
Figure 4.4.3.2.4 SDS-PAGE of induction conditions for expression of the GST-tagged full length β-galactosidase with the aid of chaperones in T1f-chap. β-Gal was induced with 1 mM IPTG at 30 °C for 4 hrs **(lanes 1-3)**, 8 hrs **(lanes 4-6)**, 15 hrs **(lanes 7-9)**, and 20 hrs **(lanes 10-12)**. **(st)** 25 µl SeeBlue® Plus2 (Invitrogen™); **(1)+(4)+(7)+(10)** 30 µl cell homogenate, 1:10 dilutions; **(2)+(5)+(8)+(11)** 30 µl pellet after sonication and centrifugation, 1:10 dilutions; **(3)+(6)+(9)+(12)** 30 µl supernatant. **(a)** DnaK; **(b)** GroEL; **(c)** DnaJ; **(d)** GrpE. 10% Tris-HCl ready gels (Bio-Rad), running buffer: Tris/glycine.

To verify data from SDS-PAGE, Western blot analysis was performed on the supernatant and the pellet fractions (Figure 4.4.3.2.5). The nitrocellulose membrane was first hybridized with the β-galactosidase antibody according to the Western blot protocol (see section 3.10 and 3.11.7.4), and after successful development for 1 min, stripped with 10 ml Restore™ Western Blot Stripping Buffer (Thermo Scientific) for 10 min at room temperature. The second hybridization was performed with an anti-GST antibody (GE Healthcare) and the blot was again developed for 1 min using the SuperSignal® West Pico Chemiluminescent Substrate Kit (Thermo Scientific). In contrast to His®-tagged β-Gal proteins, the soluble portion of GST-β-Gal seemed to be expressed in a more stable form. In this experiment, GST signals (right blot) of N-GST-Gal are more pronounced after blot development of 1 min, than His® signals of N-His®-Gal detected after development of ≥ 1 hr (cf. Figure 4.4.2.3). Major degradation fragments, like the ~30 kDa protein, were absent in the first blot even after an induction time of 20 hrs, although there were some degraded proteins just beneath the fusion protein band (Figure 4.4.3.2.5, red arrows). However, the 30 kDa protein was clearly visible in the second blot, previously hybridized with the anti-GST antibody (blue arrow).

132
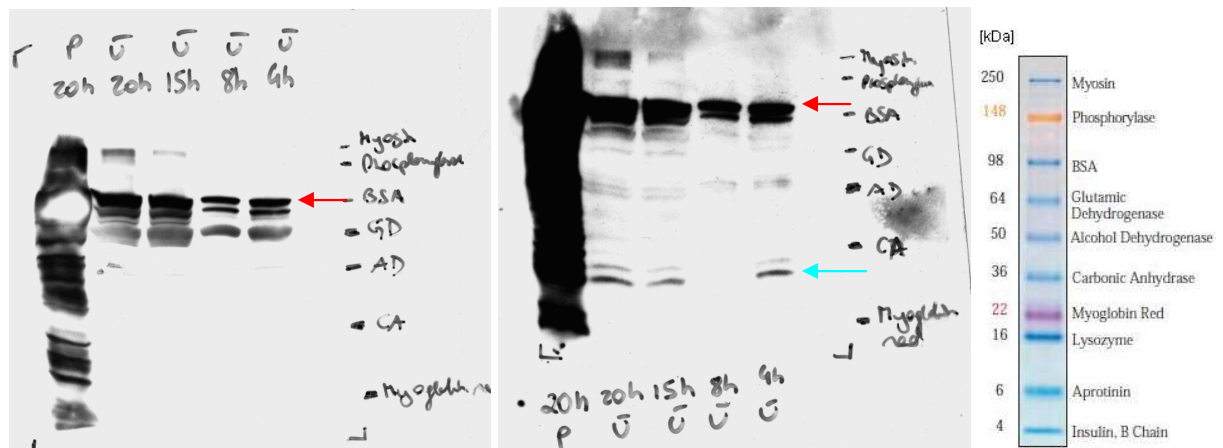
Figure 4.4.3.2.5 Western blot detection of β-Gal and GST immunoreactive material in T1f-chap. Blots were hybridized with either either α85 anti-human β-galactosidase antibody (left), or anti-GST antibody (right). Standard: 20 µl SeeBlue® Plus2 (Invitrogen™). Samples are identical with samples from Figure 4.4.3.2.4. 10% Tris-HCl ready gels (Bio-Rad), running buffer: Tris/glycine; nitrocellulose membranes. Both blots were developed for 1 min with the SuperSignal® West Pico Chemiluminescent Substrate Kit (Thermo Scientific).

Despite low expression levels of soluble N-GST-Gal, preliminary purification experiments were conducted to examine the binding characteristics of the soluble protein to the GST affinity column. For GST affinity chromatography, 250 ml LBAC-AT medium were inoculated with T1f-chap as described earlier in this chapter, and N-GST-Gal expression was induced with 1 mM IPTG at 25 °C. 200 ml of the main culture were harvested after 20 hrs, and samples for SDS-PAGE were collected from induced and uninduced cells. The pellet was resuspended in 12 ml Lysis Buffer B and homogenized by sonication. A GST affinity resin was prepared as described in section 3.5.2 and the supernatant was allowed to flow through by gravity. After washing the column with several volumes of Lysis Buffer B, bound proteins were eluted with 10 bed volumes of Elution Buffer B. Aliquots of representative fractions were prepared for SDS-PAGE and results are shown in Figure 4.4.3.2.6. Similar to purification experiments without chaperone co-expression (cf. section 4.4.3), the GST-tag of the fusion protein did not bind to the affinity column. Only the most prominent protein, the chaperone GroEL (60 kDa), was slightly visible in the eluate fractions. Due to the low expression of soluble GST-β-Gal fusion protein (cf. lane 2), the co-expression strategy was abandoned and expression of a truncated GST-β-Gal fusion protein was examined.
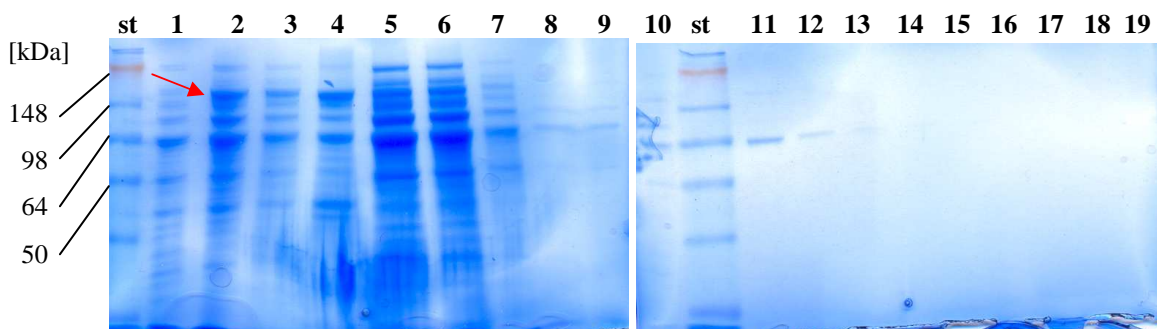
Figure 4.4.3.2.6 SDS-PAGE of fractions from purification of the GST-tagged full length β-galactosidase expressed with the aid of chaperones in T1f-chap. (st) 20 µl SeeBlue® Plus2 (Invitrogen™); **(1)** 10 µl uninduced T1f-chap; **(2)** 10 µl T1f-chap after 20 hr induction with 1 mM IPTG at 25 °C; **(3)** 30 µl cell homogenate, 1:10 dilution; **(4)** 30 µl pellet after sonication and centrifugation, 1:10 dilution; **(5)** 30 µl supernatant; **(6)** 30 µl flow through fraction; **(7)-(9)** 30 µl wash fractions; **(10)-(19)** 30 µl eluate fractions. 10% Tris-HCl ready gels (Bio-Rad), running buffer: Tris/glycine.

4.4.3.3   Expression of truncated human lysosomal acid β-galactosidase

The theoretical size of the fusion protein consisting of truncated β-Gal protein and the GST-tag (N-GST-Gal-peptide) was calculated as ~55 kDa using the program "Compute pI/Mw" (ExPASy, Swiss Institute of Bioinformatics), based on the 473 aa fusion protein sequence provided in the appendix. It was assumed that a truncated, heterologous protein sequence might be easier to express in *E. coli* cells in terms of increased protein stability and solubility. Furthermore, proper folding of small peptides might be more successful than folding of huge proteins, if expressed in a host system. However, proper folding primarily depends on other factors such as availability of appropriate molecular chaperones or post-translational modification machinery, and *E. coli* is not capable of executing such modifications.

The expression conditions for the N-terminally GST-tagged truncated β-galactosidase in the positive transformant T1p are listed in Table 4.4.3.3.1.

Temp.	Final IPTG concentration		Incub. time
	0.5 mM	**1 mM**	after induction
25 °C	expression of insoluble protein	expression of insoluble protein	4 hrs
37 °C	n.d.	expression of insoluble protein	1-5 hrs, 22 hrs

Table 4.4.3.3.1 Expression conditions for induction of N-GST-Gal-peptide in *E. coli* BL21-[pGEX-6P-2-GST-GLB1-p] (T1p). Results were obtained by SDS-PAGE.

GST-tagged β-Gal peptide was expressed with the predicted size of ~55 kDa under all conditions, but it was again insoluble. Results of a preliminary experiment are shown in Figure 4.4.3.3.2. The experimental conditions were the same as described earlier (cf. section 4.4.3.1). Samples containing N-terminal GST-tagged full length β-Gal (~104 kDa) were applied to the same SDS gel for comparative reasons. In both cases, the protein of interest was significantly overexpressed, but it was present in the pellet fraction after sonication and centrifugation (lane 3), rather than in the soluble fraction (lane 2). Therefore, all attempts to purify the protein from the supernatant fraction using GST affinity chromatography (see section 3.5.2) failed (lane 4).
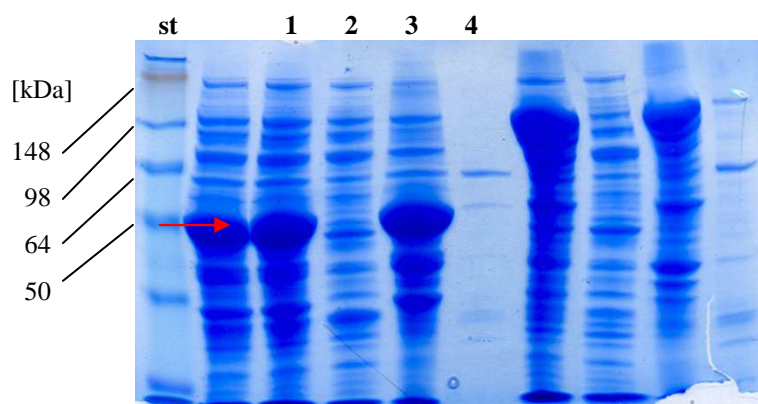
Figure 4.4.3.3.2 SDS-PAGE of fractions from purification of the GST-tagged truncated β-galactosidase peptide of T1p. β-Gal was induced with 1 mM IPTG for 4 hrs at 37 °C. **(st)** 20 µl SeeBlue® Plus2 (Invitrogen); **(1)** 30 µl cell homogenate; **(2)** 30 µl supernatant; **(3)** 30 µl pellet after sonication and centrifugation; **(4)** 30 µl concentrated and rebufferd eluate. 10% Tris-HCl ready gels (Biorad), running buffer: Tris/glycine.

Even reduction of incubation temperatures and final IPTG concentration did not result in expression of significant amounts of soluble N-GST-Gal peptide (Figure 4.4.3.3.2). Experimental procedures of this specific experiment are the same as described in section 4.4.3.1.
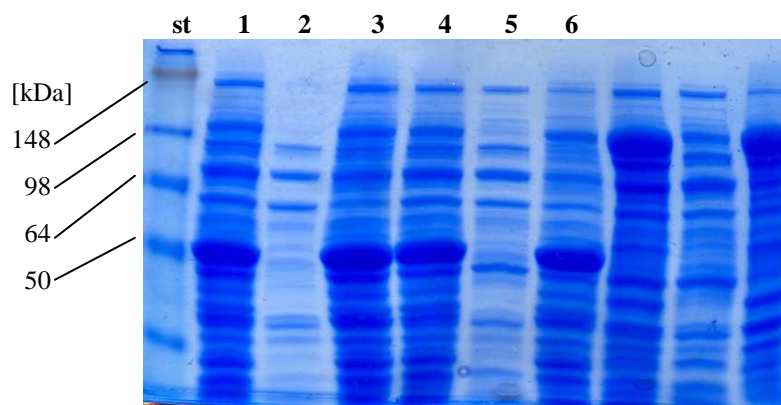
Figure 4.4.3.3.3 SDS-PAGE of induction conditions for expression of the GST-tagged truncated β-galactosidase in T1p. β-Gal was induced for 4 hrs at 25 °C with either 0.5 mM **(lanes 1-3)** or 1 mM IPTG **(lanes 4-5)**. **(st)** 20 µl SeeBlue® Plus2 (Invitrogen); **(1)+(4)** 30 µl cell homogenate; **(2)+(5)** 30 µl supernatant; **(3)+(6)** 30 µl pellet after sonication and centrifugation. 10% Tris-HCl ready gels (Biorad), running buffer: Tris/glycine

4.4.4 Solubilization of insoluble, truncated human lysosomal acid lysosomal *β*-galactosidase *in vitro*

Another, quite different approach was tested to obtain soluble GST-tagged β-Gal fusion proteins. The insoluble, truncated GST-β-Gal peptide (N-GST-Gal-peptide) expressed in T1p, was the basis for the following experiments, assuming that refolding might be easier for shorter peptides. The principle of the tested method is refolding of insoluble proteins under *in vitro* conditions. The experimental procedures are described in full detail in section 3.6, and are based on the findings of Middelberg [Middelberg, 2002]. Ten different conditions (Table 4.4.4.1) were examined using the overexpressed, insoluble N-GST-Gal-peptide of transformant T1p. Cell pellets from 50 ml cultures were used in preliminary experiments, respectively.

Buffer	Detergent/Denaturant	pH
PBS	/	7.4
Wash Buffer 1	1 M urea	7.6
Wash Buffer 2	2 M urea	7.7
Wash Buffer 3	4 M urea	7.8
Wash Buffer 4	0.2% (w/v) N-lauroyl-sarcosine	7.5
Wash Buffer 5	0.5% (w/v) N-lauroyl-sarcosine	7.5
Wash Buffer 6	1% (w/v) N-lauroyl-sarcosine	7.6
Wash Buffer 7	1% (v/v) Tween-20	7.4
Wash Buffer 8	1% (w/v) CHAPS (3-[(3-Cholamidopropyl)-dimethylammonio]-1-propanesulfonate)	7.6
Wash Buffer 9	1% (w/v) guanidine hydrochloride	7.5

Table 4.4.4.1 Washing conditions for solubilization of inclusion bodies.

The purpose of the different washing steps was the stepwise removal of contaminants from inclusion bodies, which could interfere with solubilization of the protein of interest. Triton® X-100 acts as mild, but effective detergent, often used to increase the solubility of membrane proteins, thereby permeabilizing cell membranes, and conserving the native conformation of the membrane proteins in solution [cf. references on product data sheet ckv 4/21/99, Sigma-Aldrich®]. For this reason, Triton® X-100 was always added to the lysis buffer (0.9% NaCl) for mammalian samples at a final concentration of 0.01%. In this experiment, the pellet was washed with Triton prior application of harsher conditions (e.g. urea). The aim of the overall

procedure was to obtain a solubilized form of the GST-β-Gal peptide, even if treatment with Washing Buffer 10 (8 M urea) would be necessary.

The results of a preliminary solubilization experiment are given in Figure 4.4.4.2. N-GST-Gal-peptide expression was induced with 1 mM IPTG and cells were cultured for 4 hrs at 37 °C. During the "fourth wash" under different buffer conditions, it became already clear that sarkosyl and guanidine-HCl buffers effectively solubilized former insoluble proteins, because the pellet was almost completely dissolved under these conditions, whereas the pellet was unchanged under all other tested conditions. Therefore, only the supernatants from selected sarkosyl washings were subjected to SDS-PAGE. Former insoluble N-GST-Gal-peptide (blue arrow) was successfully solubilized by washing with 0.2% or 0.5% sarkosyl (red arrows). The highest amounts of soluble fusion protein were already obtained after the "fourth wash" (lanes 7 and 13). Interestingly, the residual portion of insoluble N-GST-Gal-peptide could not be solubilized by 8 M urea treatment (lanes 11 and 17). However, the abundance of sarkosyl-soluble N-GST-Gal-peptide provided a good basis for subsequent purification experiments.

Figure 4.4.4.2 SDS-PAGE of solubilization experiments with GST-tagged truncated β-galactosidase of T1p. β-Gal was induced with 1 mM IPTG at 37 °C for 4 hrs. Inclusion bodies were washed with different detergents/ denaturants to obtain soluble N-GST-Gal-peptide. **lanes 7-11:** Wash Buffer 4 (0.2% sarkosyl); **lanes 13-17:** Wash Buffer 5 (0.5% sarkosyl); **(st)** 20 µl SeeBlue® Plus2 (Invitrogen™); **(1)** 30 µl cell homogenate; **(2)** 30 µl pellet after sonication and centrifugation; **(3)** 30 µl supernatant; **(4)** 30 µl first wash; **(5)** 30 µl second wash; **(6)+(12)** 30 µl third wash; **(7)+(13)** 30 µl fourth wash; **(8)+(14)** 30 µl fifth wash; **(9)+(15)** 30 µl sixth wash; **(10)+(16)** 30 µl 8 M urea resuspended inclusion bodies; **(11)+(17)** 30 µl 8 M urea insoluble proteins. 10% Tris-HCl ready gels (Bio-Rad), running buffer: Tris/glycine.

For a preliminary, small-scale purification of the GST-tagged fusion protein, cell pellets from 4 x 50 ml T1p culture after 4 hr induction with 1 mM IPTG at 37 °C were prepared as described

in section 3.2.2 with minor modifications. Instead of fractionating the pellet after the second wash, the pellets were combined and subsequent steps were carried out with a fourfold volume of the respective buffer, resulting in a total sample volume of ~8 ml after the "fourth wash". The pellet was washed exclusively with Wash Buffer 4 (0.2% sarkosyl; "fourth wash") and further washing steps were dispensed. Aliquots of all samples were subjected to SDS-PAGE (Figure 4.4.4.3, lanes 1-9), and bovine serum albumin (BSA; ~66 kDa) was applied to the gel for estimation of protein amounts.

The estimated amount of the fusion protein in 8 ml of the "fourth wash" supernatant was ~6 mg (0.75 mg protein/ml). This supernatant fraction was incubated with 60 units of the PreScission™ Protease (supplied as 2 U/µl; GE Healthcare) for 16 hrs at 4 °C under mild shaking. One unit of the enzyme is able to cleave ~100 µg of GST-tagged fusion proteins when incubated in the optimal buffer (50 mM Tris-HCl, 150 mM NaCl, 1 mM EDTA, 1 mM DTT, pH 7.0) at 5 °C for 16 hrs. For a first try, the sample was deliberately incubated with PreScission™ Protease in Wash Buffer 4 containing 0.2% sarkosyl. It was unclear, if sarkosyl would affect binding to the GST affinity resin. Unfortunately, no information was available from the manufacturer on inquiry. However, a tolerance of 1% Triton® X-100, 1% Tween® 20, 1% CTAB, 10 mM DTT, 0.03% SDS, or 0.1% NP-40 has been demonstrated by the manufacturer [GenScript TM0185]. In the best of cases, the GST-tag would be cleaved from the fusion protein and bind to the GST affinity resin, and PreScission™ Protease would bind to the resin as well, providing only the untagged truncated human β-Gal peptide in the flow through.

Two milliliters from the 50% slurry of the High-Affinity GST Resin (GenScript; capacity >6 mg horse liver GST/ml packed resin) were prepared as described in the manufacturer's instructions [GenScript TM0185], and equilibrated with Wash Buffer 4. The procedure yielded in 1 ml packed GST affinity resin, which was used for batching the "fourth wash" fraction (8 ml) for 3 hrs at 4 °C under mild rotating in an overhead shaker (Heidolph Reax 2, lowest level). This mixture was filled into a 0.8 x 4 cm Poly-Prep® Chromatography Column (Bio-Rad), and allowed to flow through by gravity flow. Results are shown in Figure 4.4.4.3 (lane 13).

Unfortunately, the GST-tag of the fusion peptide did not bind to the resin, nor did PreScission™ Protease cleave GST. The same sample volume was applied in lanes 12 and 13, and there is no difference in the amount of N-GST-Gal-peptide (~55 kDa), hence no cleavage of GST and no

binding of free GST to the affinity resin occurred. PreScission™ Protease (~46 kDa) itself was not visible in either lane (12 or 13), due to the high dilution factor during sample preparation (30 µl into 8 ml). To rule out any negative influence of the large sample volume, subsequent experiments were conducted with smaller volumes.
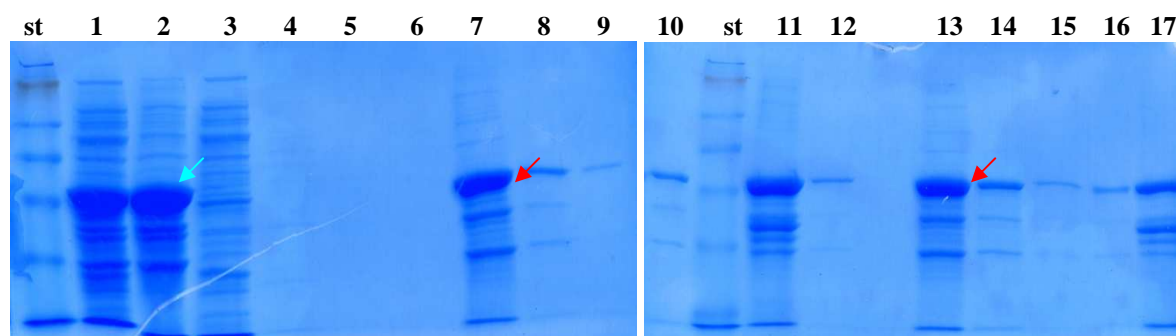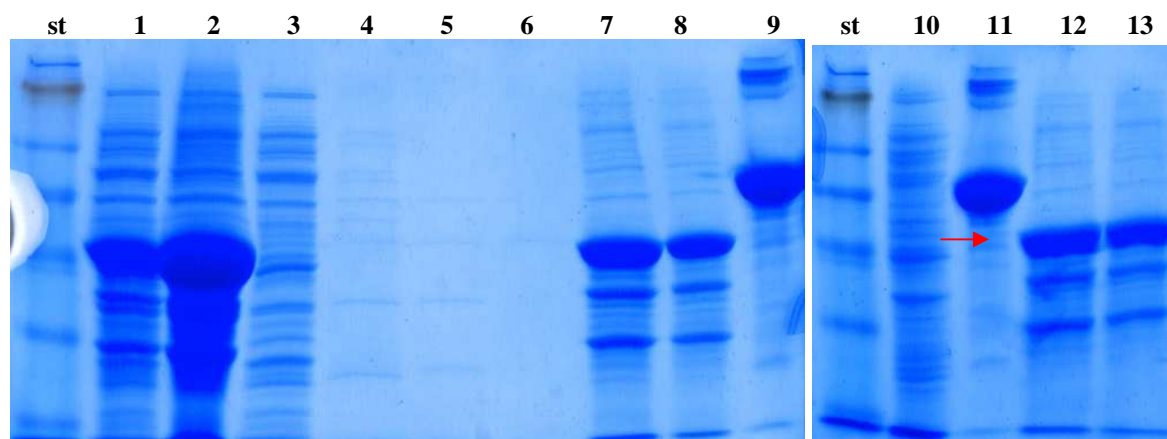

Figure 4.4.4.3 SDS-PAGE of solubilization and purification experiments with GST-tagged truncated β-galactosidase of T1p. β-Gal was induced with 1 mM IPTG at 37 °C for 4 hrs. Inclusion bodies were solubilized with 0.2% Wash Buffer 4 (0.2% sarkosyl). Soluble proteins were treated with PreScission™ Protease (GE Healthcare) prior GST affinity chromatography. **(st)** 20 µl SeeBlue® Plus2 (Invitrogen™); **(1)** 30 µl cell homogenate; **(2)** 30 µl pellet after sonication and centrifugation; **(3)** 30 µl supernatant; **(4)** 30 µl first wash; **(5)** 30 µl second wash; **(6)** 30 µl third wash; **(7)** 20 µl fourth wash; **(8)** 10 µl fourth wash; **(9)+(11)** 20 µl bovine serum albumin (BSA; 1 mg/ml); **(10)** 10 µl uninduced T1p; **(12)** 40 µl fourth wash + PP; **(13)** 40 µl flow through. 10% Tris-HCl ready gels (Bio-Rad), running buffer: Tris/glycine.

For further cleavage tests, the flow trough (~8 ml 0.2% sarkosyl solution + PreScission™ Protease from the previous experiment) was fractionated in 1 ml aliquots and diluted 1:2, 1:4, or 1:20 in PBS (pH 7.4) containing 1 mM EDTA, and 1 mM DTT, the optimal buffer for PreScission™ Protease cleavage of GST. Then, the dilutions were concentrated to final volumes of 1 ml again, using centrifugal filter units (Amicon Ultra-15, MWCO 10,000; Millipore). Finally, 10 units of PreScission™ Protease were added again to each fraction and the solutions were incubated for another 16 hrs at 4 °C under mild rotating. At this point, all samples contained a certain amount of (probably already inactive) PP from the previous experiment, but also the freshly added enzyme in the required dose. Changing the buffer composition, especially reduction of the sarkosyl concentration, might affect the solubility of N-GST-Gal-peptide. Therefore, different dilutions were prepared as described above and treated with PreScission™ Protease. Aliquots from each fraction were applied to SDS gels (Figure 4.4.4.4).

Again, the enzyme did not cleave the GST-tag from N-GST-Gal-peptide. The fusion peptide was still intact in each sample, and there were no signs of free GST-tags or untagged β-Gal peptides. In fact, there was no difference between the protease-treated fractions (lanes 1-4 and 8+9) and the original fourth wash fraction (cf. Figure 4.4.4.3, lane 7, without PP). For size comparison, samples of PreScission™ Protease (~46 kDa) were applied to the gel (lanes 5 and 6). The enzyme is not visible in other lanes. Dilution of Wash Buffer 4 and reduction of its sarkosyl content seemed to have no significant influence on the solubility of the N-GST-Gal-peptide (lanes 1-4).
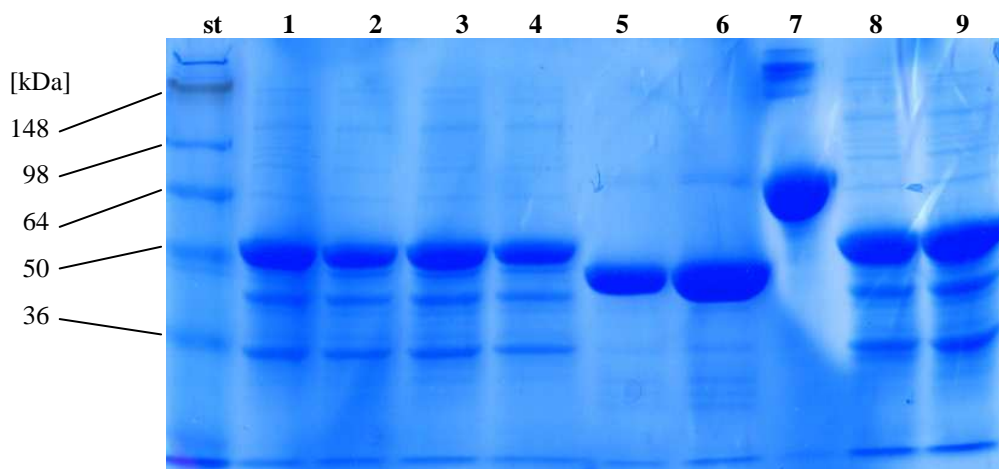
Figure 4.4.4.4 SDS-PAGE of purification experiments with GST-tagged truncated β-galactosidase of T1p. The sarkosyl-soluble protein solution was fractionated, rebuffered, concentrated, and treated once more with PreScission™ Protease. (**st**) 20 µl SeeBlue® Plus2 (Invitrogen™); (**1**) 40 µl flow through aliquot (+ PP); (**2**) 40 µl of 1:2 concentrate aliquot (+ PP); (**3**) 40 µl of 1:4 concentrate aliquot (+ PP); (**4**) 40 µl of 1:20 concentrate aliquot (+ PP); (**5**) 10 µl PreScission™ Protease; (**6**) 20 µl PreScission™ Protease; (**7**) 20 µl bovine serum albumin (BSA; 1 mg/ml); (**8**) 40 µl fourth wash aliquot (+ PP); (**9**) 40 µl fourth wash aliquot (+ PP) + freshly added PP. 10% Tris-HCl ready gels (Bio-Rad), running buffer: Tris/glycine.

There are several possible reasons why PreScission™ Protease did not cleave GST from the fusion peptide, and GST was not bound by affinity chromatography:

1. The cleavage conditions were not optimal in terms of protein concentration/sample dilution, sample buffer, or sarkosyl content.

2. Batch conditions were not optimal for purification of GST-tagged proteins. Preference might be given to "on column" procedures.

3. N-GST-Gal-peptide was not bound due to interference of the detergent sarkosyl in the buffer. No data about sarkosyl usage was available from the manufacturer of the resin. On the other hand, detergents like Triton® X-100 or 1% Tween® 20 are tolerated in concentrations up to 1% in the sample buffer.

4. The enzyme could not cleave because the fusion protein was soluble, but not correctly folded, affecting also the native state of the GST-tag hence masking the recognition site for cleavage by steric hindrance. GST binding to the affinity resin could have been impaired for the same reason.

4.5 Antibody development

Several strategies have been described to obtain antibodies or antisera directed against the human lysosomal acid β-galactosidase. These strategies comprise purification of overexpressed β-Gal precursor proteins (84 kDa) from the culture medium of CHO cells [Zhang *et al*., 1994], purification of the mature enzyme (64 kDa) from human placenta [Hubbes *et al*., 1992] and other organs (e.g. liver) or from urine [Kress and Miller, 1978; Norden *et al*., 1974], or the selective design and production of β-Gal oligopeptides [e.g. Hinek *et al*., 1993; Zhang *et al*., 1994]. Another approach to purify large amounts of the human enzyme was the cloning of its cDNA into the baculovirus genome and subsequent overexpression of the recombinant virus in insect cells [Itoh *et al*., 1990]. Most of these methods are time-consuming and expensive due to several affinity chromatographic procedures involved in the purification [e.g. Hubbes *et al*., 1992], and heterologous overexpression of proteins might be an efficient alternative to established strategies. The heterologous expression of human β-Gal in *E. coli* cells described in this work was only partially successful and requires further optimization. Due to time limitations, two other strategies were pursued in this work to obtain specific anti-β-Gal antibodies. Therefore β-Gal precursor proteins were purified from the medium of CHO-K1 cells and injected in rabbits as previously described [Zhang *et al*., 1994]. Furthermore, two novel β-galactosidase oligopeptides were designed in cooperation with the company Eurogentec (Seraing, Belgium).

4.5.1 Purification of human lysosomal acid *β-galactosidase from CHO-K1 cell culture medium*

Chinese hamster ovary (CHO) cells are convenient mammalian host cells, often utilized for expression of recombinant enzymes for enzyme replacement therapy (ERT) of lysosomal storage diseases [reviewed in Desnick, 2004 and Jayapal *et al.*, 2007]. In contrast to bacterial cells, they are able to perform post-translational modifications (e.g. glycosylations) on heterologously expressed proteins. Zhang *et al.* described the purification of overexpressed, secreted β-galactosidase precursor protein from the culture medium of CHO cells and subsequent antibody production. The method was established at the Department of Pediatrics during this work.

CHO cells (subclone K1), permanently transfected with the cDNA for human lysosomal acid β-galactosidase, and secreting the β-Gal precursor into the cell culture medium were provided by Doris Hofer, Department of Pediatrics, Medical University of Graz (see section 3.7.3). Although this approach produces stable, soluble, and correctly folded β-Gal protein there are a few drawbacks to consider when using this method for purification of human β-galactosidase. On the one hand, optimization of expression conditions and cultivation of CHO-K1 cells is time-consuming (up to 6 weeks) and expensive, and huge amounts of culture medium have to be collected (up to several liters). Furthermore, handling of such huge amounts of medium for chromatography purification is difficult, and quite often a significant portion of the target protein is lost during purification. However, it is still one of the methods of choice when purified β-Gal protein is required.

Different cultivation conditions were tested and optimized for overexpression of the human β-galactosidase. Interestingly, no significant overexpression was achieved using the previously published cell culture methods [Zhang *et al.*, 1994]. Best results were obtained by a combination of different culture media, and varying the incubation temperature (see section 3.8.4). Altogether, 2.6 L medium from CHO-K1 cells were used for the purification procedure described in section 3.12.7, yielding in ~730 µg β-galactosidase precursor protein. Briefly, the proteins from CHO-K1 culture medium were precipitated with 50% (w/v) ammonium sulfate, pelleted by centrifugation, and resuspended in 15 ml Phosphate Buffer I (pH 7.0), followed by dialysis in different buffer systems. The sample had a final volume of 40 ml prior dialysis, and 88 ml after dialysis was performed. After acidification (pH 4.3), the protein solution was

briefly centrifuged, and filtered through a filter paper. Ultimately, 83 ml of the supernatant (pH 4.3) were batched with 40 ml of the equilibrated PATG affinity resin (Sigma-Aldrich®) over night at 4 °C. Purification was performed with the ÄKTAexplorer™ system, using an XK 50/20 column as described in section 3.12.7. Fractions were collected manually, and analyzed with the UNICORN™ 4.12 software. Washing was performed with 8 bed volumes of Sodium Acetate Buffer I (pH 4.3), and bound protein was eluted with 3 bed volumes Elution Buffer GL (pH 7.0). The eluate was pooled, concentrated, dialyzed against 5 L Phosphate Buffer I (pH 7.0), and concentrated once more to a sample volume of 1.4 ml. Several charges of purified β-Gal were pooled at this point (obtained from a total of 2.6 L medium) , rebuffered with PBS (pH 7.4), and concentrated to a final sample volume of 260 µl. To remove the eluant D(-)-Galactonic acid-γ-lactone, it is important to dialyze the sample immediately. Furthermore it is important to prepare the Elution Buffer GL just prior application, because galactonolactone displayed a certain instability when dissolved for >12 hrs, leading to pH shifts of the elution buffer.

Proteins were determined according to the method of Lowry [Lowry *et al*., 1951], and β-galactosidase assays were performed with the concentrated and rebuffered eluate ("EGal"). The total protein concentration was 2.8 mg/ml, adding up to ~730 µg total protein in the EGal fraction (260 µl). β-galactosidase activity was calculated as ~2,200 mU/ml, with a specific activity of ~786 mU/mg protein. Finally, the specific β-Gal activity in the EGal fraction was ~30-fold higher than in the supernatant fraction (pH 4.3) prior application to the column (~26 mU/mg). The β-galactosidase precursor protein, secreted into the culture medium upon overexpression in CHO-K1 cells, has a molecular weight of 88 kDa [Okamura-Oho *et al*., 1996; Zhang *et al*., 1994], and was successfully purified by PATG affinity chromatography (Figure 4.5.1.1.1). Purified β-Gal was immediately subjected to SDS-PAGE. Only small amounts of other proteins where left in the EGal fraction, when compared to the main protein band. These proteins do not interfere with antibody development, as the purified β-Gal precursor can be excised from the SDS gel and directly used for immunization of rabbits.

4.5.1.1 Antigen preparation

The β-Gal specific bands (88 kDa) were excised from the gels using a sterile scalpel. After washing twice with sterile Aqua dest., the gel pieces were portioned in 8 Eppendorf tubes (~90 µg protein/tube), covered with sterile Aqua dest., and stored at room temperature until shipment (<24 hrs). The antigen was shipped at room temperature. For animal's health purposes and successful production of antibodies it was necessary to avoid chemicals like sodium azide (NaN_3), dithiothreitol (DTT), ethylenediaminetetraacetic acid (EDTA), acetic acid, urea, or other highly toxic substances in the final sample buffer. Coomassie staining does not impair antibody production. Preparation of the antigen as SDS gel piece was recommended by Eurogentec (Seraing, Belgium). According to information from Eurogentec, recognition specificity of antibodies is not necessarily influenced by the sample condition that is to say, if the antigen is provided in denatured form (e.g. SDS gel pieces), the resulting antibodies could recognize both the native and denatured form of the antigen. This is important, if the same antibody should be used for applications like immunofluorescence, Western blotting, and/or protein precipitation. These criteria were also the demands we made on the resulting anti-β-Gal antibody.
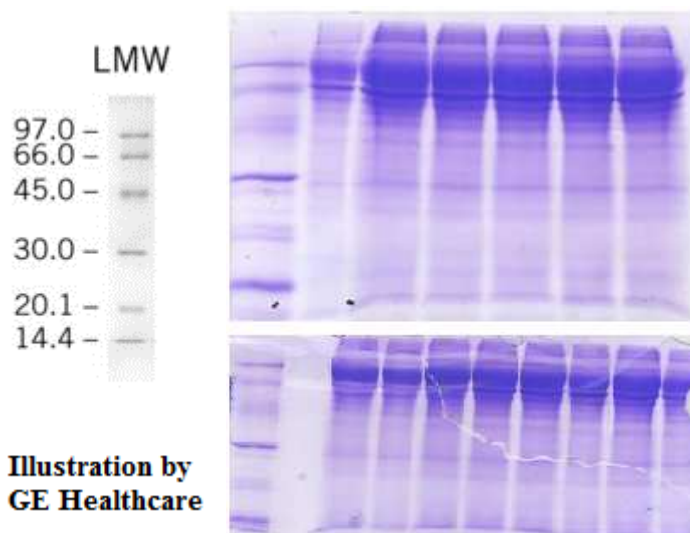
Figure 4.5.1.1.1 SDS-PAGE of the EGal fraction from PATG-chromatography for antibody development. β-Gal was overexpressed in CHO-K1 cells, secreted into the cell culture medium, and purified via PATG affinity chromatography. Standard: LMW-SDS Marker (GE Healthcare). Both gels were loaded with the EGal fraction (~730 µg total protein). 260 µl EGal were mixed with 86 µl of 4x Laemmli Sample Buffer (cf. section 3.11.7). 12.5% polyacrylamide gel, running buffer: Tris/glycine.

4.5.1.2 Immunization of rabbits and antibody production

Immunization was executed by four subcutaneous injections, with ~90 µg antigen per injection, and a total of ~360 µg antigen per rabbit. Two rabbits were used for anti-β-galactosidase antibody production. A first boost was done 21 days after the first immunization, followed by two more boosts at intervals of 28 days, respectively. Small bleeds took place 9 days after the first boost, and large bleeds were planned 9 days after the second boost. Final bleeds were scheduled on day 87, 10 days after the last boost. All described immunization procedures were conducted by Eurogentec (Seraing, Belgium).

Unfortunately, both rabbits (2206 and 2207) were killed right after the second boost, due to a technical accident by the company. It was not possible to recover serum from the rabbits, except for the small bleed sera (~2 ml each). A new immunization of a single rabbit (2513) was started using the remaining ~180 µg of the antigen. The procedure was slightly altered in terms of boost intervals, with four subcutaneous injections (~45 µg each), at intervals of 14 days (first and second boost, respectively) and 28 days (third boost). Again, small bleeds were planned 9 days after the second boost, and large bleeds 9 days after the third boost. The final bleed was done on day 87, almost a month after the last boost. Total IgG purification was performed by Eurogentec, using 50 ml of the final bleed serum (rabbit polyclonal serum; antiserum) from rabbit 2513, and both small bleed sera (~4 ml) from the previous immunization (rabbits 2206 and 2207). The resulting polyclonal IgG fraction was designated "anti-β-Gal-total IgG antibody". It should be noted that this antibody solution is not solely specific for detection of β-Gal proteins, due to other co-purified rabbit IgGs. However, the anti-β-Gal-total IgG antibody could be able to detect both precursor and mature β-Gal proteins on Western blots and, at best, also in immunofluorescence and immunoprecipitation experiments.

4.5.1.3 Quality testing of the anti-β-Gal-total IgG antibody

To assess the quality and specificity of the antibody solution, cell homogenates of COS-1 cells overexpressing human lysosomal acid β-Gal [Hofer *et al*., 2009 and 2010], as well as human skin fibroblasts were subjected to Western blots, and hybridized with different antibody concentrations. For cell homogenate preparation, protein determination, SDS-PAGE, and Western blotting, see section 3.11.7. Nitrocellulose membranes were pre-blocked in 10 ml Milk

Blocking Buffer for 1 hr at room temperature, followed by primary antibody incubation in 10 ml Milk Blocking Buffer (1:100 and 1:250) for 16 hrs at 4 °C. Additionally, one blot was hybridized with pre-immune serum (1:100 in milk), and another blot with final bleed serum (1:100 in milk). The Anti-rabbit IgG (whole molecule) alkaline phosphatase conjugate antibody produced in goat (Sigma-Aldrich®), diluted 1:40,000 in Milk Blocking Buffer, was used as secondary antibody, and incubated for 1 hr at room temperature. Blots were developed using the Bio-Rad Alkaline Phosphatase Conjugate Substrate Kit. Results are shown in Figure 4.5.1.3.1.

While the antigen (β-Gal precursor secreted from CHO-K1 cells) had a molecular weight of ~88 kDa, the resulting antibody should be able to recognize the ~84 kDa precursor protein, as well as the ~64 kDa mature enzyme of human skin fibroblast cells [Callahan, 1999; Okamura-Oho *et al*., 1996], but also secreted precursor protein itself, or any other form of heterologously expressed human β-galactosidase. The overexpressed precursor in COS-1 cells has a molecular weight of ~84 kDa as well. In fact, there was neither a constant nor a logical pattern in β-Gal detection with all tested primary "antibodies", except for the control blot (lane 11, red arrow) using the α85 anti-human β-galactosidase antibody (D'Azzo). Very similar, unspecific signals in the size of the mature enzyme (~64 kDa) and the precursor protein (~84 kDa) were obtained with pre-immune serum (blot A, lanes 1 and 3) and the anti-β-Gal-total IgG antibody (blot C, lane 5 and 7). As the pre-immune serum was collected prior immunization with the antigen, a positive β-Gal reaction is not possible, and the signals in blot A suggest an unspecific immunoglobulin reaction. Furthermore, even if positive, all signals obtained (dilution 1:100 or 1:250) were much lower than α85 antibody signals (dilution 1:1,000), but it must be noted that antibody/antisera efficiencies cannot be compared directly, due to different specific immunoglobulin concentrations.

However, the signals obtained were not in accordance with the predicted response. While healthy control fibroblasts express mainly mature β-Gal enzyme and hardly any precursor protein, the juvenile GM1 homogenate should contain almost only precursor protein, due to rapid degradation of misfolded β-Gal [Callahan 1999; Oshima *et al*., 1994; Yoshida *et al*., 1991]. Transiently transfected COS-1 cells also express only the β-Gal precursor protein (cf. lane 11, red arrow). Because of the extremely high expression efficiency, the cells are almost incapable of processing the precursor to form the mature enzyme. Only small amounts of

mature β-Gal might be found in COS-1 homogenates [Hofer *et al.*, 2009 and 2010] (cf. lane 11, blue arrow). The juvenile GM1 bands in lane 6 were almost similar to the healthy control bands in lane 7. Furthermore, signals detected in COS-1 homogenates (lanes 5 and 8) were almost completely unspecific (cf. lane 11, control blot), except for a weak signal in the approximate size of the precursor protein (lane 5, red arrow). The blue arrow in lane 7 indicates the putative location of the mature enzyme band. In all Western blots performed in this work, the β-Gal precursor protein appeared in the size of the tiny standard band (green arrows; this hardly visible standard band is not featured in the manual) between the indicated standard of 82.2 kDa and 115.5 kDa. Mature enzyme was always detected right above the 64.2 kDa standard band.

In summary, detection of precursor and mature β-Gal proteins with the anti-β-Gal-total IgG antibody or the corresponding pre-immune serum produced mainly unspecific, and weak signals in Western blot experiments. To rule out any possibility of sample confusion, experiments were performed twice.
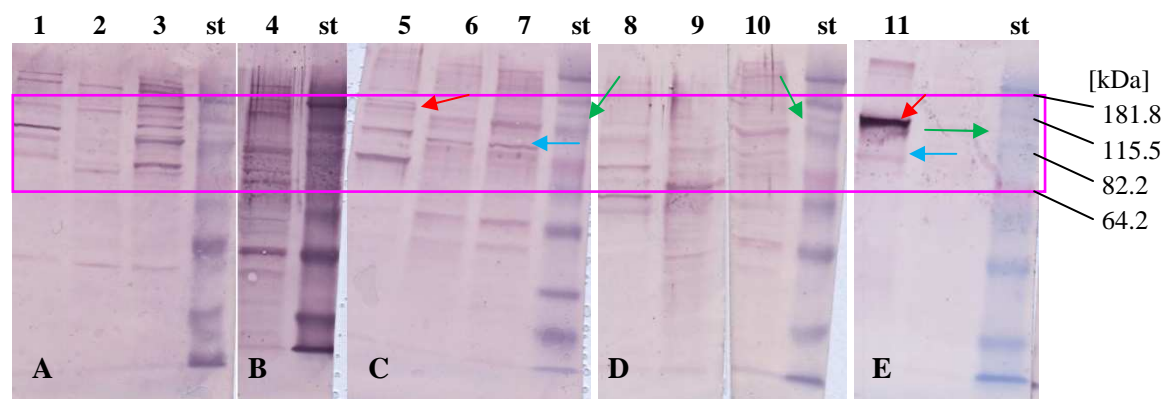
Figure 4.5.1.3.1 Western blot detection of immunoresponsive material in mammalian cell homogenates using the anti-β-Gal-total IgG antibody. For comparison, one blot was hybridized with pre-immune serum (**A**; 1:100), another blot with final bleed serum (**B**; 1:100), and a positive control blot was incubated with the α85 anti-human β-galactosidase antibody (D'Azzo; 1:1,000; **E**). Anti-β-Gal-total IgG antibody was used in a 1:100 dilution (**C**), and in a 1:250 dilution (**D**). (**st**) 25 µl BenchMark™ (Invitrogen™); (**1**) +(**5**)+(**8**)+(**11**) 20 µl COS-1 + 7 µl 4x LDS Sample Buffer (Invitrogen™) + 4 µl 10x Reducing Agent (Invitrogen™); (**2**)+(**6**)+(**9**) 16.2 µl juvenile GM1 + 5 µl SB + 2 µl RA; (**3**)+(**4**)+(**7**)+(**10**) 13.6 µl healthy control + 5 µl SB + 2 µl RA. 10% Tris-HCl ready gels (Bio-Rad), running buffer: Tris/glycine; nitrocellulose membranes.

For the purpose of comparison, Western blots of COS-1 cell homogenates were performed, and membranes were hybridized with aliquots from the original small bleed and pre-immune sera (from the killed rabbits 2206 and 2207). Hybridization conditions were the same as described

above. All sera were diluted 1:100 in Milk Blocking Buffer, and membranes were incubated over night at 4 °C. Results are shown in Figure 4.5.1.3.2. Interestingly, the membranes hybridized with the small bleed sera from both (killed) rabbits clearly showed β-Gal-specific immunoreactive signals (lanes 2 and 4), even though sera were collected only 9 days after the first boost (day 30). The β-Gal precursor protein overexpressed in COS-1 cells (cf. lane 5, control blot) was recognized by both small bleed antisera, and showed the strongest signal (red arrows). As expected, there were also numerous unspecific, but less intense, signals that can be attributed to reactions with other immunoglobulins in the serum. Most important, the pre-immune sera did not show the same band pattern as small bleed sera, supporting the results from the blots hybridized with small bleed sera.

According to this data, ~90 µg of the antigen (β-Gal precursor purified from CHO-K1 cell culture medium) per injection, and a total of two injections were sufficient for successful immune response stimulation in each rabbit (2206 and 2207) used in the first immunization round. Immunization with the reduced amount of antigen (~45 µg per injection) did not produce the desired polyclonal antibodies (rabbit 2513), and neither final bleed serum nor the purified total IgGs from this serum (plus small bleed sera from the killed rabbits) showed reproducible, β-Gal-specific immunoreactions in Western blot experiments. This result was rather surprising, as 4 injections were performed on rabbit 2513, adding up to ~180 µg of antigen, the same total amount that proved to be sufficient in rabbit 2206 and 2207, respectively.

Despite the positive results, no further tests were performed with the small bleed sera from the killed rabbits, because both sera were used for purification of total IgG as described above, and the small amounts kept in our lab were not sufficient for regular use in experiments.
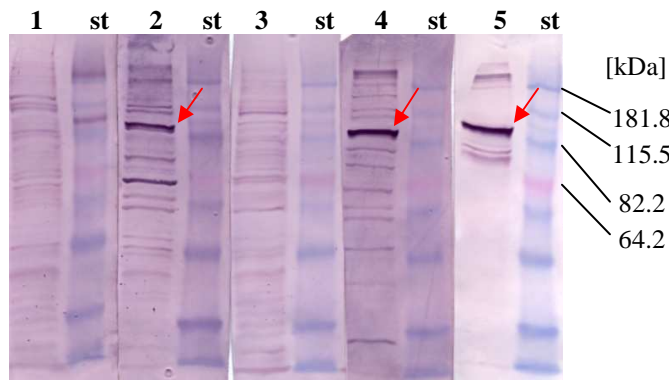
Figure 4.5.1.3.2 Western blot detection of immunoresponsive material in COS-1 cell homogenates using small bleed antisera. For comparison, blots **(1)**+**(3)** were hybridized with pre-immune sera in 1:100 dilutions, and a control blot **(5)** was incubated with the α85 anti-human β-galactosidase antibody (D'Azzo; 1:1,000). Small bleed antisera **(2)**+**(4)** were used in 1:100 dilutions. **(st)** 20 µl BenchMark™ (Invitrogen); **(1)**+**(2)** sera from rabbit 2206;

(3)+**(4)** sera from rabbit 2207. 20 µl of each sample were mixed with 7 µl 4x LDS Sample Buffer (Invitrogen™), and 3 µl 10x Reducing Agent (Invitrogen™), respectively. 10% Tris-HCl ready gels (Bio-Rad), running buffer: Tris/glycine; nitrocellulose membranes.

To further examine the qualities of the anti-β-Gal-total IgG antibody from rabbit 2513, immunofluorescence experiments were performed using different concentrations of both final bleed serum, and the antibody (Table 4.5.1.3.3). For experimental procedures see section 3.12.1. Primary antibody incubation was done for 2 hrs at room temperature and the Fluorescein (FITC)-conjugated affinity pure goat anti-rabbit IgG (H+L) antibody (1:200, 1 hr; Jackson Immuno Research) was used as secondary antibody. As anticipated after the negative Western blot results, the antibody solution and final bleed serum did not specifically react with β-galactosidase, but rather produced unspecific background signals in each tested concentration. Control experiments to eliminate failures of the secondary antibody were performed with anti-Catalase Rabbit pAb as primary antibody (Figure 4.5.1.3.4, D).

	Healthy control cells	**Juvenile GM1 cells**
Final bleed serum	1:10; 1:100; 1:200; 1:300	n.d.
Anti-β-Gal-total IgG antibody	1:10; 1:200; 1:300	1:10; 1:200; 1:300

Table 4.5.1.3.3 Antibody/Antisera concentrations tested in immunofluorescence experiments.
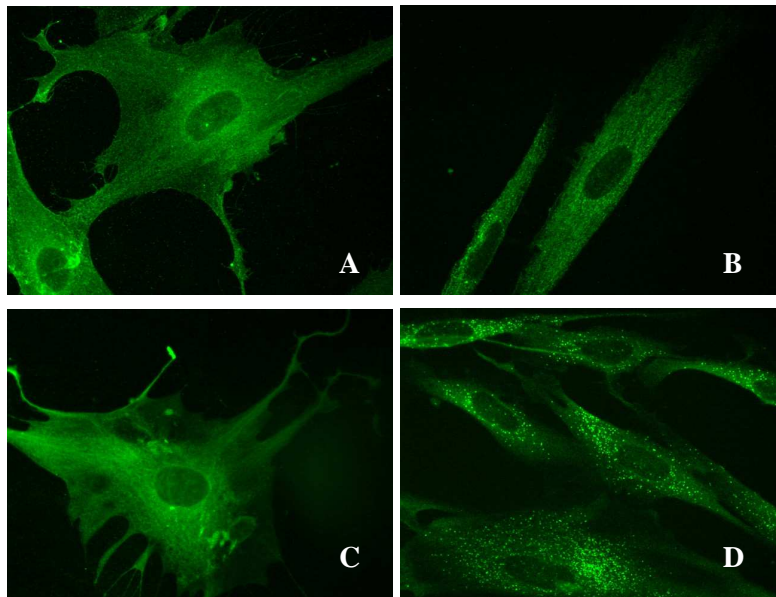
Figure 4.5.1.3.4 Immunofluorescence in fibroblasts after exposure to the anti-β-Gal-total IgG antibody, or the final bleed serum from rabbit 2513. Pictures are representative excerpts from a series of experiments (see text). Except for the control experiment **(D)**, all reactions were unspecific. **(A)** healthy control fibroblasts, total IgG antibody (1:10 dilution); **(B)** healthy control fibroblasts, final bleed serum (1:100 dilution); **(C)** juvenile GM1 fibroblasts, total IgG antibody (1:10 dilution); **(D)** healthy control cells, anti-Catalase Rabbit pAb (25 µg/ml). Cells were observed with the Olympus IX51 inverse fluorescence microscope.

4.5.2 *Production of anti-β-galactosidase peptide antibodies*

Another strategy was pursued to obtain large quantities of specific antibodies, directed against the human lysosomal acid β-galactosidase and applicable to both Western blotting and immunofluorescence experiments. Therefore, immunogenic peptides based on the protein sequence of β-Gal precursor protein [UniProt Knowledgebase accession number P16278] were designed in cooperation with Eurogentec (Seraing, Belgium). For optimal stimulation of the immune response to the antigen, two different peptides were synthesized and used for immunization of rabbits. The first peptide (LEKESILLRSSDPDY; antigen #EP084834) corresponds to position 140-154 of the polypeptide chain, and the second peptide (RFLQKRFRHHLGDDV; antigen #EP084835) was identical with position 201-215. Both sequences were verified for high recognition specificity by BLAST search (blastp; http://blast.ncbi.nlm.nih.gov), and checked for general antigenic specificity and characteristics by the company. Peptide synthesis and immunization, as well as peptide affinity chromatography were also performed by Eurogentec according to standard procedures described on their website (http://www.eurogentec.com). Briefly, the peptides were coupled to KLH (Keyhole Limpet Hemocyanin)-carrier proteins prior immunization, two rabbits were immunized with the antigens according to the AS-DOUB-LX standard package, and 20 ml of the final bleed serum from rabbit 1269 were subjected to affinity specific IgG purification to obtain β-Gal specific polyclonal antibodies. Purification was performed separately for each antigen. Polyclonal antibodies resulting from affinity purification with the antigen ligand

150

EP084834 were designated "anti-β-galactosidase peptide antibody 1", while purification with the ligand EP084835 produced "anti-β-galactosidase peptide antibody 2".

A series of Western blot and immunofluorescence experiments was performed for quality testing of the resulting polyclonal antibodies. Experimental procedures were the same as described in previous chapters and in the methods section. A representative illustration of Western blot results is shown in Figure 4.5.2.1. Both antibodies significantly reacted with β-Gal proteins in cell homogenates of human skin fibroblasts, or COS-1 cells. Most remarkably, signals were highly specific and very similar to control blots (cf. blot F and G) under all tested conditions. Best signals were obtained with 1:100 dilutions.

Unfortunately, both polyclonal antibody charges were unable to specifically localize β-Gal in immunofluorescence experiments (data not shown). However, these peptide antibodies were frequently used for Western blot experiments during this work.
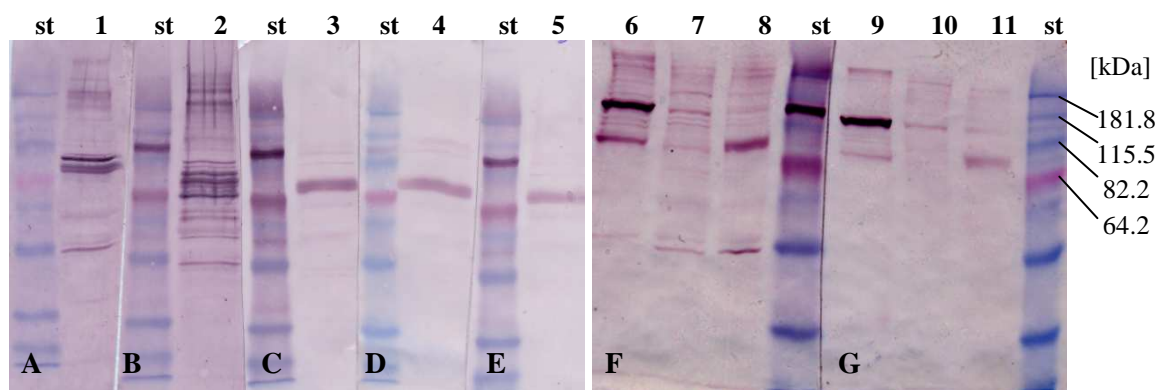
Figure 4.5.2.1 Western blot detection of immunoresponsive material in mammalian cell homogenates using the anti-β-galactosidase peptide antibodies 1 and 2 from rabbit 1269. The blots are representative for a series of experiments with both peptide antibodies, as well as pre-immune serum and final bleed serum. **(A)** pre-immune serum, dilution 1:100; **(B)** final bleed serum, dilution 1:100; **(C)** peptide antibody 1, dilution 1:100; **(D)** peptide antibody 2, dilution 1:100; **(E)** peptide antibody 1, dilution 1:250; **(F)** peptide antibody 1, dilution 1:100. A control blot was incubated with the α85 anti-human β-galactosidase antibody (D'Azzo; 1:1,000; **(G)**. **(st)** 25 µl BenchMark™ (Invitrogen™); **(1)-(5) and (8)+(11)** healthy controls; **(7)+(10)** juvenile GM1; **(6)+(9)** COS-1. 30 µg of total fibroblast proteins**,** and 20 µg COS-1 total protein were applied to gels, respectively. Samples were mixed with appropriate amounts of 4x LDS Sample Buffer (Invitrogen™) and 10x Reducing Agent (Invitrogen™). 10% Tris-HCl ready gels (Bio-Rad), running buffer: Tris/glycine; nitrocellulose membranes.

4.6 Biochemical characterization of novel iminosugars

4.6.1 Determination of inhibition constants

All of the tested substances proved to be potent inhibitors of the lysosomal β-galactosidase *in vitro* (cf. section 3.9.1, 3.12.2, and 3.12.3). The apparent inhibition constant (K_i) of most compounds was below 1 µM, while half maximal inhibitory concentrations (IC_{50}) of the novel compounds were ranging between 1 µM and 11 µM, with one exception (#2 w/o dansyl). In either case, the novel 1-deoxygalactonojirimycin (DGJ) derivatives demonstrated increased inhibition potency (lower K_i and IC_{50}) against the β-Gal enzyme, when compared to the parent compound. This effect was previously observed in kinetic experiments with specific dansylated iminosugars [Lundt *et al.*, 2006; Steiner *et al.*, 2008]. The only non-inhibitory substance in this work was compound #3. This result was not surprising, as β-Gal only binds to substrates in galacto-conformation, and compound #3 has a D-manno-configuration.

It should be noted that all inhibition assays were performed with cell homogenates of fibroblasts from healthy individuals (healthy controls), because a purified form of human lysosomal acid β-galactosidase was not available. Furthermore, an inhibitory effect of some tested iminosugars on other glucosidases in the homogenate cannot be ruled out. Therefore, calculated inhibition constants might differ from previously published values. A detailed listing of K_i and IC_{50} values of all tested substances can be found in Table 4.6.1.1.

Compound (internal name), Configuration	Chaperone activity in p.R201C fibroblasts	IC$_{50}$ [µM]	K$_i$ [µM]
#1, galacto-	yes	n.d.	0.7 ± 0.2 (n = 7)
#2 (DLHex-DGJ), galacto-	yes	6.0 ± 0.7 (n = 3)	0.6 ± 0.09 (n = 7)
#2 w/o dansyl, galacto-	yes	47.3 ± 3.9 (n = 3)	n.d.
#3, D-manno-	no	n.d.	n.d.
#4 (DGJ), galacto-	not significant	172.7 ± 26.4 (n = 5)	n.d.
#4/2 (DGJ HCl), galacto-	not significant	~150 (n = 2)	10.5 ± 2.7 (n = 3)
#6/2, galacto-	yes	11.0 ± 0.8 (n = 3)	4.9 ± 0.3 (n = 2)
#7/3, galacto-	yes	3.2 ± 0.3 (n = 5)	0.9 ± 0.09 (n = 2)
A1, galacto-	yes	8.1 ± 0.7 (n = 3)	0.8 ± 0.04 (n = 3)
A2, galacto-	yes	4.4 ± 0.4 (n = 3)	0.8 ± 0.05 (n = 1)
A3, galacto-	n.d.	2.2 ± 0.2 (n = 3)	~0.5 (n = 1)
A4, galacto-	yes	10.9 ± 0.3 (n = 3)	~2.0 (n = 1)
A5, galacto-	yes	1.08 ± 0.1 (n = 3)	~0.3 (n = 1)
A6, galacto-	yes	2.4 ± 0.7 (n = 3)	~0.7 (n = 1)

Table 4.6.1.1 Results of chaperone screenings and inhibition assays. Inhibition assays were performed with cell homogenates from healthy control fibroblasts, and chaperone activity was determined *in vitro* after incubation of cultured fibroblasts with the respective substance. n = number of individual experiments; n.d. = not determined.

The influence of the potent β-Gal inhibitor DLHex-DGJ (#2) and its parent compound DGJ (#4) on normal human β-galactosidase is demonstrated in Figure 4.6.1.2. IC$_{50}$ values were determined by addition of 0.001-100 µM DLHex-DGJ to the β-galactosidase assay. At a concentration of 100 µM, DLHex-DGJ reduced the β-Gal activity to ~6% of the basal activity, while inhibition by the parent compound DGJ resulted in approximately 60% of the basal activity. Kinetic measurements of DLHex-DGJ in cell homogenates from healthy individuals resulted in a K$_i$ of 0.6 µM. These data imply that the dansylated compound DLHex-DGJ is a much more potent β-galactosidase inhibitor than DGJ. Similar experiments with purified β-galactosidase from *Agrobacterium sp.* further support this conclusion [Steiner *et al.*, 2008].
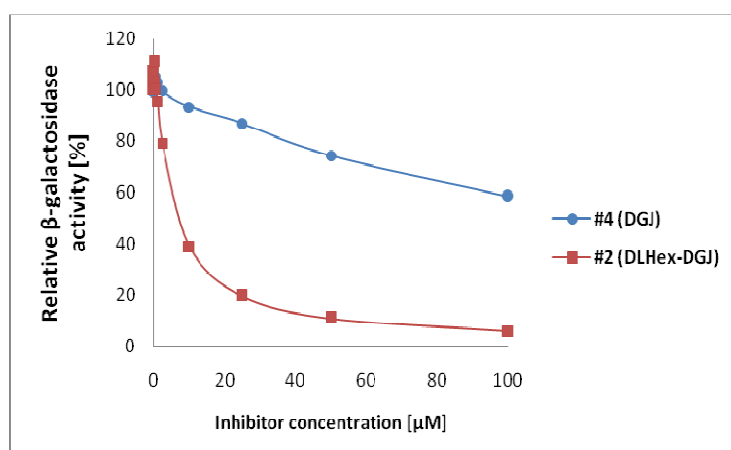
Figure 4.6.1.2 Inhibition curves of normal acid β-galactosidase. DGJ and DLHex-DGJ were added to the β-Gal assays at final concentrations of 0.001-100 µM. While at a concentration of 100 µM the parent compound DGJ reduced the β-Gal activity to ~60%, DLHex-DGJ was approximately 10-fold more effective and resulted in ~6% of the basal activity. The calculated IC_{50} of DLHex-DGJ was 6 µM.

4.6.2   Chaperone screenings in GM1 and MBD fibroblasts

The iminosugars listed in Table 4.6.1.1 were subjected to preliminary chaperone screenings in a known chaperone-sensitive cell line [Iwasaki *et al*., 2006; Tominaga *et al*., 2001], carrying the mutation p.R201C (juvenile GM1). Therefore, putative pharmacological chaperones were added to the culture media of semi-confluent fibroblasts at final concentrations of 20-500 µM, and incubated for 4 days. Cells were harvested by scraping, and cell homogenates were prepared as described for standard β-Gal assays in the methods section.

Results of preliminary experiments are shown in Figure 4.6.2.1. The relative β-Gal increase was individually calculated as compared to the activity of the respective untreated cell line. Ten of thirteen tested iminosugars were able to significantly increase the residual β-Gal activity of the chaperone-sensitive cell line. The different modifications of the acyl chain had a strong impact on the optimal chaperone concentration of each compound (indicated above the bars). Compound #2, Methyl 6-[N^2-dansyl-N^6-(1,5-dideoxy-D-galactitol-1,5-diyl)-L-lysinyl]amino hexanoate (DLHex-DGJ), was chosen for further experiments for three reasons:

1. The compound was easily soluble in aqueous buffers (e.g. PhoBI).

2. Residual β-Gal activity of p.R201C fibroblasts could be increased to up to 75% of the wildtype level in individual experiments after addition of 500 µM #2 to the cell culture medium.

154

3. Compound #2 contains a dansyl group, which renders the whole molecule autofluorescent. This feature might be helpful in immunolocalization experiments, if tracking of both β-Gal and the pharmacological chaperone is required.
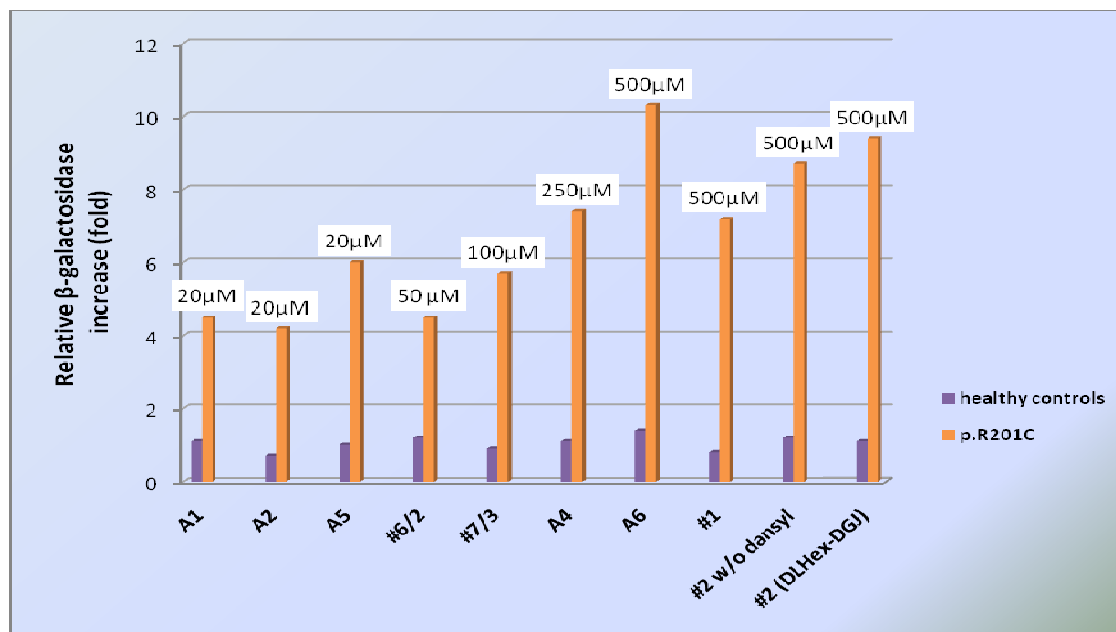
Figure 4.6.2.1 Results of preliminary chaperone screenings in chaperone-sensitive p.R201C fibroblasts. Cells were incubated with putative pharmacological chaperones at final concentrations of 20-500 µM for 4 days. Displayed data is the result of one single experiment for each compound, and was calculated as relative increase as compared to the activity without chaperone in the culture medium. Concentrations above the bars indicate optimal chaperone concentration for each compound.

4.6.2.1 The novel iminosugar DLHex-DGJ as pharmacological chaperone in GM1 cells

Several homo- and heteroallelic cell lines (cf. section 3.7.1), representative for Morquio B (MBD) and all subtypes of G_{M1}-gangliosidosis (GM1), were subjected to *in vivo* chaperone screenings with DLHex-DGJ (#2) as previously described for the known chaperone-sensitive cell line. Final chaperone concentrations in the culture medium were between 20 µM and 500 µM. Preliminary, individual experiments using the known chaperone-sensitive cell line [Iwasaki *et al*., 2006; Tominaga *et al*., 2001], homozygous for the mutation p.R201C (juvenile GM1), resulted in up to 18-fold increases of β-galactosidase residual activity, corresponding to 12%-75% of healthy control activity. Enzyme activities were significantly enhanced at low concentrations, although the optimal concentration of DLHex-DGJ was 500 µM, similar to

previous reports on its parent compound, DGJ [Tominaga *et al.*, 2001]. The results of a typical DLHex-DGJ screening in p.R201C cells are shown in Figure 4.6.2.1.1.
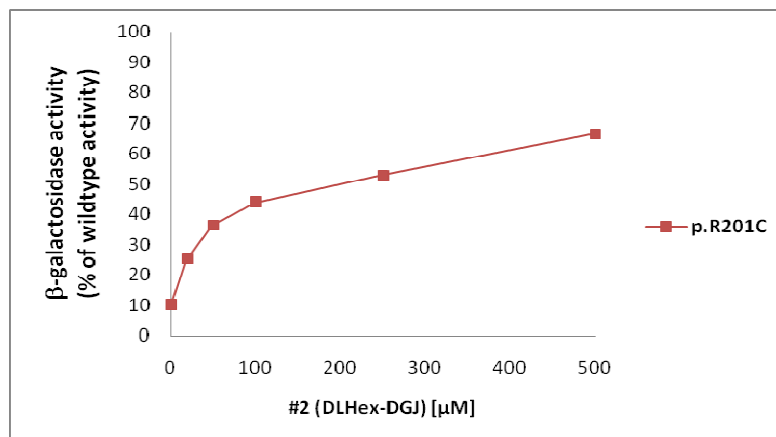
Figure 4.6.2.1.1 Characteristics of β-galactosidase enhancement after DLHex-DGJ treatment of fibroblasts. Cells were incubated with DLHex-DGJ at final concentrations of 20-500 µM for 4 days. Displayed data is the result of one single experiment, and was calculated as compared to the respective healthy control cell activities.

In all individual experiments performed with p.R201C cells, 20 µM of DLHex-DGJ resulted in β-Gal enhancement of more than 10% of the healthy control mean (28.4 nmol/hr/mg protein, see Table 4.6.2.1.3), which was previously proposed as the critical level for normal substrate turnover [Leinekugel *et al.*, 1992]. In fact, residual β-Gal activities ranging from 12%-45% of normal activity could be obtained using concentrations of 20 µM, and up to 75% with 500µM DLHex-DGJ, respectively.

At least three independent experiments on the effects of DLHex-DGJ on homo- and heteroallelic cell lines were conducted. Results are given in Figure 4.6.2.1.2 and Table 4.6.2.1.3. A positive response was defined as a more than 3-fold increase of residual β-Gal activity, or more than 10% of the healthy control mean (28.4 nmol/hr/mg protein). Altogether, six out of thirteen cell lines were chaperone-responsive. While one homoallelic (p.R201C) and three heteroallelic cell lines (p.R201H carriers) satisfied both criteria, a homoallelic adult GM1 cell line (p.G438E) showed an activity increase from 7% to 16% of the healthy control mean, and β-Gal activity in one infantile GM1 cell line, homozygous for p.C230R, was increased more than 3-fold. Beside the known chaperone-sensitive mutation p.R201C [Oshima *et al.*, 1994; Yoshida *et al.*, 1991], heteroallelic cells carrying the mutation p.R201H [Kaye *et al.*, 1997; Morrone *et al.* 2000, Santamaria *et al.*, 2006] strongly responded to chaperone treatment [Iwasaki *et al.*, Tominaga *et al.*, 2001]. Furthermore, the enzyme activity was also significantly

enhanced in cells homozygous for the novel mutation p.C230R [Hofer *et al*., 2010], and in cells carrying the adult mutation p.G438E. The p.G438E allele, originally published in a patient classified as MBD with borderline IQ and reduced expression of mature enzyme [Bagshaw *et al*., 2002; Hinek *et al*., 2000], was later found in two chronic GM1 cases with dystonia and Parkinsonism [Roze *et al*., 2005]. Interestingly, the enzyme in these infantile and adult GM1 cells was enhanced by higher concentrations compared to other responsive cells (Figure 4.6.2.1.2). It is also noteworthy that the relative increase of residual β-Gal activity after chaperone treatment in p.C230R is quite similar to the relative increase in p.R201C and p.R201H carriers (Table 4.6.2.1.3). The absolute β-Gal activities of p.C230R cells after DLHex-DGJ treatment, however, did not exceed 10% of the healthy control mean [Leinekugel *et al*., 1992], and thus remained fairly below those of treated p.R201H or p.R201C carriers.
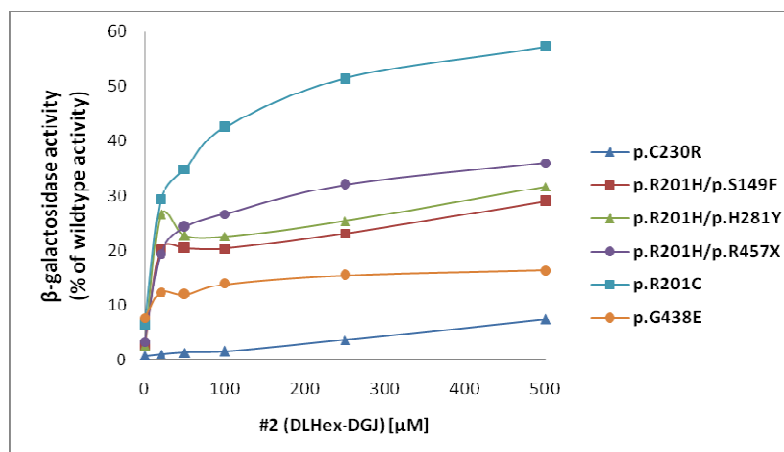
Figure 4.6.2.1.2 β-galactosidase enhancement in fibroblast homogenates after exposure of cells to DLHex-DGJ for 4 days. β-Gal activity in cells with p.R201H and p.R201C alleles was increased by low concentrations (20 µM), while other cell lines significantly responded at ≥ 250 µM to DLHex-DGJ treatment. Values are the mean of 3-24 assays. Relative β-Gal activitiy was calculated as compared to the respective healthy control cell activites.

In consistence with previous findings that the p.W273L allele produces stable, lysosomally located, but catalytically altered β-Gal proteins [Oshima *et al*., 1991], no significant enhancement could be seen in Morquio B cells or healthy controls. Likewise, all other cells from infantile GM1 (cf. Table 4.6.2.1.3) were non-responsive. Treatment with DLHex-DGJ did not alter the activity of the control enzyme β-hexosaminidase (data not shown).

| Allele 1 | Allele 2 | Phenotype | w/o DLHex-DGJ | | with DLHex-DGJ | | Increase |
			Activity	% of WT	Activity	% of WT	(fold)
WT	WT	-	284.0 ± 68.3	100.0	318.8 ± 65.2	112.3	1.1
p.I181K	**p.I181K**	infantile	0.8	0.3	1.7	0.6	2.1 *
p.R201C	**p.R201C**	juvenile	17.3 ± 5.4	6.1	162.4 ± 47.0	57.2	9.4
p.R201H	p.R457X	juvenile	8.7 ± 1.6	3.1	96.3 ± 19.6	33.9	11.1
p.R201H	p.S149F	adult/MBD	6.3 ± 0.6	2.2	77.5 ± 13.0	27.3	12.3
p.R201H	p.H281Y	juvenile	6.9 ± 1.6	2.4	86.2 ± 13.3	30.4	12.5
p.R208C	p.W161X	infantile	1.7 ± 0.2	0.6	4.2 ± 1.8	1.5	2.5
p.C230R	**p.C230R**	infantile	2.2 ± 0.8	0.8	19.8 ± 8.5	7.0	9.0
p.Y270D	**p.Y270D**	infantile	0.6 ± 0.5	0.2	1.0 ± 0.1	0.4	1.7
p.W273L	**p.W273L**	MBD	11.4 ± 4.5	4.0	14.5 ± 4.6	5.1	1.3
p.A301V	**p.A301V**	infantile	3.3 ± 0.8	1.2	4.2 ± 0.6	1.5	1.3
p.Y333H	**p.Y333H**	infantile	1.9 ± 0.9	0.7	3.5 ± 1.5	1.2	1.8
p.G438E	**p.G438E**	adult	20.5 ± 8.1	7.2	46.7 ± 17.8	16.4	2.3
p.P549L	**p.P549L**	infantile	1.4 ± 0.5	0.5	2.0 ± 0.3	0.7	1.4

Table 4.6.2.1.3 Cell lines with *GLB1* alleles tested for chaperone sensitivity against 500 μM DLHex-DGJ. Activities are given in nmol/hr/mg protein, and presumptive phenotype determining alleles are in bold letters. Experiments were performed in triplicate, except when indicated with an asterisk (data from single experiments). WT = wildtype.

4.6.2.2   DLHex-DGJ treatment affects β-galactosidase expression and maturation

To assess possible chaperone-induced changes in the expression and maturation of β-Gal, Western blot experiments were performed with selected cell lines. The appearance of mature β-Gal bands upon chaperone treatment is suggested to imply proper precursor transport to the lysosomes and subsequent processing of the C-terminal end to form the mature β-Gal enzyme. This maturation process is strictly bound to the lysosomal compartment [Okamura-Oho *et al*., 1996].

Western blot results are shown in Figure 4.6.2.2.1. While healthy controls predominantly expressed processed, mature β-Gal protein (64 kDa) together with small amounts of β-Gal precursor (84 kDa), mature β-Gal was barely detectable in untreated p.R201C and p.C230R fibroblasts, as well as in the heteroallelic p.R201H/p.R457X cell line. Upon addition of 250 μM or 500 μM DLHex-DGJ to the culture media for 4 days, the expression of both precursor and mature enzyme was remarkably enhanced in p.R201C and p.R201H/p.R457X cells.

Interestingly, only small amounts of mature β-Gal were detectable in p.C230R fibroblasts after chaperone treatment. This might be due to the fact that the residual activity (mean value 2.2

nmol/hr/mg protein) of these cells was eight times below the activity of p.R201C fibroblasts (mean value 17.3 nmol/hr/mg protein), and chaperone treatment of p.C230R cells results in β-Gal activities (mean value 19.8 nmol/hr/mg protein) comparable to untreated p.R201C cells (cf. Table 4.6.2.1.3). Mature β-Gal amounts in MBD and wildtype cells were slightly altered, corresponding to insignificant increases in enzyme activities.
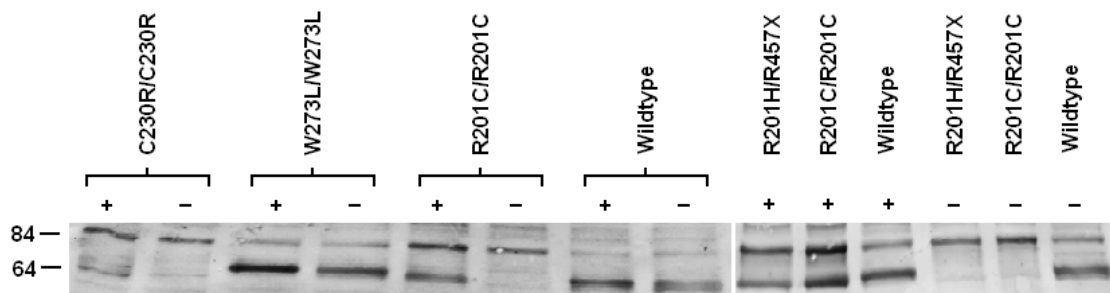
Figure 4.6.2.2.1 Western blot detection of β-galactosidase in fibroblast homogenates before and after exposure to 250 µM DLHex-DGJ. The amount of mature β-Gal protein (64 kDa) was significantly increased in p.R201C and p.R201H cells, while wildtype and MBD (p.W273L) cells show only minor changes upon DLHex-DGJ treatment. Minor changes were also observed in the infantile p.C230R mutant. Except for p.W273L, untreated mutant cells only expressed β-Gal precursor proteins (84 kDa).

4.6.2.3   Normalization of β-galactosidase transport after DLHex-DGJ treatment

To further investigate the fate of β-Gal precursor proteins after chaperone treatment, fibroblasts were stained with anti-β-galactosidase antibodies and the DNA-intercalating agent propidium iodide as counterstain. Wildtype β-Gal immunoreactive material was distributed all over the cell, corresponding to the endo-lysosomal system, with and without chaperone treatment (Figure 4.6.2.3.1). In p.R201C fibroblasts, β-Gal was predominantly found around the cell nucleus, indicating the precursor localization in the rough endoplasmic reticulum (rER) [Callahan, 1999; Oshima et al., 1994; Yoshida et al., 1991]. The unstable enzyme is labeled for degradation by molecular chaperones in the ER, initiating the endoplasmic reticulum-associated protein degradation (ERAD) machinery, followed by premature degradation in the cytoplasm [Fan, 2008; Oshima et al., 1994]. After DLHex-DGJ addition, the immunoreactive material in p.R201C fibroblasts showed wildtype-like distribution, hence DLHex-DGJ proved to be able to alter precursor trafficking.

Interestingly, β-Gal protein of p.C230R fibroblasts showed wildtype-like localization, thus no changes in distribution could be detected after DLHex-DGJ treatment. We could recently demonstrate a similar distribution of β-Gal in p.G438E fibroblasts [Hofer *et al.*, 2009], therefore, no chaperone treatment was performed on these cells.
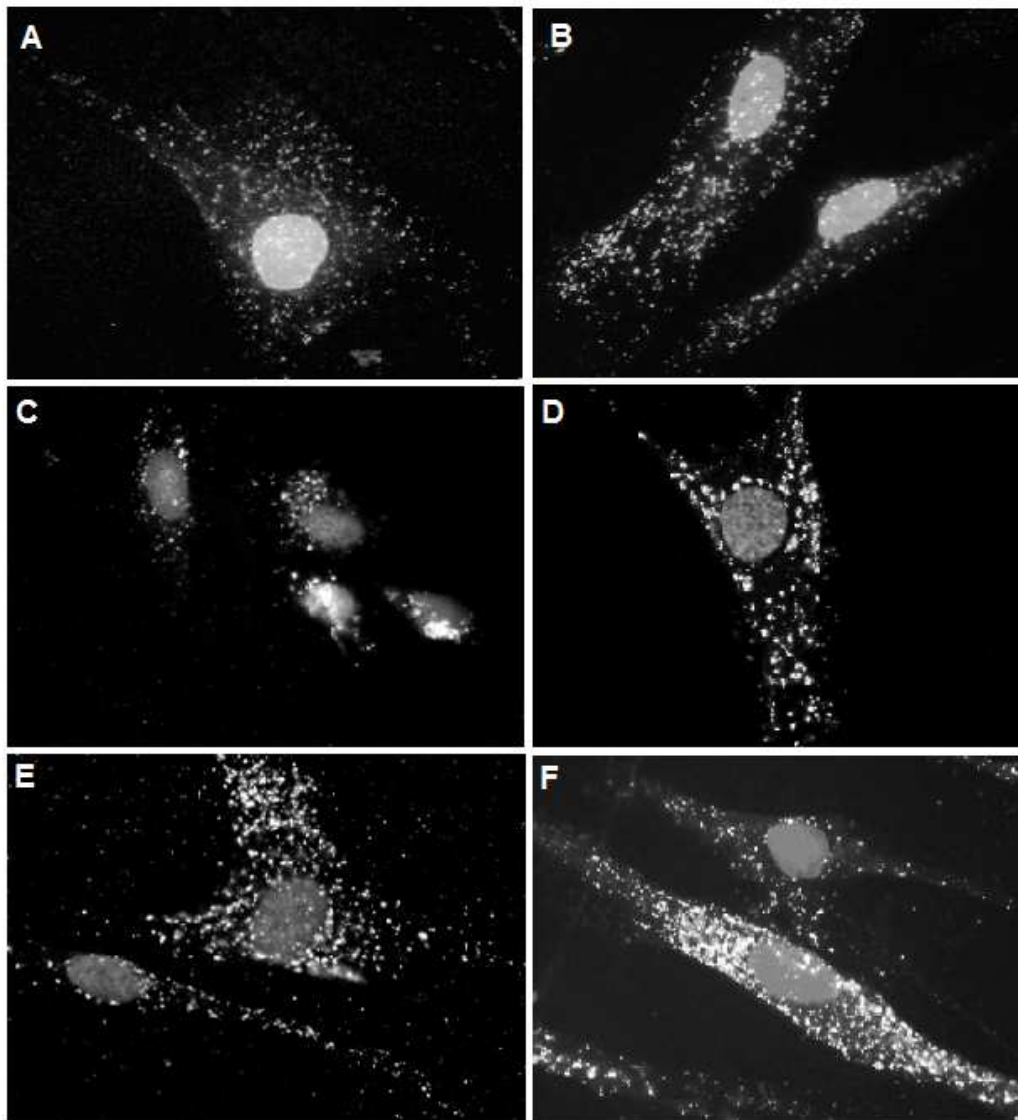
Figure 4.6.2.3.1 Immunolocalization of β-galactosidase in fibroblasts before and after DLHex-DGJ treatment. left row: untreated; right row: treated with 500 µM DLHex-DGJ for 3 days; **(A)+(B)**, wildtype; **(C)+(D)**, p.R201C; **(E)+(F)**, p.C230R. DLHex-DGJ treatment of p.R201C fibroblasts resulted in wildtype-like distribution of β-Gal immunoreactive material, suggesting precursor stabilization and transport to the lysosomes. No effect could be observed in p.C230R cells.

4.7   Investigations on natural substrate degradation in GM1 and MBD fibroblasts

4.7.1   *Uptake of natural substrate by cultured human skin fibroblasts*

To investigate the influence of DLHex-DGJ on both β-galactosidase activity and degradation of stored substrates, cultured human skin fibroblasts were loaded with radiolabeled G_{M1}-gangliosides prior incubation with the putative pharmacological chaperone (cf. section 3.9.1). β-Galactosidase from healthy individuals can perform hydrolysis on various natural substrates like G_{M1}- and G_{A1} (asialo G_{M1})-gangliosides, keratan sulfate, lactosylceramide, asialofetuin and other galactose-containing oligosaccharides, and the synthetic substrates 4-methylumbelliferyl-β-D-galactopyranoside and p-nitrophenyl-β-D-galactopyranoside, amongst others [Pshezhetsky and Ashmarina, 2001]. The β-Gal enzyme from GM1 or MBD cell lines, however, is not able to sufficiently degrade its substrates, resulting in accumulation of partially degraded substances within the cells [Suzuki *et al*., 2001].

In three individual experiments, the potential pharmacological chaperone DLHex-DGJ was added to the culture media of tritium (^{3}H)-labeled G_{M1}-ganglioside (^{3}H-G_{M1}G)-loaded cells at different final concentrations and incubated for either 2 or 4 days to examine substrate clearance. The β-glucosidase inhibitor Conduritol B Epoxide (CBE) [Datta and Radin, 1988] was added to the culture medium of selected samples to prevent degradation of glucosylceramide by inhibition of glucosylceramidase (EC 3.2.1.45) [Bieberich *et al*., 1999]. Glucosylceramide is one of the degradation products in the sphingolipid degradation pathway (Figure 4.7.1.1), and it is the final degradation product visualized by radioscanning of TLC plates in this work. Without CBE addition, glucosylceramide would be further degraded, and ultimately the tritium-label might get lost in small, unspecific and unidentifiable fragments or even in water molecules. To rule out a potential negative effect of both CBE and chaperone addition, the first experimental setup was mainly performed without CBE addition.

The human lysosomal acid β-galactosidase (EC 3.2.1.23) catalyzes the degradation of G_{M1}- to G_{M2}-gangliosides with the aid of the co-factor proteins G_{M2}-ganglioside activator (GM2A) [Li *et al*., 1979] and saposine B (Sap B) [O'Brien and Kishimoto, 1991]. G_{M2}-gangliosides are subsequently catabolized to G_{M3}-gangliosides by hydrolysis of terminal non-reducing N-acetyl-D-hexosamine residues [Knapp *et al*., 1996]. This reaction requires the action of β-

hexosaminidase A (EC 3.2.1.52) and the co-factor protein GM2A [Li *et al*., 1979]. Sialidase (EC 3.2.1.18) [Seyrantepe *et al*., 2003] and Sap B [O'Brien and Kishimoto, 1991] are necessary to for hydrolysis of G_{M3}-gangliosides to lactosylceramide. Degradation of the latter product to glucosylceramide requires the combined interaction of galactosylceramidase (galactocerebroside-β-D-galactosidase; EC 3.2.1.46) [Chen *et al*., 1993] and the human lysosomal acid β-galactosidase [Pshezhetsky and Ashmarina, 2001]. Additionally, the proteins saposine B and saposine C (Sap C) are essential interaction partners in this process [O'Brien and Kishimoto, 1991]. Finally, glucosylceramide is catabolized to ceramides and sphingosines. It is important to note that no co-factors, like saposines, are required to cleave synthetic substrates (e.g. 4-methylumbelliferyl-β-D-galactopyranoside) under *in vitro* conditions, but the presence of chloride ions (≥10 mM NaCl in lysis buffers) is necessary for the enzymatic activity [Pshezhetsky and Ashmarina, 2001]. The use of the detergent Triton is optional, but it might be necessary to add taurocholate to the enzymatic assay for specific experiments.
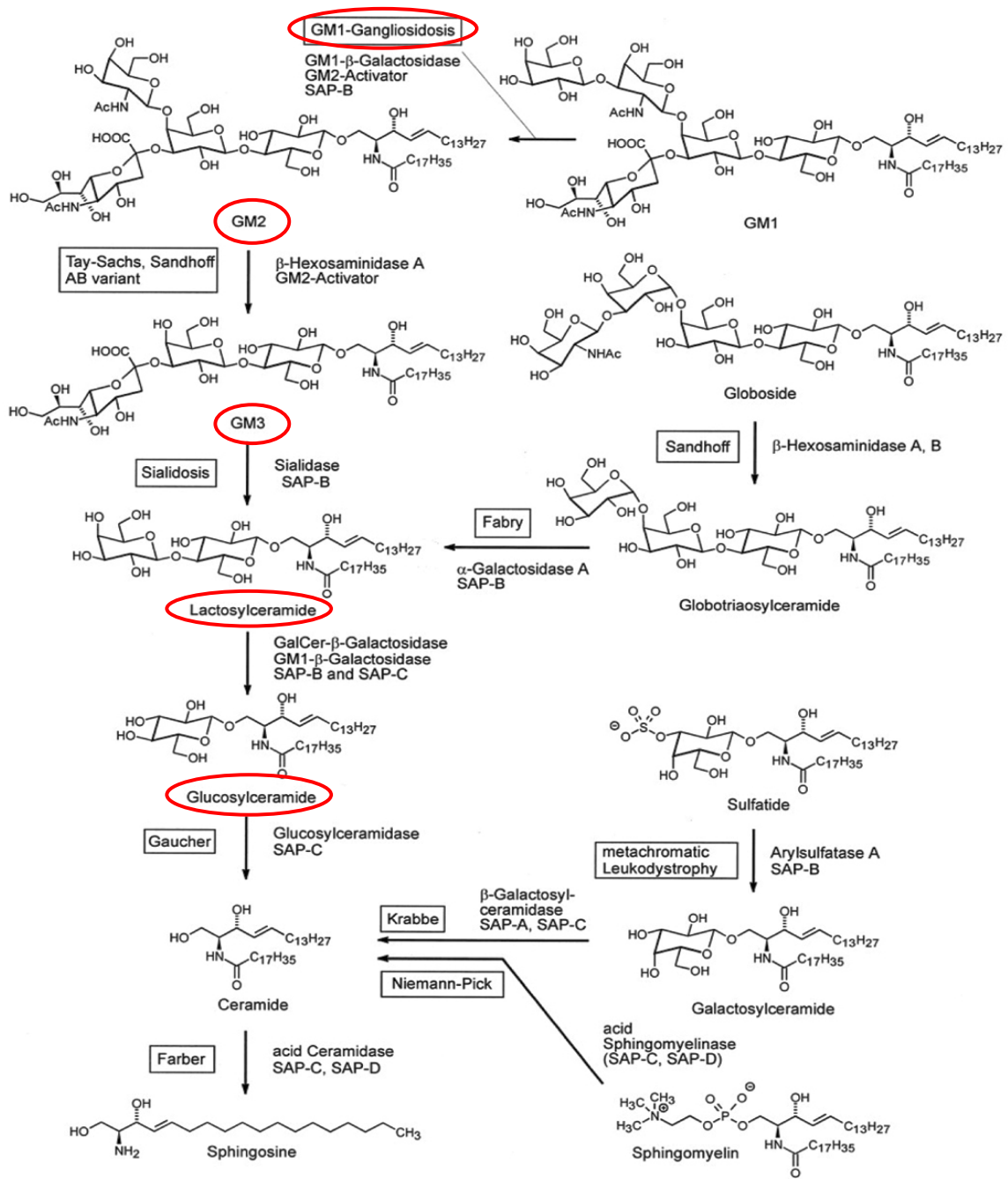
Figure 4.7.1.1 Sphingolipid degradation pathway and associated lysosomal storage diseases (excerpt).
Graphic source: http://www.lipidomicnet.org/index.php/Glycosphingolipids.

Beside wildtype (WT) cells, fibroblast cell lines with the following genotypes were loaded with tritium (^{3}H)-labeled G_{M1}-ganglioside:

- p.C230R/p.C230R (infantile GM1),

- p.R201C/p.R201C (juvenile GM1),

- p.G438E/p.G438E (adult GM1),

- p.R201H/p.S149F (adult GM1 or MBD),

- p.W273L/p.W273L (MBD).

β-Galactosidase activities were determined with alternative β-Gal assays (see section 3.11.4), and degradation of incorporated ^{3}H-G_{M1}G was analyzed by TLC. Furthermore, liquid scintillation counting was performed in all samples, and absolute amounts of radioactivity in culture media and cell homogenates were calculated. Results of the alternative β-Gal determinations with the common synthetic substrate are given in Table 4.7.1.2. Interestingly, the residual β-Gal activities determined with these alternative assays were considerably higher than activities measured with standard β-Gal assays. Those differences might be attributed to different assay conditions (cf. incubation times, substrate concentrations and solubility, buffers) and different characters of substrates. Thus the results from alternative β-Gal determinations cannot be compared directly to previous results obtained with standard assays. Alternative β-Gal or β-Hex assays were only conducted during the works at the Institute of Inherited Metabolic Disorders, First Faculty of Medicine, Charles University in Prague and General University Hospital in Prague, Czech Republic. Data from these experiments should be considered as a control for chaperone activity measured *in vitro* and supporting information for TLC results.

1st Setup	Controls - CBE			500 µM DLHex-DGJ + CBE, 4d		
	Activity nmol/hr/mg protein	% of WT	Increase (fold)	Activity nmol/hr/mg protein	% of WT	Increase (fold)
WT	779.5	100.0	1.0	914.7	117.3	1.2
p.R201C	17.8	2.3	1.0	233.5	**30.0**	**13.1**
p.C230R	4.7	0.6	1.0	27.4	3.5	**5.8**
p.W273L	23.8	3.1	1.0	57.2	7.3	2.4
p.R201H/p.S149F	14.1	1.8	1.0	174.7	**22.4**	**12.4**
p.G438E	48.8	6.3	1.0	94.9	**12.2**	1.9

1st Setup	500 µM DLHex-DGJ - CBE, 4d		
	Activity nmol/hr/mg protein	% of WT	Increase (fold)
WT	922.4	118.3	1.2
p.R201C	223.5	**28.7**	**12.6**
p.C230R	43.4	5.6	**9.2**
p.W273L	51.7	6.6	2.2
p.R201H/p.S149F	172.4	**22.1**	**12.2**
p.G438E	110.2	**14.1**	2.3

2nd Setup	Controls + CBE			20 µM DLHex-DGJ + CBE, 4d		
	Activity nmol/hr/mg protein	% of WT	Increase (fold)	Activity nmol/hr/mg protein	% of WT	Increase (fold)
WT	1,111.0	100.0	1.0	1,537.0	138.3	1.4
p.R201C	18.3	1.6	1.0	44.8	4.0	2.4
p.C230R	4.7	0.4	1.0	8.0	0.7	1.7
p.W273L	42.1	3.8	1.0	44.0	4.0	1.0
p.R201H/p.S149F	13.1	1.2	1.0	44.6	4.0	**3.4**
p.G438E	51.1	4.6	1.0	87.7	7.9	1.7

2nd Setup	100 µM DLHex-DGJ + CBE, 4d		
	Activity nmol/hr/mg protein	% of WT	Increase (fold)
WT	1,398.0	125.8	1.3
p.R201C	115.0	**10.4**	**6.3**
p.C230R	9.6	0.9	2.0
p.W273L	63.1	5.7	1.5
p.R201H/p.S149F	103.0	**9.3**	**7.9**
p.G438E	112.0	**10.1**	2.2

3rd Setup	Controls + CBE			500 µM DLHex-DGJ + CBE, 2d		
	Activity nmol/hr/mg protein	% of WT	Increase (fold)	Activity nmol/hr/mg protein	% of WT	Increase (fold)
WT	706.1	100.0	1.0	820.1	116.2	1.2
p.R201C	10.8	1.5	1.0	86.5	**12.3**	**8.0**
p.C230R	5.8	0.8	1.0	29.7	4.2	**5.2**
p.W273L	44.9	6.4	1.0	52.4	7.4	1.2

3rd Setup	250 µM #2 w/o dansyl + CBE, 2d			20 µM #2 w/o dansyl + CBE, 2d		
	Activity nmol/hr/mg protein	% of WT	Increase (fold)	Activity nmol/hr/mg protein	% of WT	Increase (fold)
WT	805.9	114.1	1.1	809.7	114.7	1.1
p.R201C	89.9	**12.7**	**8.4**	31.4	4.4	**2.9**
p.C230R	7.2	1.0	1.2	4.6	0.7	0.8
p.W273L	46.3	6.6	1.0	34.7	4.9	0.8

Table 4.7.1.2 Study of chaperone effects. Data is the result of alternative β-Gal determinations in ^{3}H-G$_{M1}$G-loaded fibroblasts based on single experiments. Enzymatic measurements were performed in duplicates.

Again, cell lines with the mutations p.R201C and p.R201H showed a more than 3-fold increase of β-galactosidase activity, corresponding to more than 10% of the respective healthy control mean, when treated with 500 µM DLHex-DGJ for 2 or 4 days. The residual β-Gal activity of infantile p.C230R cells was increased more than 3-fold, and reached more than 10% of the healthy control activity in adult p.G438E fibroblasts, respectively. Fibroblasts with the mutations p.G438E and p.R201H/p.S149F were only subjected to the 4 day DLHex-DGJ treatment. Addition of the β-glucosidase inhibitor CBE [Bieberich *et al*., 1999; Datta and Radin, 1988] had no significant influence on β-Gal activities, and treatment with DLHex-DGJ did not alter the activity of the control enzyme β-hexosaminidase (data not shown). The occurrence of major differences (cf. WT activities in control experiments) can most likely be attributed to different growth behaviour of subcultured fibroblasts, losses during preparation, but also to salvage of incorrectly folded proteins usually processed by ERAD.

In contrast to the results obtained with standard β-Gal assays, a reduction of the final DLHex-DGJ concentration in the medium to 20 µM and subsequent incubation for 4 days did not significantly increase β-Gal activity in the known chaperone-sensitive cell line (p.R201C; 2.4-fold increase). It should be noted that each experimental setup was only performed once, hence outliers are possible and results might have been significant in a second setup. However, β-Gal activity in this cell line could be enhanced above the significance threshold with a final DLHex-DGJ concentration of 100 µM and an incubation time of 4 days. Similar results were obtained in p.R201H/p.S149F fibroblasts for both concentrations. No positive response was seen in p.G438E cells or p.C230R cells, when treated with 20 µM DLHex-DGJ for 4 days. The β-Gal enzyme of p.C230R fibroblasts also did not respond to a final concentration of 100 µM in culture medium, but β-Gal activity was enhanced to ~10% of the healthy control activity in p.G438E cells. These results are consistent with previous chaperone screening results (cf. Table 4.6.2.1.3), where certain mutations (p.C230R, p.G438E) significantly responded to final DLHex-DGJ concentrations of ≥ 250 µM.

A third experimental setup included samples treated with the potential pharmacological chaperone #2 w/o dansyl. This iminosugar is a structural equivalent of DLHex-DGJ (cf. Figure 3.9.1.1.1), but does not contain the fluorescent dansyl group. The substance was available in a later phase of this work and evaluated in comparison to DLHex-DGJ to gain information on the importance of the dansyl group for the chaperone function, but also on its potential

cytotoxicity. Loading assays were performed in wildtype cells and fibroblasts carrying the mutations p.R201C, p.C230R, and p.W273L. CBE was added to the culture media of all samples and cells were incubated with a final concentration of 20 µM or 250 µM #2 w/o dansyl for 2 days, respectively. β-Gal of fibroblasts from the known chaperone-sensitive cell line p.R201C significantly responded to both concentrations (~3-fold and 8.4 fold increase), while no effect was observed in the infantile GM1 cells (p.C230R). As expected, the β-Gal enzyme of p.W273L fibroblasts was unaffected by chaperone treatment. The putative chaperone #2 w/o dansyl was previously tested in fibroblast screenings using standard β-Gal assays (cf. Table 4.6.1.1). In contrast to the experiments described above, cells were incubated with #2 w/o dansyl for 4 days, at final concentrations of 20-500 µM in the cell culture medium. β-Gal activity of p.R201C cells was significantly increased at all tested concentrations (Figure 4.7.1.3), while the activity of p.C230R fibroblasts was enhanced by concentrations ≥ 250 µM (data not shown). Treatment with #2 w/o dansyl did not alter the activity of the control enzyme β-hexosaminidase (data not shown).

Altogether, the putative pharmacological chaperones DLHex-DGJ and #2 w/o dansyl displayed the same mutation preferences, and optimal chaperone concentrations for each responsive cell line were specific and quite similar, suggesting only a moderate, but significant influence of the dansyl group on chaperone activity. On the other hand, the dansylated compound demonstrated much more inhibition potency as compared to #2 w/o dansyl (see Table 4.6.1.1), making DLHex-DGJ a useful inhibitor of human lysosomal acid β-galactosidase.
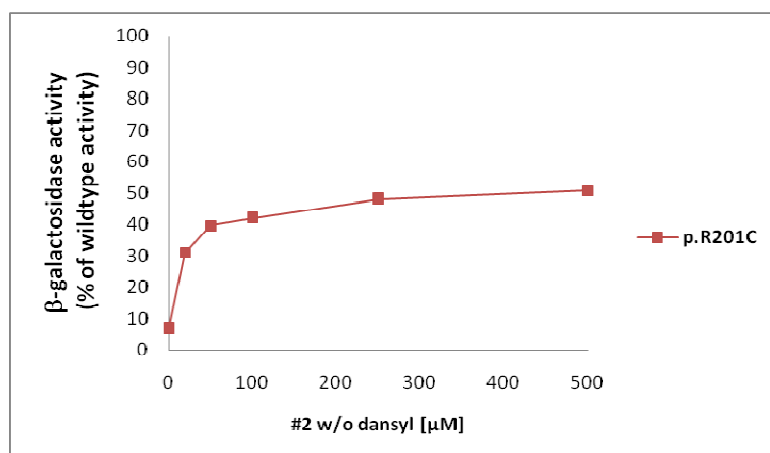
Figure 4.7.1.3 Characteristics of β-galactosidase enhancement after #2 w/o dansyl treatment of fibroblasts. Cells were incubated with #2 w/o dansyl at final concentrations of 20-500 µM for 4 days. Values are the mean of 4-6 individual experiments, and were calculated as compared to the respective healthy control cell activities.

In summary, the results from alternative β-Gal determinations in ^{3}H-G$_{M1}$G-loaded fibroblasts were almost consistent with previous results from chaperone screenings using standard β-Gal assays (Table 4.6.2.1.3). For evaluation of natural substrate degradation, the amount of incorporated, radiolabeled material was determined by liquid scintillation counting in aliquots of cell homogenates and cell culture media. The overall ^{3}H-G$_{M1}$G uptake from the medium was ranging between 2% and 7% (Table 4.7.1.4), and observed uptake rates (dpm cells/mg protein) were characteristic for each cell line. It should be noted that although the uptake rates were very low, experimental procedures were optimized in terms of ^{3}H-G$_{M1}$G concentration, incubation time, and availability of cell material for enzymatic measurements as well as lipid extractions. An incubation time of 5 days proved to be optimal for ^{3}H-G$_{M1}$G-loading of human skin fibroblasts. Extended or reduced incubation times with the radiolabeled substrate caused difficulties in signal quantitation by TLC and/or β-Gal determinations. Loading assay optimization was conducted by Befekadu Asfaw, Institute of Inherited Metabolic Disorders, First Faculty of Medicine, Charles University in Prague and General University Hospital in Prague, Czech Republic.

Sample	Genotype	dpm in cells (%)	dpm in medium (%)
Control –CBE	WT	5.9	94.1
Control +CBE	WT	4.7-5.3	94.7-95.3
500 µM #2 (DLHex-DGJ) +CBE, 4d	WT	6.0	94.0
500 µM #2 (DLHex-DGJ) –CBE, 4d	WT	4.9	95.1
500 µM #2 (DLHex-DGJ) +CBE, 2d	WT	4.2	95.8
100 µM #2 (DLHex-DGJ) +CBE, 4d	WT	4.4	95.6
20 µM #2 (DLHex-DGJ) +CBE, 4d	WT	4.8	95.2
250 µM #2 w/o dansyl +CBE, 2d	WT	4.6	95.4
20 µM #2 w/o dansyl +CBE, 2d	WT	5.4	94.6
Control –CBE	p.R201C	5.1	94.9
Control +CBE	p.R201C	3.4-3.6	96.4-96.6
500 µM #2 (DLHex-DGJ) +CBE, 4d	p.R201C	4.8	95.2
500 µM #2 (DLHex-DGJ) –CBE, 4d	p.R201C	5.1	94.9
500 µM #2 (DLHex-DGJ) +CBE, 2d	p.R201C	4.6	95.4
100 µM #2 (DLHex-DGJ) +CBE, 4d	p.R201C	3.2	96.8
20 µM #2 (DLHex-DGJ) +CBE, 4d	p.R201C	2.7	97.3
250 µM #2 w/o dansyl +CBE, 2d	p.R201C	4.6	95.4
20 µM #2 w/o dansyl +CBE, 2d	p.R201C	5.6	94.4
Control –CBE	p.C230R	5.9	94.1
Control +CBE	p.C230R	4.1-4.5	95.5-95.9
500 µM #2 (DLHex-DGJ) +CBE, 4d	p.C230R	5.8	94.2
500 µM #2 (DLHex-DGJ) –CBE, 4d	p.C230R	6.1	93.9
500 µM #2 (DLHex-DGJ) +CBE, 2d	p.C230R	5.8	94.2
100 µM #2 (DLHex-DGJ) +CBE, 4d	p.C230R	5.0	95.0
20 µM #2 (DLHex-DGJ) +CBE, 4d	p.C230R	4.6	95.4
250 µM #2 w/o dansyl +CBE, 2d	p.C230R	4.7	95.3
20 µM #2 w/o dansyl +CBE, 2d	p.C230R	6.9	93.1
Control –CBE	p.W273L	4.4	95.6
Control +CBE	p.W273L	3.3-3.5	96.5-96.7
500 µM #2 (DLHex-DGJ) +CBE, 4d	p.W273L	5.0	95.0
500 µM #2 (DLHex-DGJ) –CBE, 4d	p.W273L	4.7	95.3
500 µM #2 (DLHex-DGJ) +CBE, 2d	p.W273L	5.2	94.8
100 µM #2 (DLHex-DGJ) +CBE, 4d	p.W273L	4.5	95.5
20 µM #2 (DLHex-DGJ) +CBE, 4d	p.W273L	4.1	95.9
250 µM #2 w/o dansyl +CBE, 2d	p.W273L	5.3	94.7
20 µM #2 w/o dansyl +CBE, 2d	p.W273L	3.5	96.5
Control –CBE	p.R201H/p.S149F	2.5	97.5
Control +CBE	p.R201H/p.S149F	2.4	97.6
500 µM #2 (DLHex-DGJ) +CBE, 4d	p.R201H/p.S149F	3.3	96.7
500 µM #2 (DLHex-DGJ) –CBE, 4d	p.R201H/p.S149F	3.8	96.2
100 µM #2 (DLHex-DGJ) +CBE, 4d	p.R201H/p.S149F	2.4	97.6
20 µM #2 (DLHex-DGJ) +CBE, 4d	p.R201H/p.S149F	2.5	97.5
Control –CBE	p.G438E	3.1	96.9
Control +CBE	p.G438E	2.2	97.8
500 µM #2 (DLHex-DGJ) +CBE, 4d	p.G438E	3.9	96.1
500 µM #2 (DLHex-DGJ) –CBE, 4d	p.G438E	4.4	95.6
100 µM #2 (DLHex-DGJ) +CBE, 4d	p.G438E	3.1	96.9
20 µM #2 (DLHex-DGJ) +CBE, 4d	p.G438E	3.1	96.9

Table 4.7.1.4 Results of the liquid scintillation counting in cell homogenates and culture medium of ^{3}H-G_{M1}G-loaded human skin fibroblasts. Absolute amounts of radioactivity (in disintegrations per minute; dpm) were calculated from one single determination for each sample. Similar control experiments were summarized.

4.7.2 DLHex-DGJ treatment improves substrate clearance in p.C230R cells

Finally, lipid extracts (see section 3.12.4) of each sample were subjected to TLC and analyzed with the Raytest TLC Analyzer v2.05. Peak area calculation was performed with the Rita TLC Analysis software (v1.93.002). Peaks with lower and higher retention times than the G_{M1}-ganglioside peak were defined as degradation products (or product formation). Because this procedure takes resynthesized lipids with radiolabeling into account, the method can only be considered as semi-quantitative. Another factor preventing exact quantitation of all degradation products is the potential loss of radiolabeled signals in small, unidentifiable fragments or even in water molecules, resulting in falsified peak area ratios. To face the latter problem, CBE was added to most experiments to obtain clear TLC degradation patterns by maximal suppression of resynthesis steps. However, previous experiments with fibroblasts from other lysosomal storage diseases demonstrated a very selective action of CBE, and addition of this β-glucosidase inhibitor did not always guarantee a complete blocking of glucosylceramides degradation [personal communication, Befekadu Asfaw].

The amount of product formation (degradation) was calculated as percentage based on total incorporated radiolabeled G_{M1}-gangliosides. TLC results of all three experimental setups are illustrated in 4.7.3.1. Wildtype (WT) cells almost completely metabolized incorporated ^{3}H-G_{M1}G, yielding approximately 95% degradation. While degradation rates in control experiments of p.G438E (adult GM1) and p.R201H/p.S149F (adult GM1 or MBD) fibroblasts were almost similar to those of the untreated MBD cell line (mutation p.W273L), the juvenile GM1 case (p.R201C) showed a little less degradation in control experiments. A radical deterioration of G_{M1}-ganglioside metabolization was observed in infantile p.C230R fibroblasts. Degradation of radiolabled G_{M1}-gangliosides has never been studied in these specific GM1 and MBD fibroblasts *in situ*, hence the high degradation levels of these untreated cell lines were quite surprising. A more distinguishable outcome, corresponding to the severity of phenotypes was expected, for example less amounts of degradation in control experiments of juvenile GM1, but a bit more in the adult case. On the other hand, the experimental setup was optimized to work towards substrate saturation, and TLC analysis was semi-quantitative for reasons mentioned earlier. Therefore, the percentage of degradation/product formation is not an absolute value, but rather an approximate one.

DLHex-DGJ was added to the ^{3}H-G$_{M1}$G-loaded fibroblasts at three different final concentrations (500, 100, and 20 µM) and incubated for either 2 or 4 days. One setup using 500 µM DLHex-DGJ was performed without CBE, and two other ones with addition of the glucosylceramidase inhibitor. Upon comparison of these experiments, no synergetic or antagonistic effect of CBE and DLHex-DGJ was observed, thus the loading mixtures of subsequent experiments were supplemented with CBE. Unfortunately, results from the first experiment (Figure 4.7.3.1, A) clearly showed impaired product formation rather than chaperone-enhanced degradation of the stored radiolabeled substrate. This trend was most evident in p.R201C, p.R201H/p.S149F, and p.G438E fibroblasts. The least effected cell line beside wildtype fibroblasts were the MBD cells carrying the mutation p.W273L. It was assumed that pharmacological chaperones act on misfolded or unstable β-Gal precursor proteins [Fan, 2008], hence the positive – or in this case negative – chaperone effect is less pronounced in wildtype or MBD cells. Surprisingly, infantile GM1 cells with the mutation p.C230R showed a slight increase of ^{3}H-G$_{M1}$G degradation when treated with 500 µM of DLHex-DGJ for 4 days.

In a second experiment, DLHex-DGJ concentrations in the culture media were reduced to a final concentration of 100 µM or 20 µM (incubation time 4 days in either case). The idea behind reducing the chaperone concentration and/or incubation time was finding the optimal, non-inhibitory intracellular chaperone concentration that is able to enhance β-Gal activity under *in vivo* conditions, and minimizing inhibitory, cytotoxic effects of the putative pharmacological chaperone. In fact, a decrease of the DLHex-DGJ concentration resulted in the formation of more degradation products than observed with addition of 500 µM, but the chaperone still acted as inhibitor of β-galactosidase in almost all tested cell lines (Figure 4.7.3.1, B). Even p.C230R (infantile GM1) cells showed impaired product formation when compared to the results obtained with 500 µM DLHex-DGJ, but product formation remained unchanged compared to untreated control cells.

In chaperone screenings with subsequent *in vitro* β-Gal determinations using the synthetic substrate, the optimal chaperone concentration of DLHex-DGJ in the culture medium of all tested fibroblasts was 500 µM, although p.R201C and p.R201H cells already responded to a final concentration of 20 µM. Cells with the mutation p.C230R or p.G438E did not respond below 250 µM of DLHex-DGJ (Figure 4.6.2.1.2). TLC results indicate that the optimal DLHex-DGJ concentration for enhancing both β-Gal activity and substrate clearance in

infantile cell lines carrying the mutation p.C230R might be between 100 µM and 500 µM. On the other hand, 500 µM DLHex-DGJ was also determined as optimal concentration for chaperone action on β-Gal from p.R201C and p.R201H fibroblasts, but TLC results clearly demonstrate the inhibitory effect of this dosage. These contradictory findings point out a common problem when comparing the outcome of enzymatic assays, obtained with natural substrates, to synthetic substrate results. It is also important to note that the uptake rate of DLHex-DGJ into the cells remains unclear, but the effective chaperone concentration within the cell (e.g. in endoplasmic reticulum or lysosomes) is supposed to be sub-inhibitory, and often in the range of K_i or IC_{50} values for the respective compound [Asano, 2003; Fan, 2008; Iwasaki *et al.*, 2006; Matsuda *et al.*, 2003].

4.7.3 *The novel iminosugar #2 w/o dansyl acts as pharmacological chaperone and improves substrate clearance in p.C230R cells*

A third experiment was conducted with 500 µM DLHex-DGJ, but the incubation time was reduced to 2 days. Additionally, the potential chaperone #2 w/o dansyl was tested for its ability to clear stored substrates in GM1 and MBD cell lines. Again, DLHex-DGJ treatment of ^{3}H-G_{M1}G-loaded fibroblasts inhibited the β-Gal enzyme and impaired substrate clearance in all tested cell lines (Figure 4.7.3.1, C). In contrast to previous results (A), no enhanced product formation was observed in p.C230R cells. It should be noted that due to the semi-quantitative analysis mode, measurement differences of up to 20% were not uncommon between similar experiments. This weakness of the method impedes examination of small, chaperone-induced differences in ^{3}H-G_{M1}G degradation. The loading experiments presented in this work confirmed the assumption that this experimental setup might only be able to detect major increases or decreases of radiolabeled G_{M1}-ganglioside degradation. Another important limitation affects cell lines that presented with high amounts of basal ^{3}H-G_{M1}G degradation in control experiments. It would be impossible to detect enhanced product formation in wildtype, p.R201C, p.R201H/p.S149F, p.G438E, and p.W273L cells, or any other cell line that shows a similar degradation pattern in ^{3}H-G_{M1}G loading assays.

Figure 4.7.3.1 Degradation of incorporated ³H-labeled G_{M1}-ganglioside in MBD and GM1 fibroblasts. Cells were loaded with ^{3}H-G_{M1}G and incubated for 5 days. In some experiments, DLHex-DGJ or #2 w/o dansyl was added to the culture medium at different final concentrations and for different incubation times. Control experiments were performed without chaperone addition. Lipid extracts of cell homogenates were subjected to TLC analysis and products formation was calculated as percentage of total incorporated G_{M1}-gangliosides.

Addition of 250 µM #2 w/o dansyl also resulted in inhibition of the β-Gal enzyme in known chaperone-responsive p.R201C fibroblasts and wildtype cells. The chaperone effect of this compound was only observed in infantile p.C230R cells, consistent with findings in DLHex-DGJ experiments. A final concentration of 250 µM #2 w/o dansyl in the culture medium of p.C230R cells and incubation for 2 days resulted in enhanced degradation of the incorporated natural substrate (from ~30% to ~60%), while addition of 20 µM did not significantly alter product formation when compared to untreated controls. MBD cells (p.W273L) were unaffected by both concentrations.

Similar to DLHex-DGJ experiments, these results suggest that the effective concentration of #2 w/o dansyl in the culture medium of p.C230R fibroblasts should be considerably higher than 20 µM, presumably also between 100 µM and 500 µM. On the other hand, the #2 w/o dansyl concentration in the culture medium should be further reduced ($\leq$ 20 µM) to observe a potential chaperone effect on β-Gal of p.R201C cells. It is noteworthy that high chaperone doses significantly inhibited the β-Gal enzyme of wildtype cells. This result emphasizes the importance of accurate chaperone dosage, and supports speculation that a lower concentration

of both DLHex-DGJ and #2 w/o dansyl in the cell culture medium could reverse the storage of natural substrates in certain cell lines by enhancing β-Gal activity.

Remarkably, the principle chaperone effect of both compounds could be clearly demonstrated in infantile p.C230R cells, which also responded to DLHex-DGJ and #2 w/o dansyl treatment in chaperone screening experiments (cf. Figure 4.6.2.1.1 and 4.7.1.3). Both pharmacological chaperones markedly enhanced degradation of the incorporated radiolabeled G_{M1}-ganglioside, hence contributing to substrate clearance in certain G_{M1}-gangliosidosis fibroblasts. However, more experiments of this kind are necessary to confirm the results obtained in this work.

5 DISCUSSION

In this work the influence of novel derivatives of 1-deoxygalactonojirimycin (DGJ) on the activity of the human lysosomal acid β-galactosidase was examined under *in vitro* conditions, and *in vivo* upon treatment of cultured human skin fibroblasts from GM1 and MBD patients. The results clearly demonstrated a mutation-specific pharmacological chaperone effect of the novel iminosugars in GM1 fibroblasts and indicated dosage-dependent natural substrate degradation. Furthermore, two novel anti-human-β-Gal peptide antibodies were described in this work. Heterologous expression of the human lysosomal acid β-galactosidase in *E. coli* cells for subsequent antibody production, however, was only partially successful.

5.1 Antibody development

The limiting factor in the experimental procedures described in this work was the availability of specific anti-human-β-galactosidase antibodies. Although several procedures to obtain β-Gal antibodies are described in the literature, none of them was established at the Department of Pediatrics. Some commercially available β-Gal antibodies, based on the *E. coli* immunogen, were proposed to cross-react with the human enzyme, but this work could not provide evidence for this assumption (data not shown). The α85 anti-human β-galactosidase antibody used in several experiments in this work was kindly provided by A. d'Azzo (Department of Genetics and Tumor Cell Biology, St. Jude Children's Research Hospital, Memphis, TN). This antibody recognized the precursor and mature form of β-Gal in both native and denatured condition, which was essential for the immunofluorescence experiments and Western blots conducted in this work. However, the availability of this antibody was limited. Therefore, a major task of the present work was the purification of large amounts of the human β-Gal protein for subsequent immunization of rabbits and development of polyclonal anti-β-Gal antibodies.

The most common strategies to obtain native state β-Gal are purification of overexpressed, secreted β-Gal precursor proteins (84 kDa) from the cell culture medium of CHO cells [Zhang *et al.*, 1994] and the purification of the mature enzyme (64 kDa) from human placenta [Hubbes *et al.*, 1992]. A major disadvantage of most strategies is the need of large amounts of sample

material, and purification processes are complicated by handling of several liters urine or cell culture medium or some pounds of human tissues. Furthermore, these methods are time-consuming and expensive in terms of required materials (e.g. affinity resins). Purification of mature β-Gal from human placenta, for example, involves at least five different chromatographic steps [Hubbes *et al*., 1992]. On the other hand, purification of the secreted precursor from the culture medium of CHO cells requires only one affinity chromatographic step, but cultivation of cells to yield the required amounts of precursor in the culture media might take up to 6 weeks [Zhang *et al*., 1994; this work]. Despite the unfavorable timely aspect, this method was established at the Department of Pediatrics during this work. CHO-K1 cells, successfully prepared by Doris Hofer to overexpress and secrete the human β-Gal precursor (88 kDa), were cultivated under conditions different from that described by Zhang *et al*. and in summary, 2.6 L of culture medium were required for the purification of ~730 µg β-galactosidase precursor protein. Immunization of rabbits and purification of polyclonal total immunoglobulins (IgGs) was conducted by a commercial company (Eurogentec, Seraing, Belgium). Unfortunately, both rabbits were accidentally killed by the company and the vast majority of antigen was already injected. Quality testing of the small bleed sera from the killed rabbits clearly showed positive β-Gal signals on WB (Figure 4.5.1.3.2). The remaining antigen (~180 µg; 45 µg per injection) and a slightly altered immunization protocol were not able to produce the same immune response in a third rabbit (Figure 4.5.1.3.1). Even total IgG purification of the positively reacting small bleed sera (killed rabbits) plus the final bleed serum of the third rabbit did not result in specific anti-β-Gal antibodies. No clearly positive and reproducible signals were observed in WB or IF experiments (Figures 4.5.1.3.1 and 4.5.1.3.4). The purification of β-Gal from CHO-K1 cell culture medium was not repeated due to time limitations.

At the same time, two other antibody development strategies were pursued. One strategy comprised the design of two specific immunogenic β-Gal peptides in cooperation with Eurogentec (Seraing, Belgium), and the other was the heterologous expression of C- or N-terminal tagged human β-galactosidase in *E. coli* cells. The peptides had a length of 15 aa, respectively, and met all antigenic criteria for successful production of polyclonal anti-β-Gal antibodies in rabbits. The polyclonal antiserum from one rabbit was purified on two different peptide affinity columns, and the resulting polyclonal antibody fractions, "anti-β-galactosidase peptide antibody 1" and "anti-β-galactosidase peptide antibody 2", were tested in WB and IF

applications. Both peptide antibodies showed strong β-Gal specific signals on WB of cell homogenates from COS-1, wildtype, GM1, and MBD fibroblasts (cf. Figure 4.5.2.1), but no specific reactions were observed in IF experiments. However, these peptide antibodies were a useful amendment in WB throughout this work.

Although the heterologous expression of human β-Gal in *E. coli* cells was only partially successful, an optimized strategy might be an efficient alternative to the previously described methods. In summary, the heterologous β-Gal expression was successful in terms of significant overexpression of GST-tagged fusion proteins of full sequence length as well as a truncated fusion peptide. However, *E. coli* cells were not able to provide the machinery for proper folding of these fusion proteins, resulting in protein aggregation and inclusion body formation (cf. Figures 4.4.3.1.3 and 4.4.3.3.3). In fact, inclusion body formation of the target protein would not hinder antibody development, if the target protein could be purified from the aggregated protein complex. The insoluble β-Gal protein might as well be injected in rabbits as a purified, soluble form of the enyzme. However, β-Gal was fused with a large GST-tag (~26 kDa) in this work, which has to be cleaved from the fusion protein prior immunization of rabbits. Unfortunately, both C- and N-terminal polyhistidine-tagged β-Gal proteins were unstable in *E. coli*. They seemed to be rapidly degraded by *E. coli* proteases, visible as different sized fragments on Western blots (Figures 4.4.1.1.2, 4.4.1.1.3, and 4.4.2.3). Inclusion bodies of His®-tagged β-Gal might be used for antibody development, provided that a stable fusion protein could be purified from the insoluble protein aggregates.

Overexpression of five different *E. coli* chaperones (DnaK, DnaJ, GrpE, GroEL, and GroES) [Takara A] and co-expression of the GST-tagged full length β-Gal fusion protein (N-GST-Gal) could not significantly improve the expression of solubilized target protein (cf. Figures 4.4.3.2.3 and 4.4.3.2.4). Furthermore, the soluble portion of N-GST-Gal could not be purified on a GST-affinity resin (Figure 4.4.3.2.6). Co-expression of molecular chaperones to increase the solubility of recombinant proteins in *E. coli* has been proposed for several human proteins [reviewed in Hoffmann and Rinas, 2004], for example human procollagenases [Lee and Olins, 1992], but the choice of an appropriate chaperone system is a critical factor for success. The chaperone system used in this work (pG-KJE8 vector, Takara Bio. Inc.) did not impair the cell's viability despite high energy demands for overexpression, but potential positive effects on the solubility of the target protein were insignificant. The influence of each specific

molecular chaperone mentioned above on the solubility of heterologously expressed human β-Gal has not been determined yet. Furthermore, the effect of induction temperatures in combination with individual chaperones might be investigated in future experiments.

In contrast to the molecular chaperone approach, the solubilization of inclusion bodies by *in vitro* addition of denaturants and detergents resulted in large amounts of soluble target protein. Inclusion bodies from a positive transformant, expressing the truncated N-GST-Gal-peptide, could be solubilized by *in vitro* addition of 0.2% sarkosyl (Figure 4.4.4.2). Unfortunately, the resulting solubilized target protein was unable to bind to a GST affinity resin and could not be cleaved by a GST-specific protease. These results imply non-native state like conformation of the sarkosyl-solubilized N-GST-Gal-peptide hence impeding GST cleavage and affinity chromatography. Similar to experiments with co-expression of molecular chaperones, the influence of specific detergents and denaturants on the solubility of β-Gal inclusion bodies has to be studied in greater detail, but preliminary data obtained in sarkosyl experiments are promising.

At this point, the heterologous expression of human lysosomal acid β-Gal in *E. coli* was dispensed due to time limitations. However, not all options were exploited during this work and the collected data may provide a basis for further experiments using *E. coli* as expression host strain. Purification of large amounts of the human protein and subsequent antibody production might be easier to achieve than with established methods, and also more favorable in terms of costs.

5.2 DLHex-DGJ has pharmacological chaperone activity in human GM1 fibroblasts

Several specific inhibitors of lysosomal glycosidases [Asano, 2003] were shown to elevate residual enzyme activities after addition to the culture media of fibroblasts from patients with lysosomal diseases, and therefore, suggested to be beneficial in enzyme enhancement therapy [Begley *et al*., 2008; Fan, 2008].

For positive chaperone effects they are supposed to pass the cell membrane, to enter the ER, and to bind at neutral pH to the active site of misfolded enzyme precursors, thus facilitating proper folding or stabilizing the active site conformation of mutant proteins. Therefore, transport to the lysosomes via the mannose-6-phosphate pathway would be normalized. Within

the lysosomes, PCs may become protonated at specific groups due to the acidic pH (pH 4.5-5.0), thereby losing contact to the enzyme, and enabling the natural substrates to bind to the active site [Fan, 2008; Lieberman *et al*., 2009]. The extent and position of protonation depends on the molecular structure. The protonation sites of DLHex-DGJ are presumably the ring nitrogen of the iminoalditol (pKa ~7) as well as the aromatic amine in the dansyl moiety (pKa ~4.5). Some glycosidase inhibitors with proven chaperone activity, for example DGJ (Amigal™), are currently evaluated in clinical trials for Fabry disease [Benjamin *et al*., 2009; Fan, 2008; Khanna *et al*., 2010]. For G_{M1}-gangliosidosis, *N*-octyl-4-epi-β-valienamine (NOEV) was presented as a potent inhibitor of lysosomal β-galactosidase, and a putative pharmacological chaperone by Matsuda *et al.* [Matsuda *et al*., 2003]. It has since then been used in preclinical trials. In fibroblasts from patients with G_{M1}-gangliosidosis, NOEV displayed quite similar mutation preferences [Iwasaki *et al*., 2006], although at lower chaperone concentrations in the culture media (0.2 or 2 µM) than those used in the present work (20-500 µM). However, screening results indicate also high responses of certain mutations (p.R201C, p.R201H) below 20 µM DLHex-DGJ (Figure 4.6.2.1.2).

The novel compound, DLHex-DGJ [Fantur *et al*., 2010], is an N-alkylated derivative of 1-deoxygalactonojirimycin (DGJ), a well-known competitive inhibitor of lysosomal glycosidases [Asano, 2003]. Its chemical structure is based on the DGJ core. This is substituted at the ring nitrogen with a segmented branched spacer arm comprising of an alpha-N-dansyl-substituted (D) L-lysine residue (L), which shares the terminal amino group with the DGJ. The C-terminal end of the lysine moiety, in turn, is attached via an amide bond to the amine of methyl 6-aminohexanoate (Hex). This arrangement provides increased lipophilic character when compared to the parent compound DGJ [Steiner *et al*., 2008]. Its structural design is based on the finding that dansyl labeled, lipophilic compounds may result in increased inhibition activity compared to the non-fluorescent parent compound [Lundt *et al*., 2006].

According to the results described in this work, the novel compound DLHex-DGJ proved to be a potent inhibitor of lysosomal β-galactosidase (K_i = 0.6 µM; IC_{50} = 6 µM) *in vitro*, and a potential pharmacological chaperone *in vivo* (Figure 4.6.2.1.2 and Table 4.6.2.1.3). Previous findings [Asano, 2003; Fan, 2008; Iwasaki *et al*., 2006; Matsuda *et al*., 2003] indicated that the chaperone effect occurs at subinhibitory concentrations, although rather high doses (20-500 µM) had to be added to the culture medium for maximal effectiveness. This may be an

indication that the uptake of DLHex-DGJ into the cells may limit its chaperone activity, and the effective intracellular concentration is therefore below the concentration in the culture medium.

For Western blots and immunolocalization, 250 µM and 500 µM of DLHex-DGJ were used, since p.C230R and pG438E cells did not respond below these concentrations (Figure 4.6.2.1.2). However, only 20 µM were required for significant β-Gal enhancement in p.R201H and p.R201C carriers. Iwasaki *et al*. also demonstrated different responses of certain mutations to the same compound [Iwasaki *et al*., 2006].

Thus results of this work confirm that the efficacy of pharmacological chaperones is mutation-specific. The p.R201C allele, common for juvenile GM1 [Oshima *et al*., 1994; Yoshida *et al*., 1991], produces unstable, prematurely degraded β-Gal protein with high sensitivity for pharmacological chaperones [Iwasaki *et al*., 2006; Oshima *et al*., 1994; Tominaga *et al*., 2001; this work]. Another amino acid substitution affecting the same codon (p.R201H) has been identified in both GM1 and MBD patients [Hofer *et al*., 2009; Kaye *et al*.; 1997]. This mutation has also been shown to be chaperone-responsive [Iwasaki *et al*., 2006; Tominaga *et al*., 2001; this work]. Recent results [Hofer *et al*., 2010] imply that precursors truncated for more than 56 amino acid residues (p.E620X) are non-functional, and the phenotype-determining influence in the genotype p.R201H/p.R457X has to be limited to p.R201H. This finding enabled testing of DLHex-DGJ in heteroallelic p.R201H carriers.

Remarkably, a novel mutation, p.C230R [Hofer *et al*., 2010], recently described to cause an infantile GM1 phenotype with minor skeletal abnormalities, was identified as chaperone-sensitive cell line in this work. Immunolocalization experiments showed expression of β-Gal precursors of higher stability than in p.R201C or p.R201H cells. They are evenly distributed in the endo-lysosomal network, but lack further processing in the lysosomal compartment (Figures 4.6.2.2.1 and 4.6.2.3.1).

Homozygous p.C230R fibroblasts responded to high concentrations (≥ 250 µM) of DLHex-DGJ in the culture media, although the β-Gal activity against synthetic substrate did not exceed 10% of the normal control mean (28.4 nmol/hr/mg protein). This may be below the critical level for an influence on natural substrate turnover [Leinekugel *et al*., 1992]. Because of the high residual enzyme activities (7.2% of wildtype level), β-Gal of adult GM1 cells (p.G438E) was easily enhanced above this threshold (16.4% of wildtype level) upon addition of DLHex-DGJ (≥ 250 µM). To give an explanation for the findings, the actual concentrations of

chaperones in subcellular fractions, influence on formation and turnover of all *GLB1* gene products including EBP, as well as the degradation of natural substrates rather than of synthetic 4-methylumbelliferyl derivatives have to be studied.

Such data have to be obtained prior considering future use of DLHex-DGJ as a potential therapeutic agent in G_{M1}-gangliosidosis. In analogy to reports on the effects of various N-alkylated deoxynojirimycins (DNJ) on other lysosomal storage diseases [Butters *et al*., 2003a], one may speculate that DLHex-DGJ is able to permeate plasma membranes and the blood-brain barrier due to the length of its alkyl chain [Begley *et al*., 2008]. Although, its cytotoxicity might be higher than the non-alkylated parent compound, DGJ, the chemically inert dansyl group may rather reduce than increase its toxicity as a consequence of the protonation of the aromatic amine, resulting in dramatically increased solubility and decreased (bio)chemical reactivity. No cytotoxic effects were observed in fibroblast cultures used in this work.

Twelve other novel iminosugars were screened using the known chaperone-sensitive cell line p.R201C (juvenile GM1) and nine of them significantly increased residual β-Gal activities without affecting the control enzyme, β-Hex (cf. Figure 4.6.2.1). Several of these compounds had optimal concentrations below the one postulated for DLHex-DGJ (500 µM), but the structural and chemical characteristics of DLHex-DGJ (autofluorescent dansyl group, soluble in water) plus its ability to increase β-Gal activities in p.R201C cells to up to 75% of the healthy control activity made it the number one choice potential pharmacological chaperone in this work. Fluorescence detection of DLHex-DGJ in wildtype cells and p.R201C fibroblasts as well as co-localisation experiments with β-Gal or the lysosome marker LAMP2 never showed strong dansyl signals, despite using the optimal concentration of 500 µM in the cell culture media and an incubation time of 2-4 days (data not shown). However, we were not able to use the recommended microscopic equipment (UV-laser; cf. appendix) for optimal excitation of dansyl (~340 nm; emission at ~520 nm). Another interesting compound used in this work was substance #2 w/o dansyl, which is actually DLHex-DGJ without the dansyl group (cf. 3.9.1.1.1). It was able to increase β-Gal residual activities in p.R201C cells in the same manner as DLHex-DGJ with regard to their optimal chaperone concentration and activity enhancement in p.R201C fibroblasts. Although residual activities could be increased to up to 51% of healthy controls (Figure 4.7.1.3), the pharmacological chaperone effect of #2 w/o dansyl was always slightly below the potential of its "parent compound" DLHex-DGJ, suggesting a positive effect of the dansyl group on the chaperone activity of the molecule. DLHex-DGJ and #2 w/o dansyl

were selected for an experimental series to investigate the degradation of natural substrates upon chaperon treatment of GM1 and MBD fibroblasts.

5.3 Selective degradation of radiolabeled G_{M1}- gangliosides in chaperone - treated fibroblasts

To examine the effect of DLHex-DGJ and #2 w/o dansyl on natural substrate degradation, selected GM1 and MBD cell lines were loaded with tritium-labeled G_{M1}-gangliosides (^{3}H-G_{M1}G) and the putative pharmacological chaperones were added to the culture media at different concentrations and for different incubation times. Similar experiments were described for other types of lysosomal storage diseases [Elleder et al., 2005; Keslova-Veselikova et al., 2008; Pavlu-Pereira et al., 2005], but this is the first study on GM1 and MBD cell lines subjected to natural substrate ^{3}H-G_{M1}G-loading in combination with chaperones. It was therefore interesting to examine the relative amounts of degraded radiolabled material in fibroblasts representative for all types of GM1 and in the typical MBD cell line (p.W273L).

The principle of the experimental setup was to provide a natural substrate for β-Gal in the cell culture medium, which is transported to the lysosomes after incorporation by fibroblast cells. β-Galactosidase from healthy control cells (WT) should be able to degrade the substrate, while GM1 and MBD cells would accumulate the substance in the lysosomal compartment. It was expected that the accumulation of G_{M1}-gangliosides is less pronounced in MBD cells with the mutation p.W273L, due to the "kinetic" defect of the enzyme [Groebe et al., 1980; Okumiya et al., 2003; Paschke and Kresse, 1982]. In healthy fibroblasts, G_{M1}-gangliosides would be degraded to G_{M2}- and subsequently to G_{M3}-gangliosides, which are further catabolized to lactosylceramide and then to glucosylceramide (Figure 4.7.1.1). To possibly prevent degradation beyond glucosylceramides, the glucosylceramidase inhibitor Conduritol B Epoxide (CBE) was added in most experimental setups of this study.

Analysis of product formation/degradation, however, can only be considered semi-quantitative due to experimental restrictions resulting from unpredictable degradation beyond glucosylceramides and concomitant signal losses, and potentially falsified peak area ratios because of lipid resynthesis from degradation products. Furthermore, loading assays were optimized to result in substrate saturation, which was a surprisingly unfavourable aspect for the

experiments presented in this work. As a result, degradation rates of wildtype cells (~95%) were almost similar to rates obtained for p.G438E (adult GM1), p.R201H/p.S149F (adult GM1 or MBD), and p.W273L (MBD) cells in control experiments. Only juvenile GM1 cells (p.R201C) showed a little less degradation as compared to wildtype cells, while infantile p.C230R cells presented with a degradation pattern more apparently correlating with the severity of the underlying defect (Figure 4.7.3.1). This finding implied a very restrictive character of these specific ^{3}H-G_{M1}G-loading experiments and they are probably not suited for detection of small, chaperone-induced changes. A potential chaperone effect in p.G438E cells, for example, could not be evaluated in these experiments. Even detection of potential positive effects in p.R201C cells (juvenile GM1), the known-chaperone sensitive cell line, would be arguable. On the other side, inhibitory effects were clearly visible in this setup.

Despite the limitations described above, a significant chaperone effect could be observed for both DLHex-DGJ and #2 w/o dansyl in a specific infantile GM1 cell line carrying the mutation p.C230R. The pharmacological chaperone effect was more pronounced with #2 w/o dansyl, resulting in a ~30% increase of product formation/degradation compared to control experiments upon addition of 250 µM to the culture media for 2 days. A reduction of the chaperone concentration in the medium to 20 µM had no effect on ^{3}H-G_{M1}G degradation in this cell line. Similar to #2 w/o dansyl, 20 µM but also 100 µM of DLHex-DGJ (incubation time of 4 days, respectively) in the culture medium of p.C230R cells had no effect on the product formation of incorporated radiolabeled G_{M1}-gangliosides. Addition of 500 µM for 4 days, however, significantly increased degradation of stored material, while the same concentration incubated for only 2 days did not alter the degradation pattern as compared to untreated controls. It should be noted again that data can only be analysed in a semi-quantitative mode and furthermore, some experiments were performed only once. Hence data from loading assays should be considered as preliminary results. However, a clear trend for enhancement of substrate clearance in infantile GM1 cells with the mutation p.C230R could be observed for DLHex-DGJ as well as #2 w/o dansyl, and their effects seem to be dosage- and time-dependent. The effective chaperone concentration of these compounds in the culture medium of p.C230R fibroblasts and resulting in substance clearance is presumably between 100 µM and 500 µM.

Another striking finding was the incongruity of data obtained with the natural lipid substrate in loading assays *in situ* and the soluble synthetic substrates in enzymatic *in vitro* assays. For example, no inhibitory effects on β-Gal activity in fibroblasts treated with 500 µM DLHex-

DGJ or #2 w/o dansyl were observed in standard or alternative β-Gal assays with 4-methylumbelliferyl-β-D-galactopyranoside, but this concentration of DLHex-DGJ significantly inhibited natural substrate degradation in almost all tested cell lines, including healthy control cells. These results imply enhanced inhibition of the enzyme *in vivo*, rather than a chaperone effect for the tested concentrations. In summary, the ^{3}H-G$_{M1}$G-loading proved to be a valuable and essential addition to the preliminary chaperone screenings in fibroblast cells. Future experiments to determine effective chaperone concentrations and incubation times ought to be supported by results of experiments with natural substrates like G$_{M1}$-gangliosides rather than relying on evaluation of enzymatic *in vitro* assays using exclusively synthetic substrates.

Experimental data from preclinical trials using 1-deoxygalactonojirimycin (DGJ) in a mouse model for Fabry disease demonstrated that less frequent oral administration of the pharmacological chaperone, including repeated cycles of 4 days with DGJ followed by 3 days without DGJ, resulted in greater reductions of the stored substrate globotriaosylceramide than compared to daily administration of the compound [Khanna *et al.*, 2010]. These findings might have implications for future experiments with DLHex-DGJ, as they imply a common problem of pharmacological chaperones, which is finding the optimal dosage to achieve maximal enzymatic activity and substrate clearance, but reduce inhibitory effects to a minimum.

5.4 Outlook

In summary, the present work provides information on a novel DGJ derivative acting as inhibitor of lysosomal β-galactosidase *in vitro*, and significantly enhancing residual β-Gal activity in homozygous GM1 cell lines upon addition to the culture medium. Immunolocalization experiments revealed that pharmacological chaperone treatment causes a wildtype-like distribution of β-Gal, and Western blots confirmed intralysosomal processing of the β-Gal precursor in formerly incapable cells. Preliminary results of loading assays using a natural substrate suggested degradation of stored material in lysosomes of specific GM1 cells upon feeding with DLHex-DGJ.

There is definitely a need for more information about enzyme enhancing molecules such as iminosugars or substrate analogs in terms of mode of action and mutation specificity. The selective design of novel compounds might be helpful in understanding the interaction between

mutant enzymes and chaperones, and vice versa also provide information about the nature of the defect, caused by a certain genotype. To date, no crystallographic structure of the human lysosomal acid β-Gal is available, but elucidation of its three-dimensional structure would be interesting with regard to binding of the interaction partners from the lysosomal multienzyme complex, but also to chaperone binding and dissociation. Furthermore, exact determination of chaperone concentrations in subcellular organelles might contribute to our understanding of chaperone uptake into the cells and how cell membranes or even the blood-brain barrier are passed by these small molecules. Preliminary experiments using subcellular fractionation techniques and tandem mass spectrometry demonstrated feasibility of this approach.

The putative pharmacological chaperone DLHex-DGJ might be subjected to further, optimized loading assays using natural substrates to determine effective concentrations and incubation times for each responding cell line. Finally, oral administration of this compound to a mouse model of G_{M1}-gangliosidosis might be considered. Transgenic mice, expressing the GM1-specific mutation p.R201C, are available and proved to be helpful tools in the characterization of *N*-octyl-4-epi-β-valienamine (NOEV) and examination of potential toxic effects [Matsuda *et al*., 2003].

6 REFERENCES

Aldenhoven M, Sakkers RJ, Boelens J, de Koning TJ, Wulffraat NM. Musculoskeletal manifestations of lysosomal storage disorders. *Ann Rheum Dis* 2009; **68**: 1659-1665.

Amaxa DCT-1002, "Cell Line Nucleofector® Kit T" protocol, Vs. 07-2004.

Anderson JK, Mole JE, Baker HJ. Purification and characterization of GM1 ganglioside beta-galactosidase from normal feline liver and brain. *Biochemistry* 1978; **17**: 467-473.

Andersson U, Smith D, Jeyakumar M, Butters TD, Borja MC, Dwek RA, Platt FM. Improved outcome of N-butyldeoxygalactonojirimycin-mediated substrate reduction therapy in a mouse model of Sandhoff disease. *Neurobiol* 2004; **16**: 506-515.

Arbisser AI, Donnelly KA, Scott CI, Di Ferrante N, Singh J, Stevenson RE, Aylesworth AS, Howell RR. Morquio-like syndrome with β-galactosidase deficiency and normal hexosamine sulfatase activity: mucopolysaccharidosis IVB. *Am J Med Genet* 1977: **1**; 195-205.

Arndt V, Rogon C, Hohfeld J. To be, or not to be – molecular chaperones in protein degradation. *Cell Mol Life Sci* 2007; **64**: 2525-2541.

Asano N. Glycosidase inhibitors: update and perspecitves on practical use. *Glycobiology* 2003; **13**: 93R-104R.

Asano N, Ishii S, Kizu H, Ikeda K, Yasuda K, Kato A, Martin OR, Fan JQ. *In vitro* inhibition and intracellular enhancement of lysosomal α-galactosidase A activity in Fabry lymphoblasts by 1-deoxygalactonojirimycin and its derivatives. *Eur J Biochem* 2000; **267**: 4179-4186.

Asfaw B, Schindler D, Ledvinova J, Cerny B, Smid F, Conzelmann E. Degradation of blood group A glycolipids A-6-2 by normal and mutant human skin fibroblasts. *J Lipid Res* 1998; **39**: 1768-1780.

Bagshaw RD, Zhang S, Hinek A, Skomorowski MA, Whelan D, Clarke JT, Callahan JW. Novel mutations (Asn 484 Lys, Thr 500 Ala, Gly 438 Glu) in Morquio B disease. *Biochim Biophys Acta* 2002; **1588**: 247-253.

Bairoch A. Classification of glycosyl hydrolase families and index of glycosyl hydrolase entries in SWISS-PROT. 1999.

Ballabio A, Gieselmann V. Lysosomal disorders: from storage to cellular damage. *Biochim Biophys Acta* 2009; **1793**: 684-696.

Barrett AJ, Rawlings ND, Woessner JF (eds): *Handbook of Proteolytic Enzymes*. London: Academic Press 1998: pp 393-398.

Beck M. New therapeutic options for lysosomal storage disorders: enzyme replacement, small molecules and gene therapy. *Hum Genet* 2007; **121**: 1-22.

Beck M. Therapy for lysosomal storage disorders. *IUBMB Life* 2010; **62**: 33-40.

Begley DJ, Pontikis CC, Scarpa M. Lysosomal storage diseases and the blood-brain barrier. *Curr Pharm Des* 2008; **14**: 1566-1580.

Benjamin ER, Flanagan JJ, Schilling A, Chang HH, Agarwal L, Katz E, Wu X, Pine C, Wustman B, Desnick RJ, Lockhart DJ, Valenzano KJ. The pharmacological chaperone 1-deoxygalactonojirimycin increases alpha-galactosidase A levels in Fabry patient cell lines. *J Inherit Metab Dis* 2009; **32**: 424-440.

Bieberich E, Freischütz B, Suzuki M, Yu RK. Differential effects of glycolipid biosynthesis inhibitors on ceramide-induced cell death in neuroblastoma cells. *J Neurochem* 1999; **72**: 1040-1049.

Bio-Rad 10001677, "Profinity IMAC Resins Instruction Manual", Rev B.

Bio-Rad 4006157, "Mini-PROTEAN® 3 Cell Instruction Manual", Rev B.

Bio-Rad 4110065, "Quick Start™ Bradford Protein Assay Instruction Manual", Rev A.

Bio-Rad M1703930, "Mini Trans-Blot Electrophoretic® Transfer Cell Instruction Manual", Rev E

Booth CW, Gerbie AB, Nadler HL. Intrauterine detection of GM1-gangliosidosis, type 2. *Pediatrics* 1973; **52**:521-524.

Boustany RM, Qian WH, Suzuki K. Mutations in acid beta-galactosidase cause GM1-gangliosidosis in American patients. *Am J Hum Genet* 1993; **53**: 881-888.

Brodsky JL. The protective and destructive roles played by molecular chaperones during ERAD (endoplasmic-reticulum-associated degradation). *Biochem J* 2007; **404**: 353-363.

Brunetti-Pierri N, Scaglia F. GM1 gangliosidosis: review of clinical, molecular, and therapeutic aspects. *Mol Genet Metab* 2008; **94**: 391-396.

Buck TM, Wright CM, Brodsky JL. The activities and function of molecular chaperones in the endoplasmic reticulum. *Semin Cell Dev Biol* 2007; **18**: 751-761.

Butters TD. Pharmacotherapeutic strategies using small molecules for the treatment of glycolipid lysosomal storage disorders. *Expert Opin Pharmacother* 2007; **8**: 427-435.

Butters TD, Dwek RA, Platt FM. Imino Sugar inhibitors for treating the lysosomal glycosphingolipidoses. *Glycobiology* 2005; **15**: 43R-52R.

Butters TD, Dwek RA, Platt FM. New therapeutics for the treatment of glycosphingolipid lysosomal storage diseases. *Adv Exp Med Biol* 2003a; **535**: 219-226.

Butters TD, Mellor HR, Narita K, Dwek RA, Platt FM. Small-molecule therapeutics for the treatment of glycolipid lysosomal storage disorders. *Philos Trans R Soc Lond B Biol Sci* 2003b; **358**: 927-945.

Caciotti A, Donati MA, Boneh A, d'Azzo A, Federico A, Parini R, Antuzzi D, Bardelli T, Nosi D, Kimonis V, Zammarchi E, Morrone A. Role of beta-galactosidase and elastin binding protein in lysosomal and nonlysosomal complexes of patients with GM1-gangliosidosis. *Hum Mutat* 2005; **25**: 285-292.

Callahan JW. Molecular basis of GM1 gangliosidosis and Morquio disease, type B. Structure-function studies of lysosomal beta-galactosidase and the non-lysosomal beta-galactosidase-like protein. *Biochim Biophys Acta* 1999; **1455**: 85-103.

Callahan JW, Wolfe LS. Isolation and characterization of keratan sulfates from the liver of a patient with G_{M1}-gangliosidosis type I. *Biochim Biophys Acta* 1970; **215**: 527-543.

Chakraborty S, Rafi MA, Wenger DA. Mutations in the Lysosomal β-Galactosidase Gene That Cause the Adult Form of GM1 Gangliosidosis. *Am J Hum Genet* 1994; **54**: 1004-1013.

Chang HH, Asano N, Ishii S, Ichikawa Y, Fan JQ. Hydrophilic iminosugar active-site-specific chaperones increase residual glucocerebrosidase activity in fibroblasts from Gaucher patients. *FEBS J* 2006; **273**: 4082-4092.

Chen YQ, Rafi MA, de Gala G, Wenger DA. Cloning and expression of cDNA encoding human galactocerebrosidase, the enzyme deficient in globoid cell leukodystrophy. *Hum Molec Genet* 1993, **2**: 1841-1845.

Chothia C, Lesk AM. The relation between the divergence of sequence and structure in proteins. *EMBO J* 1986; **5**: 823-826.

Compain P, Martin OR, Boucheron C, Godin G, Yu L, Ikeda K, Asano N. Design and synthesis of highly potent and selective pharmacological chaperones for the treatment of Gaucher's disease. *ChemBioChem* 2006; **7**: 1356-1359.

D'Agrosa RM, Hubbes M, Zhang S, Shankaran R, Callahan JW. Characteristics of the beta-galactosidase-carboxypeptidase complex in GM1-gangliosidosis and beta-galactosialidosis fibroblasts. *Biochem J* 1992; **285**: 833-838.

Datta SC, Radin NS. Normalization of liver glucosylceramide levels in the „Gaucher" mouse by phosphatidylserine injection. *Biochem Biophys Res Commun* 1988; **152**: 155-160.

Davies G, Henrissat B. Structures and mechanisms of glycosyl hydrolases. *Structure* 1995; **3**: 853-859.

D'Azzo A, Hoogeveen A, Reuser AJ, Robinson D, Galjaard H. Molecular defect in combined beta-galactosidase and neuraminidase deficiency in man. *Proc Natl Acad Sci USA* 1982; **79**: 4535-4539.

De Maio A. Heat shock proteins: facts, thoughts, and dreams. *Shock* 1999; **11**: 1-12.

Desnick RJ. Enzyme replacement and enhancement therapies for lysosomal diseases. *J Inherit Metab Dis* 2004; **27**: 385-410.

Dimri GP, Lee X, Basile G, Acosta M, Scott G, Roskelly C, Medrano EE, Linskens M, Rubelj I, Pereira-Smith O, Peacocke M, Campisi J. A biomarker that identifies senescent human cells in culture and in aging skin in vivo. *Proc Natl Acad Sci* 1995; **92**: 9363-9367.

Dorland, L, Haverkamp J, Viliegenthart JF, Strecker G, Michalski JC, Fournet B, Spik G, Montreuil J. 360-MHz 1H nuclear-magnetic-resonance spectroscopy of sialyl-oligosaccharides from patients with sialidosis (mucolipidosis I and II). *Eur J Biochem* 1978; **87**: 323-329.

Elleder M, Jerabkova M, Asfaw B, Hrebicek M, Berna L, Ledvinova J, Hulkova H, Rosewich H, Schymik N, Paton BC, Harzer K. Prosaposin deficiency -- a rarely diagnosed, rapidly progressing, neonatal neurovisceral lipid storage disease. Report of a further patient. *Neuropediatrics* 2005; **36**: 171-180.

Fan JQ. A counterintuitive approach to treat enzyme deficiencies: use of enzyme inhibitors for restoring mutant enzyme activity. *Biol Chem* 2008; **389**: 1-11.

Fan JQ, Ishii S, Asano N, Suzuki Y. Accelerated transport and maturation of lysosomal α-galactosidase A in Fabry lymphoblasts by an enzyme inhibitor. *Nat med* 1999; **5**: 112-115.

Fantur K, Hofer D, Schitter G, Steiner AJ, Pabst BM, Wrodnigg TM, Stütz AE, Paschke E. DLHex-DGJ, a novel derivative of 1-deoxygalactonojirimycin with pharmacological chaperone activity in human G_{M1}-gangliosidosis fibroblasts. *Mol Genet Metab* 2010; **100**: 262-268.

Frost RG, Holmes EW, Norden AG, O'Brien JS. Characterization of purified human liver acid beta-D-galactosidases A2 and A3. *Biochem J* 1978; **175**: 181-188.

GE Healthcare 28-9184-51 AB, "pGEX-6P-2 Vector", 05/2007.

GenScript TM0185, „High-Affinity GST Resin" technical manual, 01042010.

Giugliani R, Jackson M, Skinner SJ, Vimal CM, Fensom AH, Fahmy N, Sjövall A, Benson PF. Progressive mental regression in siblings with Morquio disease type B (mucopolysaccharidosis IV B). *Clin Genet* 1987; **32**: 313-325.

Glössl J, Truppe W, Kresse H. Purification and properties of N-acetylgalactosamine 6-sulphate sulphatase from human placenta. *Biochem J* 1979; **181**: 37-46.

Gluzman Y. SV40-transformed simian cells support the replication of early SV40 mutants. *Cell* 1981; **23**: 175-182.

Groebe H, Krins M, Schmidberger H, von Figura K, Harzer K, Kresse H, Paschke E, Sewell A, Ullrich K. Morquio syndrome (mucopolysaccharidosis IV B) associated with beta-galactosidase deficiency. Report of two cases. *Am J Hum Genet* 1980; **32**: 258-272.

Grudnik P, Bange G, Sinning I. Protein targeting by the signal recognition particle. *Biol Chem* 2009; **390**: 775-782.

Hahn CN, del Pilar Martin M, Schroder M, Vanier MT, Hara Y, Suzuki K, Suzuki K, d'Azzo A. Generalized CNS disease and massive GM1-ganglioside accumulation in mice defective in lysosomal acid beta-galactosidase. *Hum Mol Genet* 1997; **6**: 205-211.

Hartree EF. Determination of protein: a modification of the Lowry method that gives a linear photometric response. *Anal Biochem* 1972; **48**: 422-427.

Hasilik A, Lemansky P. Defects in lysosomal enzyme trafficking. in Platt FM, Walkley SU (eds): Lysosomal Disorders of the Brain. New York: Oxford University Press 2004: pp 141-169.

Henrissat B, Callebaut I, Fabrega S, Lehn P, Mornon JP, Davies G. Conserved catalytic machinery and the prediction of a common fold for several families of glycosyl hydrolases. *Proc Natl Acad Sci* 1995; **92**: 7090-7094.

Henrissat B, Coutinho PM. Carbohydrate-Active Enzymes server. 1999.

Hinek A. Biological roles of the non-integrin elastin/laminin receptor. *Biol Chem* 1996; **377**: 471-480.

Hinek A, Rabinovitch M, Keeley F, Okamura-Oho Y, Callahan J. The 67-kD elastin/laminin-binding protein is related to an enzymatically inactive, alternatively spliced form of beta-galactosidase. *J Clin Invest* 1993; **91**: 1198-1205.

Hinek A, Zhang S, Smith AC, Callahan JW. Impaired elastic-fiber assembly by fibroblasts from patients with either Morquio B disease or infantile GM1-gangliosidosis is linked to deficiency in the 67-kD spliced variant of beta-galactosidase. *Am J Hum Genet* 2000; **67**:23-26.

Hiraiwa M, Saitoh M, Arai N, Shiraishi T, Odani S, Uda Y, Ono T, O'Brien JS. Protective protein in the bovine lysosomal beta-galactosidase complex. *Biochim Biophys Acta* 1997; **1341**: 189-199.

Ho MW, Cheetham P, Robinson D. Hydrolysis of GM1-ganglioside by human liver β-galactosidase isoenzymes. *Biochem J* 1973; **136**: 351-359.

Hoeksema HL, van Diggelen OP, Galjaard H. Intergenic complementation after fusion of fibroblasts from different patients with beta-galactosidase deficiency. *Biochim Biophys Acta* 1979; **566**: 72-79.

Hofer D, Paul K, Fantur K, Beck M, Bürger F, Caillaud C, Fumic K, Ledvinova J, Lugowska A, Michelakakis H, Radeva B, Ramaswami U, Plecko B, Paschke E. GM1 gangliosidosis and Morquio B disease: expression analysis of missense mutations affecting the catalytic site of acid beta-galactosidase. *Hum Mutat* 2009; **30**: 1214-1221.

Hofer D, Paul K, Fantur K, Beck M, Rouberge A, Vellodi A, Poorthuis BJ, Michelakakis H, Plecko B, Paschke E. Phenotype determining alleles in GM1 gangliosidosis patients bearing novel *GLB1* mutations. *Clin Genet* 2010. *[in press]*

Hoffmann F, Rinas U. Roles of heat-shock chaperones in the production of recombinant proteins in Escherichia coli. *Adv Biochem Eng Biotechnol* 2004; **89**: 143-161.

Hollemans M, Reijngoud DJ, Tager JM. Evidence against a MgATP-dependent proton pump in rat-liver lysosomes. *Biochim Biophys Acta* 1979; **551**: 55-66.

Hoogeveen AT, Graham-Kawashima H, d'Azzo A, Galjaard H. Processing of human beta-galactosidase in GM1-gangliosidosis and Morquio B syndrome. *J Biol Chem* 1984; **259**: 1974-1977.

Hoogeveen AT, Verheijen FW, Galjaard H. The relation between human lysosomal beta-galactosidase and its protective protein. *J Biol Chem* 1983; **258**: 12143-12146.

Hubain P, Adam E, Dewelle A, Druez G, Farriaux JP, Dupont A. Étude d'une observation de gangliosidose á G_{M1}. *Helv Paediatr Acta* 1969; **24**: 337-351.

Hubbes M, D'Agrosa RM, Callahan JW. Human placental beta-galactosidase. Characterization of the dimer and complex forms of the enzyme. *Biochem J* 1992; **285** (Pt 3): 827-831.

Ida H, Eto Y, Maekawa K. GM1-gangliosidosis: Morphological and biochemical studies. *Brain Dev* 1989; **11**: 394-398.

Invitrogen™ 711-011109, "T4 DNA Ligase" user manual, 051502.

Invitrogen™ 28-0182, "One Shot® BL21(DE3) chemically competent *E. coli* cells" user manual, Version G.

Invitrogen™ MAN0000735, "SimplyBlue™ SafeStain" user manual, IM-6050

Ishii S, Chang HH, Yoshioka H, Shimada T, Mannen K, Higuchi Y, Taguchi A, Fan JQ. Preclinical efficacy and safety of 1-deoxygalactonojirimycin in mice for Fabry disease. *J Pharmacol Exp Ther* 2009; **328**: 723-731.

Itoh K, Oshima A, Sakuraba H, Suzuki Y. Expression, glycosylation, and intracellular distribution of human beta-galactosidase in recombinant baculovirus-infected Spodoptera frugiperda cells. *Biochem Biophys Res Commun* 1990; **167**: 746-753.

Iwasaki H, Watanabe H, Iida M, Ogawa S, Tabe M, Higaki K, Nanba E, Suzuki Y. Fibroblast screening for chaperone therapy in beta-galactosidosis. *Brain Dev* 2006; **28**: 482-486.

Jackman HL, Tan FL, Tamei H, Beurling-Harbury C, Li XY, Skidgel RA, Erdös EG. A peptidase in human platelets that deamidates tachykinins. Probable identity with the lysosomal "protective protein". *J Biol Chem* 1990; **265**: 11265-11272.

Jatzkewitz H, Sandhoff K. On a biochemically special form of infantile amaturotic idiocy. *Biochim Biophys Acta* 1963; **70**: 354-356.

Jayapal KP, Wlaschin KF, Yap MGS, Hu WS. Recombinant protein therapeutics from CHO cells – 20 years and counting. *Chem Eng Prog* 2007; **103**: 40-47.

Jeyakumar M, Dwek RA, Butters TD, Platt FM. Storage solutions: treating lysosomal disorders of the brain. *Nat Rev Neurosci* 2005; **6**: 713-725.

Jones CS, Mahuran D, Lowden JA, Callahan JW. Human placental beta-galactosidase: structural and immunological observations. *Can J Biochem Cell Biol* 1984; **62**: 529-534.

Kaback MM, Sloan HR, Sonneborn M, Herndon RM. GM1-gangliosidosis type I: in utero detection and fetal manifestations. *J Pediatr* 1973; **82**: 1037-1041.

Kasperzyk JL, d'Azzo A, Platt FM, Alroy J, Seyfried TN. Substrate reduction reduces gangliosides in postnatal cerebrum-brainstem and cerebellum in GM1 gangliosidosis mice. *J Lipid Res* 2005; **46**: 744-751.

Kaye EM, Shalish C, Livermore J, Taylor HA, Stevenson RE, Breakefield XO. β-galactosidase gene mutations in patients with slowly progressive GM1 gangliosidosis. *J Child Neurol* 1997; **12**: 242-247.

Kenyon KR, Sensenbrenner JA. Mucolipidosis II (I-cell disaease): ultrastructural observations of conjunctiva and skin. *Invest Ophthalmol* 1971; **10**: 555-567.

Keslova-Veselikova J, Hulkova H, Dobrovolny R, Asfaw B, Poupetova H, Berna L, Sikora J, Golan L, Ledvinova J, Elleder M. Replacement of alpha-galactosidase A in Fabry disease: effect on fibroblast cultures compared with biopsied tissues of treated patients. *Virchows Arch* 2008; **452**: 651-665.

Khanna R, Soska R, Lun Y, Feng J, Frascella M, Young B, Brignol N, Pellegrino L, Sitaraman SA, Desnick RJ, Benjamin ER, Lockhart DJ, Valenzano KJ. The pharmacological chaperone 1-deoxygalactonojirimycin reduces tissue globotriaosylceramide levels in a mouse model of Fabry disease. *Mol Ther* 2010; **18**: 23-33.

Kleijer WJ, Van der Veer E, Niermeijer MF. Rapid prenatal diagnosis of GM1-gangliosidosis using microchemical methods. *Hum Genet* 1976; **33**: 299-305.

Knapp S, Vocadlo D, Gao Z, Kirk B, Lou J, Withers SG. NAG-thiazoline, An N-Acetyl-β-hexosaminidase Inhibitor That Implicates Acetamido Participation. *J Am Chem Soc* 1996; **118**: 6804-6805.

Kollmann K, Pohl S, Marschner K, Encarnação M, Sakwa I, Tiede S, Poorthuis BJ, Lübke T, Müller-Loennies S, Storch S, Braulke T. Mannose phosphorylation in health and disease. Eur *J Cell Biol* 2010; **89**: 117-123.

Kress BC, Miller AL. Characterization of the acid beta-D-galactosidases from human urine. *Clin Chim Acta* 1978; **85**: 23-32.

Kudoh T, Kikuchi K, Nakamura F, Yokoyama S, Karube K, Tsugawa S, Minami R, Nakao T. Prenatal diagnosis of GM1-gangliosidosis: Biochemical manifestations in fetal tissues. *Hum Genet* 1978; **44**: 287-293.

Kurz DJ, Decary S, Hong Y, Erusalimsky JD. Senescence-associated β-galactosidase reflects an increase in lysosomal mass during replicative ageing of human endothelial cells. *J Cell Sci* 2000; **113**: 3613-3622.

Laemmli UK. Cleavage of structural proteins during the assembly of the head of bacteriophage T4. *Nature* 1970; **227**: 680-685.

Lee BY, Han JA, Im JS, Morrone A, Johung K, Goodwin EC, Kleijer WJ, DiMaio D, Hwang ES. Senescence-associated beta-galactosidase is lysosomal beta-galactosidase. *Aging Cell* 2006; **5**: 187-195.

Lee SC, Olins PO. Effect of overproduction of heat shock chaperones GroESL and DNaK on human procollagenase production in Escherichia coli. *J Biol Chem*. 1992; **267**: 2849-2852.

Leinekugel P, Michel S, Conzelmann E, Sandhoff K. Quantitative correlation between the residual activity of β-hexosaminidase A and arylsulfatase A and the severity of the resulting lysosomal storage disease. *Hum Genet* 1992; **88**: 513-523.

Leroy JG, DeMars. Mutant enzymatic and cytological phenotypes in cultured human fibroblasts. *Science* 1967; **157**: 804-806.

Li SC, Nakamura T, Ogamo A, Li YT. Evidence for the presence of two separate protein activators for the enzymic hydrolysis of GM1 and GM2 gangliosides. *J Biol Chem* 1979; **254**: 10592-10595.

Li Z, Srivastava P. Heat-shock proteins. *Curr Protoc Immunol* 2004; Appendix 1: Appendix 1T.

Lieberman RL, D'Aquino JA, Ringe D, Petsko GA. Effects of pH and iminosugar pharmacological chaperones on lysosomal glycosidase structure and stability. *Biochemistry* 2009; **48**: 4816-4827.

Lin H, Sugimoto Y, Ohsaki Y, Ninomiya H, Oka A, Taniguchi M, Ida H, Eto Y, Ogawa S, Matsuzaki Y. N-octyl-β-valienamine up-regulates activity of F213I mutant β-glucosidase in cultured cells: a potential chemical chaperone therapy for Gaucher disease. *Biochim Biophys Acta* 2004; **1689**: 219-228.

Little L, Alcouloumre M, Drotar AM, Herman S, Robertson R, Yeh RY, Miller AL. Properties of N-acetylglucosamine 1-phosphotransferase from human lymphoblasts. *Biochem J* 1987; **248**: 151-159.

Little LE, Mueller OT, Honey NK, Shows TB, Miller AL. Heterogeneity of N-acetylglucosamine 1-phosphotransferase within mucolipidosis III. *J Biol Chem* 1986; **261**: 733-738.

Lodish H, Berk A, Zipursky LS, Matsudaira P, Baltimore D, Darnell JE. in *Molecular cell biology*. New York: WH Freeman & Co. 1999.

Lowden JA, Cutz E, Conen PE, Rudd N, Doran TA. Prenatal diagnosis of GM1-gangliosidosis. *N Engl J Med* 1973; **288**: 225-228.

Lowry OH, Rosebrough NJ, Farr AL, Randall RJ. Protein measurement with the Folin phenol reagent. *J Biol Chem* 1951; **193**: 265-275.

Lundt I, Steiner AJ, Stütz AE, Tarling CA, Ully S, Withers SG, Wrodnigg TM. Fluorescently tagged iminoalditol glycosidase inhibitors as novel biological probes and diagnostics. *Bioorg Med Chem* 2006; **14**: 1737-1742.

Maegawa GH, Tropak M, Buttner J, Stockley T, Kok F, Clarke JT, Mahuran DJ. Pyrimethamine as a potential pharmacological chaperone for late-onset forms of GM2 gangliosidosis. *J Biol Chem* 2007; **282**: 9150-9161.

Matalon R, Arbogast B, Justice P, Brandt EK, Dorfman A. Morquio's syndrome. Deficiency of a chondroitin sulfate N-acetylhexosamine sulfate sulfatase. *Biochem Biophys Res Commun* 1974; **61**: 759-765.

Matsuda J, Suzuki O, Oshima A, Ogura A, Noguchi Y, Yamamoto Y, Asano T, Takimoto K, Sukegawa K, Suzuki Y, Naiki M. Beta-galactosidase-deficient mouse as an animal model for GM1-gangliosidosis. *Glycoconj J* 1997; **14**: 729-736.

Matsuda J, Suzuki O, Oshima A, Yamamoto Y, Noguchi A, Takimoto K, Itoh M, Matsuzaki Y, Yasuda Y, Ogawa S, Sakata Y, Nanba E, Higaki K, Ogawa Y, Tominaga L, Ohno K, Iwasaki H, Watanabe H, Brady RO, Suzuki Y. Chemical chaperone therapy for brain pathology in GM1-gangliosidosis. *Proc Natl Acad Sci USA* 2003; **100**: 15912-15917.

McCarter JD, Burgoyne DL, Miao S, Zhang S, Callahan JW, Withers SG. Identification of Glu-268 as the catalytic nucleophile of human lysosomal beta-galactosidase precursor by mass spectrometry. *J Biol Chem* 1997; **272**: 396-400.

Meikle PJ, Hopwood JJ, Clague AE, Carey WF. Prevalence of lysosomal storage disorders. *JAMA* 1999; **281**: 249-254.

Michalski JC, Strecker G, Fournet B, Cantz M, Spranger J. Structures of sialyl-oligosaccharides excreted in the urine of a patient with mucolipidosis I. *FEBS Lett* 1977; **79**: 105-108.

Middelberg AP. Preparative protein folding. *Trends Biotechnol* 2002; **20**: 437-443.

Millipore PR02842, "Amicon®Ultra-15 Centrifugal Filter Devices" user manual, Rev.B10/09.

Morita M, Saito S, Ikeda K, Ohno K, Sugawara K, Suzuki T, Togawa T, Sakuraba H. Structural bases of GM1 gangliosidosis and Morquio B disease. *J Hum Genet* 2009; **54**: 510-515.

Morreau H, Bonten E, Zhou XY, D'Azzo A. Organization of the gene encoding human lysosomal β-galactosidase. *DNA Cell Biol* 1991; **10**: 495-504.

Morreau H, Galjart NJ, Gillemans N, Willemsen R, van der Horst GT, d'Azzo A. Alternative splicing of beta-galactosidase mRNA generates the classic lysosomal enzyme and a beta-galactosidae-related protein. *J Biol Chem* 1989; **264**: 20655-20663.

Morrone A, Bardelli T, Donati MA, Giorgi M, Di Rocco M, Gatti R, Parini R, Ricci R, Taddeucci G, d'Azzo A, Zammarchi E. beta-galactosidase gene mutations affecting the lysosomal enzyme and the elastin-binding protein in GM1-gangliosidosis patients with cardiac involvement. *Hum Mutat* 2000; **15**: 354-366.

Ni X, Canuel M, Morales CR. The sorting and trafficking of lysosomal proteins. *Histol Histopathol* 2006; **21**: 899-913.

Nishimoto J, Nanba E, Inui K, Okada S, Suzuki K. GM1-Gangliosidosis (Genetic β-Galactosidase Deficiency): Identification of Four Mutations in Different Clinical Phenotypes among Japanese Patients. *Am J Hum Genet* 1991; **49**: 566-574.

Norden AG, Tennant LL, O'Brien JS. GM1 ganglioside beta-galactosidase. A. Purification and studies of the enzyme from human liver. *J Biol Chem* 1974; **249**: 7969-7976.

Novagen TB009, "BL21 competent *E. coli* cells" user manual, Rev. F 0104.

Novagen TB036, "pET-21a-d(+) Vectors" user manual, 12/98.

O'Brien JS. β-Galactosidase deficiency (GM1-gangliosidosis, galactosialidosis, and Morquio syndrome type B); ganglioside sialidase deficiency (mucolipidosis IV). in Scriver CR, Beaudet AL, Sly WS, Valle D (eds): *The Metabolic Basis of Inherited Disease*. 6th ed. New York: McGraw-Hill 1989: pp 1797-1806.

O'Brien JS. Generalized gangliosidosis. *J Pediatr* 1969; **75**: 167-186.

O'Brien JS, Gugler E, Giedion A, Wiesmann U, Herschkowitz N, Meier C, Leroy J. Spondyloepiphyseal dysplasia, corneal clouding, normal intelligence and acid β-galactosidase deficiency. *Clin Genet* 1976; **9**: 495-504.

O'Brien JS, Kishimoto Y. Saposin proteins: structure, function, and role in human lysosomal storage disorders. *FASEB J* 1991; **5**: 301-308.

Okada S, O'Brien JS. Generalized gangliosidosis: Beta-galactosidase deficiency. *Science* 1968; **160**: 1002-1004.

Okamura-Oho Y, Zhang S, Hilson W, Hinek A, Callahan JW. Early proteolytic cleavage with loss of a C-terminal fragment underlies altered processing of the beta-galactosidase precursor in galactosialidosis. *Biochem J* 1996; **313** (Pt 3): 787-794.

Okumiya T, Kroos MA, Vliet LV, Takeuchi H, Van der Ploeg AT, Reuser AJ. Chemical chaperones improve transport and enhance stability of mutant α-glucosidases in glycogen storage disease type II. *Mol Genet Metab* 2007; **90**: 49-57.

Okumiya T, Sakuraba H, Kase R, Sugiura T. Imbalanced substrate specifity of mutant beta-galactosidase in patients with Morquio B disease. *Mol Genet Metab* 2003; **78**: 51-58.

Oshima A, Yoshida K, Itoh K, Kase R, Sakuraba H, Suzuki Y. Intracellular processing and maturation of mutant gene products in hereditary beta-galactosidase deficiency (beta-galactosidosis). *Hum Genet* 1994; **93**: 109-114.

Oshima A, Yoshida K, Shimmoto M, Fukuhara Y, Sakuraba H, Yanagisawa N, Suzuki Y. Human beta-galactosidase gene mutations in Morquio B disease. *Am J Hum Genet* 1991; **49**: 1091-1093.

Parenti G. Treating lysosomal storage diseases with pharmacological chaperones. From concept to clinics. *EMBO Mol Med* 2009; **1**: 268-279.

Parenti G, Zuppaldi A, Gabriela-Pittis M, Rosaria-Tuzzi M, Annunziata I, Meroni G, Porto C, Donaudy F, Rossi B, Rossi M, Filocamo M, Donati A, Bembi B, Ballabio A, Andria G. Pharmacological enhancement of mutated alpha-glucosidase activity in fibroblasts from patients with Pompe disease. *Mol Ther* 2007; **15**: 508-514.

Paschke E and Kresse H. Morquio disease, type B: activation of GM1-beta-galactosidase by GM1-activator protein. *Biochem Biophys Res Commun* 1982; **109**: 568-575.

Paschke E, Milos I, Kreimer-Erlacher H, Hoefler G, Beck M, Hoeltzenbein M, Kleijer W, Levade T, Michelakakis H, Radeva B. Mutation analyses in 17 patients with deficiency in acid beta-galactosidase: three novel point mutations and high correlation of mutation W273L in Morquio disease type B. *Hum Genet* 2001; **109**: 159-166.

Paschke E, Niemann R, Strecker G, Kresse H. Aggregation properties of beta-galactosidase of human urine and degradation of its natural substrates by a purified preparation of the enzyme. *Biochim Biophys Acta* 1982; **704**: 134-143.

Pavlu-Pereira H, Asfaw B, Poupcotva H, Ledvinova J, Sikora J, Vanier MT, Sandhoff K, Zeman J, Novotna Z, Chudoba D, Elleder M. Acid sphingomyelinase deficiency. Phenotype variability with prevalence of intermediate phenotype in a series of twenty-five Czech and Slovak patients. A multi-approach study. *J Inherit Metab Dis* 2005; **28**: 203-227.

Pharmacia A, Affinity Chromatography: Principles & Methods, *Pharmacia Fine Chemicals*, 1983; p.24.

Pieper U, Eswar N, Webb BM, Eramian D, Kelly L, Barkan DT, Carter H, Mankoo P, Karchin R, Marti-Renom MA, Davis FP, Sali A. MODBASE, a database of annotated comparative protein structure models and associated resources. *Nucleic Acids Res* 2009; **37** (Database issue): D347-354.

Platt FM, Butters TD. Inhibition of substrate synthesis: a pharmacological approach for glycosphingolipid storage disease therapy. in Platt FM, Walkley SU (eds): *Lysosomal Disorders of the Brain.* New York: Oxford University Press 2004: pp 381-408.

Platt FM, Butters TD. Substrate deprivation: a new therapeutic approach for the glycosphingolipid lysosomal storage diseases. *Expert Rev Mol Med* 2000; **2**: 1-17.

Platt FM, Lachmann RH. Treating lyososmal storage disorders: current practice and future prospects. *Biochim Biophys Acta* 2009; **1793**: 737-745.

Platt FM, Neises GR, Reinkensmeier G, Townsend MJ, Perry VH, Proia RL, Winchester B, Dwek RA, Butters TD. Prevention of lysosomal storage in Tay-Sachs mice treated with N-butyldeoxynojirimycin. *Science* 1997; **276**: 428-431.

Poorthuis BJ, Wevers RA, Kleijer WJ, Groener JE, de Jong JG, van Weely S, Niezen-Koning KE, van Diggelen OP. The frequency of lysosomal storage diseases in The Netherlands. *Hum Genet* 1999; **105**: 151-156.

Pshezhetsky AV, Ashmarina M. Lysosomal multienzyme complex: biochemistry, genetics, and molecular pathophysiology. *Prog Nucleic Acid Res Mol Biol* 2001; **69**: 81-114.

Pshezhetsky AV, Potier M. Stoichiometry of the human lysosomal carboxypeptidase-beta-galactosidase complex. *Biochem Biophys Res Commun* 1993; **195**: 354-362.

QIAGEN 1034639, "EndoFree® Plasmid Purification Handbook", 11/2005.

QIAGEN 1043788, "QIAprep® Miniprep Handbook", 12/2006.

QIAGEN 1051746, "QIAquick® Spin Handbook", 03/2008.

Radin NS. Inhibitors and stimulators of glucocerebroside metabolism. *Prog Clin Biol Res* 1982; **95**: 357-383.

Roze E, Paschke E, Lopez N, Eck T, Yoshida K, Maurel-Ollivier A, Doummar D, Caillaud C, Galanaud D, Billete de Villemeur T, Vidailhet M, Roubergue A. Dystonia and parkinsonism in GM1 type 3 gangliosidosis. *Mov Disord* 2005; **20**: 1366-1369.

Sano R, Annunziata I, Patterson A, Moshiach S, Gomero E, Opferman J, Forte M, d'Azzo A. GM1-ganglioside accumulation at the mitochondria-associated ER membranes links ER stress to Ca(2+)-dependent mitochondrial apoptosis. *Mol Cell* 2009; **36**: 500-511.

Santamaria R, Blanco M, Chabas A, Grinberg D, Vilageliu L. Identification of 14 novel *GLB1* mutations, including five deletions, in 19 patients with GM1 gangliosidosis from South America. *Clin Genet* 2007: **71**: 273-279.

Santamaria R, Chabas A, Coll MJ, Miranda CS, Vilageliu L, Grinberg D. Twenty-one novel mutations in the *GLB1* gene identified in a large group of GM1-gangliosidosis and Morquio B patients: possible common origin for the prevalent p.R59H mutation among gypsies. *Hum Mutat* 2006; **27**: 1060.

Sartorius SLU2004-e07 103, "Vivaspin 4 & 15 ml" user manual, 85030-516-16.

Sawkar AR, Adamski-Werner SL, Cheng WC, Wong CH, Beutler E, Zimmer KP, Kelly JW. Gaucher disease-associated glucocerebrosidases show mutation-dependent chemical chaperoning profiles. *Chem Biol* 2005; **12**: 1235-1244.

Sawkar AR, Cheng WC, Beutler E, Wong CH, Balch WE, Kelly JW. Chemical chaperones increase the cellular activity of N370S β-glucosidase: a therapeutic strategy for Gaucher disease. *Proc Natl Acad Sci* 2002; **99**: 15428-15433.

Schitter G, Fantur K, Mahuran DJ, Mayer C, Paschke E, Pototschnig G, Scheucher E, Steiner AJ, Stütz AE, Tarling CA, Thonhofer M, Tropak M, Withers SG, Wrodnigg TM. Fluorous Iminoalditols: A new Family of N-Modified Glycosidase Inhibitors. *Chembiochem* 2010a. *[accepted]*

Schitter G, Scheucher E, Steiner AJ, Stütz AE, Thonhofer M, Tarling CA, Withers SG, Wicki J, Fantur K, Paschke E, Mahuran DJ, Rigat BA, Tropak M, Wrodnigg TM. Synthesis of lipophilic 1-deoxygalactonojirimycin derivatives as D-galactosidase inhibitors. *Beilstein J Org Chem* 2010b; **6** (21).

Seyrantepe V, Poupetova H, Froissart R, Zabot MT, Maire I, Pshezhetsky AV. Molecular pathology of NEU1 gene in sialidosis. *Hum Mutat* 2003; **22**: 343-352.

Sheth JJ, Sheth FJ, Bhattacharya R. Morquio-B syndrome (MPS-IV B) associated with beta-galactosidase deficiency in two siblings. *Indian J Pediatr* 2002; **69**: 109-111.

Shield JP, Stone J, Steward CG. Bone marrow transplantation correcting beta-galactosidase activity does not influence neurological outcome in juvenile GM1-gangliosidosis. *J Inherit Metab Dis* 2005; **28**: 797-798.

Sinigerska I, Chandler D, Vaghjiani V, Hassanova I, Gooding R, Morrone A, Kremensky I, Kalaydjieva L. Founder mutation causing infantile GM1-gangliosidosis in the Gypsy population. *Mol Genet Metab* 2006; **88**: 93-95.

Steiner AJ, Schitter G, Stütz AE, Wrodnigg TM, Tarling CA, Withers SG, Fantur K, Mahuran D, Paschke E, Tropak M. 1-deoxygalactonojirimycin-lysine hybrids as potent D-galactosidase inhibitors. *Bioorg Med Chem* 2008; **16**: 10216-10220.

Strecker G, Peers MC, Michalski JC, Hondi-Assah T, Fournet B, Spik G, Montreuil J, Farriaux JP, Maroteaux P, Durand P. Structure of nine sialyl-oligosaccharides accumulated in urine of eleven patients with three different types of sialidosis. Mucolipidosis II and two new types of mucolipidosis. *Eur J Biochem* 1977; **75**: 391-403.

Suzuki K. Cerebral G_{M1}-gangliosidosis: chemical pathology of visceral organs. *Science* 1968; **159**: 1471-1472.

Suzuki Y, Oshima A, Nanba E. β-galactosidase deficiency (β-galactosidosis): GM1 gangliosidosis and Morquio B disease. in Scriver CR, Beaudet AL, Sly WS, Valle D (eds): *The Metabolic and Molecular Bases of Inherited Disease.* New York: McGraw-Hill 2001: pp 3775-3809.

Suzuki K, Suzuki KI, Kamoshita S. Chemical pathology of G_{M1}-gangliosidosis (generalized gangliosidosis). *J Neuropathol Exp Neurol* 1969; **28**: 25-73.

Takara A, "Chaperone Plasmid Set" user manual, v.0401.

Takara B, "Chaperone Competent Cell BL21 Series" user manual, v.0707.

Tominaga L, Ogawa Y, Taniguchi M, Ohno K, Matsuda J, Oshima A, Suzuki Y, Nanba E. Galactonojirimycin derivatives restore mutant human beta-galactosidase activities expressed in fibroblasts from enzyme-deficient knockout mouse. *Brain Dev* 2001; **23**: 284-287.

Tomino S, Meisler M. Biochemical and immunological studies of purified mouse beta-galactosidase. *J Biol Chem* 1975; **250**: 7752-7758.

Tropak MB, Blanchard JE, Withers SG, Brown ED, Mahuran D. High-throughput screening for human lysosomal β-N-acetyl hexosaminidase inhibitors acting as pharmacological chaperones. *Chem Biol* 2007; **14**: 153-164.

Tropak MB, Reid SP, Guiral M, Withers SG, Mahuran D. Pharmacological enhancement of β-hexosamindase activity in fibroblasts from adult Tay-Sachs and Sandhoff patients. *J Biol Chem* 2004; **279**: 13478-13487.

Tylki-Szymańska A, Maciejko D, Kidawa M, Jablońska-Budaj U, Czartoryska B. Amniotic tissue transplantation as a trial of treatment in some lyososomal storage diseases. *J Inherit Metab Dis* 1985; **8**: 101-104.

Van der Spoel A, Bonten E, d'Azzo A. Processing of lysosomal beta-galactosidase. The C-terminal precursor fragment is an essential domain of the mature enzyme. *J Biol Chem* 2000; **275**: 10035-10040.

Van der Spoel A, Bonten E, d'Azzo A. Transport of human lysosomal neuraminidase to mature lysosomes requires protective protein/cathepsin A. *EMBO J* 1998; **17**; 1588-1597.

Van Dongen JM, Willemsen R, Ginns EI, Sips HJ, Tager JM, Barranger JA, Reuser AJ. The subcellular localization of soluble and membrane-bound lysosomal enzymes in I-cell fibroblasts: a comparative immunocytochemical study. *Eur J Cell Biol* 1985; **39**: 179-189.

Van Pelt J, Kamerling JP, Vliegenthart JF, Verheijen FW, Galjaard H. Isolation and structural characterization of sialic acid-containing storage material from mucolipidosis I (sialidosis) fibroblasts. *Biochim Biophys Acta* 1988; **965**: 36-45.

Vyas NK. Atomic features of protein-carbohydrate interactions. *Curr Opin Struct Biol* 1991; **1**: 732-740.

Wenger D, Williams C. Screening for lysosomal disorders. in Hommes FA (ed): *Techniques in diagnostic human biochemical genetics*. New York: Wiley-Liss 1991; pp 587–617.

Wraith JE. Enzyme replacement therapy for the management of the mucopolysaccharidoses. *Int J Clin Pharmacol Ther* 2009; **47**: S63-65.

Yamamoto Y, Fujie M, Nishimura K. The interrelation between high- and low-molecular-weight forms of GM1-beta-galactosidase purified from porcine spleen. *J Biochem* 1982; **92**: 13-21.

Yamamoto Y, Hake CA, Martin BM, Kretz KA, Ahern-Rindell AJ, Naylor SL, Mudd M, O'Brien JS. Isolation, characterization, and mapping of a human acid beta-galactosidase cDNA. *DNA Cell Biol* 1990; **9**:119-127.

Yayon A, Klagsbrun M, Esko JD, Leder P, Ornitz DM. Cell surface, heparin-like molecules are required for binding of basic fibroblast growth factor to its high affinity receptor. *Cell* 1991; **64**: 841-848.

Yoshida K, Oshima A, Shimmoto M, Fukuhara Y, Sakuraba H, Yanagisawa N, Suzuki Y. Human beta-galactosidase gene mutations in GM1-gangliosidosis: a common mutation among Japanese adult/chronic cases. *Am J Hum Genet* 1991; **49**: 435-442.

Yu L, Ikeda K, Kato A, Adachi I, Godin G, Compain P, Martin O, Asano N. α-1-C-Octyl-1-deoxynojirimycin as a pharmacological chaperone for Gaucher disease. *Bioorg Med Chem* 2006; **14**: 7736-7744.

Zhang S, McCarter JD, Okamura-Oho Y, Yaghi F, Hinek A, Withers SG, Callahan JW. Kinetic mechanism and characterization of human beta-galactosidase precursor secreted by permanently transfected Chinese hamster ovary cells. *Biochem J* 1994; **304** (Pt 1): 281-288.

Zhou XY, van der Spoel A, Rottier R, Hale G, Willemsen R, Berry GT, Strisciuglio P, Morrone A, Zammarchi E, Andria G, d'Azzo A. Molecular and biochemical analysis of protective protein/cathepsin A mutations: correlation with clinical severity in galactosialidosis. *Hum Mol Genet* 1996; **5**: 1977-1987.

7 APPENDIX

Affinity resins

High-Affinity GST Resin	GenScript, L00206
p-Aminophenyl β-D-thiogalactopyranoside-Agarose (PATG)	Sigma-Aldrich®, A8648
Profinity™ IMAC Resin	Bio-Rad, 156-0133

Antibodies

α85 anti-human β-galactosidase antibody produced in rabbits	provided by A. D'Azzo, St. Jude Children's Res. Hosp. Memphis, USA
Anti-Catalase Rabbit pAb	Calbiochem®, 219010
Anti-GST antibody produced in goat	GE Healthcare, 27457701
Anti-rabbit IgG (whole molecule) alkaline phosphatase conjugate antibody produced in goat	Sigma-Aldrich®, A3687
Fluorescein (FITC)-conjugated AffiniPure Goat Anti-Rabbit IgG (H+L)	Jackson Immuno Research, 111-095-045
ImmunoPure® Goat Anti-Rabbit IgG (H+L), Peroxidase Conjugated	Thermo Scientific, 31460
Peroxidase-conjugated AffiniPure Donkey Anti-Goat IgG (H+L)	Jackson Immuno Research, 705-035-147
Rabbit Polyclonal anti-6-Histidine	Novus Biologicals®, NB600-318
Rhodamine (TRITC)-conjugated AffiniPure Sheep Anti-Mouse IgG (H+L)	Jackson Immuno Research, 515-025-062

Centrifuges and rotors

Avanti™ 30 Centrifuge	Beckman Coulter
GS-15R Centrifuge	Beckman Coulter
Sorvall RC 5B Plus	Sorvall
Table Top Centrifuge, Biofuge pico	Heraeus Instruments
Table Top Centrifuge, Z200A	Hermle
UV Spectrophotometer UV-1800	Shimadzu
C0650 rotor, fixed angle rotor	Beckman Coulter

F21S, fixed angle rotor		Sorvall
F2402H rotor, fixed angle rotor		Beckman Coulter
S4180 rotor, swinging bucket rotor		Beckman Coulter

Chemicals and solutions

Substance	M_r	**Company, catalog no.**
0.9% Sodium chloride solution (NaCl)		Baxter, HCA1413AR
2-Mercaptoethanol	78.13	Sigma-Aldrich®, M3148
2-Propanol	60.1	Merck, 100995
3-[(3-Cholamidopropyl)dimethylammonio]-1-propanesulfonate (CHAPS)	614.88	Sigma-Aldrich®, C9426
4-Methylumbelliferone	198.2	Sigma-Aldrich®, M1808
4-Methylumbelliferyl-β-D-galactopyranoside	338.3	Sigma-Aldrich®, M1633
4-Methylumbelliferyl-N-acetyl-β-D-glucosaminide	379.4	Sigma-Aldrich®, M2133
Acetic acid (glacial) 100%	60.05	Merck, 100063
Agarose, LE		Biozym®, 850074
Ammonium persulfate (APS)	228.2	Roth®, 9178.1
Ampicillin	371.4	Roche, 10835242001
Aqua destillata (Aqua dest.), Ampuwa®		Fresenius Kabi
Boric acid	61.83	Sigma-Aldrich®, 339067
Bovine serum albumin (BSA)	~66 kDa	Sigma-Aldrich®, A7906
BSA, 100x for DNA restriction analysis		New England Biolabs®, B9001S
Brilliant Blue R	825.97	Sigma-Aldrich®, 27816
Bromophenol blue (BPB)	691.94	Merck, 111746
Chloramphenicol	323.14	Fluka, 23275
Chloroform	119.38	Merck; 102445
Citric acid monohydrate	210.14	Merck, 100244
Conduritol B Epoxide	162.1	Sigma-Aldrich®, C5424
Copper(II) sulfate pentahydrate ($CuSO_4$ x $5H_2O$)	249.68	Merck, 102790
D(-)-Galactonic acid-γ-lactone	178.1	SeqChem, SRP01100g
Dimethyl sulfoxide (DMSO)	78.13	Sigma-Aldrich®, 154938
Di-sodium hydrogen phosphate dihydrate (Na_2HPO_4 x $2H_2O$)	177.99	Merck, 106580
Dithiothreitol (DTT)	154.25	Sigma-Aldrich®, D9163
Dry milk, non fat		Bio-Rad, 170-6404

Ethidium bromide, UltraPure™		Invitrogen™, 15585011
Ethylenediaminetetraacetic acid (EDTA)	372.24	Sigma-Aldrich®, E5134
Ethanol (EtOH)	46.07	Merck, 100983
Geneticin®		Gibco®, 11811023
Gentamicin, Gibco®		Invitrogen™, 15750037
Glycerol	92.1	Fluka, 49767
Glycine	75.07	Roth®, 3908.2
Guanidine hydrochloride	95.53	Sigma-Aldrich®, 43272
Hydrochloric acid, fuming 37% (HCl)		Merck, 100317
Imidazole	68.08	Fluka, 56748
Isopropyl β-D-1-thiogalactopyranoside (IPTG)	238.31	Sigma-Aldrich®, I5502
L-(+)-Arabinose	150.13	Sigma-Aldrich®, A3256
L-Glutathione, reduced	307.32	Sigma-Aldrich®, G4251
Methanol (MeOH)	32.04	Merck, 106009
Nickel(II) sulfate (NiSO$_4$)	154.8	Sigma-Aldrich®, 656895
N-lauroyl-sarcosine	293.4	Sigma-Aldrich®, L9150
Orcinol, 97%		Sigma-Aldrich®, 447420
Phosphate buffered saline (PBS), pH 7.4		Sigma-Aldrich®, P3813
Phosphate buffered saline (PBS), pH 7.1-7.2		LKH Apotheke
Potassium sodium tartrate tetrahydrate	282.23	Merck, 108087
Propidium iodide	668.40	Invitrogen™, P3566
S.O.C. medium		Invitrogen™, 15544034
Sodium acetate	82.03	Sigma-Aldrich®, S2889
Sodium azide (NaN$_3$)	65.01	Sigma-Aldrich®, S8032
Sodium dihydrogen phosphate monohydrate (NaH$_2$PO4 x H$_2$O)	137.99	Merck,106346
Sodium carbonate (Na$_2$CO$_3$)	105.99	Merck, 106398
Sodium chloride (NaCl)	58.44	Merck, 106404
Sodium dodecyl sulfate (SDS)	288.38	Roth®, 2326.1
Sodium hydrogen carbonate (NaHCO$_3$)	84.01	Merck, 106329
Sodium hydroxide (NaOH)	40.0	Merck, 106498
Tetracycline		
Tetramethylethylendiamine (TEMED)	116.24	Roth®, 2367.1
Tris(hydroxymethyl)-aminomethane (Tris base)	121.13	Merck, 108382
Tris(hydroxymethyl)-aminomethanhydro-chlorid (Tris-HCl)	157.60	Merck, 108219
Tri-sodium citrate dihydrate	294.1	Merck, 106448
Triton® X-100		Sigma-Aldrich®, T9284
Tween® 20	1,227.72	Merck, 822184
Urea	60.06	Sigma-Aldrich®, 208884

DNA molecular weight markers

AmpliSize DNA Mol. Ruler	Bio-Rad, 170-8200
SmartLadder, molecular weight marker	Eurogentec, MW-1700-10

E. coli strains and plasmid DNA

BL21 competent *E. coli* cells	Novagen, 694494
BL21(DE3)pLysS, Induction Control A	Invitrogen™, 697393
Chaperone Plasmid Set feat. pG-KJE8 plasmid DNA	Takara Bio. Inc., 3340
NovaBlue competent *E. coli* cells	Karl-Franzens-University of Graz
One Shot® BL21(DE3) chemically competent *E. coli* cells	Invitrogen™, C600003
pET-21d(+) DNA	Novagen, 69743
pGEX-6P-2 vector	GE Healthcare, 27459801

Enzymes

AmpliTaq Gold® DNA Polymerase, with Buffer II and MgCl$_2$ solution	Applied Biosystems™, N8080243
Deoxyribonuclease I from bovine pancreas, (DNase I)	Sigma-Aldrich®, DN25
*Msc*I, 5 U/µl	New England Biolabs®, R0534S
*Nco*I, 10 U/µl	New England Biolabs®, R0193S, or Roche, 10835315001
*Nde*I, 20 U/µl	New England Biolabs®, R0111S
*Not*I, 10 U/µl	New England Biolabs®, R0189S
Pfu DNA Polymerase	Promega, M7741
PreScission™ Protease	GE Healthcare, 27084301
*Sal*I, 20 U/µl	New England Biolabs®, R0138S
*Sca*I, 10 U/µl	Roche, 10775266001
*Sma*I, 20 U/µl	New England Biolabs®, R0141S
Trypsin-EDTA (1x), Lot L00409-1823	PAA, L11-004
*Xho*I, 20 U/µl	New England Biolabs®, R0146S

Media and supplements

CHO-S-SFM II, with L-Glutamine, Gibco®, Lot 467818	Invitrogen™, 12052
DMEM High Glucose (pH 7.85), with L-, Glutamine, w/o Phenol Red, Lot E87709-2098	PAA, E15-877
Fetal bovine/calf serum Mycoplex (FCS),	PAA, A15-105
Ham's F-12, w/o L-Glutamine, Lot E01608-1640	PAA, E15-016
L-Glutamine solution	Sigma-Aldrich®, G7513
Luria Agar	Sigma-Aldrich®, L3147
Luria Broth	Sigma-Aldrich®, L3522
MEM with Earle's Salts (pH 7.5), w/o L-Glutamine, Lot E02409-2104 Lot A10507-0361	PAA, E15-024

Other materials

Amersham Hyperfilm™ MP	GE Healthcare, 28906835
Amicon® Ultra-15 Centrifugal Filter Units, MWCO 10,000	Millipore, UFC901024
Cell Line Nucleofector® Kit T	Amaxa, VCA-1002
Corning Costar® Strippetes®	Corning Incorporated
Cuvettes, "Halb-Mikro-Küvetten"	Sarstedt, 67.742
Easy-Grip™ Tissue Culture Dishes, 35 x 10 mm	Beckton Dickinson, 353001
EndoFree® Plasmid Maxi Kit	QIAGEN, 12362
Microplate, 6well, flat bottom	IWAKI, 3810-006
Nitrocellulose membrane, 0.45 µM pore size	Invitrogen™, LC2001
Petri Dishes, 100 x 15 mm	Beckton Dickinson, 351029
Poly-Prep® Chromatography Columns	Bio-Rad, 731-1550
QIAprep® Spin Miniprep Kit	QIAGEN, 27106
QIAquick® Gel Extraction Kit	QIAGEN, 28706
Quartz SUPRASIL® Cuvette, 10 mm	Hellma, 104.002B-QS
Quartz SUPRASIL® Micro Cuvette, (0.6 ml), 10 mm; plus Adapter	PerkinElmer, B0631123
Ready Gel Tris-HCl, 10%	Bio-Rad, 161-1155
Silica gel (Kieselgel) 60, 20 x 20 cm	Merck, 5721
Tissue Culture Flask, 25 cm², vented cap	Beckton Dickinson, 353109
Tissue Culture Flask, 75 cm², vented cap	IWAKI, 3123-075

Vivaspin 4 columns, MWCO 5,000	Vivascience, Sartorius GmbH, VS0413
Vivaspin 4 columns, MWCO 10,000	Vivascience, Sartorius GmbH, VS0403
XK 16/20 Column (chromatography)	GE Healthcare, 18877301

Protein molecular weight markers

BenchMark™ Pre-Stained Protein Ladder	Invitrogen™, 10748-010
LMW-SDS Marker	GE Healthcare, 17044601
SeeBlue® Plus2 Pre-Stained Standard	Invitrogen™, LC5925

Reagents and Kits

Bio-Rad Alkaline Phosphatase Conjugate Substrate Kit	Bio-Rad, 170-6432
Bio-Rad Protein Assay Dye Reagent	Bio-Rad, 500-0006
Calf Intestinal Alkaline Phosphatase (CIAP)	Invitrogen™, 18009027
DNA Ligase, T4	Invitrogen™, 15224025
DNA Polymerization Mix dNTP Set, (20 mM each A,C,G,T)	GE Healthcare, 28406557
Folin-Ciocalteu's phenol reagent	Merck, 109001
Liquid Scintillation Cocktail, BCS	GE Healthcare, NBCS104
Mowiol 4-88 Mounting Medium pH 8.5	Hoechst
NuPAGE® LDS 4x LDS Sample Buffer	Invitrogen™, NP0007
NuPAGE® Sample Reducing Agent 10x	Invitrogen™, NP0004
Quick Start™ Bradford Dye Reagent	Bio-Rad, 500-0205
Restore™ Western Blot Stripping Buffer	Thermo Scientific, 21059
Rotiphorese® Gel 40 (19:1)	Roth®, 3030.1
SimplyBlue™ SafeStain	Invitrogen™, LC6060
SuperSignal® West Pico Chemiluminescent Substrate Kit	Thermo Scientific, 34080

Technical equipment

AGFA CURIX 60™ table-top processor	Development of x-ray films from Western blots
ÄKTAexplorer™ coupled with Frac-900 Fractionator; UNICORN™ 4.12 software; Amersham Pharmacia Biotech	Fast protein liquid chromatography (FPLC); Purification of β-galactosidase from CHO-K1 cell culture medium

ATI Unicam, UV/VIS Spectrometer UV4	Photometric measurement of proteins
Beckman LS 6000IC Scintillation Counter	Measurement of radiation from β-emitters
Bio-Rad Mini-PROTEAN® 3 Cells	SDS-PAGE
Bio-Rad Mini Trans-Blot® Electrophoretic Transfer Cells	Western blotting
Branson Sonifier II, W-250	Cell homogenization (mammalian cells)
Braun Labsonic L	Cell homogenization (*E. coli*)
Braun Labsonic U	Cell homogenization (*E. coli*)
Cole-Parmer Co. Ultrasonic Homogenizer, 4710 series, Cup Horn Sonicator	sterile homogenization of mammalian cells, and liposome vesicle preparation (loading assays)
Eppendorf Mastercycler (epgradient S)	Polymerase chain reaction (PCR)
Eppendorf Thermomixer comfort	Temperature-dependent incubations of 1.5 ml tubes
Heidolph Reax 2 overhead shaker	Overhead shaking of samples and resins
Heraeus HERASafe® Clean Bench	Tissue culture
Herolab E.A.S.Y Win32 Gel Documentation	UV gel documentation of agarose gels
Olympus IX51 inverse fluorescence microscope, View III camera, Analysis B Software	Fluorescence imaging of live- and fixed-cell samples
PerkinElmer Luminescence Spectrometer, LS50B	Detection of fluorescence signals in enzymatic assays
Pharmacia Biotech Electrophoresis System with Power Supply EPS 600	Agarose gel electrophoresis
PowerPac HC™ 250 Volt	SDS-PAGE, Western blotting
Raytest TLC Analyzer v2.05 including Rita TLC Analysis software (v1.93.002)	Analysis of radiolabeled samples on TLC plates; peak analysis and quantification
Spectrophotometer UV-1800, Shimadzu	Photometric measurements of proteins and DNA
Zeiss Axiovert 25 microscope	Optical microscope for cell observation during growth or fibroblast preparation
Zeiss LSM510 META Confocal Imaging System	Confocal laser scanning microscopy of live- and fixed-cell samples

Amino acid sequences of heterologously expressed fusion proteins

Amino acid sequence of the C-terminal polyhistidine-tagged full length β-galactosidase (685 residues):

```
  1 MPGFLVRILP LLLVLLLLGP TRGLRNATQR MFEIDYSRDS FLKDGQPFRY ISGSIHYSRV
 61 PRFYWKDRLL KMKMAGLNAI QTYVPWNFHE PWPGQYQFSE DHDVEYFLRL AHELGLLVIL
121 RPGPYICAEW EMGGLPAWLL EKESILLRSS DPDYLAAVDK WLGVLLPKMK PLLYQNGGPV
181 ITVQVENEYG SYFACDFDYL RFLQKRFRHH LGDDVVLFTT DGAHKTFLKC GALQGLYTTV
241 DFGTGSNITD AFLSQRKCEP KGPLINSEFY TGWLDHWGQP HSTIKTEAVA SSLYDILARG
301 ASVNLYMFIG GTNFAYWNGA NSPYAAQPTS YDYDAPLSEA GDLTEKYFAL RNIIQKFEKV
361 PEGPIPPSTP KFAYGKVTLE KLKTVGAALD ILCPSGPIKS LYPLTFIQVK QHYGFVLYRT
421 TLPQDCSNPA PLSSPLNGVH DRAYVAVDGI PQGVLERNNV ITLNITGKAG ATLDLLVENM
481 GRVNYGAYIN DFKGLVSNLT LSSNILTDWT IFPLDTEDAV RSHLGGWGHR DSGHHDEAWA
541 HNSSNYTLPA FYMGNFSIPS GIPDLPQDTF IQFPGWTKGQ VWINGFNLGR YWPARGPQLT
601 LFVPQHILMT SAPNTITVLE LEWAPCSSDD PELCAVTFVD RPVIGSSVTY DHPSKPVEKR
661 LMPPPPQKNK DSWLDHVLEH HHHH
```

Amino acid sequence of the N-terminal polyhistidine-tagged full length β-galactosidase (684 residues):

```
  1 MAHHHHHPG FLVRILPLLL VLLLLGPTRG LRNATQRMFE IDYSRDSFLK DGQPFRYISG
 61 SIHYSRVPRF YWKDRLLKMK MAGLNAIQTY VPWNFHEPWP GQYQFSEDHD VEYFLRLAHE
121 LGLLVILRPG PYICAEWEMG GLPAWLLEKE SILLRSSDPD YLAAVDKWLG VLLPKMKPLL
181 YQNGGPVITV QVENEYGSYF ACDFDYLRFL QKRFRHHLGD DVVLFTTDGA HKTFLKCGAL
241 QGLYTTVDFG TGSNITDAFL SQRKCEPKGP LINSEFYTGW LDHWGQPHST IKTEAVASSL
301 YDILARGASV NLYMFIGGTN FAYWNGANSP YAAQPTSYDY DAPLSEAGDL TEKYFALRNI
361 IQKFEKVPEG PIPPSTPKFA YGKVTLEKLK TVGAALDILC PSGPIKSLYP LTFIQVKQHY
421 GFVLYRTTLP QDCSNPAPLS SPLNGVHDRA YVAVDGIPQG VLERNNVITL NITGKAGATL
481 DLLVENMGRV NYGAYINDFK GLVSNLTLSS NILTDWTIFP LDTEDAVRSH LGGWGHRDSG
541 HHDEAWAHNS SNYTLPAFYM GNFSIPSGIP DLPQDTFIQF PGWTKGQVWI NGFNLGRYWP
601 ARGPQLTLFV PQHILMTSAP NTITVLELEW APCSSDDPEL CAVTFVDRPV IGSSVTYDHP
661 SKPVEKRLMP PPPQKNKDSW LDHV
```

Amino acid sequence of the N-terminal GST-tagged full length β-galactosidase (920 residues):

```
  1 MSPILGYWKI KGLVQPTRLL LEYLEEKYEE HLYERDEGDK WRNKKFELGL EFPNLPYYID
 61 GDVKLTQSMA IIRYIADKHN MLGGCPKERA EISMLEGAVL DIRYGVSRIA YSKDFETLKV
121 DFLSKLPEML KMFEDRLCHK TYLNGDHVTH PDFMLYDALD VVLYMDPMCL DAFPKLVCFK
181 KRIEAIPQID KYLKSSKYIA WPLQGWQATF GGGDHPPKSD LEVLFQGPLG SPGIPGSTSA
241 IAAAPGFLVR ILPLLLVLLL LGPTRGLRNA TQRMFEIDYS RDSFLKDGQP FRYISGSIHY
301 SRVPRFYWKD RLLKMKMAGL NAIQTYVPWN FHEPWPGQYQ FSEDHDVEYF LRLAHELGLL
361 VILRPGPYIC AEWEMGGLPA WLLEKESILL RSSDPDYLAA VDKWLGVLLP KMKPLLYQNG
421 GPVITVQVEN EYGSYFACDF DYLRFLQKRF RHHLGDDVVL FTTDGAHKTF LKCGALQGLY
481 TTVDFGTGSN ITDAFLSQRK CEPKGPLINS EFYTGWLDHW GQPHSTIKTE AVASSLYDIL
541 ARGASVNLYM FIGGTNFAYW NGANSPYAAQ PTSYDYDAPL SEAGDLTEKY FALRNIIQKF
601 EKVPEGPIPP STPKFAYGKV TLEKLKTVGA ALDILCPSGP IKSLYPLTFI QVKQHYGFVL
661 YRTTLPQDCS NPAPLSSPLN GVHDRAYVAV DGIPQGVLER NNVITLNITG KAGATLDLLV
721 ENMGRVNYGA YINDFKGLVS NLTLSSNILT DWTIFPLDTE DAVRSHLGGW GHRDSGHHDE
781 AWAHNSSNYT LPAFYMGNFS IPSGIPDLPQ DTFIQFPGWT KGQVWINGFN LGRYWPARGP
841 QLTLFVPQHI LMTSAPNTIT VLELEWAPCS SDDPELCAVT FVDRPVIGSS VTYDHPSKPV
901 EKRLMPPPPQ KNKDSWLDHV
```

Amino acid sequence of the N-terminal GST-tagged truncated β-galactosidase (473 residues):

```
  1 MSPILGYWKI KGLVQPTRLL LEYLEEKYEE HLYERDEGDK WRNKKFELGL EFPNLPYYID
 61 GDVKLTQSMA IIRYIADKHN MLGGCPKERA EISMLEGAVL DIRYGVSRIA YSKDFETLKV
121 DFLSKLPEML KMFEDRLCHK TYLNGDHVTH PDFMLYDALD VVLYMDPMCL DAFPKLVCFK
181 KRIEAIPQID KYLKSSKYIA WPLQGWQATF GGGDHPPKSD LEVLFQGPLG SPGIPGSTSA
241 IAAAPGFLVR ILPLLLVLLL LGPTRGLRNA TQRMFEIDYS RDSFLKDGQP FRYISGSIHY
301 SRVPRFYWKD RLLKMKMAGL NAIQTYVPWN FHEPWPGQYQ FSEDHDVEYF LRLAHELGLL
361 VILRPGPYIC AEWEMGGLPA WLLEKESILL RSSDPDYLAA VDKWLGVLLP KMKPLLYQNG
421 GPVITVQVEN EYGSYFACDF DYLRFLQKRF RHHLGDDVVL FTTDGAHKTF LKC
```

8 CURRICULUM VITAE

MAG. KATRIN MEDEA-EMMA FANTUR

Year of birth	1979
Nationality	Austrian
E-Mail	katrin.fantur@gmail.com

UNIVERSITY TRAINING / CAREER

Since 2007/02	PhD Thesis at the Graz University of Technology under supervision of Prof. Peter Macheroux and conducted at the Department of Pediatrics and Adolescence Medicine (PI: Prof. Eduard Paschke), Medical University of Graz, Austria. Project title: "Investigations for the early diagnosis and prognosis of the phenotype in lysosomal storage diseases" (Grant no. GZ 200.156/2-VI/1a/2006, Austrian Ministry of Science and Research).
2009/08 – 2009/12	Several short-termed research stays at the laboratory of Prof. Jana Ledvinová at the First Faculty of Medicine, Charles University in Prague and General Univ. Hospital in Prague, Czech Republic, and at the laboratory of Prof. Lukas Mach at the Department of Applied Genetics and Cell Biology, University of Agricultural Sciences, BOKU Vienna, Austria.
2006/08 – 2006/12	Project employee in the laboratory of Prof. Peter Macheroux at the Department of Biochemistry, Graz University of Technology, Austria.
2006/06	Graduation (Master's degree "Mag. rer. nat.") with emphasis on biochemistry / molecular biology and genetics.
1998 – 2006	Studies in microbiology at the Karl-Franzens University in Graz, Austria.

LANGUAGES

German	mother tongue
English	fluent, certified by a TOEFL-PBT in 2005 (score: 620 of 677)
Italian	basic skills

MEMBERSHIPS

Austrian Association of Molecular Life Sciences and Biotechnology (ÖGMBT)

Austrian Association of Artificial Intelligence (ÖGAI)

PUBLICATIONS

Peer reviewed publications:

Schitter G, **Fantur K**, Mahuran DJ, Mayer C, Paschke E, Pototschnig G, Scheucher E, Steiner AJ, Stütz AE, Tarling CA, Thonhofer M, Tropak M, Withers SG, Wrodnigg TM
Fluorous Iminoalditols: A new Family of N-Modified Glycosidase Inhibitors
Chembiochem (2010), *[accepted]*.

Schitter G, Scheucher E, Steiner AJ, Stütz AE, Thonhofer M, Tarling CA, Withers SG, Wicki J, **Fantur K**, Paschke E, Mahuran DJ, Rigat BA, Tropak M, Wrodnigg TM
Synthesis of lipophilic 1-deoxygalactonojirimycin derivatives as D-galactosidase inhibitors
Beilstein Journal of Organic Chemistry 6, 21 (2010).

Fantur K, Hofer D, Schitter G, Steiner AJ, Pabst BM, Wrodnigg TM, Stütz AE, Paschke E
DLHex-DGJ, a novel derivative of 1-deoxygalactonojirimycin with pharmacological chaperone activity in human G_{M1}-gangliosidosis fibroblasts
Molecular Genetics and Metabolism 100, 3 (2010), 262-268.

Hofer D, Paul K, **Fantur K**, Beck M, Roubergue A, Vellodi A, Poorthuis B, Michelakakis H, Plecko B, Paschke E
Phenotype determining alleles in G_{M1}-gangliosidosis patients bearing novel GLB1 mutations
Clinical Genetics (2010), *[in press]*.

Hofer D, Paul K, **Fantur K**, Beck M, Bürger F, Caillaud C, Fumic K, Ledvinova J, Lugowska A, Michelakakis H, Radeva B, Ramaswami U, Plecko B, Paschke E
G_{M1}-gangliosidosis and Morquio B disease: expression analysis of missense mutations affecting the catalytic site of acid beta-galactosidase
Human Mutation 30, 8 (2009), 1214-1221.

Steiner AJ, Schitter G, Stütz AE, Wrodnigg TM, Tarling CA, Withers SG, **Fantur K**, Mahuran D, Paschke E, Tropak M
1-Deoxygalactonojirimycin-lysine hybrids as potent D-galactosidase inhibitors
Bioorganic & Medicinal Chemistry 16, 24 (2008), 10216-10220.

ORAL PRESENTATIONS

Iminoanaloga der Galaktose – pharmakologische Chaperone für die Therapie von G_{M1}-Gangliosidose?
35. Jahrestagung der Gesellschaft für Neuropädiatrie
Graz, Austria, 2009/04/24

Die Dosis macht das Gift: Iminozucker – Inhibitoren lysosomaler Enzyme oder pharmakologische Chaperone in lysosomalen Speicherkrankheiten
13. Österreichischer Kohlenhydratworkshop *[invited talk]*
Graz, Austria, 2009/02/19

Biochemical characterization of novel galactose analogues with presumptive chaperone activity in fibroblasts from patients with G_{M1}-gangliosidosis and Morquio B disease
13. Pädiatrisches Stoffwechselsymposium – Homocysteinstoffwechsel, Lysosomen, Neurometabolische Störungen
Graz, Austria, 2008/04/25

CONFERENCE POSTERS (SELECTION)

Fantur K, Hofer D, Schitter G, Wrodnigg TM, Stütz AE, Paschke E
Novel iminosugars acting as chaperones of lysosomal β-galactosidase – impact on therapy of G_{M1}-gangliosidosis?
17th ESGLD Workshop, Bad Honnef, Germany, September 10-13, 2009.

Hofer D, **Fantur K**, Paul K, Plecko B, Paschke E
Expression analysis of novel missense mutations of the GLB1 (acid β-galactosidase) gene in COS-1 cells
17th ESGLD Workshop, Bad Honnef, Germany, September 10-13, 2009.

Schitter G, **Fantur K**, Paschke E, Rigat B, Stütz A, Tarling C, Tropak M, Withers S, Wrodnigg TM
Elevated biological activity of 1-deoxygalactonojirimycin by lipophilic and fluorophilic substitution?
13. Österreichische Chemietage, Vienna, Austria, August 24-27, 2009.

Hofer D, **Fantur K**, Paul K, Plecko B, Paschke E

G_{M1}-Gangliosidose und Morquio Typ B: Expression von Missense-Mutationen des katalytischen Zentrums der sauren β-Galaktosidase

35. Jahrestagung der Gesellschaft für Neuropädiatrie, Graz, Austria, April 23-26, 2009.

Fantur K, Hofer D, Schitter G, Wrodnigg TM, Stütz AE, Paschke E

Imino analogues of galactose: specific inhibitors of human acid β-D-galactosidase and putative pharmacological chaperones for the treatment of inherited lysosomal storage diseases

Life Sciences 2008, Joint Annual Meeting of the Austrian Network for Gene Therapy (ANGT), Austrian Society for Biotechnology (ÖGBT), Austrian Society for Genetics and Genetic Engineering (ÖGGGT) and the Austrian Society for Biochemistry and Molecular Biology (ÖGBM), Graz, Austria, September 22-24, 2008.

Paschke E, Hofer D, **Fantur K**, Paul K, Morrone A, D'Azzo A

Expression analysis in COS-1 cells of missense alleles of the GLB1 (acid β-Galactosidase) gene with presumptive influence on catalytic enzyme function

Annual Symposium of the Society for the Study of Inborn Errors of Metabolism, Lisbon, Portugal, September 2-5, 2008.

Stütz AE, **Fantur K**, Paschke E, Schitter G, Steiner AJ, Tarling CA, Tropak MB, Withers SG, Wrodnigg TM

Novel N-modified derivatives of 1-deoxygalactonijirimycin are powerful inhibitors of galactosidases and restore mutant galactosidase activity in a G_{M1}-gangliosidosis cell line

XX. International Symposium on Medicinal Chemistry (EFMC-ISCM), Vienna, Austria, August 31-September 4, 2008.

Wrodnigg TM, Schitter G, Stütz AE, Paschke E, **Fantur K**, Tropak M, Withers SG

Helping glycosidases with glycosidase inhibitors: design and evaluation of inhibitors as potential chemical chaperones based on active site structure data of lysosomal glycosidases

XX. International Symposium on Medicinal Chemistry (EFMC-ISCM), Vienna, Austria, August 31-September 4, 2008.

Schitter G, **Fantur K**, Paschke E, Stütz AE, Steiner G, Tarling C, Tropak M, Withers S, Wrodnigg TM

Sticky helpers: novel liphophilic as well as bolaamphiphilic iminoalditol derivatives support mutant lysosomal galactosidase folding

XX. International Symposium on Medicinal Chemistry (EFMC-ISCM), Vienna, Austria, August 31-September 4, 2008.

Fantur K, Hofer D, Schitter G, Wrodnigg TM, Stütz AE, Paschke E.
Biochemical characterization of novel galactose analogues with presumptive chaperone activity in fibroblasts from patients with G_{M1}-gangliosidosis and Morquio B disease
10th International MPS Symposium, Vancouver, Canada, June 26-30, 2008.

Leber R, Kurat C, Petschnigg J, Natter K, Scholz H, Rechberger G, Streith IEF, **Fantur K**, Malanovic N, Kohlwein SD
Neutral lipid homeostasis in the yeast Saccharomyces cerevisiae
ELSO Meeting, Dresden, Germany, September 3-5, 2005.

Petschnigg J, Kurat CF, Leber R, Natter K, Scholz, H, Wolinski H, **Fantur K**, Gruber A, Winkler K, Kohlwein SD
Neutral lipid homeostasis in the yeast Saccharomyces cerevisiae
22nd YGM Conference, Bratislava, Slovak Republic, August 7-12, 2005.

DIPLOMA THESIS

Supervisors: Dr. Regina Maria Leber and Prof. Sepp-Dieter Kohlwein (PI)

Title: Charakterisierung lipolytischer Enzyme in der Hefe *Saccharomyces cerevisiae*
(Characterization of lipolytic enzymes in the yeast *Saccharomyces cerevisiae*)